ecp
Educational Control Products

Manual For Model 220

Industrial Emulator / Servo Trainer

(Instructor's Edition)

Important Notice

Section 2.3 of this manual contains important safety information that must be read by all users prior to operating the ECP system.

This manual is for use in direct association with ECP experimental systems only and may be reproduced only for that purpose. All other use, dissemination, or reproduction in whole or in part without the written permission of ECP is strictly prohibited.

© COPYRIGHT 1995, by ECP Educational Control Products. All rights reserved.

This Edition is compatible with Executive Software Version 2.3

ecp
Educational Control Products
1 Buckskin Court
Bell Canyon, CA 91307

ph: (818) 703-0802 fax: (818) 703-6040

The Model 220 Emulator Apparatus

CONTENTS

1 Introduction 1

1.1 System Overview 1

1.2 Manual Overview 2

2 System Description & Operating Instructions 3

2.1 ECP Executive Software 3

2.2 Electromechanical Plant 26

2.3 Safety 34

3 Start-up & Self-Guided Demonstration 37

3.1 Hardware Set-up Verification 37

3.2 Demonstration Of ECP Executive Program 39

3.3 Nonintuitive System Behavior 46

4 Real-time Control Implementation 47

4.1 Servo Loop Closure 47

4.2 Command Generation 49

4.3 Servo Motor & Amplifier 54

4.4 Multi-tasking Environment 57

4.5 Sensors 57

4.6 Auxiliary Analog Output 59

5 Plant Dynamic Models 61

5.1 Rigid Body Plants 61

5.2 Flexible Drive Dynamics 62

6 Experiments 68

6.1 System Identification 68

6.2 Rigid Body PD & PID Control 78

6.3 Fundamentals of Servo Control 83

6.4 Control of Plant With Drive Flexibility 94

6.5 Control of Plant With Backlash 100

(Instructor's Manual Only)

6i Instructor's Supplement To Experiments 102

6.1i System Identification 102

6.2i Rigid Body PD & PID Control 107

6.3i Fundamentals of Servo Control 113

6.4i Control of Plant With Drive Flexibility 126

6.5i Control of Plant With Backlash 138

6.5i Suggestions For Further Experiments 142

Ai Useful Scripts 144

A.1i Plant Model Builders 144

A.2i PD Gain Selector 150

A.2i LQR Synthesis 151

1 Introduction

Welcome to the ECP line of educational control systems. These systems are designed to provide insight to control system principles through hands-on demonstration and experimentation. Each consists of an electromechanical plant and a full complement of control hardware and software. The user interface to the system is via a user-friendly, PC window environment which supports a broad range of controller specification, trajectory generation, data acquisition, and plotting features. The systems are designed to accompany introductory through advanced level controls courses and support either high level usage (i.e. direct controller specification and execution) or detailed user-written algorithms.

The electromechanical apparatus may be transformed into a variety of dynamic configurations which represent important classes of "real life" systems. The Model 220 apparatus represents many such physical plants including rigid bodies; flexibility in drive shafts, gearing and belts; and coupled discrete vibration with actuator at the drive input and sensor collocated or at flexibly coupled output (noncollocated). Several other important non-ideal properties are readily introduced and removed including backlash, drive friction, and disturbances. This allows them to be characterized in a controlled manner and facilitates study of control approaches to mitigate their effects.

1.1 System Overview

The experimental control system is comprised of the three subsystems shown in Figure 1.1-1. The first of these is the electromechanical plant which consists of the emulator mechanism, its actuator and sensors. The design features brushless DC servo motors for both drive and disturbance generation, high resolution encoders, adjustable inertias and changeable gear ratios. It also has features to introduce coulomb and viscous friction, drive train flexibility, and backlash.

The next subsystem is the real-time controller unit which contains the digital signal processor (DSP) based real-time controller[1], servo/actuator interfaces, servo amplifiers, and auxiliary power supplies. The DSP is capable of executing control laws at high sampling rates allowing the implementation to be modeled as continuous or discrete time. The controller also interprets trajectory commands and supports such functions as data acquisition, trajectory generation, and system health and safety checks. A logic gate array performs motor commutation and encoder

[1]The system is also available in a PC bus installation form in which the DSP based real-time controller resides in the PC and all other control unit hardware remains in a separate box. This form has faster PC/controller communication rates. (Controller speed is unaffected.)

© ECP 1994, All rights reserved.

pulse decoding. Two auxiliary digital-to-analog converters (DAC's) provide for real-time analog signal measurement. This controller is representative of modern industrial control implementation.

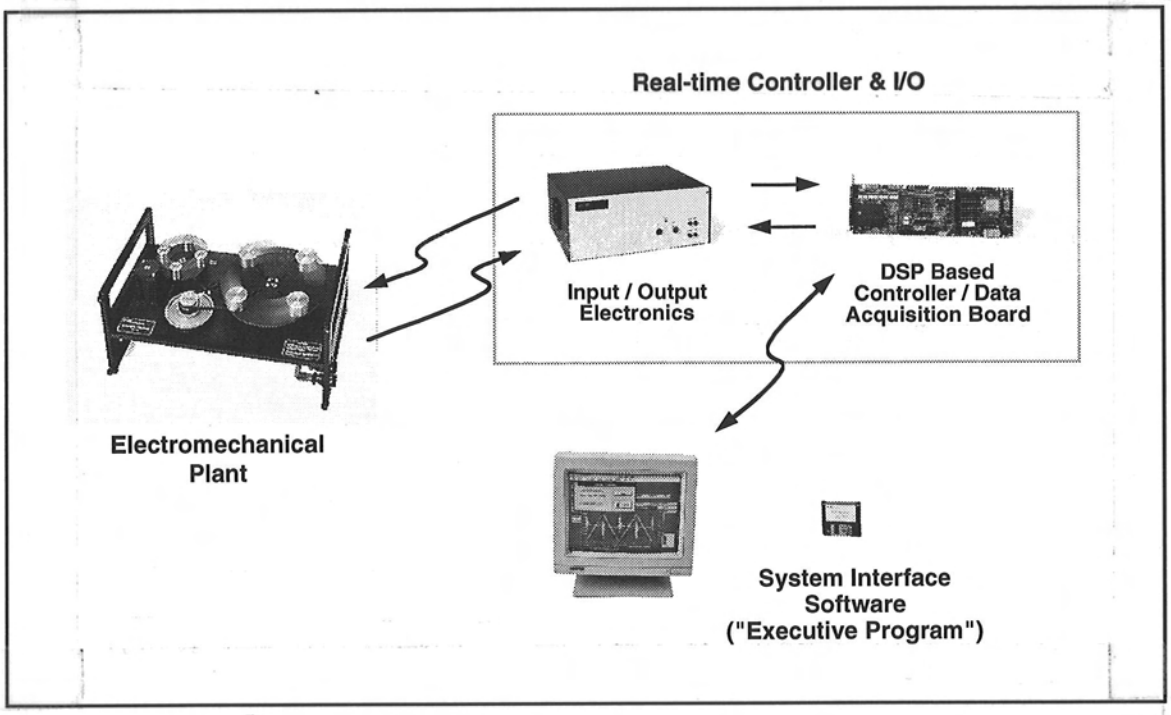

Figure 1.1-1. The Experimental Control System

The third subsystem is the executive program which runs on a PC under the DOS operating system. This menu-driven program is the user's interface to the system and supports controller specification, trajectory definition, data acquisition, plotting, system execution commands, and more. Controllers may assume a broad range of selectable block diagram topologies and dynamic order. The interface supports an assortment of features which provide a friendly yet powerful experimental environment.

1.2 Manual Overview

The next chapter, Chapter 2, describes the system and gives instructions for its operation. Section 2.3 contains important information regarding safety and is mandatory reading for all users prior to operating this equipment. Chapter 3 is a self-guided demonstration in which the user is quickly walked through the salient system operations before reading all of the details in Chapter 2. A description of the system's real-time control implementation as well as a discussion of generic implementation issues is given in Chapter 4. Chapter 5 presents dynamic equations useful for control modeling. Chapter 6 gives detailed experiments including system identification and a study of important implementation issues and practical control approaches.

© ECP 1995, All Rights Reserved

2 System Description & Operating Instructions

This chapter contains descriptions and operating instructions for the executive software and the mechanism. The safety instructions given in Section 2.3 must be read and understood by any user prior to operating this equipment.

2.1 ECP Executive Software

The ECP Executive software is the user's interface to the system. It is a menu driven / window environment that the user will find is intuitively familiar and quickly learned. This software runs on an IBM PC or compatible computer and communicates with ECP's digital signal processor (DSP) based real-time controller. Its primary functions are supporting the downloading of various control algorithm parameters (gains), specifying command trajectories, selecting data to be acquired, and specifying how data should be plotted. In addition, various utility functions ranging from saving the current configuration of the Executive to specifying analog outputs on the auxiliary DAC's are included as menu items.

2.1.1 PC System Requirements

The ECP Executive runs on any PC/AT or compatible computer. You will need at least 1 megabyte of RAM and a hard disk drive with at least 3 megabytes of space. All versions of the Executive program run under any DOS versions 3.x, 4.x, 5.x, and 6.x. Be aware that DOS version 4.x has had reported problems working with various software packages. The Executive requires a VGA monitor with a VGA graphics card installed on the PC.

The Executive Program runs best on a 386 or 486 with 2 megabytes of memory (or more) under DOS 5.0 with `HIGHMEM.SYS` driver included in your `CONFIG.SYS` file.[1] Also, if the software does not "see" at least 2 megabytes of free RAM, you may find the program executing somewhat slowly since it will use the hard disk as virtual memory.

[1] A faster computer, such as a 25 Mhz 486 with the real-time controller on the PC bus provides a much more expeditious working environment than a 386 or 286 and/or RS232 controller/PC communication. Real-time control speed, however, is unaffected.

© ECP 1995, All rights reserved.

2.1.2 Installation Procedure

The ECP Executive Program consists of several files on either a 5.25" 1.2 megabyte (high density) or 3.25" 1.44 megabyte distribution diskette in a compressed form. The files on the distribution diskette are:

```
ECP.EXE
ECP.DAT
ECPBMP.DAT
*.CFG
*.PLT
*.PMC
```

The "ECP.*" files are needed to run the Executive Program. The "*.CFG" and "*.PLT" files are some controller configuration and plotting files that are included for the initial self-guided demonstration. The "*.PMC" file is the controller Personality File and should only be used in the case of a non curable system failure (see "Utility Menu" below).

To install the Executive program, we recommend that you make a dedicated sub directory on the hard disk and enter this sub directory. For example type:

```
>MD ECP
>CD ECP
```

Next insert the distribution diskette in either "A:" or "B:" drive, as appropriate. Copy all files in the distribution diskette to the hard disk under the "ECP" sub directory. For example if the "B:" drive is used:

```
>COPY B:*.* C:
```

Next execute INSTALL.EXE by typing:

```
>INSTALL
```

You will notice some file decompression activities. This completes the installation procedure. You may run the ECP Executive by typing:

```
>ECP
```

The Executive program is window based with pull-down menus and dialog boxes. You may either use the cursor keys on the keyboard or a mouse to make selections from the pull-down menus. Vertical movement within these menus is accomplished by the up and down arrow keys, respectively. To make a selection with the keyboard, simply highlight the desired choice and press <ENTER>. Menu choices with highlighted letters may also be selected by pressing the corresponding function key. (The indicated key for menus; "alt" plus the indicated key within dialog boxes).

© ECP 1995, All rights reserved.

Within dialog boxes, movement from one object to the next is accomplished by using the <TAB> and the <SHIFT-TAB> keys. Here, "objects" includes input lines, check boxes, and "radio buttons". As you move from one object to the next, the focused object is highlighted, indicating that it is selected. Pressing <ENTER> will select the highlighted button (e.g. termination of the dialog box will result if the **OK** button is highlighted).

2.1.3 Background Screen

The *Background Screen* , shown in Figure 2.1.-1, remains in the background during system operation including times when other menus and dialog boxes are active. It contains the main menu and a display of real-time data, system status, and an *Abort Control* button to immediately discontinue control effort in the case of an emergency.

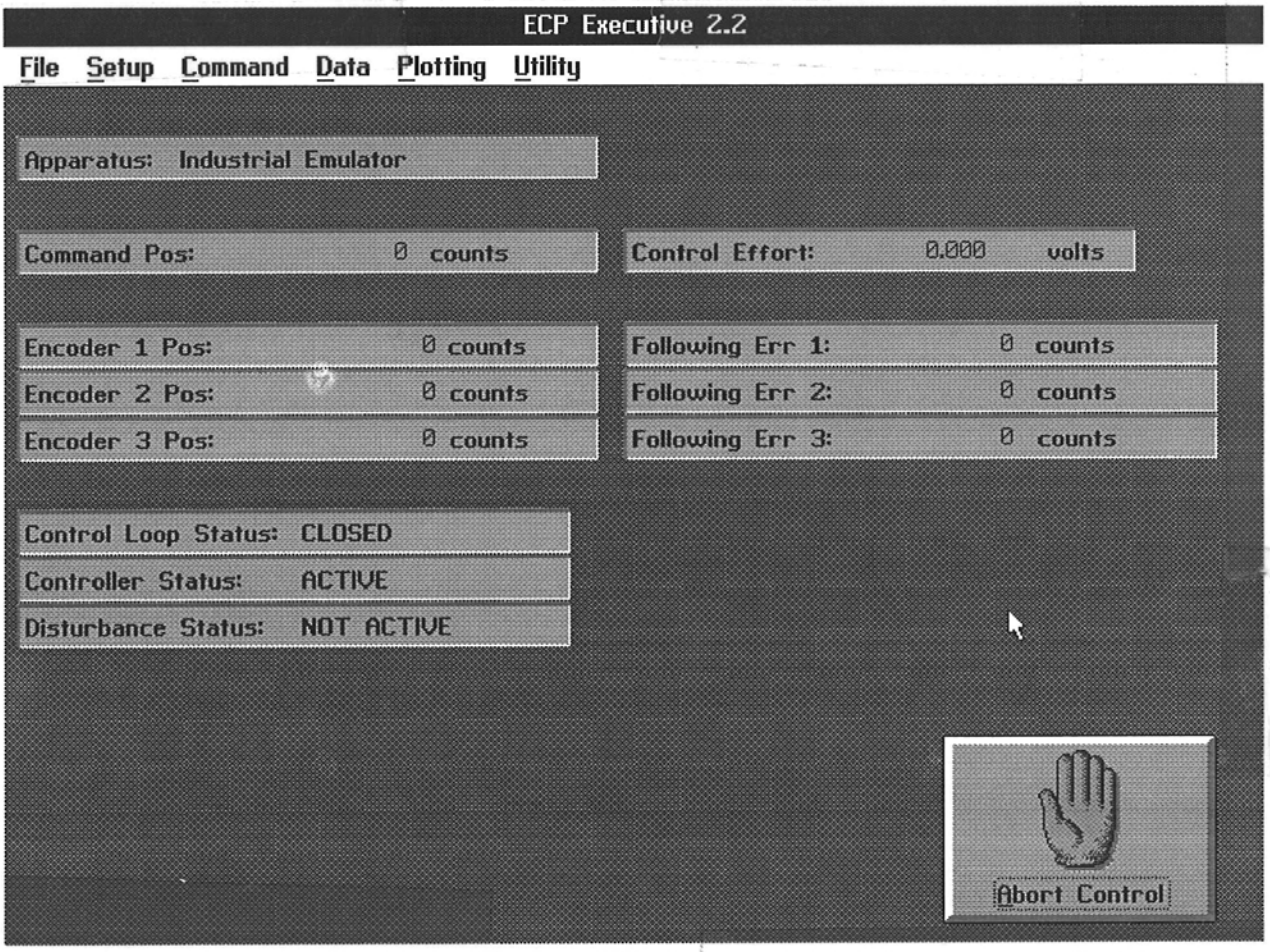

Figure 2.1-1. The Background Screen

© ECP 1995, All rights reserved.

2.1.3.1 Real-Time Data Display

In the *Data Display* fields, the instantaneous commanded position, the encodcr positions, the following errors (instantaneous differences between the commanded position and the actual encoder positions), and the control effort in volts (on the DAC) are shown.

2.1.3.2 System Status Display

The **Control Loop Status** ("Open" or "Closed"), indicates "Closed" unless an open loop trajectory is being executed or a "Limit Exceeded" condition has occurred. In either of these cases the Control Loop Status will indicate "Open". The **Controller Status** will indicate "Active" unless a motor overspeed, a shaft over-deflection, or motor/amplifier over-temperature condition has occurred (see Section 2.3 for more details). In either of these cases the Controller Status will indicate "Limit Exceeded". The Limit Exceeded indicator will reoccur unless the user takes one of the two following actions depending on the nature of the over-limit cause. Either a stable controller (one that does not cause limiting conditions) must be implemented via the **Control Algorithm** box under the **Setup** menu or an acceptable trajectory must be executed under the **Command** menu. An "acceptable" trajectory is one that does not overspeed the motor , over-deflect the flexible shaft or result in sustained high current to the motor. The controller must be "re implemented" in order to clear the Limit Exceeded condition – see Section 2.1.5.1.1.

The **Disturbance Status** will indicate "Active" when the viscous friction disturbance is invoked and/or when a profile disturbance torque is selected during a trajectory execution. It will otherwise indicate "Not Active" unless, due to disturbance motor amplifier over-current or load shaft over-speed, a "Limit Exceeded" condition develops. In this situation the "Limit Exceeded" indication will continue to appear until a new disturbance torque is implemented which does not cause a limit exceeding condition.

2.1.3.3 Abort Control Button

Also included on the Background Screen is the **Abort Control** button. Clicking the mouse on this button simply opens the control loop. This is a very useful feature in various situations including one in which a marginally stable or a noisy closed loop system is detected by the user and he/she wishes to discontinue control action immediately. Note also that control action may always be discontinued immediately by pressing the red "OFF" button on the control box.

2.1.3.4 Main Menu Options

The *Main menu* is displayed at the top of the screen and has the following choices:

File
Setup
Command
Data
Plotting
Utility

© ECP 1995, All rights reserved.

2.1.4 **File** Menu

The File menu contains the following pull-down options:

Load Settings
Save Settings
About
Exit

2.1.4.1 The **Load Settings** dialog box allows the user to load a previously saved configuration file into the Executive. A configuration file is any file with a "`.cfg`" extension which has been previously saved by the user using **Save Settings**. Any "`*.cfg`" file can be loaded at any time. The latest loaded "`*.cfg`" file will overwrite the previous configuration settings in the ECP Executive *but* changes to an existing controller residing in the DSP real-time control card will not take place until the new controller is "implemented" – see Section 2.1.5.1. The configuration files include information on the control algorithm, trajectories, data gathering, and plotting items previously saved. To load a "`*.cfg`" file simply select the **Load Settings** command and when the dialog box opens, select the appropriate file from the directory.[1] Note that every time the Executive program is entered, a particular configuration file called "`default.cfg`" is loaded.

2.1.4.2 The **Save Settings** option allows the user to save the current control algorithm, trajectory, data gathering and plotting parameters for future retrieval via the **Load Settings** option. To save a "`*.cfg`" file, select the **Save Settings** option and save under an appropriately named file (e.g. "`pid1dsk.cfg`"). By saving the configuration under a file named "`default.cfg`" the user creates a default configuration file which will be automatically loaded on reentry into the Executive program. You may tailor "`default.cfg`" to best fit your usage.

2.1.4.3 Selecting **About** brings up a dialog box with the current version number of the Executive program.

2.1.4.4 The **Exit** option brings up a verification message. Upon confirming the user's intention, the Executive is exited.

2.1.5 **Setup** Menu

The **Setup** menu contains the following pull-down options:

Control Algorithm
User Units
Communications

[1] Its fastest to simply double-click on the desired file.

© ECP 1995, All rights reserved.

2.1.5.1 **Setup Control Algorithm** allows the entry of various control structures and control parameter values to the real-time controller – see Figure 2.1-2. In addition to feedforward which will be described later, the currently available feedback options are:

PID
PI With Velocity Feedback
PID+Notch
Dynamic Forward Path
Dynamic Prefilter/Return Path
State Feedback
General Form

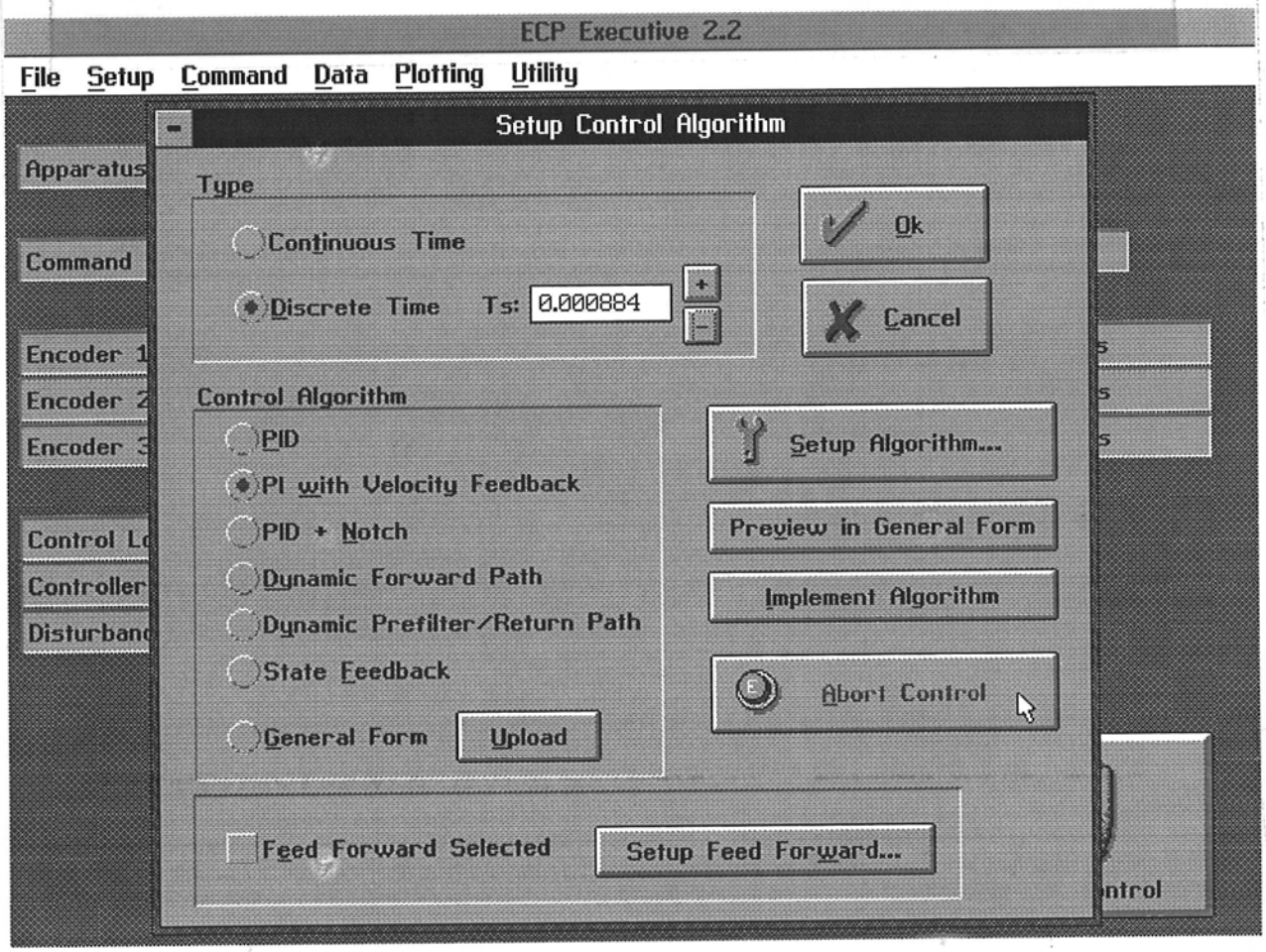

Figure 2.1-2. Setup Control Algorithm Dialog Box

© ECP 1995, All rights reserved.

2.1.5.1.1 Discrete Time Control Specification

The user chooses the desired option by selecting the appropriate "radio button" and then clicking on **Setup Algorithm**. The user must also select the sampling period which is always in multiples of 0.000884 seconds (1.1 KHz is the maximum sampling frequency).[1] To run the selected choice on the real-time controller click on the **Implement Algorithm** button. The control action will begin immediately. To stop control action and open the loop with zero control effort click on the **Abort** button. To upload the current controller select **General Form** then click on the **Upload Algorithm** button followed by **Setup Algorithm**. Here you will find the current controller in the form that is actually executed in real-time – see Figure 2.1-3.

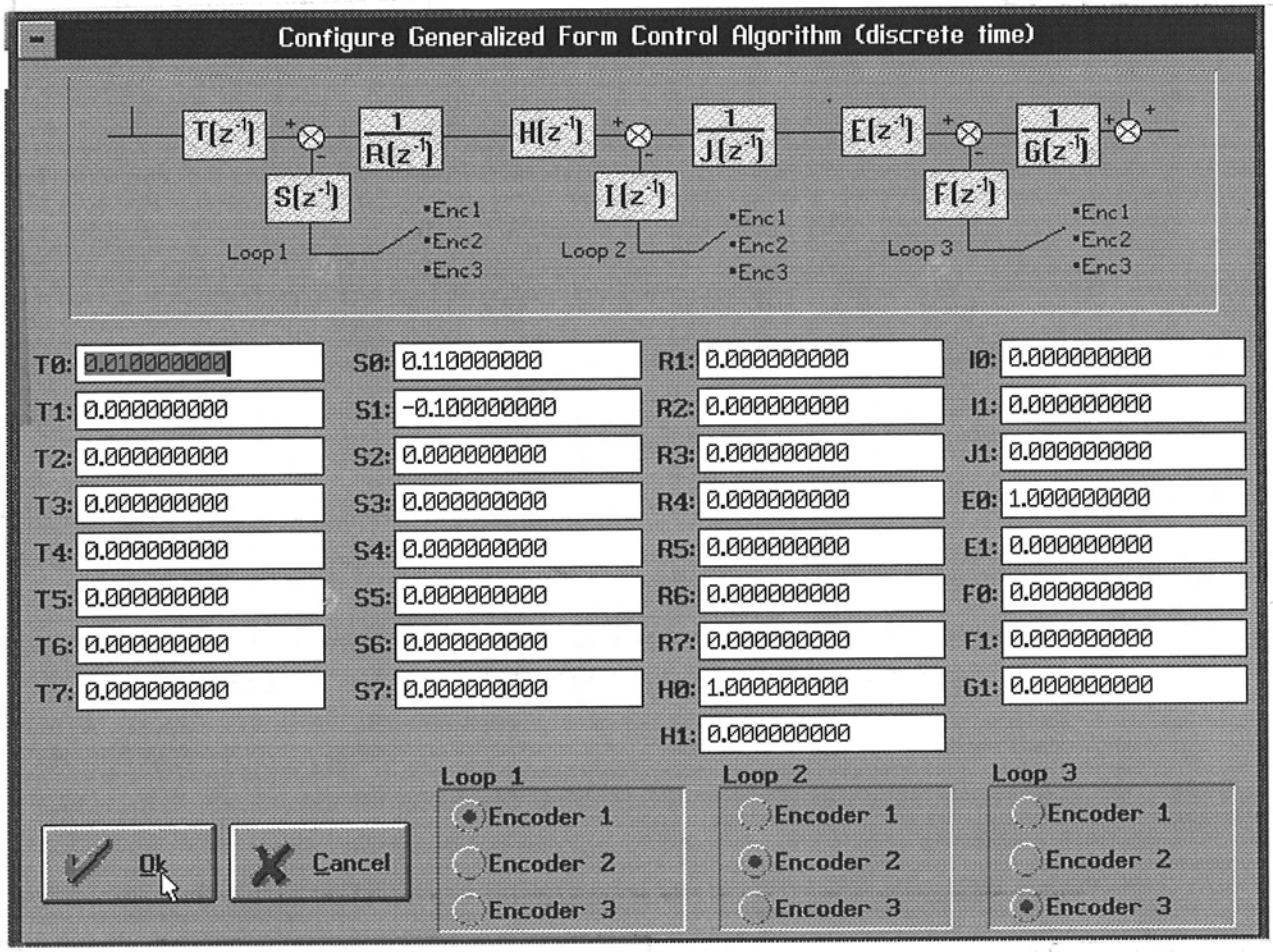

Figure 2.1-3. Dialog Box For Generalized Control Algorithm Input

A typical sequence of events is as follows: Select the desired servo loop closure sampling time T_S in multiples of 0.000884 seconds. Then select the control structure you wish to implement (e.g.

[1] For many designs, the value T_s = .00442 sec is a good midpoint between the spatial quantization induced noise associated with rate derivation over small sample periods and the phase lag associated with large ones.

© ECP 1995, All rights reserved.

radio buttons for PID, PID+Notch etc.). Select **Setup Algorithm** to input the gain parameters (coefficients). You must also select the desired feedback channel by choosing the correct encoder(s) used for your particular control design. Exit **Setup** by selecting **OK**. Now you should be back in the **Setup Control Algorithm** dialog box with a selected set of gains for a specified control structure. To down load this set of control parameters to the real-time controller click on **Implement Algorithm**. This action results in an immediate running of your selected control structure on the real-time controller. If you notice unacceptable behavior (instability and/or excessive ringing or noise) simply click on **Abort Control** which opens up the control loop with zero control effort commanded to the actuator.

To inspect the form by which your particular control structure is actually implemented on the real-time controller, simply click on **Preview In General Form**. You may edit the algorithm in the **General Form** box, however when you exit, you must select **General Form** prior to "implementing" if you want the changes to become effective. (i.e. the radio button will still indicate the box you were in prior to previewing and this one will be downloaded unless **General Form** is selected).

The **Setup Feed Forward** option allows the user to add feedforward action to any of the above feedback structures. By clicking on this button a dialog box appears which allows the feedforward control parameters (coefficients) to be entered. To augment the feedforward action to the feedback algorithm the user must then check the **Feedforward Selected** check-box. Any subsequent down loading (via the **Implement Algorithm** button) combines the feedforward control algorithm with the selected feedback control algorithm The feedforward action remains in effect until all of its coefficients are cleared and downloaded again even when the check-box has been cleared. Thus to disable the feedforward action the user must go to its dialog box, set all of the coefficients to zero and download (via **Implement Algorithm**) the zero set of coefficients to the real-time controller with the check box checked. Alternatively, the user can reset the controller via **Reset** option in the **Utility** menu (see below). This action also clears out all of the coefficients of both the feedback and feedforward controllers.[1]

Important Note: Every time a set of control coefficients are downloaded via **Implement Algorithm** button, the commanded position as well as all of the encoder positions are reset to zero. This action is taken in order to prevent any instantaneous unwanted transient behavior from the controller. The control action then begins immediately.

Important Note: For high order control laws (those using more than 2 or 3 terms of either the R, S, T, K, or L polynomials), it is often important that the coefficients be entered with relatively high precision– say at least 5 to 6 points after the decimal. The real-time controller works with 96-bit real number arithmetic (48-bit integer plus 48-bit fraction). Although the Executive displays the coefficients with nine points after the decimal, it accepts higher precision numbers and downloads them correctly.

[1]The feedback gains will generally still reside in the appropriate feedback controller dialog box and may be re-downloaded via **Implement** once they have been verified.

© ECP 1995, All rights reserved.

2.1.5.1.1 Continuous Time Control Specification

Depending on your course of study, It may be desirable to specify the control algorithm in continuous time form.[1] The method for inputting control parameters is identical to that described for the discrete time case. Again you may preview your controller in the continuos **General Form** prior to implementing. Upon selecting either **Implement Algorithm** or **Preview in General Form,** the algorithm also gets mapped into the discrete General Form where it may be viewed either before (following "**Preview**") or after (following "**Implement**") downloading to the real time controller.[2]

Again it is the discrete time general form that is actually executed in real time. The input coefficients are transformed to discrete time using one of the two following substitutions. For polynomials: ***n(s), d(s)*** in **PID + Notch**; ***s(s), t(s),*** and ***r(s)*** in **Dynamic Forward Path, Dynamic Prefilter / Return Path**, and the **General Form**; and ***k(s), l(s)*** in **Feed Forward**, the Tustin (bilinear) transform

$$s = \frac{2}{T_s}\frac{1-z^{-1}}{1+z^{-1}}$$

is used. All other cases (first order) use the Backwards Difference method:

$$s = \frac{1-z^{-1}}{T_s}$$

Blocks using the Tustin transform must be proper in ***s*** while those using backwards difference may be improper – e.g. a differentiator.

2.1.5.2 The **User Units** dialog box provides the user with various choices of angular or linear units. For Model 220 the choices are *counts, degrees and radians.* There are 16000 counts, 360 degrees and 2π radians per revolution of both the load and drive inertia disks. By clicking on the desired radio button the units are changed automatically for trajectory inputs as well as the

[1] A often used rule of thumb is that the continuous time approximation of sampled data systems is acceptably accurate if the sampling frequency is at least 10 times the system bandwidth. (This rule is not always conservative however, see Section 6.3.5 & 6.3.5i). Since the attainable closed loop bandwidths for the system are generally less than 10 Hz, sampling rates above 100 Hz usually provide results that are indistinguishable between equivalent continuous and discrete controller designs. I.e. for sampling rates above 100 Hz, the user may generally design and specify the controller in continuous time with no measurable difference in system behavior than if the controller were designed in discrete time.

[2] Note that in previewing the discrete generalized form of a continuous controller you should select **Discrete Time , General Form**, then **Setup Algorithm.** If instead the sequence **Discrete Time, Preview In General Form,** is used, then the selected discrete time algorithm (the one with the red dot next to it and which will not generally contain parameters that correspond to the continuous time design) will be previewed. Subsequent "Implementing" will then download the wrong design.

© ECP 1995, All rights reserved.

Background Screen displays, plotting and jogging activities. Units of *counts* are used exclusively for the examples in this manual.

2.1.5.3 The **Communications** dialog box is usually used only at the time of installation of the real-time controller. The choices are serial communication (RS232 mode) or PC-bus mode – see Figure 2.1-4. If your system was ordered for PC-bus mode of communication, you do not usually need to enter this dialog box unless the default address at 528 on the ISA bus is conflicting with your PC hardware. In such a case consult the factory for changing the appropriate jumpers on the controller. If your system was ordered for serial communication the default baud rate is set at 34800 bits/sec. To change the baud rate consult factory for changing the appropriate jumpers on the controller. You may use the **Test Communication** button to check data exchange between the PC and the real-time controller. This should be done after the correct choice of **Communication Port** has been made.

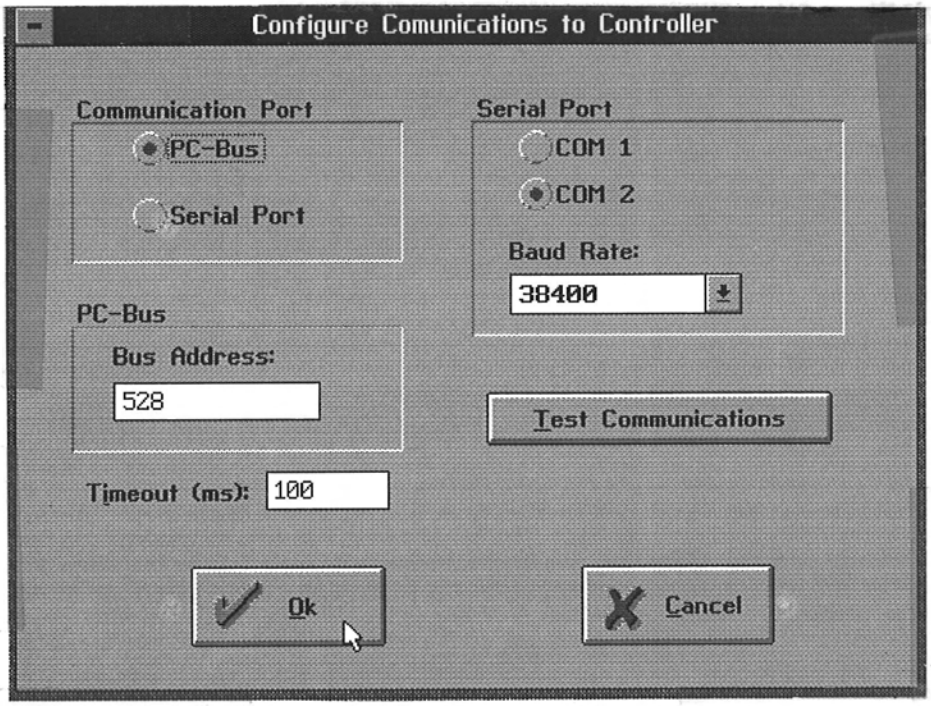

Figure 2.1-4. The Communications Dialog Box

2.1.6 **Command** Menu

The **Command** menu contains the following pull-down options

Trajectory . . .
Disturbance . . .
Execute . . .

© ECP 1995, All rights reserved.

2.1.6.1 The **Trajectory Configuration** dialog box (see Figure 2.1.-5) provides a selection of trajectories through which the apparatus can be maneuvered. These are:

Step
Ramp
Parabolic
Cubic
Sinusoidal
Sine Sweep
User Defined

A mathematical description of these is given later in Section 4.1.

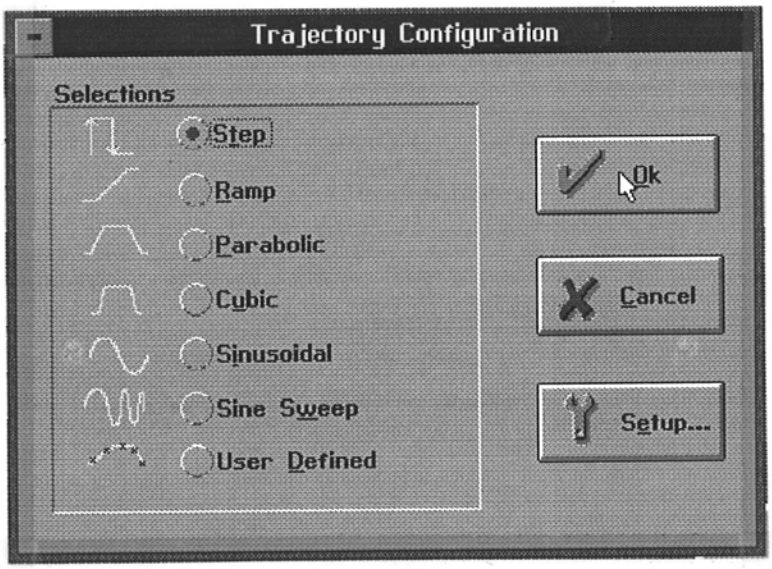

Figure 2.1-5. The Trajectory Configuration Dialog Box

By clicking the desired radio button followed by the Setup button one selects a specific dialog box for each trajectory.

The **Step** dialog box allows both **Closed Loop** and **Open Loop** step inputs. The **Closed Loop** step subjects the closed loop system to a step command and is always in units of displacement (counts, inches, degrees etc.). The step size is incremental from the current commanded position and is always forward and backward with a specified dwell time and a number of repetitions. There are range limits for the maximum step size and dwell time which are apparatus-specific. Out-of-bounds inputs will cause an error message indicating the acceptable parameter range. The

© ECP 1995, All rights reserved.

Open loop step subjects the plant to a step input and its units are always in volts. The maximum voltage is +/- 5 volts. Remember that a large open loop step size combined with a large open loop dwell time may result in an overspeed condition which is detected by the real-time controller. This condition will cause the open loop step test to be aborted and the **Controller Status** display in the Background screen to indicate **Limit Exceeded.** To run the test again you should reduce either or both the step size and the dwell time. Also note that for very large closed loop step sizes the **Limit Exceeded** condition may occur. This is generally true for all trajectories whose parameters have been selected such that they generate either too high a speed, too large a deflection , or a motor/amplifier over temperature (stalled) condition (see Section 2.3 on safety).

The **Ramp** dialog box allows a constant speed closed loop input command. The displacement size is incremental from the current commanded position and is always forward and backward with a specified speed, dwell time, and number of repetitions.

The **Parabolic** trajectory allows a constant acceleration (quadratic in position) closed loop input command. The displacement size is again incremental from the current position and is always forward and backward with a specified acceleration time, speed, dwell time and number of repetitions. Note that the total displacement time may be longer than acceleration/deceleration time depending on the selected displacement size and the speed input. In this case the parabolic acceleration/deceleration curves are joined by a constant velocity ramp.

The **Cubic** option allows a constant jerk (cubic in position) closed loop input command. As before, displacement size is incremental from the current position and is always forward and backward with a specified acceleration time, speed, dwell time and number of repetitions. Again, the total displacement time may be longer than acceleration/deceleration time depending on the selected displacement size and the speed input.

Note that the only difference between a parabolic trajectory and a cubic trajectory is that, during the acceleration/deceleration times a constant acceleration is commanded in a parabolic input and a constant jerk (linearly changing acceleration) is commanded in the cubic input. Of course, in a ramp input the commanded acceleration/deceleration is infinite at the ends of a commanded displacement stroke and zero at all other times during the motion.

The **Sinusoidal** dialog box provides for both **Closed loop** and **Open loop** sine wave inputs. The **Closed loop** option subjects the closed loop system to a sine wave command with amplitude in units of displacement (counts, inches, degrees etc.). The amplitude is incremental from the current commanded position. The user also specifies the frequency in Hz and the number of cycles. The **open loop** option specifies a sine wave input to the plant with amplitude in volts (at the DAC). The maximum voltage is +/- 5 volts. Remember that a large open loop amplitude combined with a low frequency may result in an overspeed condition which is detected by the

© ECP 1995, All rights reserved.

real-time controller. Similarly, even modest commanded amplitude near or at a resonance frequency can cause an excessive shaft deflection. These conditions will cause the open loop test to be aborted and the **Controller Status** display in the Background Screen to indicate **Limit Exceeded.** To run the test again you should reduce the amplitude size. Also note that very high frequency large amplitude closed loop tests or smaller commands near a resonant frequency result in the **Limit Exceeded** condition. In general, all trajectories which generate either too high a speed, too large a deflection, or excessive motor power will cause this condition – see the safety section 2.3.

The **Sine Sweep** dialog box supports both **Closed Loop** and **Open Loop** sine sweep inputs. The **Closed Loop** option specifies a sine sweep in units of displacement (counts, inches, degrees etc.). The amplitude is incremental from the current commanded position. The user also specifies the starting and the ending frequencies in Hz and the sweep time. The frequency increase is linear in time. For example a sweep from 0 Hz to 10 Hz in 10 seconds results in a one Hertz per second frequency increase. There is an apparatus-specific amplitude limit beyond which the Executive will not accept the inputs. The **Open Loop** sine sweep subjects the plant to a sine sweep input whose units are always in volts. The maximum voltage is +/- 5 V. Remember again that any of the following may result in a **Limit Exceeded** condition: large open loop amplitude size combined with a low frequency; high frequency large amplitude closed loop tests and operation near or through resonances.[1]

The **User Defined** trajectory dialog box provides the interface for the input of any form of trajectory created by the user. In order to make use of this feature the user must first create an ASCII text file with an extension "`.trj`" (e.g. "`random.trj`"). The content of this file should be as follows:

The first line should provide the number of points in the trajectory. The maximum number of points is limited to 100. This line should not contain any other information. The subsequent lines (up to 100) should contain the consecutive set points. For example to input twenty points equally spaced in distance one can create a file called "`example.trj`' using any text editor as follows

```
20
5
10
15
20
25
30
```

[1]Sweeping through resonances is very useful in visualizing the frequency response dynamics, but must be done at a sufficiently low input amplitude. When viewing open loop sine sweep results, it is often best to view velocity rather than position data to reduce position drift effects. By selecting a relatively long sweep period, the transient effects of freq. change are minimized and the true freq. response is best approximated.

© ECP 1995, All rights reserved.

```
35
40
45
50
55
60
65
70
75
80
85
90
95
100
```

Now the **segment time** which is a time between each consecutive point can be changed in the dialog box. For example if a 100 milliseconds segment time is selected, the above trajectory would take 2 seconds to complete (100*20=2000 ms). The minimum **segment time** is restricted to five milliseconds by the real-time controller. The format of any "`.trj`" file is the same regardless of whether it was created for an open loop test or a closed loop test. When the points of a "`.trj`" file are selected for an open loop test their units are assumed to be in DAC bits (+32767 = 9.99 V, -32767 = -10.0 V for the 16 bit DAC). For the closed loop tests the units are the current displacement units (counts, degrees, or radians). Obviously a user defined trajectory may also cause overspeed or over-deflection of the plant if the segment time is too short and the distance between the consecutive points is too long. Finally note that the closed loop user defined trajectories are cubic spline fitted in-between consecutive points by the real-time controller.

2.1.6.2 The **Disturbance Configuration** dialog box (see Figure 2.1.-5a) provides a selection of disturbance torque profiles for the disturbance motor. These are:

Viscous

Step

Sinusoidal (time)

Sinusoidal (theta)

User Defined

© ECP 1995, All rights reserved.

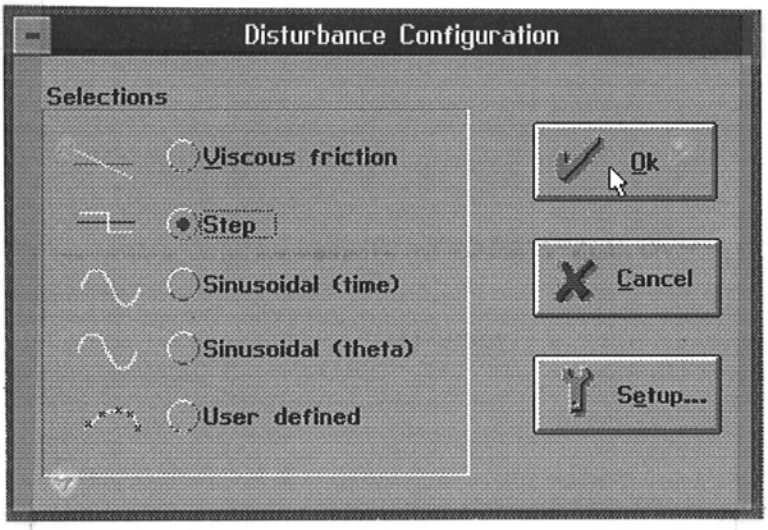

Figure 2.1-6. The Disturbance Configuration Dialog Box

By clicking on the desired radio button followed by **Setup**, one enters a dialog box for the disturbance profile selected.

The **Viscous Friction** window allows the user to input a disturbance signal proportional to the angular speed of the load shaft as sensed by the load encoder (encoder #2). The Amplitude entry is the magnitude of the viscous coefficient in units of volts/radian/second. Once the disturbance motor is calibrated this entry translates to a certain number of N-m/rad./sec. The user has a choice of implementing the viscous disturbance either directly through this dialog box or later prior to running a trajectory in the **Execute** dialog box. The maximum amplitude of viscous disturbance is limited to 10 volts/radian/second.

The **Step** disturbance dialog box allows the user to input the parameters for a square wave torque disturbance. The entries in this dialog box are identical to the **Open Loop Step** trajectory discussed above.

The **Sinusoidal (time)** dialog box allows the user to input a torque disturbance to the load shaft via the disturbance motor in the form of a sinusoidal function of time. The entries in this dialog box are identical to the **Open Loop Sinusoidal** trajectory discussed above.

The **Sinusoidal (theta)** dialog box allows the user to input a function of angle sine wave torque disturbance to the load shaft. This allows the simulation of cogging torque and or other spatially dependent disturbances. The amplitude of the disturbance torque is entered in terms of volts. The user must enter the number of cogging torque cycles per revolution of the load shaft (maximum number is limited to 100). In addition the period of time for which the cogging torque disturbance is required to be active must be specified.

© ECP 1995, All rights reserved.

The **User Defined** disturbance box provides the interface for the input of any form of disturbance trajectory created by the user. In order to make use of this feature the user must first create an ASCII text file with an extension `.trj` (e.g. `random.trj`). The format is identical to the **User Defined** trajectories discussed in the pervious section. Note that the maximum number of points are still 100 and the first entry must be the number of points in a particular file. The units of inputs are in DAC bits (for our 16-bit bipolar DACs: +32767= 9.999 volts and -32768 = -10.0 volts) After the calibration of the disturbance motor, the exact ratio between a DAC bit and the actual disturbance torque on the load shaft may be determined.

During the active period of any of the above disturbance profiles the **Disturbance Status** would indicate "Active". It is, however, possible that the disturbance motor enters the "**Limit Exceeded**" condition either as a result of over current or over speed. To return to the "Active" condition, the user must modify the disturbance parameters and implement the disturbance torque again via the **Execute** dialog box (note that the **Viscous** friction disturbance may also be implemented within its own dialog box).

The following rules govern disturbance implementation:

1. You must have selected a disturbance (and verified its parameters) under the **Disturbance Configuration** dialog box and checked "**Include XXX** (any of the above) **Disturbance**" when Executing a trajectory.
2. The disturbance will only be active while the trajectory is executing. If the trajectory terminated before the specified disturbance duration, the disturbance will also terminate.
3. The only exception to rules 1 and 2 is viscous damping which may be invoked either via its own dialog box (under **Disturbance Configuration**) or when a trajectory is executed (by checking **Include Viscous Friction** before Executing). Viscous friction may run simultaneously with other disturbances. Note that **Viscous Friction**, if implemented, will remain in effect until either it is removed in its own dialog box, or a new trajectory is run without checking **Include Viscous Friction**.

2.1.6.3 The **Execute** dialog box (see Figure 2.1-7) is entered after a trajectory is selected. Here the user has a choice of including viscous friction and another additional disturbance with a set of parameters previously selected within the appropriate dialog box. The user also has a choice of sampling the data by clicking the **Sample Data** check box or not sampling data by clearing this check box (for the details of data gathering see Section 2.1.7.1 **Setup Data Acquisition**). Once the choice is made as to whether to sample data, the user normally selects **Run**. The specified trajectory will start to be executed by the real-time Controller. Once finished, and provided the **Sample Data** box was checked, the data will be uploaded back into the Executive for plotting, saving and exporting. At any time during the execution of the trajectory or during the uploading of data the process may be terminated by clicking on the **Abort** button. Finally, if the disturbance

© ECP 1995, All rights reserved.

torque profile has a time period longer than the selected trajectory period, it will be terminated at the end of the trajectory profile.

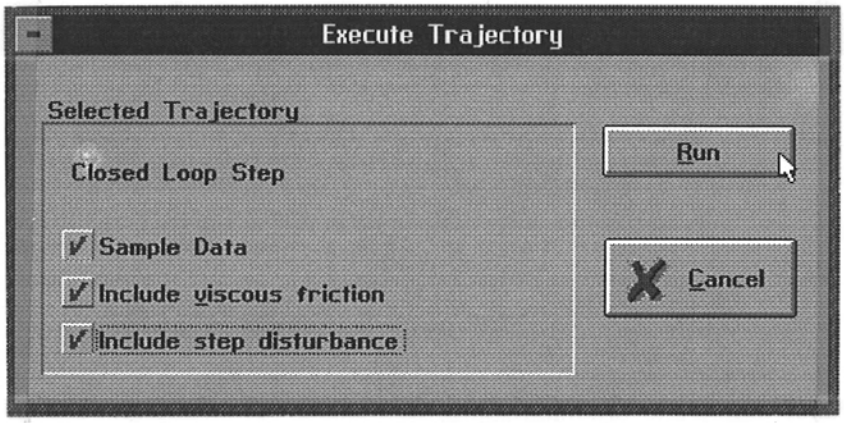

Figure 2.1-7. The Execute Dialog Box

2.1.7 **Data** Menu

The **Data** menu contains the following pull-down options

Setup Data Acquisition
Upload Data
Export Raw Data

2.1.7.1 **Setup Data Acquisition** allows the user to select one or more of the following data items to be collected at a chosen multiple of the servo loop closure sampling period while running any of the trajectories mentioned above – see Figures 2.1-8 and 4.1-1:

Commanded Position
Encoder 1 Position
Encoder 2 Position
Encoder 3 Position
Control Effort (output to the servo loop or the open loop command)
Disturbance Effort (disturbance motor command)
Node A (input to the H polynomial in the Generalized Control Algorithm)
Node B (input to the E polynomial in the Generalized Control Algorithm)
Node C (output of the 1/G polynomial in the Generalized Control Algorithm)

© ECP 1995, All rights reserved.

Node D (output of the feedforward controller which is added to the node C value to form the combined regulatory and tracking controller).

In this dialog box the user adds or deletes any of the above items by first selecting the item, then clicking on the **Add Item** or **Delete Item** button. The user must also select the data gather sampling period (in multiples of the servo period). For example, if the sample time (T_S in the **Setup Control Algorithm**) is 0.00442 seconds and you choose 5 for your gather period here, then the selected data will be gathered once every fifth sample or once every 0.0221 seconds. Usually for trajectories with fast frequency contents (e.g. Step, or high frequency Sine Sweep), one should choose a low data gather period. On the other hand, one should avoid gathering more often (or more data types) than needed since the upload and plotting routines become slower as the data size increase.

2.1.7.2 Selecting **Upload Data** allows any previously gathered data to be uploaded into the Executive. This feature is useful when one wishes to switch and compare between plotting previously saved raw data and the currently gathered data. Remember that the data is automatically uploaded into the executive whenever a trajectory is executed and data acquisition is enabled. However, once a previously saved raw data file is loaded into the Executive, the currently gathered data is overwritten. Now the **Upload Data** feature allows the user to bring the overwritten data back from the real-time controller into the Executive.

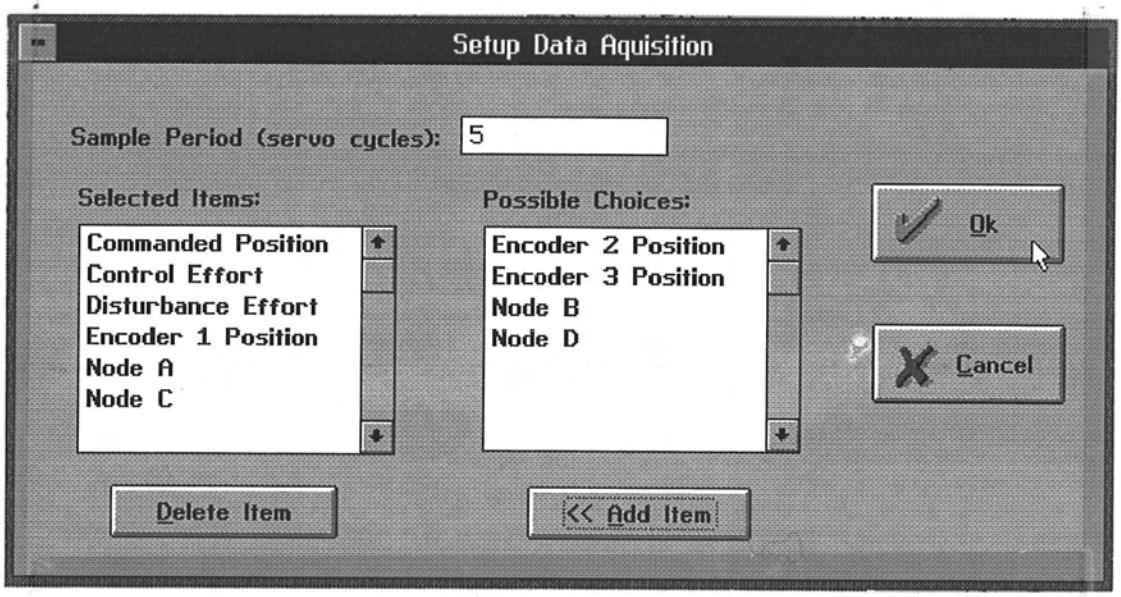

Figure 2.1-8. The Setup Data Acquisition Dialog Box

© ECP 1995, All rights reserved.

2.1.7.3 The **Export Raw Data** function allows the user to save the currently acquired data in a text file in a format suitable for reviewing, editing, or exporting to other engineering/scientific packages such as Matlab®.[1] The first line is a text header labeling the columns followed by bracketed rows of data items gathered. The user may choose the file name with a default extension of "`.txt`" (e.g. `lqrstep.txt`). The first column in the file is sample number, the next is time, and the remaining ones are the acquired variable values. Any text editor may be used to view and/or edit this file.

2.1.8 **Plotting** Menu

The **Plotting** menu contains the following pull-down options

Setup Plot
Plot Data
Axis Scaling
Print Data
Load Plot Data
Save Plot Data
Close Window

2.1.8.1 The **Setup Plot** dialog box (see Figure 2.1-9) allows up to four acquired data items to be plotted simultaneously – two items using the left vertical axis units, and two using the right vertical axis units[2]. More than four items cannot appear on the same plot. Simply click on the item you wish to add to the left or the right axis and the click on the **Add to Left Axis** or **Add to Right Axis** buttons. You must select at least one item for the left axis before plotting is allowed – i.e. if only one item is plotted, it must be on the left axis. You may also change the plot title from the default one in this dialog box.

Items for comparison should appear on the same axis (e.g. commanded vs. encoder position) to ensure the same axis scaling and bias. Items of dissimilar scaling or bias (e.g. control effort in volts and position in counts) should be placed on different axes.

[1]The bracketed rows end in semicolons so that the entire file may be read as an array in Matlab by running it as a script once the header is stripped i.e. the script should be: <array name>= [exported data file]. Variable values over time are the columns of this array; the rows are the variable value set at successive sample numbers.

[2]You will see in the box plotting selections of velocity and acceleration for the position variables acquired. These are automatically generated during the uploading process.

© ECP 1995, All rights reserved.

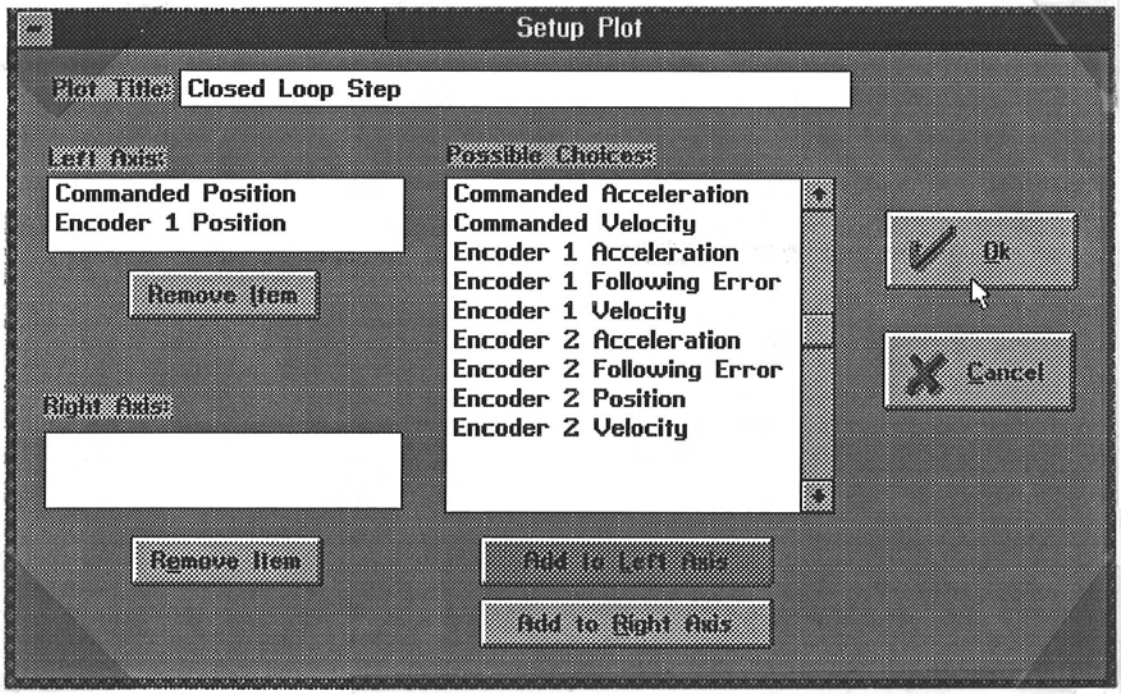

Figure 2.1-9 The Setup Plot Dialog Box (Shows case where data was gathered for encoders 1 & 2 and commanded input. Up to 20 variables may be made available for plotting)

2.1.8.2 **Plot Data** generates a plot of the selected items. By clicking on the upper blue border of the plots , they may dragged across the screen. The view size may be maximized by clicking on the up arrow of the upper right hand corner. It can also be shrunk to an icon by clicking on the down arrow of the upper left hand corner. This function is very useful for comparing several graphs. It can be expanded back to the full size at any time by double-clicking on the icon. Also more than one plot can be cascaded on the Background Screen[1]. By clicking on any point within the area of the desired plot it will appear over the others. Plots may be arbitrarily shaped by moving the cursor to the lower right hand corner to the position where it becomes a double-arrow . The corner may then be "dragged" to reshape the plot. Finally by clicking on the top left hand corner of a plot screen one can close the plot window.

2.1.8.3 The **Axis Scaling** provides for scaling of the horizontal and vertical axes for closer data inspection – both visually and for printing. Grid lines may be selected or de selected and data points may be labeled.

[1]To avoid system slow-down, the number of open plots on the background screen should not become excessive.

© ECP 1995, All rights reserved.

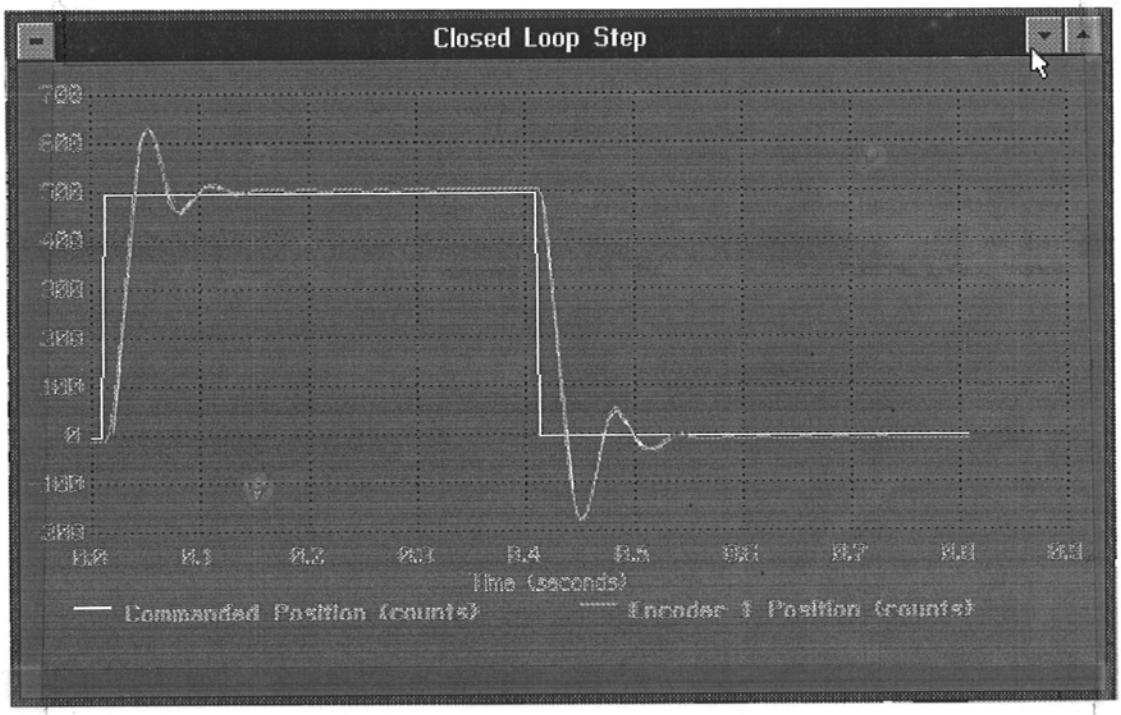

Figure 2.1-10. A Typical Plot Window

2.1.8.4 The **Print Data** option allows the user to provide a hard copy of the selected plot on either an Epson compatible dot matrix printer or a HP Laserjet compatible printer.

2.18.5 The **Load Plot Data** dialog box enables the user to bring into the Executive previously saved "`.plt`" plot files. Note that such files are not stored in a format suitable for use by other programs. The "`.plt`" plot files contain the sampling period of the previously saved data. As a result, after plotting any previously saved plot files and before running a trajectory, you should check the servo loop sampling period **Ts** in the **Setup Control Algorithm** dialog box. If this number has been changed, then correct it. Also, check the data gathering sampling period in the **Data Acquisition** dialog box, this too may be different and need correction.

2.1.8.6 The **Save Plot Data** dialog box enables the user to save as a plot file of the data gathered by the controller. The default extension is "`.plt`" under the current directory. Note that "`.plt`" files are not saved in a format suitable for use by other programs. For this purpose the user must use the **Export Raw Data** option of the **Data** menu.

2.1.8.7 The **Close Window** option allows the currently marked plot window to close. This can also be done by clicking on the top left hand corner of the plot window.

© ECP 1995, All rights reserved.

2.1.9 Utility Menu

The **Utility** menu contains the following pull-down options:

Configure Auxiliary DACs
Jog Position
Zero Position
Reset Controller
Rephase Motor
Down Load Controller Personality File

2.1.9.1 The **Configure Auxiliary DACs** dialog box (see Figure 2.1-11) enables the user to select various items for analog output on the two analog channels in front of the ECP Control Box. Using equipment such as an oscilloscope, plotter, or spectrum analyzer the user may inspect the following items continuously in real time:

Commanded Position
Encoder 1 Position
Encoder 2 Position
Encoder 3 Position
Control Effort
Node A
Node B
Node C
Node E

The scale factor which divides the item can be less than 1 (one). The DACs analog output is in the range of +/- 10 volts corresponding to +32767 to -32768 counts. For example to output the commanded position for a sine sweep of amplitude 2000 counts you should choose the scale factor to be 0.061 (2000/32767=0.061) This gives close to full +/- 10 volt reading on the analog outputs. In contrast, if the numerical value of an item is greater than +/- 32767 counts, for full scale reading, you must choose a scale factor of greater than one. Note that the above items are always in counts (not degrees or radians) within the real time controller and since the DAC's are 16-bit wide, + 32767 counts corresponds to +9.999 volts, and -32768 counts corresponds to -10 volts.

© ECP 1995, All rights reserved.

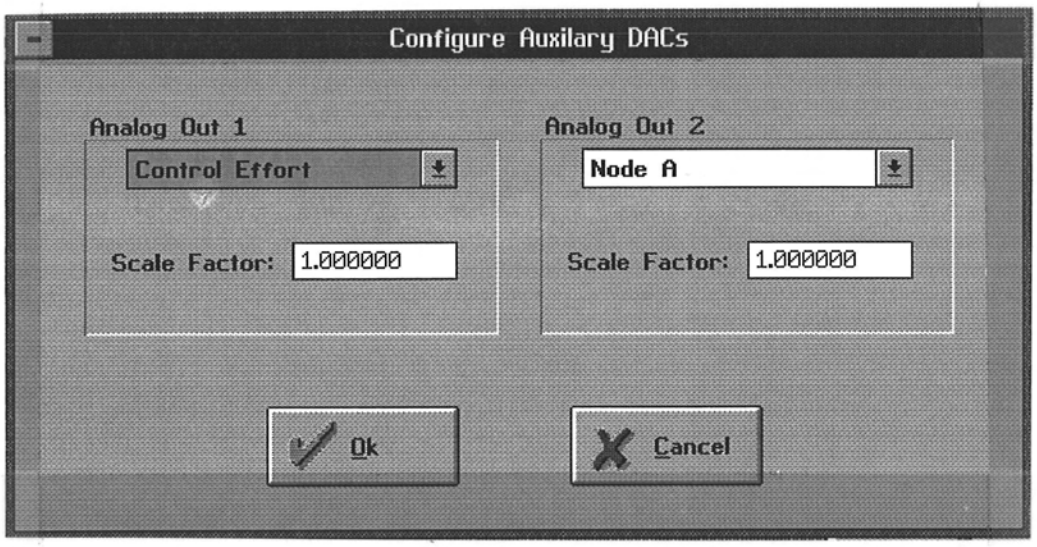

Figure 2.1-11. The Configure Auxiliary DACs Dialog Box

2.1.9.2 The **Jog Position** option enables the user to move the mechanism to a different commanded position. In contrast to displacements executed under the **Trajectory** dialog box, during a **Jog** command no data is acquired for plotting purposes. Since this motion is effected via the current controller, one can only jog under closed loop control with a stable controller. By selecting the appropriate radio button either incremental and absolute displacements may be carried out. The jogging feature allows the user to return to a known position after the execution of the various forms of open and closed loop trajectories.

2.1.9.3 The **Zero Position** option enables the user to reinitialize the current position as the zero position. Note that if following errors exists, then the actual positions may be other than zero even though the commanded position is at zero (since the action is similar to commanding an instantaneous zero set point, a sudden small jerk in position may occur).

2.1.9.4 The **Reset Controller** option allows the user to reset the real-time controller. Upon Power up and after a reset activity, the loop is closed with zero gains and there it behaves in the same way as in the open loop state with zero control effort. Thus the user should be aware that even though the **Control Loop Status** indicates "closed loop", all of the gains are zeroed after a Reset. In order to implement (or re implement) a controller you must go to the **Setup Control Algorithm** box.

© ECP 1995, All rights reserved.

2.1.9.5 The **Rephase Motor** option enables a user to simply rephase a brushless motor's commutation phase angle. This feature is not used by the Model 220 system since its motors use absolute sensors for commutation.

2.1.9.6 The **Download Controller Personality File** is an option which should not be used by most users. In a case where the real-time controller irrecoverably malfunctions, and after consulting ECP, a user may download the personality file if a ".pmc" file exists. In the case of Model 220, this file is named "m220xxx.pmc". Note that this downloading process takes a few seconds.

2.2 Electromechanical Plant

2.2.1 Design Description

The plant, shown in Figure 2.2-1 is designed to emulate a broad range of typical servo control applications. The Model 220 apparatus consists of a *drive motor* (servo actuator) which is coupled via a timing belt to a *drive disk* with variable inertia. Another timing belt connects the drive disk to the *speed reduction (SR)* assembly while a third belt completes the drive train to the *load disk.* The load and drive disks have variable inertia which may be adjusted by moving (or removing) brass weights. Speed reduction is adjusted by interchangeable belt pulleys in the SR assembly. Backlash may be introduced through a mechanism incorporated in the SR assembly, and flexibility may be introduced by an elastic belt[1] between the SR assembly and the drive disk. The drive disk moves one-for-one with the drive motor so that its inertia may be thought of as being *collocated* with the motor. The load inertia however will rotate at a different speed than the drive motor due to the speed reduction. Also, drive flexibility and/or backlash may exist between it and the drive motor and hence its inertia is considered to be *noncollocated* with the motors.

A disturbance motor connects to the load disk via a 4:1 speed reduction and is used to emulate viscous friction and disturbances at the plant output. A brake below the load disk may be used to introduce Coulomb friction. Thus friction, disturbances, backlash, and flexibility may all be introduced in a controlled manner. These effects represent non-ideal conditions that are present to some degree in virtually all physically realizable electromechanical systems.

All rotating shafts of the mechanism are supported by precision ball bearings. Needle bearings in the SR assembly provide low friction backlash motion (when backlash is desired).

[1]Either a "rigid" or flexible belt may be used between the SR assembly and the load disk.

© ECP 1995, All rights reserved.

High resolution incremental encoders[1] couple directly to the drive (θ_1) and load (θ_2) disks providing position (and derived rate) feedback. The drive and disturbance motors are electrically driven by servo amplifiers and power supplies in the Controller Box. The encoders are routed through the Controller box to interface directly with the DSP board via a gate array that converts their pulse signals to numerical values[2].

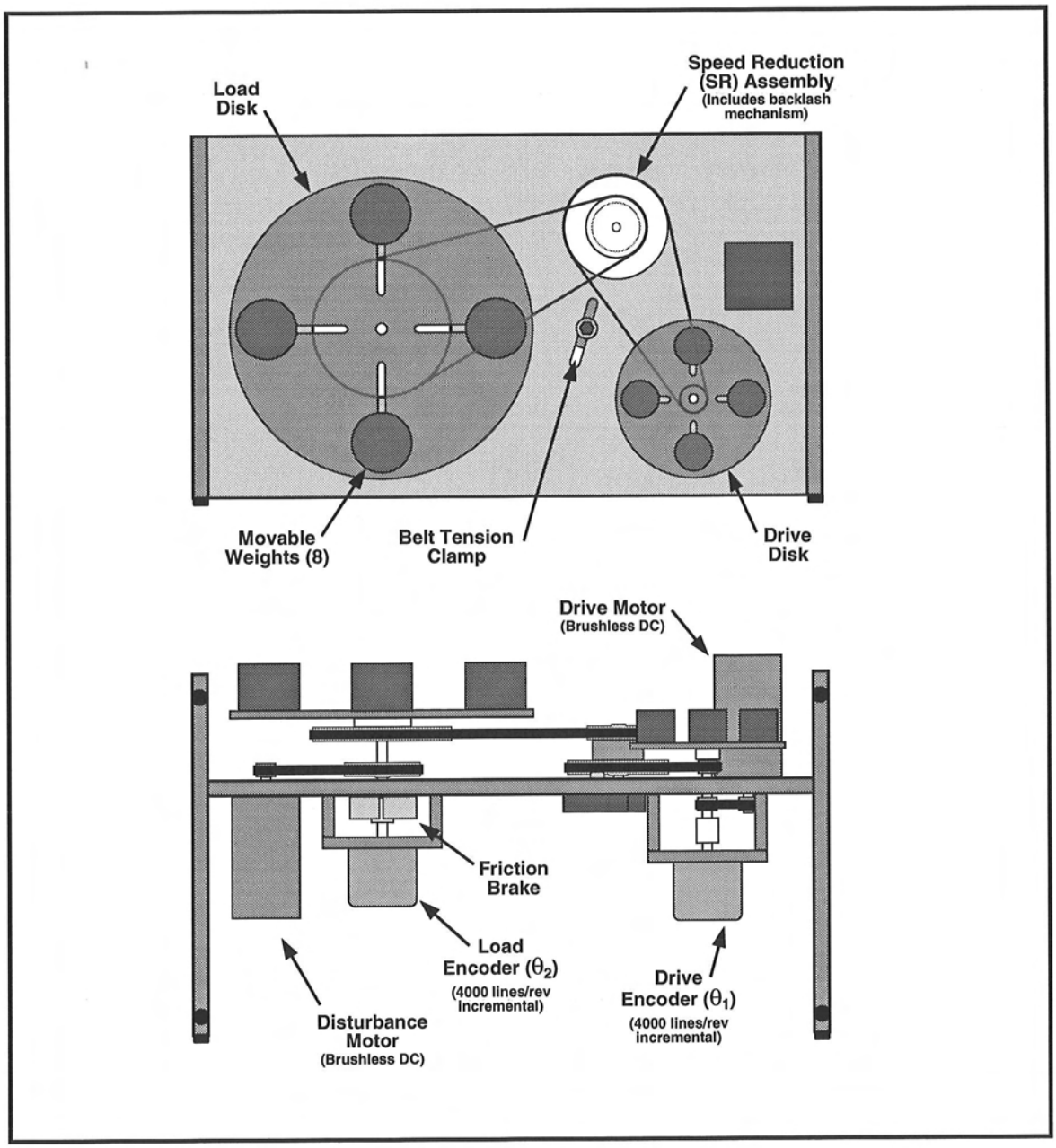

Figure 2.2-1. Emulator Apparatus

[1]4000 lines per revolution with 4X hardware interpolation provide 16,000 count per rev. resolution for control.

[2]See Chapter 4 for a description of component functionality (e.g. actuators and sensors) and I/O processing (e.g. motor commutation and encoder pulse counting)

© ECP 1995, All rights reserved.

2.2.2 Instructions for Changing Configurations

Important notices:

1. **Disconnect power to the electrical Controller Box prior to performing any procedure in this section.**
2. **Replace and secure the plexiglass safety cover immediately after completing all procedures.**

2.2.2.1 Changing Pulleys & Gear Ratio[1] (Refer to Figure 2.2-2)

Gear ratios are changed via selection of the sizes of the upper and lower pulleys in the SR assembly. Fixed pulleys at the drive and inertia disks have 12 and 72 teeth respectively so that in combination with the interchangeable pulleys, end-to-end gear ratios ranging from 1.5:1 to 24:1 are achieved. Table 2.2-1 gives the pulley combinations to establish a desired ratio and identifies the recommended timing belts for each combination. Once the user becomes familiar with the system, the proper belt lengths may generally be seen by inspection and gear ratios (end-to-end) resulting from the SR gear selection become obvious.

1. Remove the existing pulleys by first loosening the belt tension clamp screw to allow the belts to become slack. Loosen the clamp screw and the backlash adjustment screw. Lift the SR assembly off the idler shaft and unscrew the upper and lower pulley attach screws to free the existing pulleys.
2. Replace the new pulleys in reverse order of step 1. Be sure that the bearing contact boss is facing downward in the lower pulley and upward in the upper pulley and that the backlash contact boss on the lower backlash member is facing upward (away from the lower pulley). Also be sure that the backlash adjustment screw is tightened (only light torque is necessary – do not over tighten) unless backlash effects are desired.

2.2.2.2 Changing & Tightening Belts

1. Refer to Table 2.2-1 for proper belt selection. If the lower pulley is unchanged then the existing lower belt should be the correct one.
2. Fit the lower then upper belts over their respective pulleys. Simultaneously tighten both belts by applying 5-10 pounds (25-50 N.) of force in the direction shown in Figure 5.2-2. You may need to apply the force in an off-center direction to adequately tension both belts[2]. Tighten the belt tension clamp screw while applying the force.
3. Manually rotate the disks for several rotations of the load disk and observe the belts. They should be just taught enough so that their nominally straight lengths do not further visibly straighten (they should already be straight) when the load and drive disks are manually counter-

[1]We apply the term "gear ratio" due to its common usage even though the speed reduction is effected by pulleys and belts.

[2]Precise measurement of the force is not necessary.

© ECP 1995, All rights reserved.

rotated. Belts that are too slack add flexibility and belts that are too tight add excess friction – both generally unwanted.

2.2.2.3 Changing Brass Weights

Instructions for changing or relocating the brass weights for the drive and load inertia disks are given in Figure 2.2-3.

2.2.2.4 Installing Flexible Drive Belt

It is recommended that the flexible drive belts be used with the 36 tooth pulley only (I.e. the 36 tooth pulley in the upper position in the SR assembly.) The flexible belt should be in place only for the duration of active testing. Prolonged periods (more than several hours) may permanently stretch the belts.

1. With the upper belt (from the SR assembly to the load disk) removed tighten the lower belt – see "Changing & Tightening Belts" above. Since the upper belt is removed, the SR assembly is free to move for a limited range along a circular arc about the drive disk. It is usually preferred to position the SR assembly as close as possible to the load disk.[1]
2. Stretch the flexible belt to fit it past the load disk and around the load disk pulley. Stretch the belt and begin to fit it about the 36 tooth pulley. By rotating the pulley with one section of the belt on the pulley edge, the belt is easily fed into place. The result should be as shown in Figure 2.2-4.

2.2.2.5 Adjusting Backlash

Backlash is adjusted (0 to 20 deg @ the SR) via the backlash adjustment screw (see Figure 2.2-2). You may measure the amount of backlash by temporarily tightening the friction clamp below the load disk and manually rotating the drive disk back and forth while noting the encoder readings at each extreme.[2] You must have the "feedback connector connected to the control box and the ECP executive program operating. Drive power to the apparatus however must be disconnected. Be certain that you loosen the friction clamp before proceeding

[1]If the flexible belt is found to slip during later testing, the SR assembly may be positioned further from the load disk to increase the flexible belt tension.

[2]Note here that 1 disk revolution = 16,000 encoder counts.

© ECP 1995, All rights reserved.

2.2.2.6 Adjusting Friction Brake

Coulomb friction is adjusted via the tightening screw in the friction brake. The brake should not be set greater than 1 N-m to avoid excessive friction[1] and hence excessive drive current[2] (under subsequent closed loop control) which can lead to amplifier burn-out.

Note:

1. Always move the drive disk manually prior to operation to verify that excessive brake torque does not exist.
2. Always loosen tightening screw on friction brake immediately after performing any needed tests. The brake should be used infrequently.

[1]This is approximately the torque produced by two 0.5 kg brass weights at a 10 cm radius under the force of gravity when the mechanism is placed in the disk-vertical position. The two weights should be horizontally oriented from the load disk axle.

[2]While there are safety checks embedded in the control software, it is bad practice to leave the motor stalled or with significant steady state load such as that required to overcome high friction. ECP is not responsible for equipment failures resulting from excessive brake friction.

© ECP 1995, All rights reserved.

Table 2.2-1. Pulley and Belt Configurations For Various Gear Ratios

Bottom Pulley (No. of Teeth)	Top Pulley (No. of Teeth)	Gear Ratio (End-to-end)	Bottom Belt* (Drive to SA ass'y)	Top Belt* (SA ass'y to load)
18	24	4.5:1	140	250
	36	3:1	140	260
	72	1.5:1	140	300
24	18	8:1	140	250
	36	4:1	140	260
	72	2:1	140	300
36	18	12:1	150	250
	24	9:1	150	250
	72	3:1	150	300
72	18	24:1	200	250
	24	18:1	200	250
	36	12:1	200	260

* Numbers given are twice the number of belt teeth and are equal to the inner length of the flattened belt divided by 0.050 inches. These numbers appear on the belts (among other markings). E.g. a marking "250XLO37" corresponds to "250" in this table.

© ECP 1995, All rights reserved.

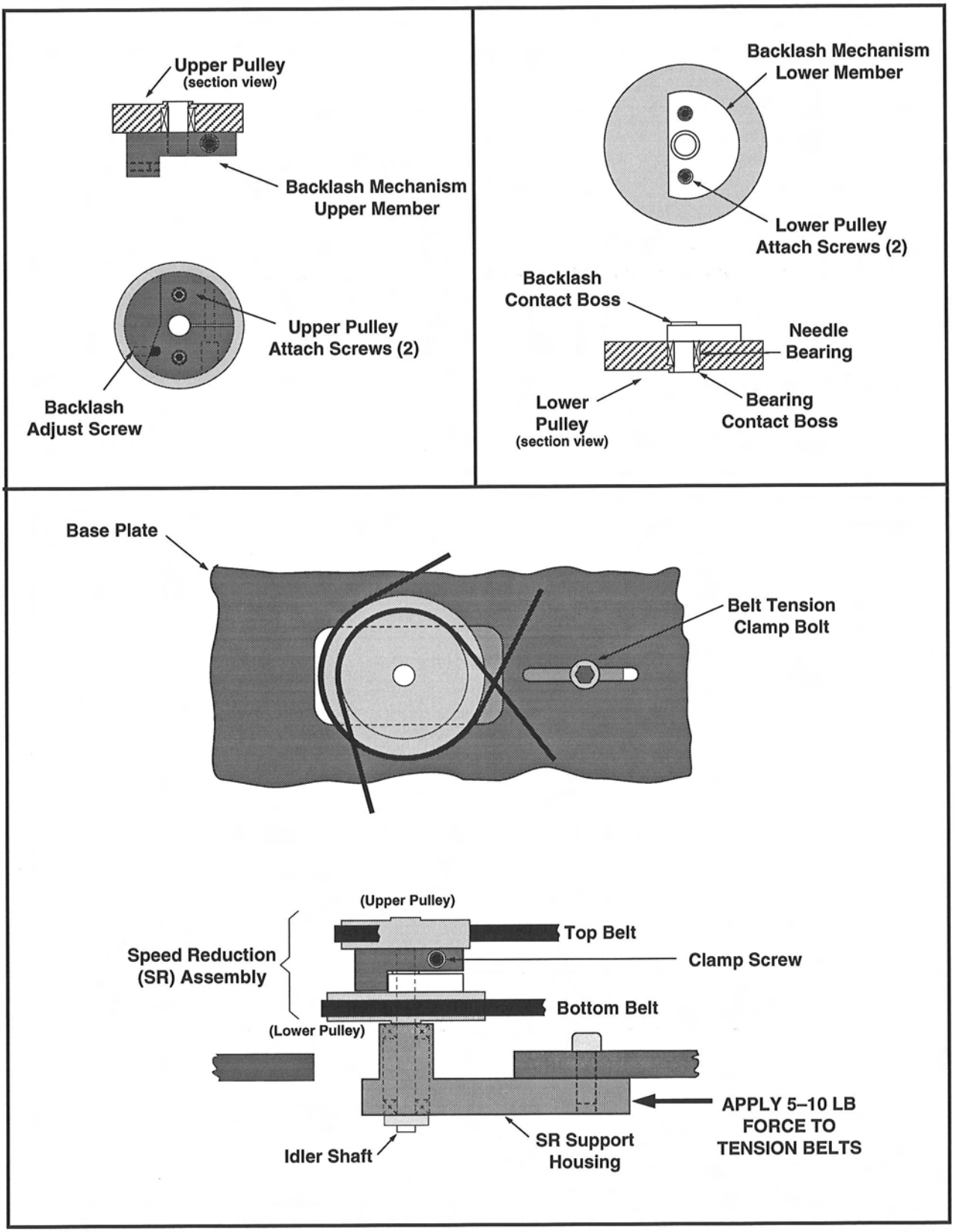

Figure 2.2-2. Components Used In Changing Gear Ratio & Adjusting Backlash

© ECP 1995, All rights reserved.

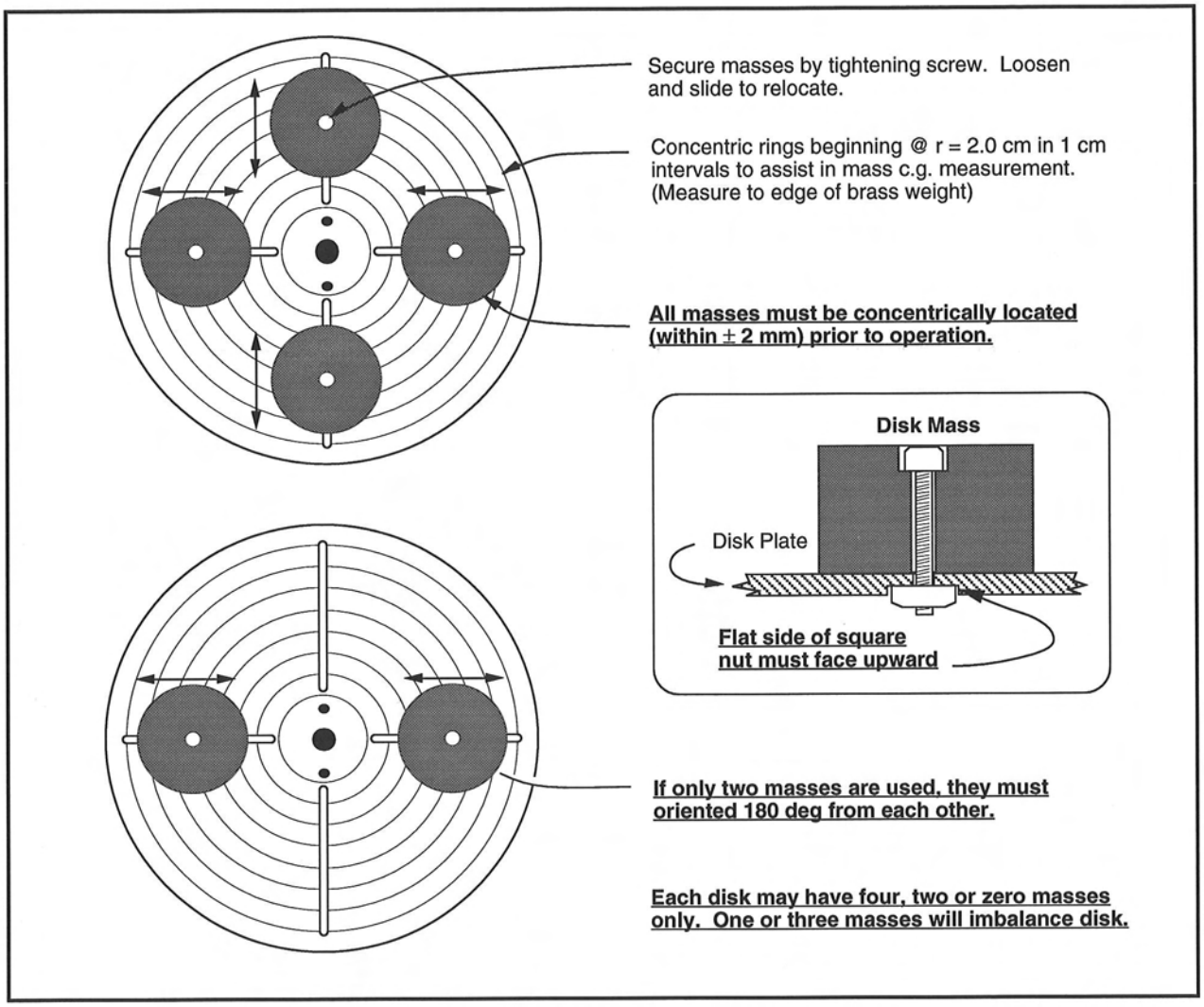

Figure 2.2-3. Guidelines For Changing Or Adjusting Disk Masses

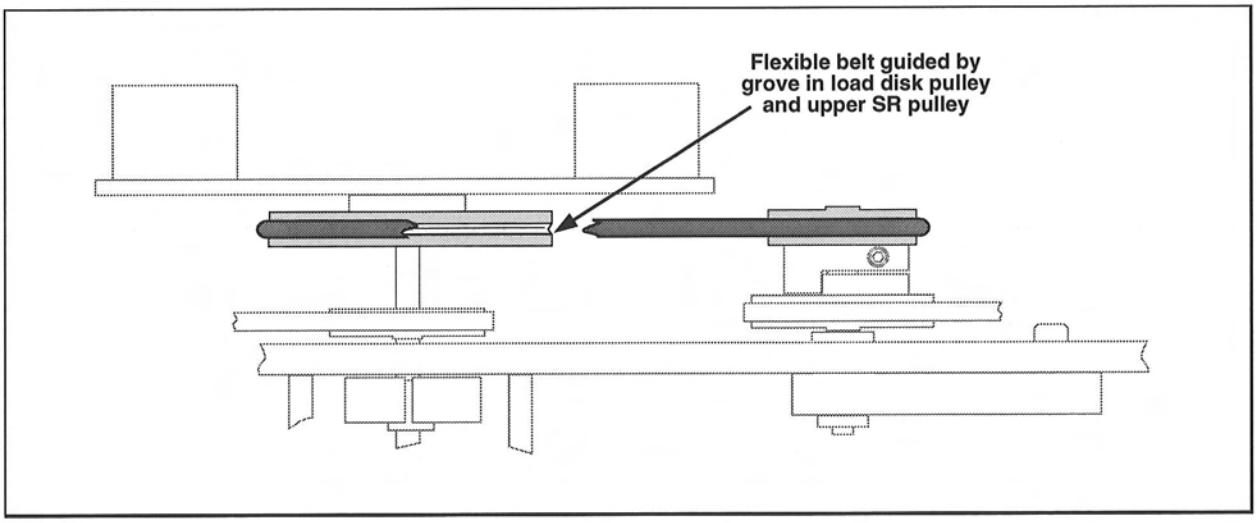

Figure 2.2-4. Installing Flexible Drive Belt

© ECP 1995, All rights reserved.

2.3 Safety

The following are safety features of the system and cautions regarding its operation. This section must be read and understood by all users prior to operating the system. If any material in this section is not clear to the reader, contact ECP for clarification before operating the system.

Important Notice: In the event of an emergency, control effort should be immediately discontinued by pressing the red "OFF" button on front of the control box.

2.3.1 Hardware

A relay circuit is installed within the Control Box which automatically turns off power to the Box whenever the real-time Controller (within the PC) is turned on or off. Thus for the PC bus version[1] of the real-time Controller the user should turn on the computer prior to pressing on the black ON switch. This feature is implemented to prevent uncontrolled motor response during the transient power on/off periods. The power to the Control Box may be turned off at any time by pressing the red OFF switch.

Although not recommended, it will not damage the hardware to apply power to the Control-Box even when the PC is turned off. However, doing so does not result in motor activation as the motor current amplifier will be disabled. The *amplifier enable* signal input to the Control Box is connected to the real-time Controller via the 60-pin flat ribbon cable. This input operates in a normally closed mode. When power to the real-time Controller is off, this input becomes open which in turn disables the motor amplifier.

The recommended procedure for **start up** is as follows:

First : Turn on the PC with the real-time Controller installed in it.
Second: Turn on the power to Control Box (press on the black switch).

You must execute the third step (rephasing) every time the PC bus version of the real-time Controller is powered on and (due to a software safety feature) whenever the Executive program is entered.

The recommended **shut down** procedure is:

First: Turn off the power to the Control Box.
Second: Turn off the PC..

[1]The majority of this section (2.3.1) pertains to the PC bus installation of the real-time controller. For the controller box/RS-232 version, the control box should generally be powered on before entering the executive software.

© ECP 1995, All rights reserved.

FUSES: There are two 3.0A 120V slow blow fuses within the Control Box. One of them is housed at the back of the Control Box next to the power cord plug. The second one is inside the box next to the large blue colored capacitor.

2.3.2 Software

The **Limit Exceeded** indicator of the **Controller Status** display indicates either one or more of the following conditions have occurred:

Over deflection of the flexible shaft.
Over speed of the motor.
Excessive drive motor power

The real-time Controller continuously monitors the above limiting conditions in its background routine (intervals of time in-between higher priority tasks). When one if these conditions occurs, the real-time Controller opens up the control loop with a zero torque command sent to the actuator. The **Limit Exceeded** indicator stays on until a new set of (stabilizing) control gains are downloaded to the real-time Controller via the **Implement Algorithm** button of the **Setup Control Algorithm** dialog box, or a new trajectory is executed via the **Command** menu. Obviously the new trajectory must have parameters that do not cause the **Limit Exceeded** condition.

The **Limit Exceeded** indicator of the **Disturbance Motor Status** display indicates either one or both of the following conditions have occurred:

Over speed of the disturbance motor.
Excessive disturbance motor power

Also included is a *watch-dog timer*. This subsystem provides a fail-safe shutdown to guard against software malfunction and under-voltage conditions. The use of the watch-dog timer is transparent to the user. This shutdown condition turns on the red LED on the real-time Controller card, and will cause the control box to power down automatically. You may need to cycle the power to the PC in order to reinitialize the real-time Controller should a watch-dog timer shutdown occur.

2.3.3 Safety Checking The Controller

While it should generally be avoided, in some cases it is instructive or useful to manually contact the mechanism when a controller is active. This should always be done with caution and never in such a way that clothing or hair may be caught in the apparatus. By staying clear of the mechanism when it is moving or when a trajectory has been commanded, the risk of injury is greatly reduced.

© ECP 1995, All rights reserved.

Being motionless, however, is not sufficient to assure the system is safe to contact. In some cases an unstable controller may have been implemented but the system may remains motionless until perturbed – then it could react violently.

In order to eliminate the risk of injury in such an event, you should always safety check the controller prior to physically contacting the system. This is done by lightly grasping a slender, light object with no sharp edges (e.g. a ruler without sharp edges or an unsharpened pencil) and using it to slowly move either the load or drive disk from side to side. Keep hands clear of the mechanism while doing this and apply only light force to the disk. If the disk does not spin up or oscillate then it may be manually contacted – but with caution. This procedure must be repeated whenever any user interaction with the system occurs (either via the Executive Program of the Controller Box) if the mechanism is to be physically contacted again.

2.3.4 Warnings

WARNING #1: Stay clear of and do not touch any part of the mechanism while it is moving, while a trajectory has been commanded, or before the active controller has been safety checked – see Section 2.3.3.

WARNING #2: The following apply at all times except when motor drive power is disconnected (consult ECP if uncertain as to how to disconnect drive power):

a) Stay clear of the mechanism while wearing loose clothing (e.g. ties, scarves and loose sleeves) and when hair is not kept close to the head.

b) Keep head and face well clear of the mechanism.

WARNING #3: Verify that the masses and inertia disks are secured per section 2.2 of this manual prior to powering up the Control Box or transporting the mechanism.

WARNING #4: Do not take the cover off or physically touch the interior of the Control Box unless its power cord is unplugged (first press the "Off" button on the front panel) and the PC is unpowered or disconnected.

WARNING #5: The power cord must be removed from the box prior to the replacement of any fuses.

© ECP 1995, All rights reserved.

3. Start-up & Self-guided Demonstration

This chapter provides an orientation "tour" of the system for the first time user. In Section 3.1 certain hardware verification steps are carried out. In Section 3.2 a self-guided demonstration is provided to quickly orient the user with key system operations and Executive program functions. Finally, in Section 3.3, certain system behaviors which may be nonintuitive to a first time user are pointed out .

3.1 Hardware Setup Verification

At this stage it is assumed that

a) The ECP Executive program has been successfully installed on the PC's hard disk (see Section 2.1.2).

b) The actual printed circuit board (the real-time Controller) has been correctly inserted into an empty slot of the PC's extension (ISA) bus (this applies to the PC bus version only).

c) The supplied 60-pin flat cable is connected between the J11 connector (the 60-pin connector) of the real-time Controller and the JMACH connector of the Control Box[1].

d) The other two supplied cables are connected between the Control Box and the Emulator apparatus;

e) The apparatus has the two disks securely installed with no weights fastened to any disks and all clamps removed. (i.e. the plant should be set up as shown in Figure 2.2-1 except with no masses on the disks. This is the configuration the mechanism is shipped in.)

f) You have read the safety Section 2.3. All users must read and understand that section before proceeding.

Please check the cables again for proper connections.

[1]This applies to the PC-bus installation only. For the controller in the Control Box, the RS-232 cable must be connected between the Control Box and the PC.

© ECP 1995, All rights reserved.

3.1.1 Hardware Verification (For PC-bus Installation)

Step 1: Switch off power to both the PC and the Control Box.

Step 2: With power still switched off to the Control Box, switch the PC power on. Enter the ECP program by typing ">ECP" in the appropriate directory. You should see the Background Screen (see Section 2.1.3). Gently rotate the drive or load disk by hand. You should observe some following errors and changes in encoder counts. The **Control Loop Status** should indicate "**CLOSED**" and the **Controller Status** should indicate "**ACTIVE**". If this is the case skip Step 3 and go to Step 4.

Step 3: If the ECP program cannot find the real-time Controller (a pop-up message will notify you if this is the case), try the **Communication** dialog box under the **Setup** menu. Select PC-bus at address 528, and click on the test button. If the real-time Controller is still not found, try increasing the time-out in 20 ms increments up to a maximum of 300 ms. If this doesn't correct the problem, switch off power to your PC and then take its cover off. With the cover removed check again for the proper insertion of the Controller card. Switch the power on again and observe the two LED lights on the Controller card. If the green LED comes on all is well; if the red LED is illuminated, you should contact ECP for further instructions. If the green LED comes on, turn off power to your PC, replace the cover and turn the power back on again. Now go back to the ECP program and you should see the positions change as you gently rotate the disks.

Step 4: Make sure that you can rotate disks freely. Now connect the power cord to the Control Box and press the black "ON" button to turn on the power to the Control Box. You should notice the green power indicator LED lit, but the motor should remain in a disabled state. Do not touch the disks whenever power is applied to the Control Box since there is a potential for uncontrolled motion of the disks (see the warnings in Section 2.3) unless the controller has been safety checked.

This completes the hardware verification procedure. Please refer again to Section 2.3 for future start up and shut down procedures.

© ECP 1995, All rights reserved.

3.2 Demonstration of ECP Executive Program

This section walks the user through the salient functions of the system. By following the instructions below you will actually implement a controller, maneuver the system through various trajectories, and acquire and plot data. The procedures given in this section are specific to the Model 220 system.

Step 1: Loading A Configuration File. With the power to the Control box turned off, enter the ECP Executive program. You should see the Background Display. Turn on power to the Control Box (press on the black button). Now enter the **File** menu, choose **Load Settings** and select the file `default.cfg`. This configuration file is supplied on the distribution diskette and should have been copied under the ECP directory by now. Note that this file would have been loaded into the Executive automatically (see section 2.1.4.1). This particular `default.cfg` file contains the controller gain parameters and other trajectory, data gathering and plotting parameters specifically saved for the activities within this section.

Note that the plant type for which this file has been created has a 4:1 mechanical advantage (speed deduction) between the Load Disk and the Drive Disk with no brass weights on either disks. This is the standard set up for the Model 220 when shipped from factory.

Step 2: Implementing The Controller. Now enter the **Setup** menu and choose **Setup Control Algorithm**. You should see the sampling time **Ts** = 0.00442 seconds, and the **PI + Velocity Feedback** "radio button" selected. Now click on the **Setup Algorithm** button and you should see the following gains: k_p = 0.20, k_d = 0.010, k_i = 0. These are *continuous time* gains designed for a closed loop natural frequency of approximately 4 Hz and a damping ratio of 1 (critical damping). Note that the feedback loop is closed around Encoder #1. Exit this box and then click on **Implement algorithm**. The control law is now down-loaded to the real-time Controller. If you do not notice any motor power, click again until you notice the servo loop closed.

Now select **Discrete Time** and click on **Upload Algorithm** then on **General Form** and again select **Setup Algorithm**. You should see the general form algorithm with some non zero coefficients. These coefficients correspond to PID gains mapped to the general form algorithm structure. Notice that the general form algorithm is the only structure that actually runs in real-time. All other structures (e.g. dynamic filters, State Feedback etc.) are translated to the general form by the Executive prior to the implementation. Prior to leaving the **Setup Control Algorithm** dialog box select the **Continuous Time** radio button again.

© ECP 1995, All rights reserved.

Step 3: Setting Up Data Acquisition. Enter the **Data** menu and select **Setup Data Acquisition**. In this box make sure that the following five items are selected: Commanded Position, Encoder 1, Encoder 2, Control effort and Disturbance Effort. *Data sample period* should be 3 which means that the data will be collected every second servo cycle (in this case every 3*0.00442 = 0.0133 seconds).

Step 4: Executing A Trajectory & Plotting. Enter the **Command** menu and select **Trajectory**. In this box select **Step** and then **Setup**. You should see *step size = 4000*, *dwell time = 1000* ms, and *no. of repetitions = 1*. If not, change the values to this parameter set. Exit this box and go to the **Command** menu. Select **Execute** and, with *only* the **Sample Data** box checked, run the trajectory and wait for the data to be uploaded from the real-time Controller. You should have noticed a step move of 4000 counts (1/4 of revolution of the smaller Disk, a dwell of 1 second and a return step move. Now enter the **Plotting** menu and choose **Setup Plot**. Select Commanded Position and Encoder 1 Position for plotting (both on left axis) and click on **Plot Data**. You should see a plot similar to the one shown in Figure 3.2-1. This is the step response of a critically damped system with an (underdamped) natural frequency of approximately 6 Hz.

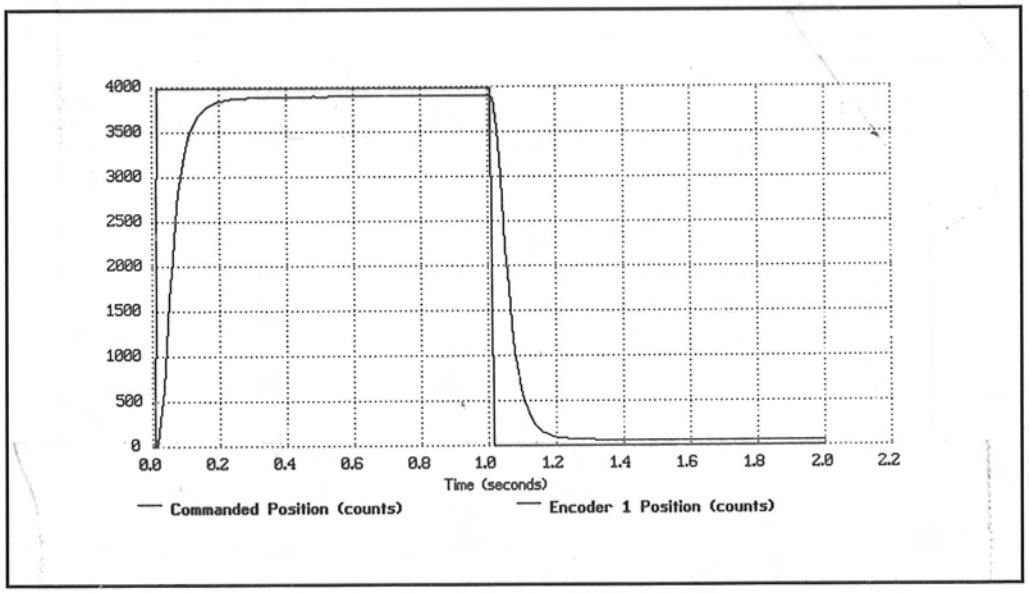

Figure 3.2-1 Critically Damped Step Response at Encoder 1

Note that all plot screens may be repositioned by dragging the plot frame bar using the mouse. A plot screen may be minimized or "shrunk" by clicking on the down arrow on the top right hand corner. By double clicking on a minimized plot screen it may be expanded again. In general, to speed up the screen graphics, one should avoid minimizing more than 4 to 5 plot screens on the Background screen. It is best to close unwanted plot screens rather than minimize them. You can re-size the plots using the cursor to "drag" the lower right hand corner of the plot frame (position cursor at corner and begin "dragging" when cursor becomes double arrow).

© ECP 1995, All rights reserved.

Step 5: Underdamped Step Response. Now enter the **Setup** menu again and choose **Setup Control Algorithm**. You should again see **Ts** = 0.00442 s., **PI + Velocity Feedback,** and **Continuous Time** selected. Now click on **Setup Algorithm** and you should see the following gains: $k_p = 0.20$, $k_d = 0.010$, $k_i = 0$. Change the derivative gain to $k_d = 0.002$ leaving the values for the other two gains unchanged. You have just reduced the velocity feedback gain. By reducing the amount of derived velocity feedback a critically damped second order system becomes under damped. To demonstrate this, **Implement** the algorithm in the **Setup Control Algorithm** box. Repeat Step 4 above with the new set of gains and plot the response of the Encoder #1 position to the same commanded step input. The response should look like the graph shown in Figure 3.2-2 which exhibits characteristics of an under damped system. Now change the derivative gain back to 0.010 for critical damping, implement the new gains via the **Setup Control Algorithm** dialog box.

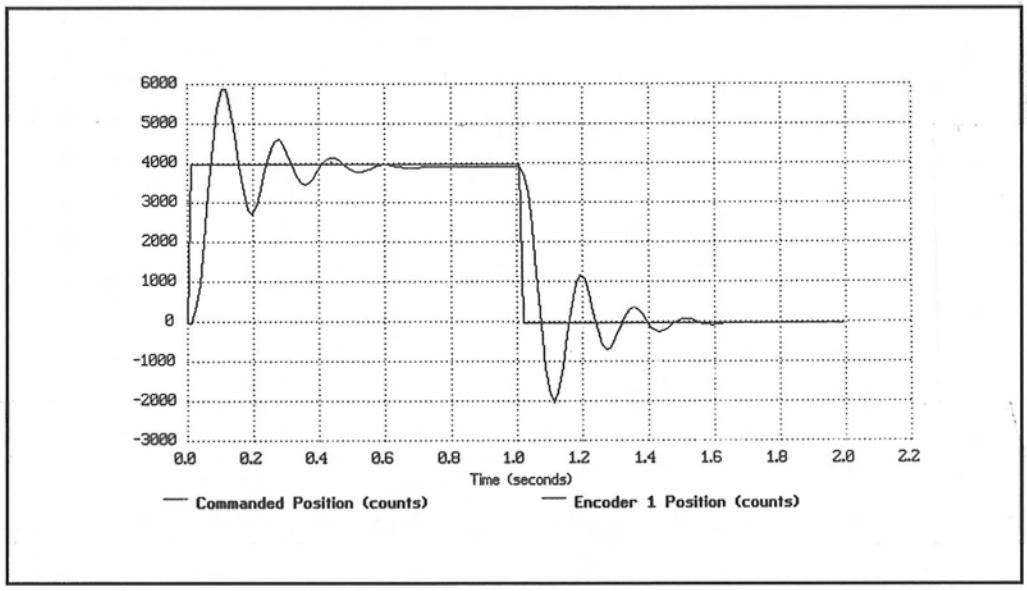

Figure 3.2-2 Underdamped Step Response

Step 6: Tracking Response. Enter the **Command** menu and select **Trajectory**. Choose **Ramp** and **Setup** to enter the *Ramp* dialog box. You should see *distance = 10000* counts, *velocity = 10000* counts/s, *dwell time = 100* ms, and *no. of repetitions = 1*. If not, change the values to this set. Exit this dialog box and go to the **Command** menu. Now select **Execute** and with only **Sample Data** checked, run the trajectory and wait for the data to be uploaded. You should have noticed a ramp (constant velocity) move of 10,000 counts (5/8 of a revolution of the small disk) followed by an 100 ms dwell and then the return motion. Now enter the **Plotting** menu and choose **Setup Plot**. Select Commanded position and Encoder 1 Position and then plot the data. You should see a plot similar to the one shown in Figure 3.2-3. Repeat the last step but this time add the

© ECP 1995, All rights reserved.

Commanded Velocity and Encoder 1 Velocity for plotting on the right axis. Note that you may save the plot data under `anyname.plt` using the **Save Plot Data** option. Any plot data thus saved may be reloaded from the disk using the **Load Plot Data** option for future inspection, plotting or printing. To print simply choose the **Print Data** menu option and select the appropriate printer before the printing command. You may also save the data in an ASCII format suitable for entry to other software packages via the **Export Data** option under the **Data** menu. The file extension for ASCII data is `*.txt`. Now close all plot windows.

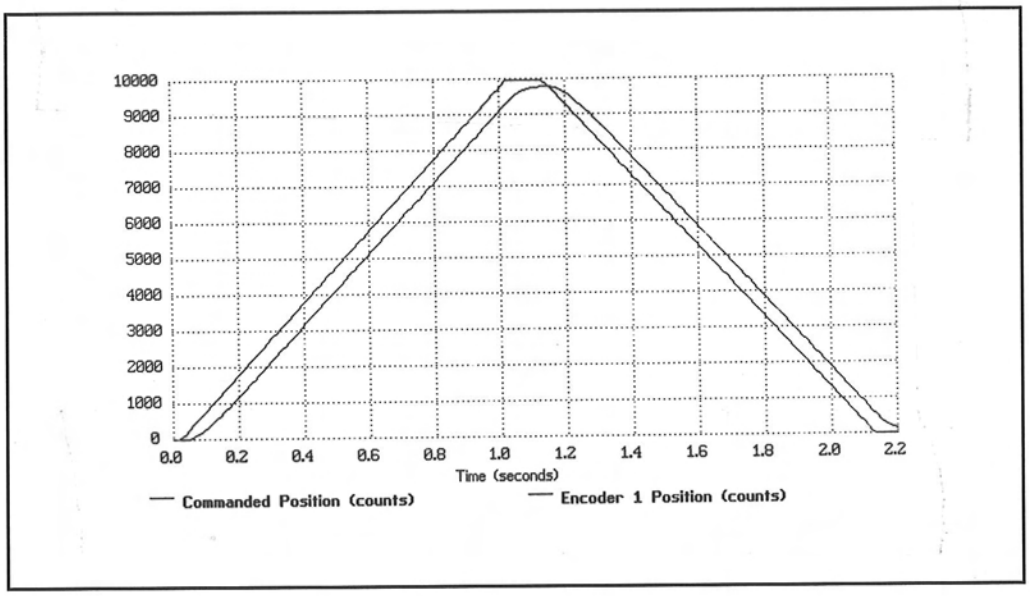

Figure 3.2-3 Ramp Tracking With PD Control

Step 7: Frequency Response. Again enter **Trajectory** and select **Sine Sweep** then **Setup**. You should see: Amplitude = 500 counts, min. freq. = 0.1 Hz, max. freq.= 12 Hz and sweep time = 30 seconds. Exit this box and go to **Command** menu and **Execute**. With only **Sample Data** checked, run the trajectory and wait for the data to be uploaded. You should notice a sinusoidal motion with increasing frequency and reducing amplitude for about 30 seconds. After the data has been uploaded at the end, go to the Plotting menu and choose Setup Plot. Remove the velocities from the right axis and Command Position from the left axis, then plot the Encoder 1 Position. The plot should look like the one shown in Figure 3.2-4. This is a typical response associated with a damped second order system when excited sinusoidally with an increasing frequency (frequency response).

Now as done previously, change to $k_d = 0.002$ (underdamped) and **Implement**. Exit and the repeat the same sine sweep trajectory maneuver. The response should now indicate the characteristic peak associated with the frequency response of an under damped second order system (resonance at approximately 6 Hz in this case) as shown in Figure 3.2-5.

© ECP 1995, All rights reserved.

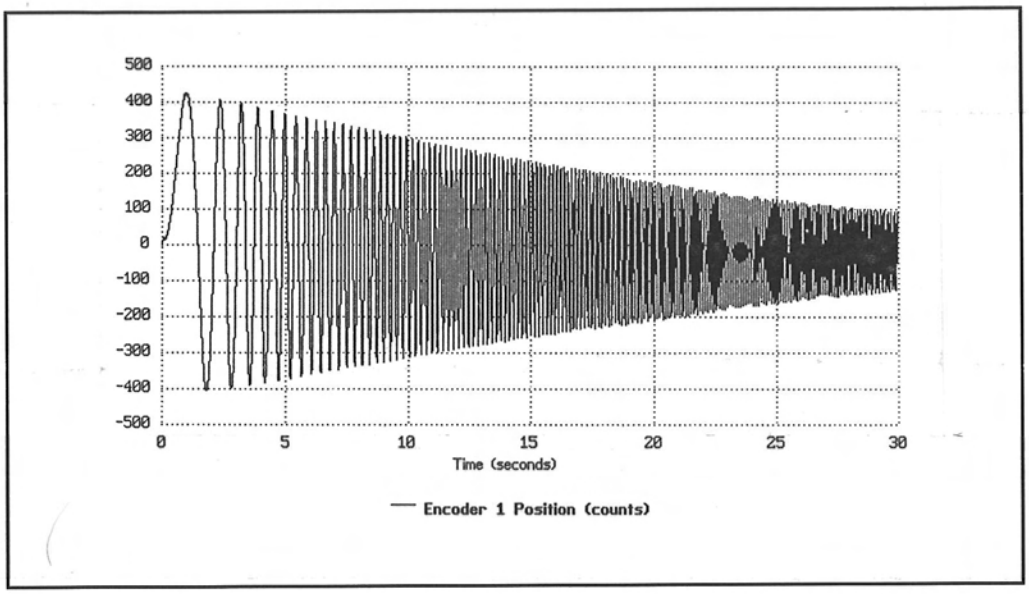

Figure 3.2-4 Sine Sweep Response of Critically Damped System

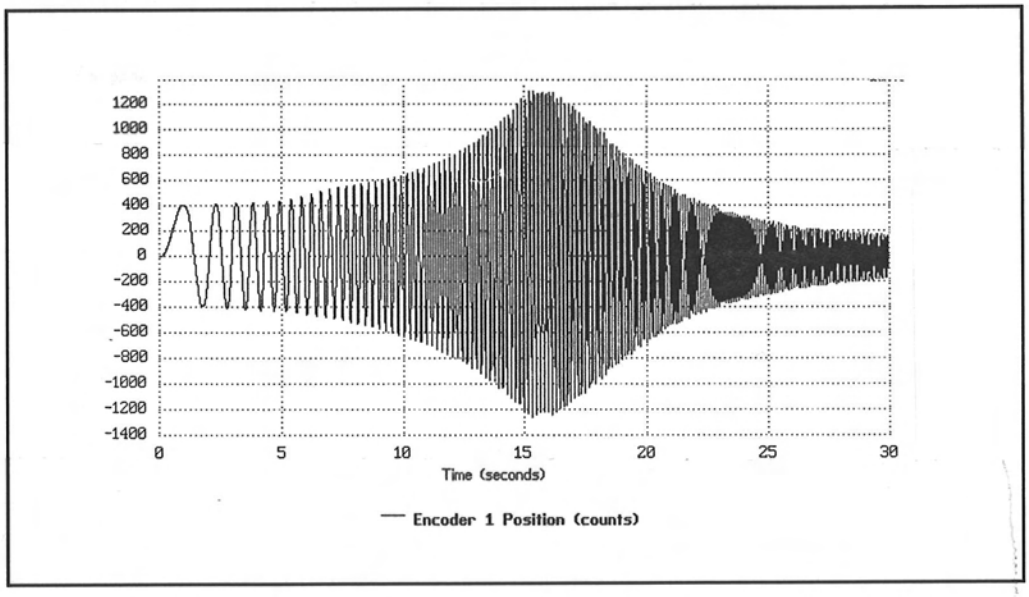

Figure 3.2-5 Sine Sweep Response of Underdamped System

Step 8: Adding Viscous Damping. Enter the **Disturbance** dialog box under the **Command** menu. Select **Viscous Friction** and then **Setup**. Using this menu you may enter the parameters for the viscous friction coefficient in units of volts/radian/second. It should be set to 1.0 volts/radian/second. Exit this dialog box and go to the **Execute** dialog box. This time check both **Sample Data** and **Include viscous friction** prior to running the previously used Step trajectory. The response observed should look similar to the one shown in Figure 3.2-6. Relative to Figure 3.2-2, this response shows that the effect of viscous friction is to add damping which is the same as the effect of derivative feedback. Note that the viscous friction torque, if implemented, will remain in effect until either it is *removed* in its own dialog box, or a new trajectory is run without checking the

© ECP 1995, All rights reserved.

Include viscous friction check box. For the Model 220 system, viscous friction is effected via the disturbance motor coupled to the Load Disk.

Return to **Setup Control Algorithm** menu and return the derivative gain to $k_d = 0.010$ for critical damping. Implement the new gain and then exit the dialog box. Set up a 0 (zero) count step for 7500 ms duration and 1 repetition via **Step** under **Trajectory** in the **Command** menu. This prepares the system for regulation and data collection.

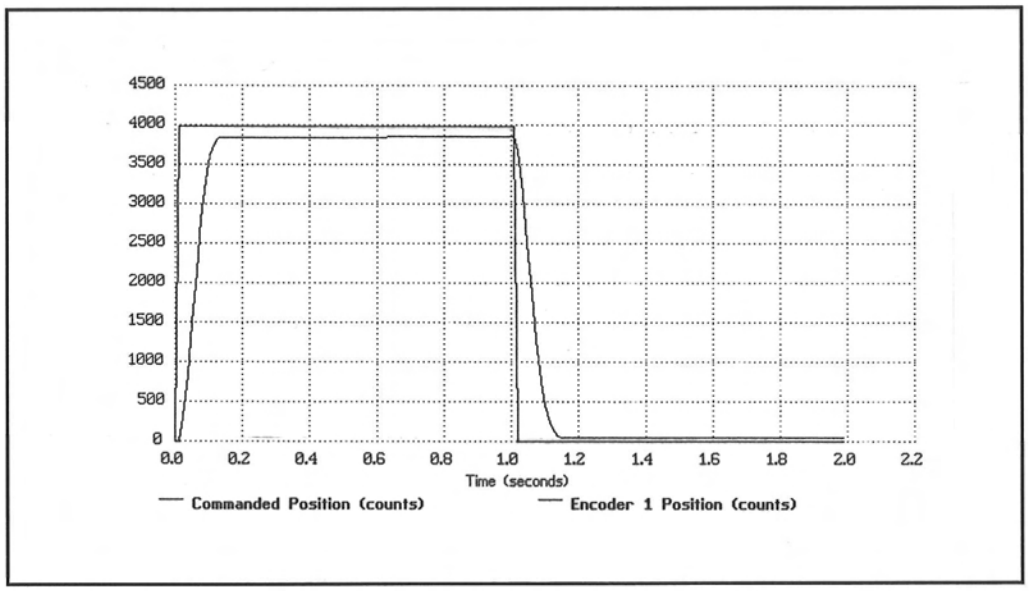

Figure 3.2-6 Damping Of Underdamped System Via Viscous Friction

Step 8: Disturbance Regulation & Integral Control. Enter the **Disturbance** dialog box under the **Command** menu. Select **Step** and then **Setup**. Using this menu you may enter the parameters for a step torque disturbance (all disturbance torque profiles are physically activated from the motor connected to the larger "load" disk via the 4:1 pulley below the disk). The parameters should be: *Step Size = 0..5* volts, *Dwell time =2500* ms and *no. of repetitions = 2*. Exit and **Execute** the (zero amplitude) Step trajectory making sure to check both **Sample Data** and **Include Step Disturbance** prior to running. The response observed after plotting Encoder 1 position should look similar to the one shown in Figure 3.2-7 (You may want to plot Disturbance Effort as well to see the overall regulation effect). Notice the increased size of the steady state error due to the step disturbance. After plotting this data, shrink it for later comparison.

Now re-enter **Setup Control Algorithm** and the **PI + velocity Feedback** window and add integral gain by setting $k_i = 1.0$ leaving the other two gains unchanged. Exit and **Implement**. Repeat the above procedure and plot the response. You should notice that the response overshoots but the steady state errors due to the step torque disturbance are eliminated by the addition of the integral action. A plot similar to the one shown in Figure 3.2-8 should have been obtained. All disturbance torque profiles (except viscous friction) are synchronized to start of any selected trajectory maneuver. If a disturbance

© ECP 1995, All rights reserved.

profile's selected duration is longer than the selected duration for a particular trajectory, the disturbance effort is brought to zero at the end of the trajectory maneuver. This means that the disturbance torque profiles may be cut short if the end of trajectory motion is reached first. Also the scaling for the disturbance effort between volts and Newton meters of torque is discussed in the chapter 6.

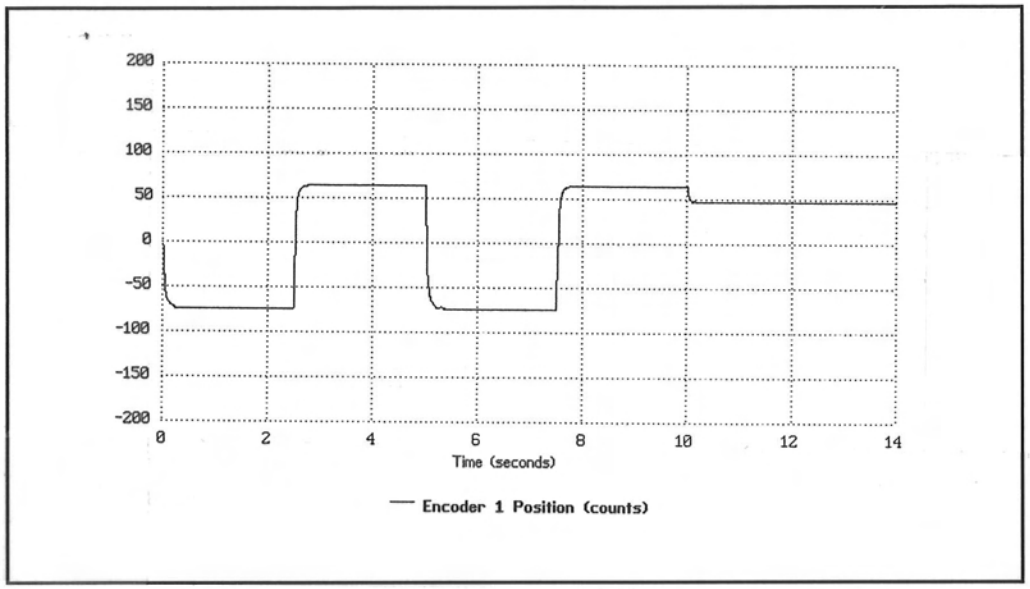

Figure 3.2-7 Response Of PD controlled System To Step Disturbance Torque

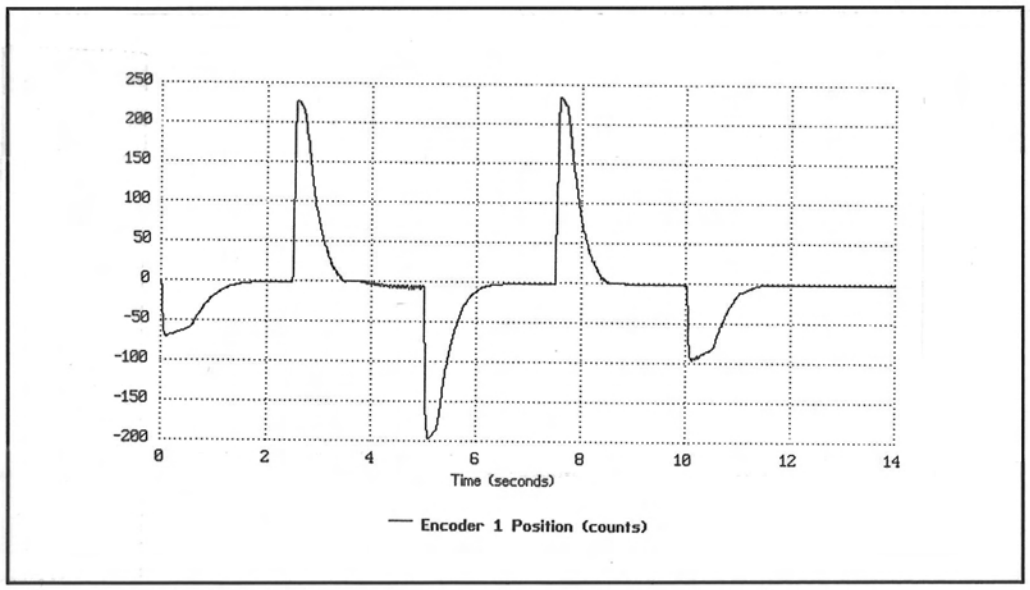

Figure 3.2-6 Elimination Of Steady State Error Via Integral Action

This completes the self-guided tour. It is strongly advised that the user read all material in Chapters 2 and 3 before further operation of the system.

© ECP 1995, All rights reserved.

3.3 Nonintuitive System Behavior

An explanation of system functionality which may be nonintuitive to first time (or first few time) users is given below.

Point 1: Upon PC power up, the control loop is closed but all gains are cleared to zero. As a result, even though the status display indicates **CLOSED LOOP**, the control effort is zero indicating that there is no torque demand from the actuator. With zero gains, the closed loop system behaves like an open loop one. This initialization of the gains to zero also takes place every time the real-time controller is **Reset** under the **Utility** menu. Note that **Reset** also carries out a rephasing procedure which results in a short sudden motion.

Point 2: Even though the parameters for a particular control algorithm may exist within the Executive, the real-time Controller does not carry them until the **Implement Algorithm** button of the **Setup Control Algorithm** dialog box is activated. Then control is implemented immediately

Point 3: The **Limit Exceeded** message comes on as a result of either motor over-speed, shaft over-deflection or drive over-current. In either case the message does not clear until a stable set of control gains are downloaded and if necessary a less abrupt trajectory is requested (see Section 2.1.3). This condition may also occur under the following two conditions:

a) With the control loop closed, a motor rephasing command is issued.

b) With the control loop closed, the power to the Control Box is turned off and the disks are rotated manually and then the power is turned back on again.

In either case the sudden motions of the disks may cause the limiting conditions.

© ECP 1995, All rights reserved.

4. Real-Time Control Implementation

This chapter is a description of the real-time controller functionality and a tutorial on related implementation issues.

The ECP real-time Controller is a Digital Signal Processor (DSP) based single board computer which executes the following real-time tasks:

Servo loop closure
Command generation
Sensor Interface

In addition, in the background (while not executing the above tasks) it carries out the following:

User Interface via PC and/or RS232 Bus

Limits and Safety Activities

4.1 Servo Loop Closure

Servo loop closure involves computing the control algorithm at the sampling time. The real-time Controller executes the General Form equation of the control law at each sample period T_s. This period can be as short as 0.000884 seconds (approx. 1.1 KHz) or any multiple of this number. The Executive program's **Setup Control Algorithm** dialog box allows the user to alter the sampling period. All forms of control laws are automatically translated by the Executive program to the General Form prior to downloading ("implementing") to the Controller. The General Form uses 96-bit real number (48-bit integer and 48-bit fractional) arithmetic for computation of the control effort. The control effort is saturated in software at +/- 16384 to represent +/- 5 volts on the 16-bit DACs whose range is +/- 10 volts. The +/-5 volt limitation is due to the actuator 's amplifier input voltage scaling.

Referring to Figure 4.1-1, the control equations are as follows:

$$R(q^{-1})\text{nodeA}(k) = T(q^{-1})*c_p(k)-S(q^{-1})*f_{b1}(k)$$

Here T ,S , and R are seventh order polynomials of the unit time shift operator q, and the letter k represents the k^{th} sampling period for k=0, 1,2, ... The variable nodeA is an intermediate value

© ECP 1995, All rights reserved.

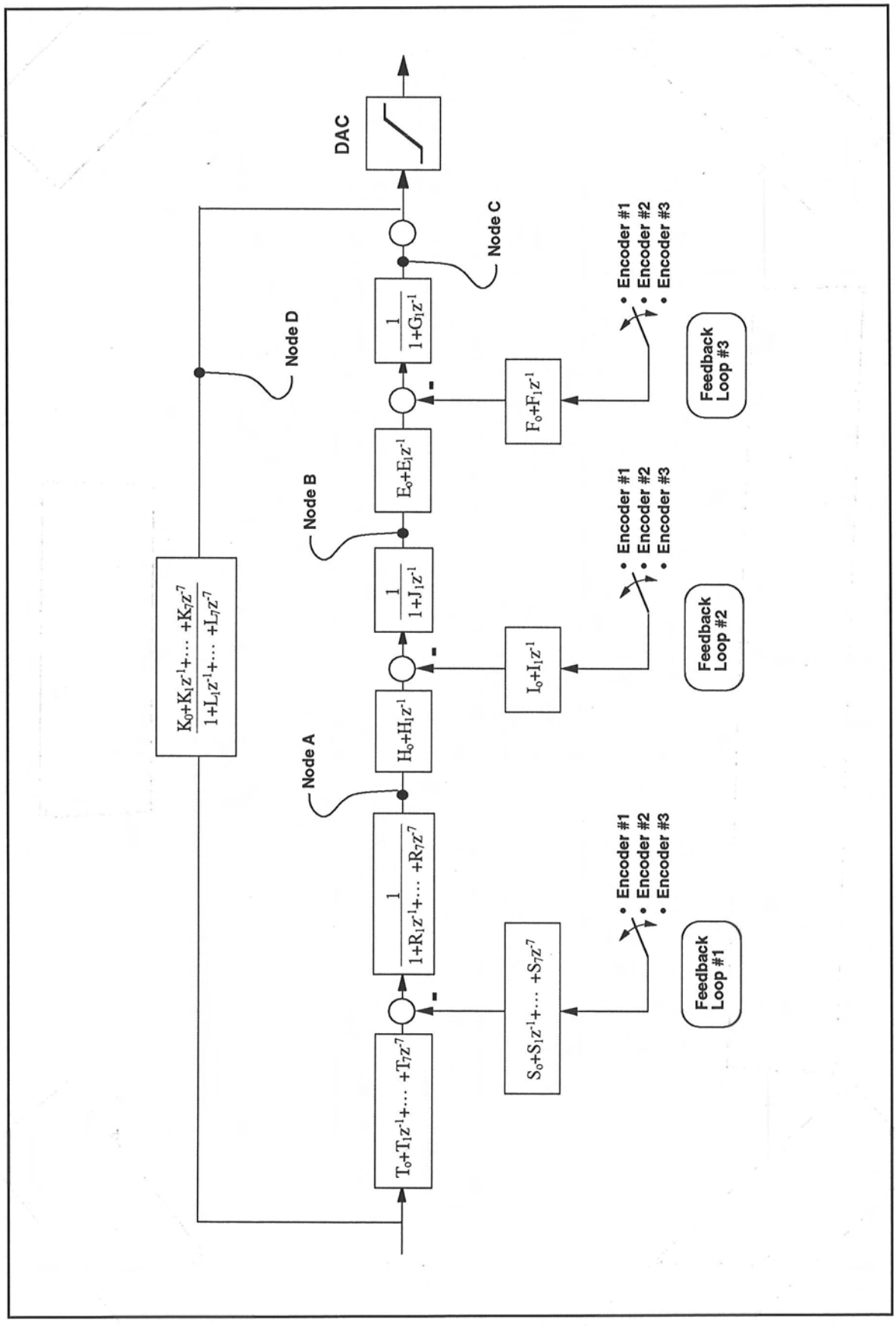

Figure 4.1-1. General Form Of The ECP Control Algorithm

© ECP 1995, All rights reserved.

of the overall control law equation which is stored in the memory and may be acquired by the user through the Data Acquisition feature of the Executive program. The variable $c_p(k)$ is the commanded position which is generated by the real-time Controller as described in the next section. The variable $f_{b1}(k)$ may be from any of the three possible feedback sensors depending on the state of software loop switch 1.

Next the intermediate loop is computed as follows

$$J(q^{-1})*nodeB(k) = H(q^{-1})*nodeA(k)-I(q^{-1})*f_{b2}(k)$$

Here again nodeB is an intermediate value stored in the memory and f_{b2} is the sensor feedback selected via loop switch 2. J, H, and I are second order polynomials. For the inner loop we have

$$G(q^{-1})*nodeC(k) = E(q^{-1})*nodeB(k)-F(q^{-1})*f_{b3}(k)$$

NodeC is the contribution to the value of the control effort generated by the overall regulator and f_{b3} is the sensor feedback selected via loop switch 3. G, E, and F are second order polynomials. For the feedforward loop we have

$$L(q^{-1})*nodeD(k) = K(q^{-1})*c_p(k)$$

In this case nodeD is the contribution to the value of the control effort generated by the feedforward terms, L and K are sixth order polynomials.

The combined regulatory and tracking controller generates the control effort as:

$$control\ effort(k) = nodeC(k)+nodeD(k)$$

The general control structure described above supports the implementation of a broad range of specific control forms.

4.2 Command Generation

Command generation is the real-time generation of motion trajectories specified by the user. The parameters of these trajectories are downloaded to the real-time Controller through the Executive program via the **Trajectory Configuration** dialog box. This section describes the trajectories generated in the current control version.

© ECP 1995, All rights reserved.

4.2.1 Step Move

Figure 4.2-1a shows a step move demand. The desired trajectory for such a move can be described by

$$c_p(t) = c_p(0)+C \qquad \text{for } t>0$$
$$c_v(t)=0 \qquad \text{for } t>0$$
$$c_v(0)=\infty$$

Where $c_p(t)$ and $c_v(t)$ represent commanded position and velocity at time t respectively and C is the constant step amplitude. Such a move demand generates a strong impulsive torque from the control actuator. The response of a mechanical system connected to the actuator would depend on the dynamic characteristics of the controller and the system itself. However, in a step move, the instantaneous velocity and its derivatives are not directly controllable. Usually step moves are used only for test purposes; more gentle trajectories are nearly always used for practical maneuvers.

4.2.2 Ramp Move

A ramp demand is seen in Figure 4.2-1b. The trajectory can be described by

$$c_p(t) = c_p(0)+V*t \qquad \text{for } t>0$$
$$c_v(t) = V \qquad \text{for } t>0$$
$$c_a(0) = \infty$$

where $c_a(0)$ represents commanded acceleration at time zero and V is a constant velocity. Relative to a step demand, a ramp demand is more gentle, however the acceleration is still impulsive. The commanded velocity is a known constant during the maneuver.

4.2.3 Parabolic Move

Figure 4.2-1c shows a parabolic move demand. Its trajectory can be expressed as:

$$c_p(t) = c_p(0)+c_v(0)*t+1/2\ A*t^2 \qquad \text{for } t>0 <1/2\ t_f$$
$$c_v(t) = c_v(0)+A*t \qquad \text{for } t>0 <1/2\ t_f$$
$$c_a(t) = A \qquad \text{for } t>0 <1/2\ t_f$$
$$c_j(0) = \infty$$

© ECP 1995, All rights reserved.

where $c_j(t)$ represents commanded jerk at time t and A is a constant acceleration, and t_f is the final destination time. Relative to a ramp demand, a parabolic demand is more gentle, however the rate of change of acceleration (jerk) is still impulsive. Note that the commanded acceleration is a known constant during the maneuver. The second half of a parabolic demand uses -A for deceleration.

4.2.4 Cubic Move

Figure 4.2-1d shows a cubic demand which can be described by

$$c_p(t) = c_p(0)+c_v(0)*t+1/2\ c_a(0)*t^2+1/6\ J*t^3 \qquad \text{for } t>0<1/4\ t_f$$

$$c_v(t) = c_v(0)+c_a(0)*t+1/2\ J*t^2 \qquad \text{for } t>0<1/4\ t_f$$

$$c_a(t) = c_a(0)+J*t \qquad \text{for } t>0<1/4\ t_f$$

$$c_j(0) = J$$

where J represents a constant jerk. Relative to all the above demands, a cubic demand is more gentle. The commanded acceleration is linearly changing during the three sections of the maneuver. The second half of a cubic demand uses -J and the third part uses J again for the jerk input.

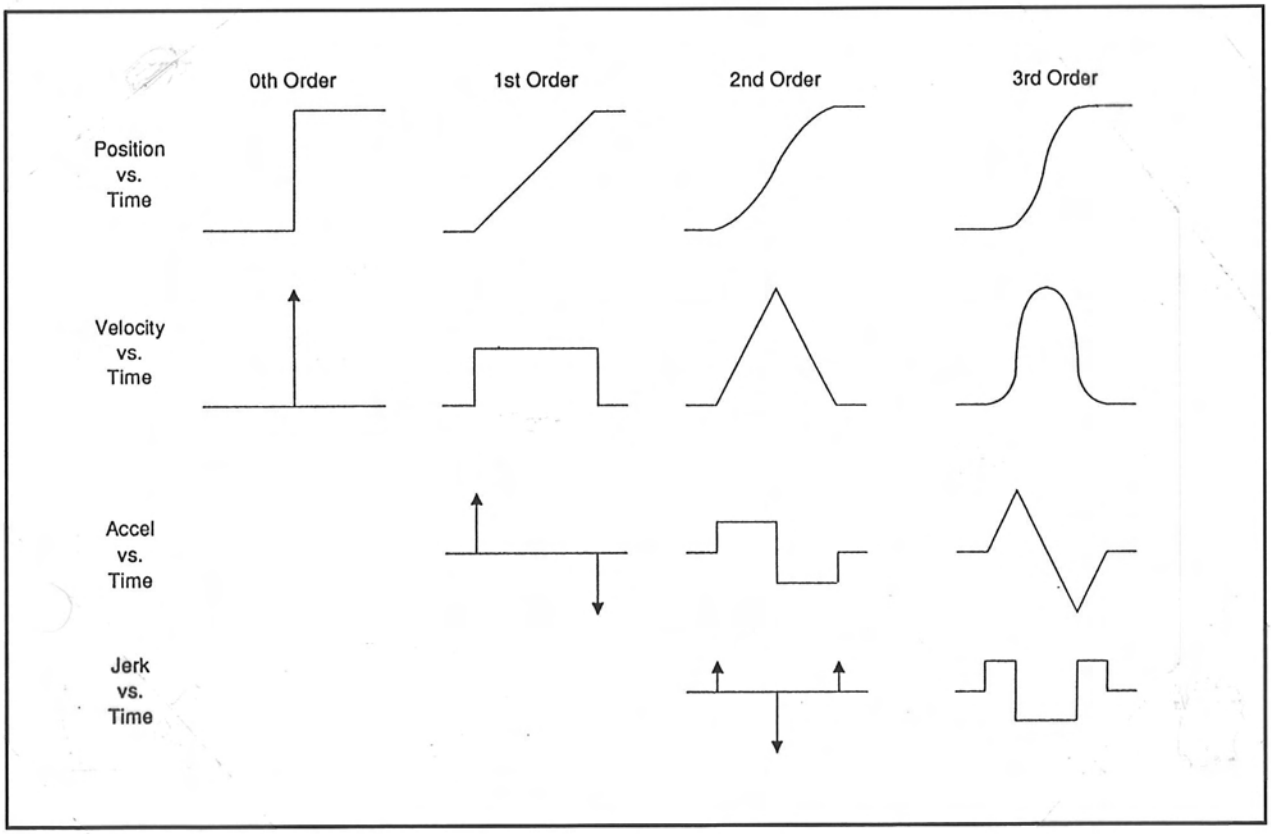

Figure 4.2-1. Geometric Command Trajectories Of Increasing Order

© ECP 1995, All rights reserved.

4.2.5 The Blended Move

Any time a ramp, a parabolic or a cubic trajectory move is demanded the real-time Controller executes a general blended move to produce the desired reference input to the control algorithm. The move is broken into five segments as shown in the velocity profile of Figure 4.2-2. For each section a cubic (in position) trajectory is planned. Five distinct cubic equations can describe the forward motion . After the dwell time, the reverse motion can be described by five more cubic trajectories. Each cubic has the form:.

$$cp_i(t)= cp_i(0)+V_i*t+1/2\ A_i*t^2+1/6\ J_i*t^3 \qquad i = 1,...,5$$

Using a known set of trajectory data (i.e. the requested total travel distance, acceleration time t_{acc}, and the maximum speed v_{max}, for each move), the constant coefficients V_i, A_i, and J_i are determined for each segment of the move by the real-time Controller. This function is known as the "motion planning" task. Note that for a parabolic profile $J_i=0$, and for a ramp profile A_i is also zero which further simplifies the task. Having determined the coefficients for each section, the real-time Controller uses these values at the servo loop sampling periods to update the commanded position (reference input). For example if the segment is a cubic ($J \neq 0$):

$$c_a(k)= c_a(k-1) +J*T_s$$
$$c_v(k)=c_v(k-1)+c_a(k)*T_s$$
$$c_p(k)=c_p(k-1)+c_v(k)*T_s$$

where T_s is the sampling period and $c_a(k)$, $c_v(k)$, $c_p(k)$ represent commanded acceleration, velocity and position at the k^{th} sampling period.

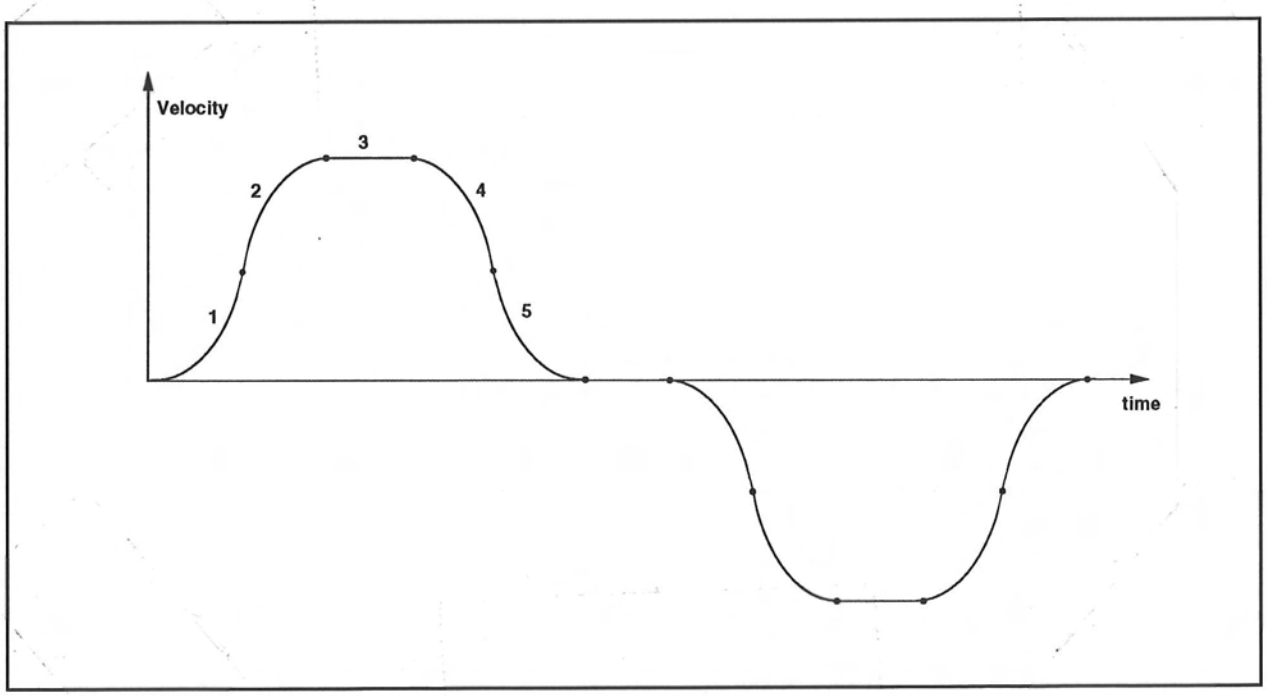

Figure 4.2-2 Velocity Profile for General Blended Move

© ECP 1995, All rights reserved.

4.2.6 Sinusoidal Move

The sinusoidal move is generated using the following equation:

$$c_p(k) = R^* \sin(\theta(k))$$

where R is the amplitude, $\theta(k)=\omega^*k^*T_p$ for k=0,1,..., and ω is the commanded frequency in Hz. T_p is set to five milliseconds. To further smooth out the trajectory, a cubic spline is fitted between the points as follows:

$$c_p'(k) = (c_p(k-1)+4^*c_p(k)+c_p(k+1))/6$$

For the linear sine sweep, $\omega(k) = \alpha^*T_p$, where α is a constant determined by the difference between the maximum and the minimum frequency divided by the sweep time

$$\alpha = (\omega_{max} - \omega_{min}) / \text{sweep time}$$

4.3 Brushless Motor Commutation and Torque Control

The main advantage of a DC brushless motor (otherwise known as a *permanent magnet synchronous* motor) over the conventional DC brush motor is the elimination of both brush friction associated wear.

Figure 4.3-1 shows a cross sectional view of a typical DC brushless motor. In contrast to the conventional DC brush motor, the permanent magnets are fixed to the rotor. The phase windings (typically 3 phases) are distributed in slots of the stator. This arrangement also provides for greater heat dissipation (i^2R), which in turn leads to improved life and typically greater volume-to-power ratios for brushless motors than for brush motors.

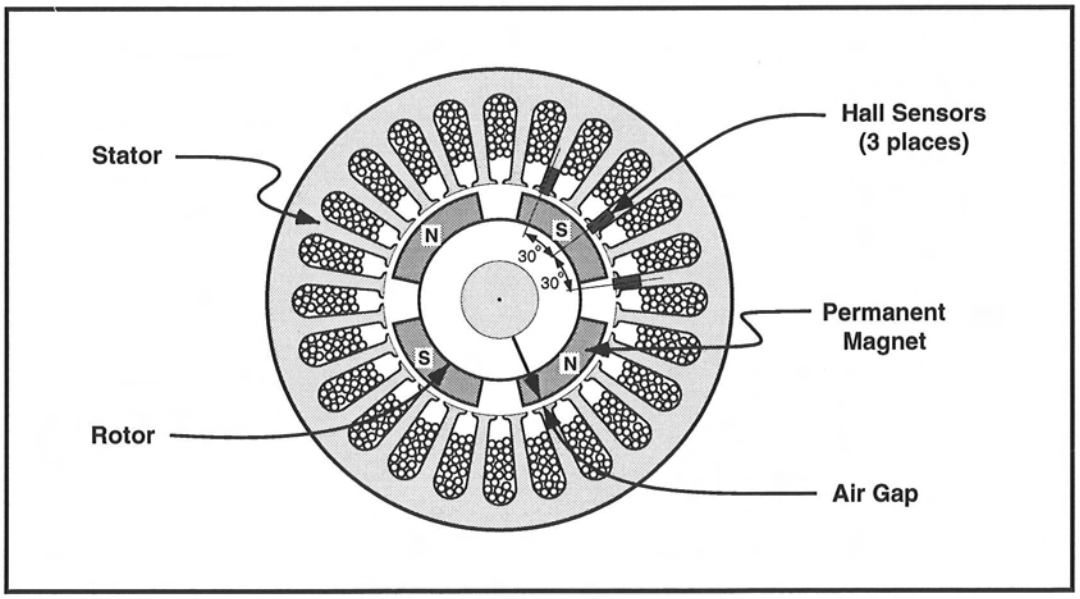

Figure 4.3-1. Cross-section of a Typical DC Brushless Motor. (Four pole type shown)

© ECP 1995, All rights reserved.

In any continuously rotating motor, to provide continuous torque, the current must be successively altered or switched depending on the absolute position of the rotor. In a DC brush motor, this switching is implemented mechanically by the commutator. In a DC brushless motor, a rotor positioning sensor is used and the commutation procedure is done electronically. We will consider two different types of commutation procedures for DC permanent magnet brushless motors: rectangular and sinusoidal.

4.3.1 Rectangular (Hall-Effect) Commutation

Figure 4.3-2 shows a simplified schematic of the drive system(s) used in this mechanism. This is a typical drive scheme for a 4-pole 3-phase star-wound brushless motor with Hall-effect (rectangular) commutation. The three Hall-effect sensors are positioned on the stator. The sensed magnetic field switches between the adjacent north/south poles as the rotor rotates. This switching sequence is then used to direct the commanded motor current to individual winding phases (Figure 4.3-3). A simple electronic logic circuit is used for the generation of the switching steps (six steps per electrical cycle or 12 steps per mechanical cycle for a 4-pole motor). Analog high bandwidth *proportional plus integral* (PI) current feedback loops are then used on two of the three phases to assure almost instantaneous response of the actual winding current following any commanded current changes. The third phase does not require a current feedback loop because (as per Kirchhoff's law) the current in the third phase is the negative of the sum of the current in the other two phases.

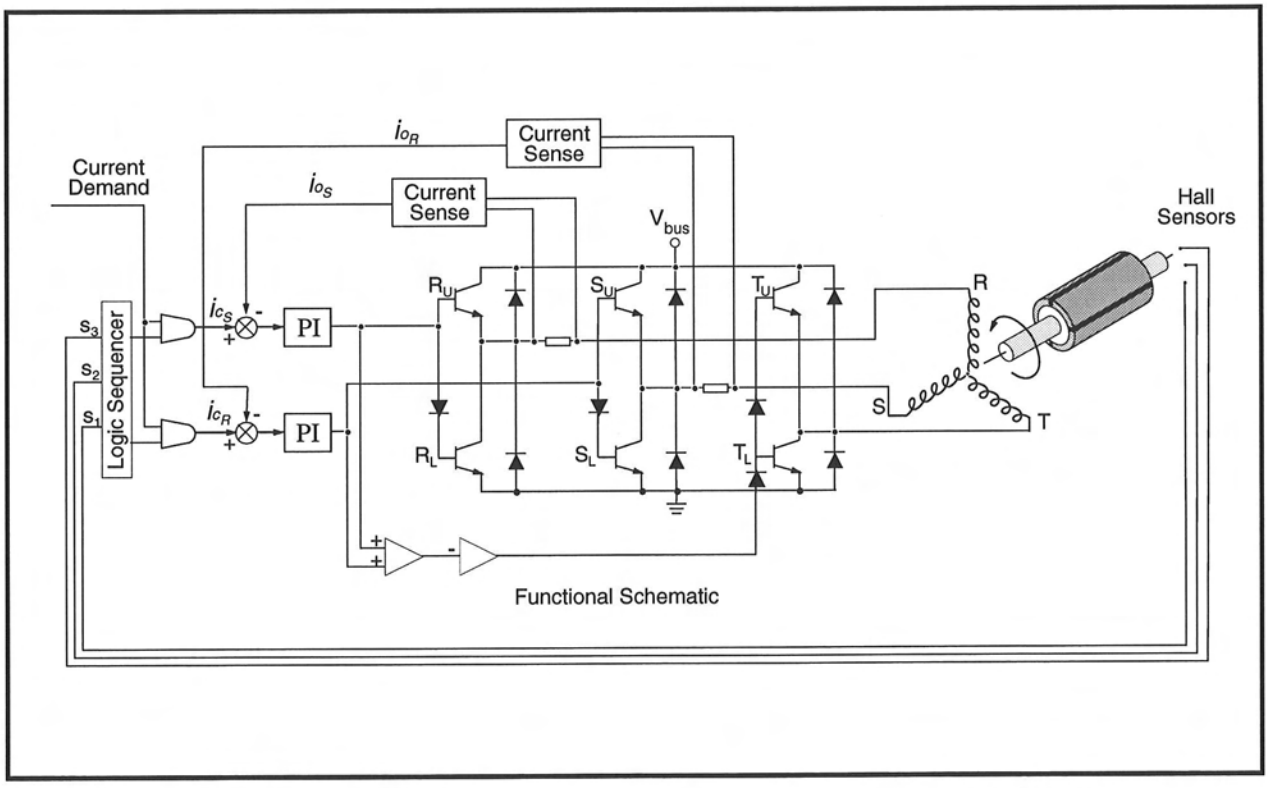

Figure 4.3-2 Simplified Schematic of Hall-effect Commutated DC Brushless Motor Drive System

© ECP 1995, All rights reserved.

We assume that, due to the relatively high bandwidth of the current loops, nearly instantaneous matching of the commanded current (torque) and the actual current occurs.[1] With the rectangular drive scheme shown in Figure 4.3-3b, at any position only two of the three phases are operational so that the current in the third phase is zero. Consider a 60 electrical degree interval $30 \leq \theta \leq 90$. The torque input from phase R is

$$T_R = K_t I_R \sin\theta \qquad (4.3\text{-}1)$$

and

$$I_R = -I_T \text{ with } I_S = 0$$

where $K_t = Z*B_p*r*l$ is the torque constant per phase in N-m. Z is the number of turns per winding, r is the inside radius of the stator in meters, and l is the active length of conductors in meters. B_p is the peak air gap flux density in Teslas.

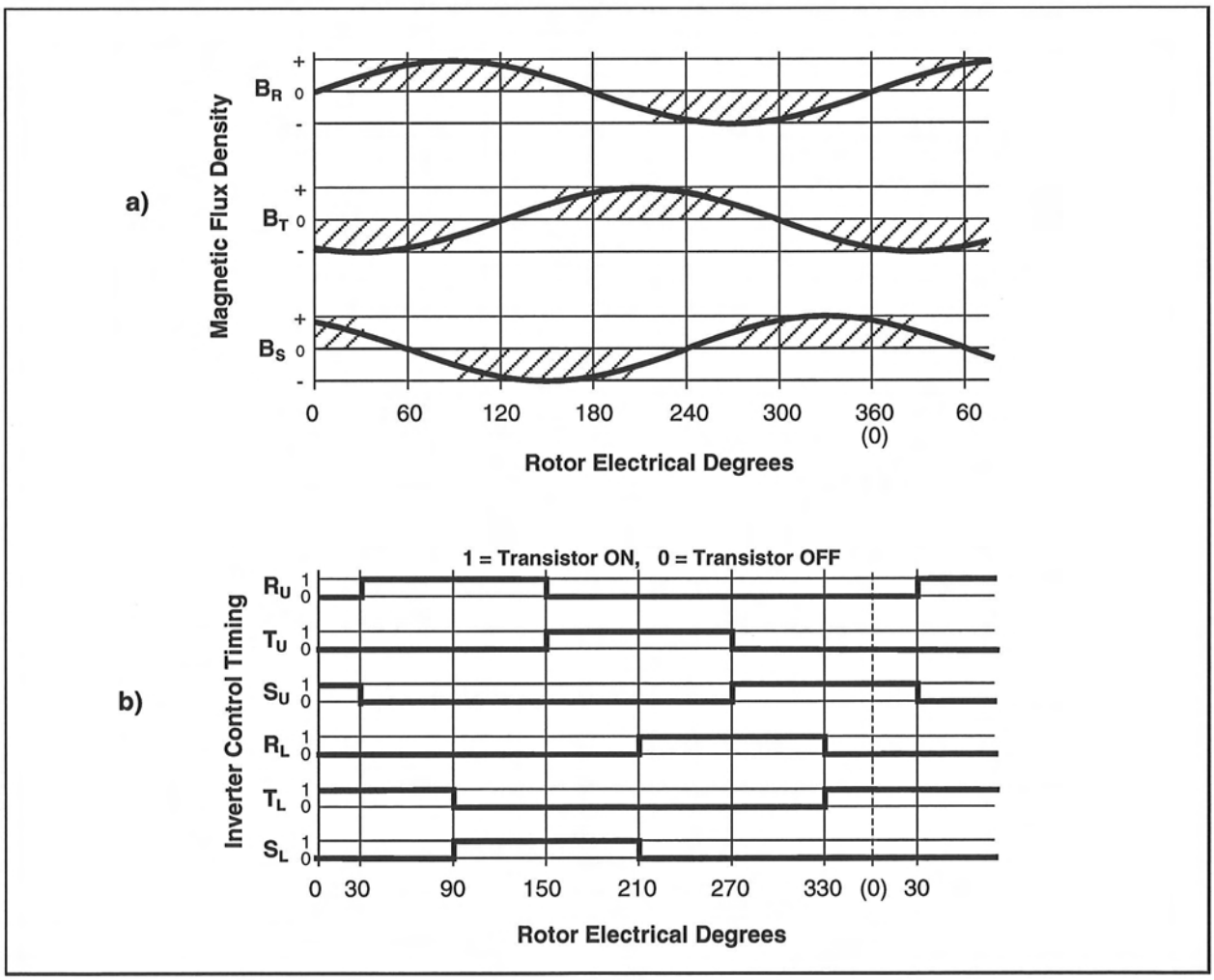

Figure 4.3-3 Hall-effect Commutation Timing Diagram

[1]We qualify the validity of this assumption later when we discuss the PI current loops.

© ECP 1995, All rights reserved.

To produce positive torque, the flux density must be negative for phase T. This is the case for a sinusoidally wound motor (see Figure 4.3-3a):

$$\begin{aligned} T_T &= K_t I_T \sin(\theta-120) \\ &= K_t I_R \sin(120-\theta) \qquad \text{for } 30 \le \theta \le 90 \\ &= K_t I_R (0.5\sin\theta+0.886\cos\theta) \end{aligned} \tag{4.3-2}$$

The total torque is given by the addition of T_T and T_R over the interval $30 \le \theta \le 90$:

$$T = T_R+T_T = K_t(1.5\sin\theta+0.886\cos\theta)*I_R \tag{4.3-3}$$

Equation 4.3-3 shows that the effective torque constant, $K_t(1.5\sin\theta+0.886\cos\theta)$, changes as a function of rotor angle producing a torque ripple as much as 13% for rectangular commutation. This torque ripple can be treated as a disturbance which, in most practical applications, is reduced by closing outer velocity and position loops around the current loop.

4.3.2 Sinusoidal Commutation

For a motor with sinusoidally wound stator coils the air gap flux densities are:

$$\begin{aligned} B_R &= B_p \sin \\ B_S &= B_p \sin(\theta+120) \\ B_T &= B_p \sin(\theta+240) \end{aligned} \tag{4.3-4}$$

Where B_R, B_S, and B_T are the per phase flux densities for the motor phases R, S, and T respectively and B_p is the peak value in Tesla. If we assume that the PI controllers around the current loop maintain the phase currents in phase with the air gap flux densities, then the current in each phase in terms of the peak current I_p are given by

$$\begin{aligned} I_R &= I_p \sin \\ I_S &= I_p \sin(\theta+120) \\ I_T &= I_p \sin(\theta+240) \end{aligned} \tag{4.3-5}$$

From equation 4.3-4 and 4.3-5, the instantaneous torque being produced in each phase is

$$\begin{aligned} T_R &= K_t I_p \sin^2\theta \\ T_S &= K_t I_p \sin^2(\theta+120) \\ T_R &= K_t I_p \sin^2(\theta+240) \end{aligned} \tag{4.3-6}$$

The total torque is the sum of the above torque components, which is given by

$$\begin{aligned} T &= T_R+T_S+T_T \\ &= K_t I_p (\sin^2\theta+\sin^2(\theta+120)+\sin^2(\theta+240)) \end{aligned}$$

© ECP 1995, All rights reserved.

To produce positive torque, the flux density must be negative for phase T. This is the case for a sinusoidally wound motor (see Figure 4.3-3a):

$$\begin{aligned} T_T &= K_t I_R \sin(\theta+240) \\ &= K_t I_R (0.5\sin\theta+0.886\cos\theta) \qquad \text{for } 0 \le \theta \le 60 \end{aligned} \tag{4.3-2}$$

The total torque is given by the addition of T_T and T_R over the interval $0 \le \theta \le 60$:

$$T = T_R+T_T = K_t(1.5\sin\theta+0.886\cos\theta)*I_R \tag{4.3-3}$$

Equation 4.3-3 shows that the effective torque constant, $K_t(1.5\sin\theta+0.886\cos\theta)$, changes as a function of rotor angle producing a torque ripple as much as 13% for rectangular commutation. This torque ripple can be treated as a disturbance which, in most practical applications, is reduced by closing outer velocity and position loops around the current loop.

4.3.2 Sinusoidal Commutation

For a motor with sinusoidally wound stator coils the air gap flux densities are:

$$\begin{aligned} B_R &= B_p \sin \\ B_S &= B_p \sin(\theta+120) \\ B_T &= B_p \sin(\theta+240) \end{aligned} \tag{4.3-4}$$

Where B_R, B_S, and B_T are the per phase flux densities for the motor phases R, S, and T respectively and B_p is the peak value in Tesla. If we assume that the PI controllers around the current loop maintain the phase currents in phase with the air gap flux densities, then the current in each phase in terms of the peak current I_p are given by

$$\begin{aligned} I_R &= I_p \sin \\ I_S &= I_p \sin(\theta+120) \\ I_T &= I_p \sin(\theta+240) \end{aligned} \tag{4.3-5}$$

From equation 4.3-4 and 4.3-5, the instantaneous torque being produced in each phase is

$$\begin{aligned} T_R &= K_t I_p \sin^2\theta \\ T_S &= K_t I_p \sin^2(\theta+120) \\ T_R &= K_t I_p \sin^2(\theta+240) \end{aligned} \tag{4.3-6}$$

The total torque is the sum of the above torque components, which is given by

$$\begin{aligned} T &= T_R+T_S+T_T \\ &= K_t I_p (\sin^2\theta+\sin^2(\theta+120)+\sin^2(\theta+240)) \\ &= 3/2\ K_t I_p \end{aligned} \tag{4.3-7}$$

© ECP 1995, All rights reserved.

Equation 4.3-7 shows that "perfect" sinusoidal commutation of a "perfectly" sinusoidally wound motor provides for a ripple free torque constant. In practice, however, a small amount of torque ripple may exist due to imperfections in the windings and the current loop elements and misalignment of the rotor position sensor. Note that for this method of commutation, a high resolution absolute position sensor is required.

4.3.3 Proportional Plus Integral (PI) Current Loop

Each phase of the motor winding coil is characterized by its resistance R and its inductance L. If we assume that the per-phase back emf of motor is negligible in the high torque / low speed region of operation, then the block diagram shown in Figure 4.3-4 represents the per-phase PI loop for two of the three phases. (There is no need for PI loop on the third phase, as the sum of the total current must be zero in a star winding circuit).

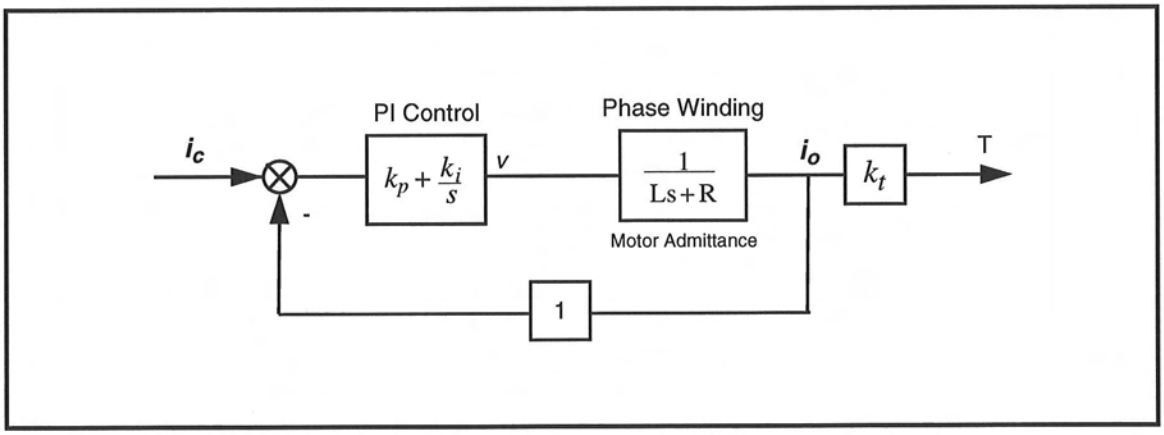

Figure 4.3-4 Simplified Block Diagram of Analog PI Controller (applies to each motor winding phase)

This is a second order system with the transfer function

$$\frac{i_o(s)}{i_c(s)} = \frac{(k_p/L)s + k_i/L}{s^2 + \left(R + k_p/L\right)s + k_i/L} \tag{4.3-8}$$

having natural frequency

$$\omega_n = \sqrt{\frac{k_i}{L}} \tag{4.3-9}$$

and damping ratio

$$\zeta = \frac{k_p + R}{2\sqrt{k_i L}} \tag{4.3-8}$$

By choosing the appropriate values for k_i and k_p, very high bandwidths for closed loop current (torque) response may be achieved (>500 Hz). In comparison to the achievable bandwidths for the outer velocity and/or position loops, the bandwidth of the current loop is generally about two orders of magnitude greater. This means that the current (torque) response is essentially instantaneous and therefore its dynamics may usually be ignored. Note also that the addition of the integrator has made this closed loop system a type one system. This, in turn, results in zero steady state error and a unity DC gain.

© ECP 1995, All rights reserved.

4.4 Multi-Tasking Environment

Digital control implementation is intimately coupled with the hardware and software that supports it. Nowhere is this more apparent than in the architecture and timing used to support the various data processing routines. A well prioritized time multi-tasking scheme is essential to maximizing the performance attainable from the processing resources.

The priority scheme for the ECP real-time Controller's multi-tasking environment is tabulated in Table 4.4-1. The highest priority task is the trajectory update and servo loop closure computation which takes place at the maximum rate of 1.131 KHz (minimum sampling period is 0.000884 seconds). In this case, the user may reduce the sampling rate through the Executive Program via changes to T_s in the **Setup Control Algorithm** dialog box.

The trajectory planning task has the third highest priority and is serviced at a maximum rate of 377 Hz. Here the parameters for a new trajectory need not be calculated every time this task is serviced by the real-time Controller. Whenever a new trajectory is required (i.e. the current trajectory is near its completion) this task is executed. The lower priority tasks are system house keeping routines including safety checks, interface and auxiliary analog output.

Table 4.4-1 The Multi-Tasking Priority Scheme of the Real-Time Controller

Priority	Task Description	Service Frequency
1	Servo Loop Closure & Command Update	1.31 KHz
2	Trajectory Planning	377 Hz
3	Background Tasks including User Interface, Auxiliary DAC Update, Limit checks etc.	Background (In time between other tasks)

The higher priority tasks always prevail over lower ones in obtaining the computational power of the DSP. This multi-tasking scheme is realized by a real-time clock which generates processor interrupts.

4.5 Sensors

There are two incremental rotary shaft encoders used in the Model 220. Each has a resolution of 4000 pulses per revolution. These encoders measure the incremental displacement of the motor and the load shaft.

© ECP 1995, All rights reserved.

The encoders are an optical type whose principle of operation is depicted in Figure 4.5-1. A low power light source is used to generate two 90 degrees out of phase sinusoidal signals on the detectors as the moving plate rotates with respect to the stationary plate. These signals are then squared up and amplified in order to generate quadrate logic level signals suitable for input to the programmable gate array on the real-time Controller. The gate array uses the A and B channel phasing to decode direction and detects the rising and falling edge of each to generate 4x resolution – see Figure 4.5-2.[1] The pulses are accumulated continuously within 24-bit counters (hardware registers). The contents of the counters are read by the DSP once every servo (or commutation) cycle time and extended to 48-bit word length for high precision numerical processing. Thus the accumulation of encoder pulses provides an angular position measurement (signal) for the servo routines.

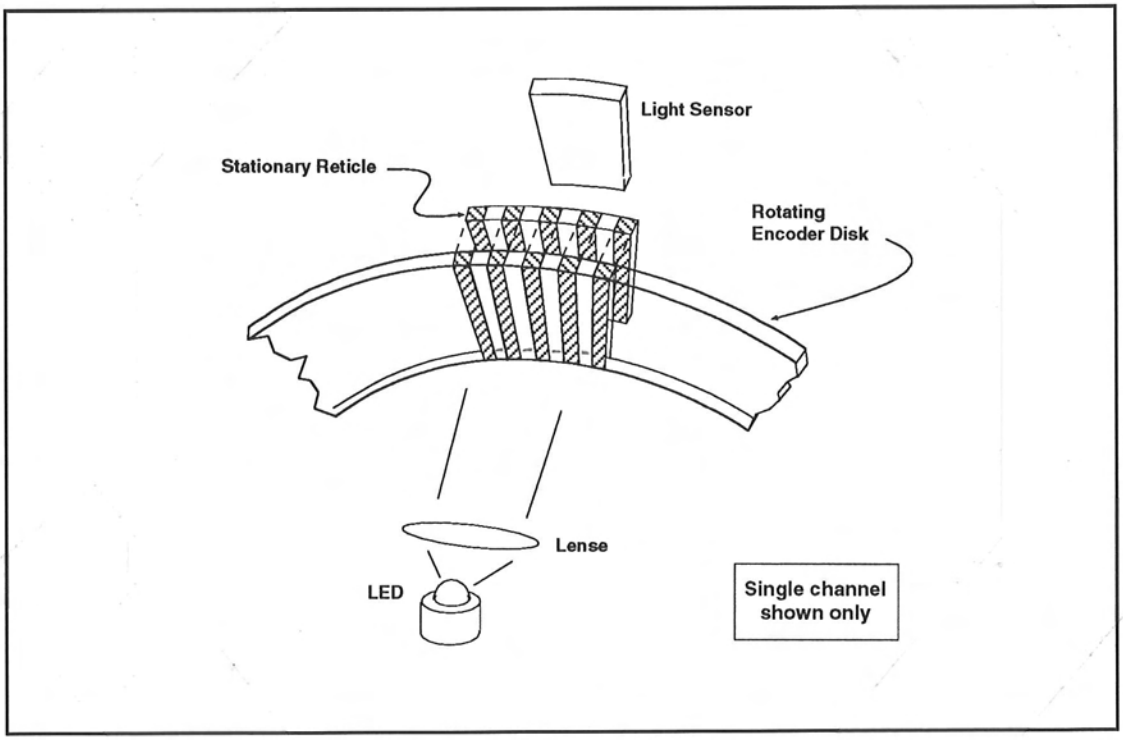

Figure 4.5-1 The Operation Principle of Optical Incremental Encoders

[1] I.e. the disk encoder resolution effectively becomes 16,000 counts per revolution.

© ECP 1995, All rights reserved.

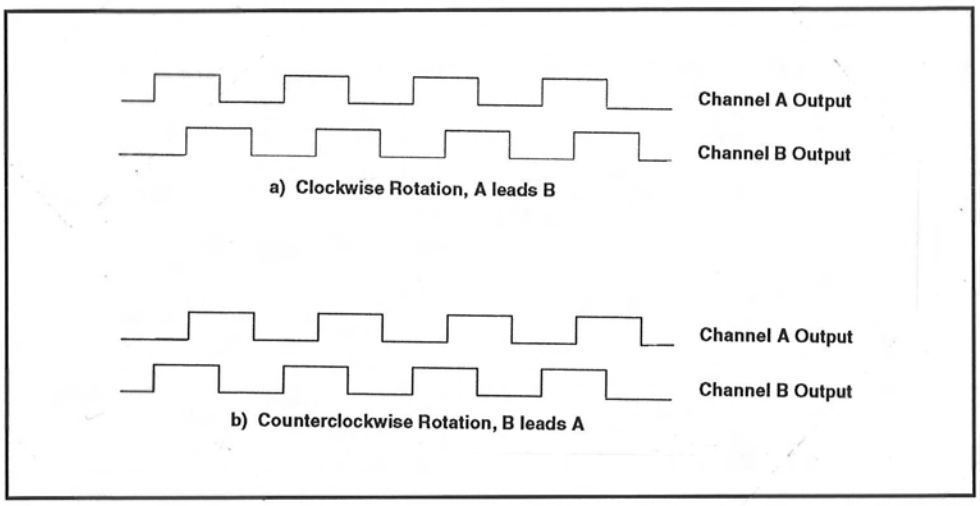

Figure 4.5-2. Optical Encoder Output

4.6 Auxiliary Analog Output

There are two analog output channels in the Control Box which are connected to two 16-bit DACs which physically reside on the real-time Controller. Each analog output has the range of +/- 10 volts (-32768 to +32767 counts) with respect to the analog ground. The outputs on these DACs are updated by the real-time Controller as a low priority task. However, for virtually all trajectories (e.g. for sine sweep up to approx. 25 Hz) the update rate is sufficiently fast for an oscilloscope or other analog equipment to inspect the various internal Controller signals. See the section on the Executive Program's **Utility** menu for the available signals to output on these DACs.

© ECP 1995, All rights reserved.

5. Plant Dynamic Models

This Chapter provides time and Laplace domain expressions which are useful for linear control implementation and are used in the experiments described later in this manual.

5.1 Rigid Body Plant

5.1.1 Basic Speed Ratio Effects

By inspection of Figure 5.1-1, the overall drive train gear ratio, *gr*, is such that $\theta_1 = gr\theta_2$, i.e.:[1]

$$gr = \frac{r_l r_{p1}}{r_{p2} r_d} \tag{5.1-1}$$

We shall refer to the partial gear ratio between the idler pulley assembly and the drive disk *gr'*, i.e.:

$$gr' = r_{p1}/r_d \tag{5.1-2}$$

so that $\theta_1 = gr'\theta_p$.

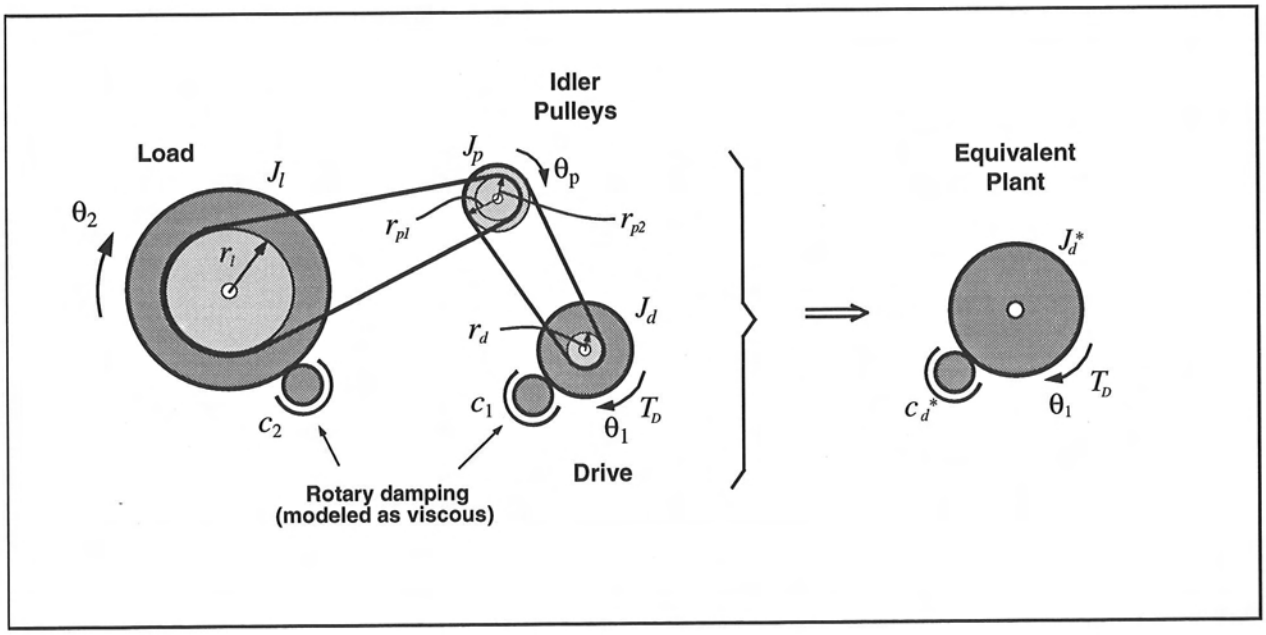

Figure 5.1-1. Rigid Body Plant Model

[1]Although the our mechanism does not use gears, we use the term "gear ratio" to refer to speed reduction because of its common usage in practice.

© ECP 1993, All Rights Reserved

If we call the torque acting on the load T_l, and equate this to the portion of the drive torque acting on the load, T_{Dl}, we have:

$$T_l = gr\,T_{Dl} \tag{5.1-3}$$

so that from

$$T_l = J_l \ddot{\theta}_l \tag{5.1-4}$$

we have

$$gr\,T_{Dl} = J_l \ddot{\theta}_l = J_l gr^{-1} \ddot{\theta}_d \quad \rightarrow \quad T_{Dl} = J_{lr} \ddot{\theta}_d \tag{5.1-5}$$

where

$$J_{lr} = J_l gr^{-2} \tag{5.1-6}$$

is the load inertia *reflected* to the drive or input.

The same squared scaling of inertia with speed ratio between elements holds in general. The drive inertia reflected to the load location, for example, is $J_{dr} = J_d gr^2$. We may then express for Figure 5.1-1:

$$J_d^* = J_d + J_p\, gr'^{-2} + J_l gr^{-2} \tag{5.1-7}$$

and

$$J_l^* = J_d\, gr^2 + J_p(gr/gr')^2 + J_l \tag{5.1-8}$$

where J_d^* and J_l^* are the total inertias reflected to the drive and load respectively.

Similarly for the friction coefficients it may be shown that[1]

$$c_d^* = c_1 + c_2 gr^{-2} \tag{5.1-9}$$

and

$$c_l^* = c_1 gr^2 + c_2 \tag{5.1-10}$$

where c_d^* *and* c_l^* are the total reflected friction constants at the drive and load.

5.1.2 Rigid Body Dynamics

For many applications involving servo drives, non-ideal effects such as drive flexibility, backlash, static and kinetic friction, and other nonlinearities are sufficiently small that the plant may be

[1] In this model we neglect the bearing friction at the speed reduction idler shaft.

© ECP 1995, All Rights Reserved

modeled as a simple rigid body obeying Newton's second law. That is, modeling friction effects as being viscous, from Figure 5.1-1 we may express:

$$J_d^* \ddot{\theta}_1 + c_d^* \dot{\theta}_1 = T_D \tag{5.1-11}$$

or:

$$J_l^* \ddot{\theta}_2 + c_l^* \dot{\theta}_2 = grT_D \tag{5.1-12}$$

which have the Laplace transforms:

$$\frac{\theta_1(s)}{T_D(s)} = \frac{1}{s(J_d^* s + c_d^*)} \tag{5.1-13}$$

$$\frac{\theta_2(s)}{T_D(s)} = \frac{gr}{s(J_l^* s + c_l^*)} \tag{5.1-14}$$

When friction may be neglected these reduce further to

$$J_d^* \ddot{\theta}_1 = T_D \tag{5.1-15}$$

$$J_l^* \ddot{\theta}_2 = grT_D \tag{5.1-16}$$

$$\frac{\theta_1(s)}{T_D(s)} = \frac{1}{J_d^* s^2} \tag{5.1-17}$$

$$\frac{\theta_2(s)}{T_D(s)} = \frac{gr}{J_l^* s^2} \tag{5.1-18}$$

5.2 Flexible Drive Dynamics

5.2.1 Equations Of Motion

An approximation of the emulator plant with flexibility in the drive train is shown in Figure A-1a . Using the free body diagram of Figure 5.2-1b and summing torques acting on J_l we have via Newton's second law (in its rotational form)[1]

[1]The term F_o in Figure 5.2-1 is the static tension in the flexible belt. It is assumed that this value is never exceeded during dynamic motion (i.e. that no section of the belt becomes slack).

© ECP 1995, All Rights Reserved

$$(F_1\text{-}F_2)r_l - c_2\dot{\theta}_2 = J_l\ddot{\theta}_2 \tag{5.2-1}$$

or

$$J_l\ddot{\theta}_2 + c_2\dot{\theta}_2 + 2k_{\mathcal{L}}(r_l\theta_2 - r_{p2}\theta_p)r_l = 0 \tag{5.2-2}$$

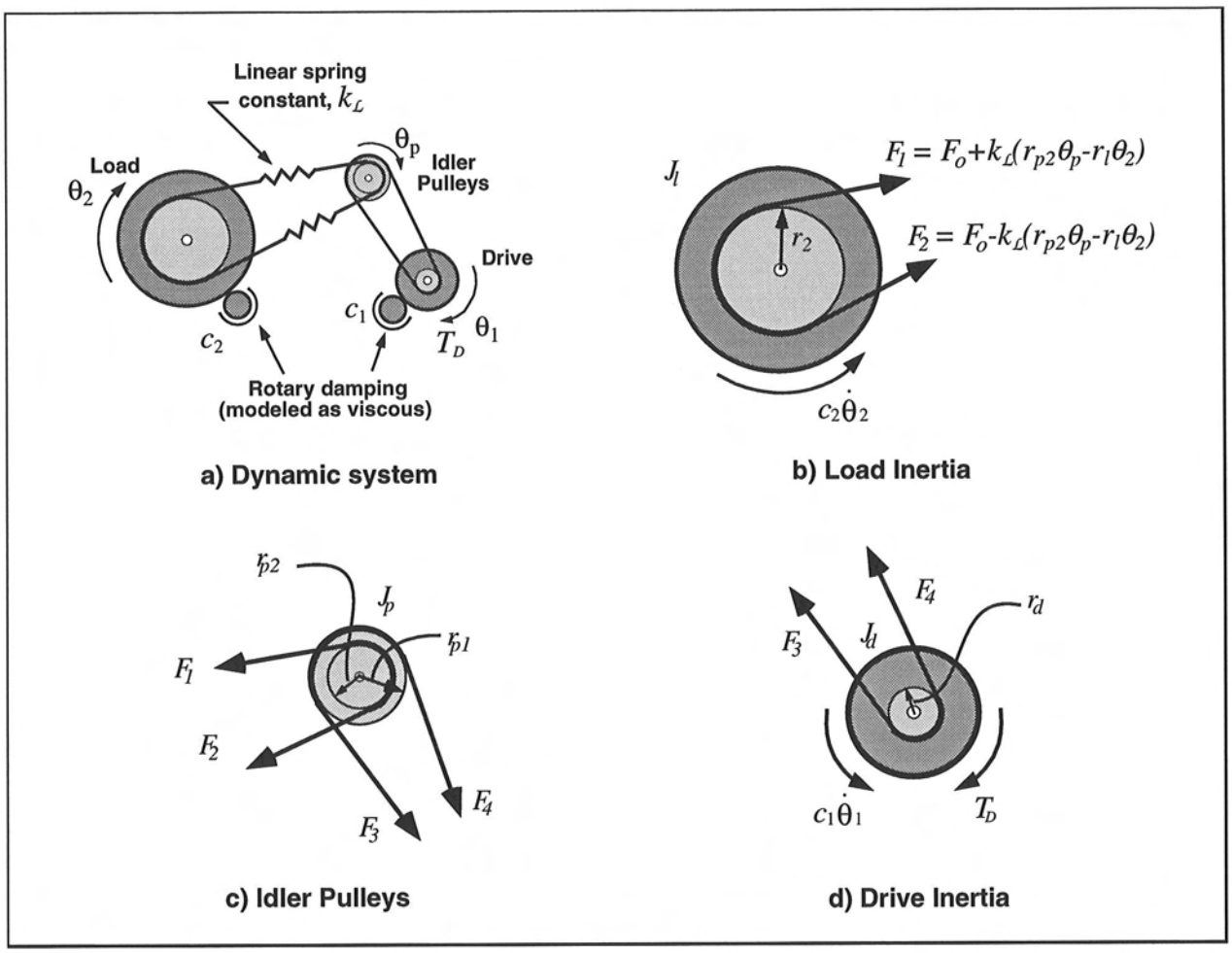

Figure 5.2-1. Plant Description And Free Body Diagrams For Dynamics Modeling

By defining a torsional (or rotary) spring constant

$$k \triangleq 2k_{\mathcal{L}}r_l^2 \tag{5.2-3}$$

Eq.(5.2-2) becomes:

$$J_l\ddot{\theta}_2 + c_2\dot{\theta}_2 + k(\theta_2 - r_{p2}/r_l\theta_p) = 0 \tag{5.2-4}$$

© ECP 1995, All Rights Reserved

For the idler (Fig. 5.2-1c) we have:

$$(F_2\text{-}F_1)r_{p2} + (F_4\text{-}F_3)r_{p1} = J_p\ddot{\theta}_p \tag{5.2-5}$$

or:

$$\begin{aligned}(F_4\text{-}F_3)r_{p1} &= J_p\ddot{\theta}_p + 2k_{\Delta}(F_1\text{-}F_2)r_{p2} \\ &= J_p\ddot{\theta}_p + 2k_{\Delta}\left(r_{p2}\theta_p\text{-}r_l\theta_2\right)r_{p2}\end{aligned} \tag{5.2-6}$$

For the drive inertia:

$$T_D + (F_3\text{-}F_4)r_d - c_1\dot{\theta}_1 = J_d\ddot{\theta}_1 \tag{5.2-7}$$

which combines with (5.2-6) as:

$$T_D - \frac{r_d}{r_{p1}}\left(J_p\ddot{\theta}_p + 2k_{\Delta}\left(r_{p2}\theta_p\text{-}r_l\theta_2\right)r_{p2}\right) - c_1\dot{\theta}_1 = J_d\ddot{\theta}_1 \tag{5.2-8}$$

Using (5.1-2 and 5.2-3) we have

$$\left(J_d+gr^{-2}J_p\right)\ddot{\theta}_1 + c_1\dot{\theta}_1 + k\left(r_{p2}\theta_p\text{-}r_l\theta_2\right)\frac{r_d r_{p2}}{r_{p1}r_l^2} = T_D \tag{5.2-9}$$

Finally, by defining

$$J_d^* \triangleq J_d+gr^{-2}J_p \tag{5.2-10}$$

equations (5.2-9, -4) yield, with obvious substitution, the desired equations of motion in two coordinates:

$$J_d^*\ddot{\theta}_1 + c_1\dot{\theta}_1 + k\left(gr^{-2}\theta_1\text{-}gr^{-1}\theta_2\right) = T_D \tag{5.2-11}$$

$$J_l\ddot{\theta}_2 + c_2\dot{\theta}_2 + k(\theta_2\text{-}gr^{-1}\theta_1) = 0 \tag{5.2-12}$$

In matrix notation we may express:

$$\boldsymbol{J}\ddot{\boldsymbol{\theta}} + \boldsymbol{c}\,\dot{\boldsymbol{\theta}} + \boldsymbol{k}\,\boldsymbol{\theta} = \boldsymbol{T} \tag{5.2-13}$$

where

$$\begin{gathered}\boldsymbol{\theta} = \begin{bmatrix}\theta_1 \\ \theta_2\end{bmatrix},\ \boldsymbol{J} = \begin{bmatrix}J_d^* & 0 \\ 0 & J_l\end{bmatrix},\ \boldsymbol{c} = \begin{bmatrix}c_1 & 0 \\ 0 & c_2\end{bmatrix}, \\ \boldsymbol{k} = k\begin{bmatrix}gr^{-2} & gr^{-1} \\ gr^{-1} & 1\end{bmatrix},\ \boldsymbol{T} = \begin{bmatrix}T_D \\ 0\end{bmatrix}\end{gathered} \tag{5.2-14}$$

© ECP 1995, All Rights Reserved

5.2.2 State Space Realization

A state space realization which is useful in several control approaches to this system follows directly from Eq 5.2-13. i.e.:

$$\dot{x} = Ax + BT(t)$$
$$Y = Cx \qquad (5.2\text{-}15)$$

where:

$$X = \begin{bmatrix} \theta_1 \\ \dot{\theta}_1 \\ \theta_2 \\ \dot{\theta}_2 \end{bmatrix}, \quad A = \begin{bmatrix} 0 & 1 & 0 & 0 \\ -k\,gr^{-2}/J_d^* & -c_1/J_d^* & k\,gr^{-1}/J_d^* & 0 \\ 0 & 0 & 0 & 1 \\ k\,gr^{-1}/J_l & 0 & -k/J_l & -c_2/J_l \end{bmatrix},$$

$$B = \begin{bmatrix} 0 \\ 1/J_d^* \\ 0 \\ 0 \end{bmatrix}, \quad C = \begin{bmatrix} C_1 & 0 & 0 & 0 \\ 0 & C_2 & 0 & 0 \\ 0 & 0 & C_3 & 0 \\ 0 & 0 & 0 & C_4 \end{bmatrix}$$

and $C_i = 1$ (i=1,2,3,4) when X_i is an output and equals 0 otherwise.

5.2.3 Transfer Functions

From the Laplace transform of Eq's(A.2-8,9) we have:

$$\frac{\theta_1(s)}{T_D(s)} = \frac{J_l s^2 + c_2 s + k}{D(s)} \qquad (5.2\text{-}16)$$

$$\frac{\theta_2(s)}{T_D(s)} = \frac{k/gr}{D(s)} \qquad (5.2\text{-}17)$$

where:

$$D(s) = J_d^* J_l s^4 + \left(J_d^* c_2 + J_l c_1\right)s^3 + \left(J_d^* k + J_l gr^{-2} k + c_1 c_2\right)s^2 + \left(c_1 k + c_2 gr^{-2} k\right)s \qquad (5.2\text{-}18)$$

© ECP 1995, All Rights Reserved

The above models are useful when the plant parameters J_x, k_x & c_x are known or are measurable explicitly. In many cases, the plant is identified via its natural frequencies, damping ratios, and gains. The above transfer function types may also be expressed in the form:

$$\frac{\theta_1(s)}{T(s)} = \frac{K_1\left(s^2 + 2\zeta_z\omega_z s + \omega_z^2\right)}{s\left(s+c^*\right)\left(s^2 + 2\zeta_p\omega_{p1} s + \omega_p^2\right)} \tag{5.2-19}$$

$$\frac{\theta_2(s)}{T(s)} = \frac{K_2}{s\left(s+c^*\right)\left(s^2 + 2\zeta_p\omega_{p1} s + \omega_p^2\right)} \tag{5.2-20}$$

where the gains K_1 & K_2, are nominally equal to $1/J_d^*$ and $k/(grJ_d^*J_l)$ respectively (but may be measured more directly in some cases). The coefficient c^* is nominally equal to $c/(J_d^*+J_l)$ where c is the damping (modeled as viscous) associated with the scaled rigid body mode (i.e. the mode where the rotating members move uniformly without oscillatory motion).
Measurement of parameters to establish the explicit plant transfer functions for the Model 220 plant is covered in Section 6.1 of this manual.

5.2.4 Damping In Flexible Drive

In systems where the flexible element contains a significant fraction of the plant damping, it may be useful to include this damping in the plant model. An example of where such damping may arise is when the flexible element is a drive belt[1] such as the one in the Model 220 apparatus employed specifically to impart drive flexibility. Figure 5.2-1 depicts the approximation used to derive the dynamic model.

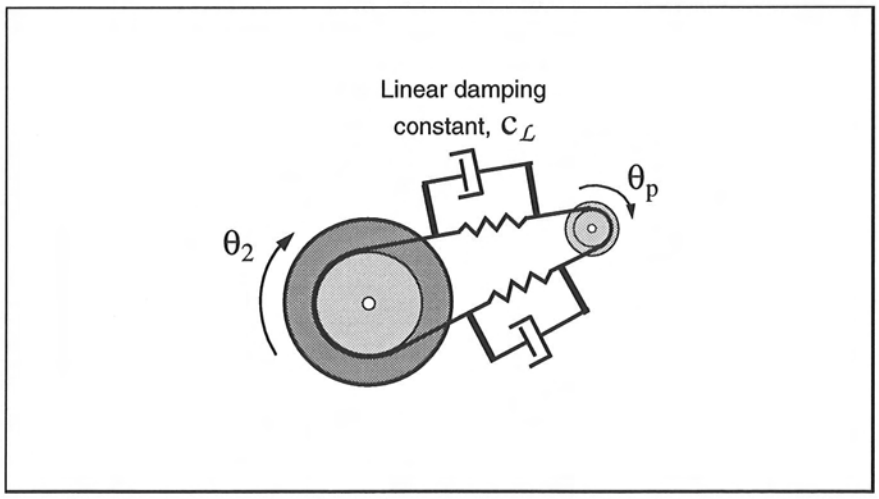

Figure 5.2-1. Model of Flexible Drive Damping

[1]Metallic drive elements on the other hand typically have very low material damping and this added model complexity would be of no value.

© ECP 1995, All Rights Reserved

By performing the dynamic analysis according to the steps in Section 5.2.1 and defining

$$c_{12} \triangleq 2c_{\mathcal{L}} r_l^2 \tag{5.2-21}$$

The following equations of motion are obtained.

$$J_d^* \ddot{\theta}_1 + (c_1 + gr^{-2} c_{12})\dot{\theta}_1 - gr^{-1} c_{12}\dot{\theta}_2 + k\left(gr^{-2}\theta_1 - gr^{-1}\theta_2\right) = T_D \tag{5.2-22}$$

$$J_l \ddot{\theta}_2 + (c_2 + c_{12})\dot{\theta}_2 - gr^{-1} c_{12}\dot{\theta}_1 + k(\theta_2 - gr^{-1}\theta_1) = 0 \tag{5.2-23}$$

Which have the state space realization form of Eq.(5.2-15) with

$$A = \begin{bmatrix} 0 & 1 & 0 & 0 \\ -kgr^{-2}/J_d^* & -(c_1 + c_{12}gr^{-2})/J_d^* & kgr^{-1}/J_d^* & c_{12}gr^{-1}/J_d^* \\ 0 & 0 & 0 & 1 \\ kgr^{-1}/J_l & c_{12}gr^{-1}/J_l & -k/J_l & -(c_2 + c_{12})/J_l \end{bmatrix} \tag{5.2-24}$$

and all else unchanged.

The transfer functions become.

$$\frac{\theta_1(s)}{T_D(s)} = \frac{J_l s^2 + (c_2 + c_{12})s + k}{D(s)} \tag{5.2-25}$$

$$\frac{\theta_2(s)}{T_D(s)} = \frac{(k + c_{12})/gr}{D(s)} \tag{5.2-26}$$

where

$$\begin{aligned} D(s) = {} & J_d^* J_l s^4 + \left(J_d^*(c_2 + c_{12}) + J_l(c_1 + c_{12}gr^{-2})\right)s^3 \\ & + \left(J_d^* k + J_l gr^{-2} k + c_1 c_2 + c_1 c_{12} + c_{12} c_2 gr^{-2}\right)s^2 + \left(c_1 k + c_2 gr^{-2} k\right)s \end{aligned} \tag{5.2-27}$$

The inclusion of the coupled friction c_{12}, is not necessary in many practical applications. It does render better agreement between simulation and system test results however when it is included in the dynamic model of the Model 220 apparatus.

© ECP 1995, All Rights Reserved

6. Experiments

This chapter presents experiments which identify the plant parameters, implement a variety of control schemes, and demonstrate many important control principles. The versatility of this software / hardware system allows for a much broader range of experimental uses than will be described here and the user is encouraged to explore whatever topics and methodologies may be of interest – subject of course to your school and laboratory guidelines and the safety notations of this manual. The safety portion of this manual, Section 2.4, must be read and understood by any user prior to operating this equipment.

The instructions in this chapter begin at a high level of detail so that they may be followed without a great deal of familiarity with the PC system interface, and become more abbreviated in details of system operation as the chapter progresses. To become more familiar with these operations, it is strongly recommended that the user read Chapter 2 in its entirety prior to undertaking the operations described here. Remember here, as always, it is recommended to save data and control configuration files regularly to avoid undue work loss should a system fault occur.

6.1 System Identification

In this section, the inertia, gain, and damping of the various system components are found indirectly by measuring their effect on system response characteristics. In these tests, we will close a proportional plus rate feedback loop about the drive feed back encoder (Encoder #1). The corresponding block diagram is shown in Figure 6.1-1 and has the output/input transfer function:

$$\mathbf{c}(s) = \frac{\theta_1(s)}{r(s)} = \frac{k_p k_{hw}/J}{s^2+(c+k_d k_{hw}/J)s + k_p k_{hw}/J} \qquad (6.1\text{-}1)$$

© ECP 1995, All Rights Reserved

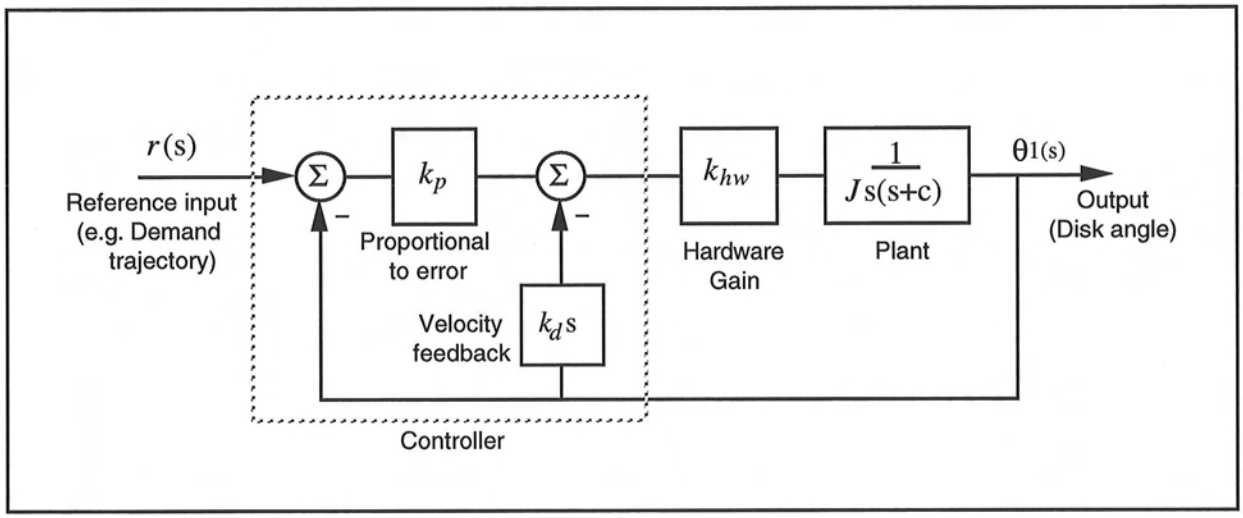

Figure 6.1-1. Controller Configuration for Plant Identification

which has the form of the classical second order system:

$$\mathbf{c}(s) = \frac{\omega_n^2}{s^2+2\zeta\omega_n s+\omega_n^2} \tag{6.1-2}$$

where

$$\omega_n \triangleq \sqrt{\frac{k_p k_{hw}}{J}} \tag{6.1-3}$$

is called the system *natural frequency,* and

$$\zeta \triangleq \frac{1}{2\omega_n}\left(\frac{c+k_d k_{hw}}{J}\right) \tag{6.1-4}$$

is the system *damping ratio.* When the plant friction (modeled here as viscous) is negligible compared to that supplied by k_d, the damping ratio takes on the familiar form

$$\zeta \approx \frac{k_d k_{hw}}{2J\omega_n} = \frac{k_d k_{hw}}{2\sqrt{J k_p k_{hw}}} \tag{6.1-5}$$

The so-called hardware gain, k_{hw},[1] of the system is comprised of the product:

$$k_{hw} = k_c k_a k_t k_e k_s \tag{6.1-6}$$

[1]It contains software gain also. This software gain, k_s is used to give higher controller-internal numerical resolution and improves encoder pulse period measurement for very low rate estimates.

© ECP 1995, All Rights Reserved

where:

k_c, the DAC gain, = 10V / 32,768 DAC counts
k_a, the Servo Amp gain, = approx. 2 (amp/V)
k_t, the Servo Motor Torque constant = approx. 0.1 (N-m/amp)
k_e, the Encoder gain, = 16,000 pulses (counts) / 2π radians
k_s, the Controller Software gain, = 32 (controller input counts / encoder or ref. input counts)[1]

Hence, k_{hw} has the *dimensions* of torque but is more precisely expressed in *units* of [(N-m / rad) * (controller input count) / (DAC count)]. In this section we shall measure k_{hw} directly.

In the model above the inertia J must be *reflected* to the sensor output location. In the work that follows, we use the following notation for the reflected inertia to the motor for each of the test cases shown in Table 6.1-1:

$$J^*_{d\,i} = (J_{dd} + J_{dl} + J_{wdi} + J_{wli} + J_{pi})_{\text{reflected}} \quad , \text{i = Test Case number} \tag{6.1-7}$$

where:

J_{dd} is the inertia of the bare drive disk plus the drive motor, encoder, drive disk/motor belt and pulleys
J_{dl} is the inertia of the bare load disk plus the disturbance motor, encoder, load disk/motor belt and pulleys
J_{wdi} is the inertia associated with the brass weights at the drive disk.
J_{wli} is the inertia associated with the brass weights at the load disk.
J_{pi} is the inertia associated with the pulleys in the SR assembly.

Since reflected inertia of a given component is proportional to the square of the ratio of its speed to the motor speed (can you show this?), Eq 6.1-7 becomes:

$$J^*_{d\,i} = J_{dd} + J_{wdi} + J_{pi}\,(n_{pd}/12)^2 + (J_{dl} + J_{wli})(n_{pl}/n_{pd}/6)^2 \tag{6.1-8}$$

Where the last term is the overall gear ratio squared. Similarly we have for the damping constant, c, that damping at the load, c_2 is reduced by $(n_{pl}/n_{pd}/6)^2$ when reflected at the drive.

Using the above relationships, we are prepared to measure system parameters.

[1]Controller counts are those that are actually operated on in the control algorithm. i.e. The reference input (trajectory) counts and encoder counts are multiplied by 32 prior to control law execution.

© ECP 1995, All Rights Reserved

Table 6.1-1. Test Cases For Plant Identification And Other Experiments

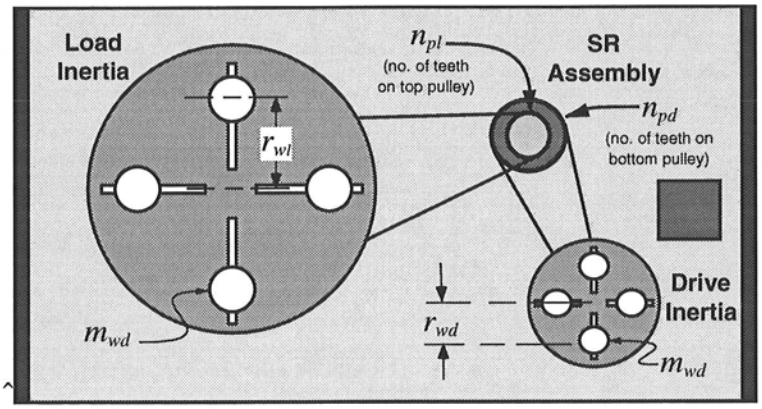

Test Case	n_{pd}	n_{pl}	m_{wd} (kg)	r_{wd} (cm)	m_{wl} (kg)	r_{wl} (cm)	Description
1	N/A	N/A	4x .500	5.0	0	N/A	Drive Inertia only. Belt to SR assembly pulleys disconnected.
2	N/A	N/A	4x .200	5.0	0	N/A	Drive Inertia only. Belt to SR assembly pulleys disconnected.
3	N/A	N/A	0	N/A	0	N/A	Same as case #1 except brass weights removed from drive inertia disk.
4	18	72	0	N/A	0	N/A	1.5:1 overall speed reduction. No brass weights on either disk.
5	18	72	4x .200	5.0	0	N/A	1.5:1 overall speed reduction. Brass weights on drive disk only.
6	18	72	4x .200	5.0	4x .500	10.0	1.5:1 overall speed reduction. Brass weights on both disks
7	72	18	4x .200	5.0	0	N/A	24:1 overall speed reduction. Brass weights on drive disk only.
8	72	18	4x .200	5.0	4x .500	10.0	24:1 overall speed reduction. Brass weights on both disks
9	72	18	0	N/A	4x .500	10.0	24:1 overall speed reduction. Brass weights on load disk only.
10	18	24	2x .200	5.0	4x .500	10.0	4.5:1 overall speed reduction. 2 brass weights on drive disk, 4 on load disk .
11	24	36	0	N/A	4x .500	10.0	4:1 overall speed reduction. Brass weights on load disk only.
12	24	36	4x .200	5.0	4x .500	10.0	4:1 overall speed reduction. Brass weights on both disks.

© ECP 1995, All Rights Reserved

We first measure the hardware gain, k_{hw} via acceleration of a known inertia, then find the unknown inertias by measuring ω_n under closed loop feedback.

6.1.1 Gain Measurement

Calculate the total inertia at the drive disk when four 500 g (includes attachment bolts and nuts) weights are attached as described in Test Case 1 in Table 6.1-1. The following data apply:

a. Brass weight diameter = 4.95 cm.

b. Thickness of drive disk plate = 0.47 cm. Diameter of drive disk = 13.21 cm. $\rho_{aluminum} = 2.71$ g/cm^3. (neglect the cutout slots – you may wish to verify that their inertia contribution is negligible)

c. From manufacturer specifications, the motor inertia, $J_{motor} = 3.8*10^{-5}$ kg-m^2. (Note that the motor to drive disk gear ratio is 1.)

You may neglect the inertia of the encoder, and the belt and pulleys between the motor and the drive disk.

Procedure:

1. Turn off power to the Controller box (red button) and temporarily remove the plexiglass safety cover on the mechanism. Loosen the SR assembly clamp screw and remove the belt connecting the SR assembly to the drive inertia disk. Secure four 500 g weights at 5.0 cm radius on the drive disk. Verify that the masses are secured per Section 2.2.2 and that each is at a center distance of 5.0 cm from the shaft center-line. Be certain that the plexiglass safety cover is securely installed before proceeding.

2. Select user units under the **Set-up** menu to be **counts**. With the controller powered up (both the Controller box and the host PC), enter the **Control Algorithm** box under the **Set-up** menu and set **T_S=0.002652 s**. Enter the **Command** menu, go to **Trajectory** and select **Step, Set-up**. Select **Open Loop Step** and input a step size of **2.0 volts**, a duration of **200 ms** and **1 repetition**. Go to **Set up Data Acquisition** in the **Data** menu and select **encoder #1** as data to acquire and specify data sampling every **5** (five) servo cycles[1] (I.e. every 5 T_S's). Select **OK** to exit. This sets up the system to accelerate the drive disk with 2.0 V input to the servo amplifier for 200 ms forward then backward while acquiring Encoder #1 position data every 13 ms.

3. Select **Execute** from the **Command** menu and select **Run**. The drive disk will accelerate forward, then return. Encoder data is collected to record this response. Select **Set-up Plot** from the **Plotting** menu and choose **Encoder #1 Velocity** then select **Plot Data**. You will see approximately linear positive and negative slopes in the velocity response. (It is possible to read this value directly by plotting encoder #1 acceleration. This data, obtained by double numerical differentiation, is typically fairly noisy however. The student may want to verify this by observing the acceleration plot).

[1]Here there is no servo cycle per se since the system will be operated open loop. Data sampling is at a moderate frequency to avoid excessive noise in the subsequent velocity measurement obtained via numerical differentiation.

© ECP 1995, All Rights Reserved

4. Carefully measure the time difference and the velocity difference through the linear section of both the positive and negative going curves.[1] Obtain the acceleration (counts/s^2) by dividing the velocity difference by the time difference in each case; then take the average of the two values. From $T = J\ddot{\theta}$, we have (the student should verify the validity of this expression):

$$2V^{*}k_a k_t k_e = J_{dtest}{}^{*}\textit{acceleration measured in Step 4}$$

where J_{dtest} is the total inertia at the disk calculated at the beginning of this section. Calculate $k_a k_t k_e$ and hence determine k_{hw} via Eq (6.1-6).

6.1.2 Inertia Measurement

In this procedure, a frequency measurement technique is utilized to first measure the previously calculated load disk inertia (Steps b and c at the beginning of the previous section). The technique is then applied to find the unknown load disk inertia.

Procedure:

1. Turn off power to the Controller box (red button) and temporarily remove the plexiglass safety cover on the mechanism. Place the mechanism in the Test Case #3 configuration (Table 1.1-1). Be certain that the plexiglass safety cover is securely installed before proceeding.

2. With the controller powered up (both the Controller box and the host PC), enter the **Control Algorithm** box under the **Set-up** menu and set **T_S=0.002652 s** and select **Continuous Time Control**. Select **PI With Velocity Feedback** and **Set-up Algorithm**. Enter the k_p **= 0.5** and k_d **= 0.001** ($k_i = 0$) and select **OK**.

   In this and all future work, be sure to stay clear of the mechanism before doing the next step. Selecting **Implement Algorithm** immediately implements the specified controller; if there is an instability or large control signal[2], the plant may react violently.

   Select **Implement Algorithm**, then **OK**.

   If the system appears stable after implementing the controller, first displace the disk with a light, non sharp object (e.g. a plastic ruler) to verify stability prior to touching plant

3. Enter the **Command** menu, go to **Trajectory** and select **Step, Set-up**. Select **Closed Loop Step** and input a step size of **1000 counts**, a duration of **1000 ms** and **1 repetition**. Exit to the Background Screen by consecutively selecting **OK**. This puts the controller board in a mode for performing a pair of closed loop steps (one forward then one backward) of one second duration. This procedure may be repeated and the duration adjusted to vary the maneuver and data acquisition period.

---

[1] For more precise measurement you may "zoom in" on this region of the plot using **Axis Scaling** in the **Plotting** menu.

[2] E.g. a large error at the time of implementation.

© ECP 1995, All Rights Reserved

4. Go to **Set up Data Acquisition** in the **Data** menu and select **encoder #1** and **Commanded Position** as data to acquire and specify data sampling every **1** (one) servo cycles (I.e. every T_s. Usually it is not necessary to acquire data at such a high frequency. Here however we wish to have high resolution data to make fairly precise measurements of the response frequencies.). Select **OK** to exit. Select **Zero Position** from the **Utility** menu to zero the encoder positions.

5. Select **Execute** from the **Command** menu and select **Run**. The drive disk will step, oscillate, and attenuate, then return. Encoder data is collected to record this response. Select **OK** after data is uploaded.

6. Select **Set-up Plot** from the **Plotting** menu and choose **Encoder #1 Position** then select **Plot Data**. You will see the drive disk time response similar to that shown in Figure 6.1-1.

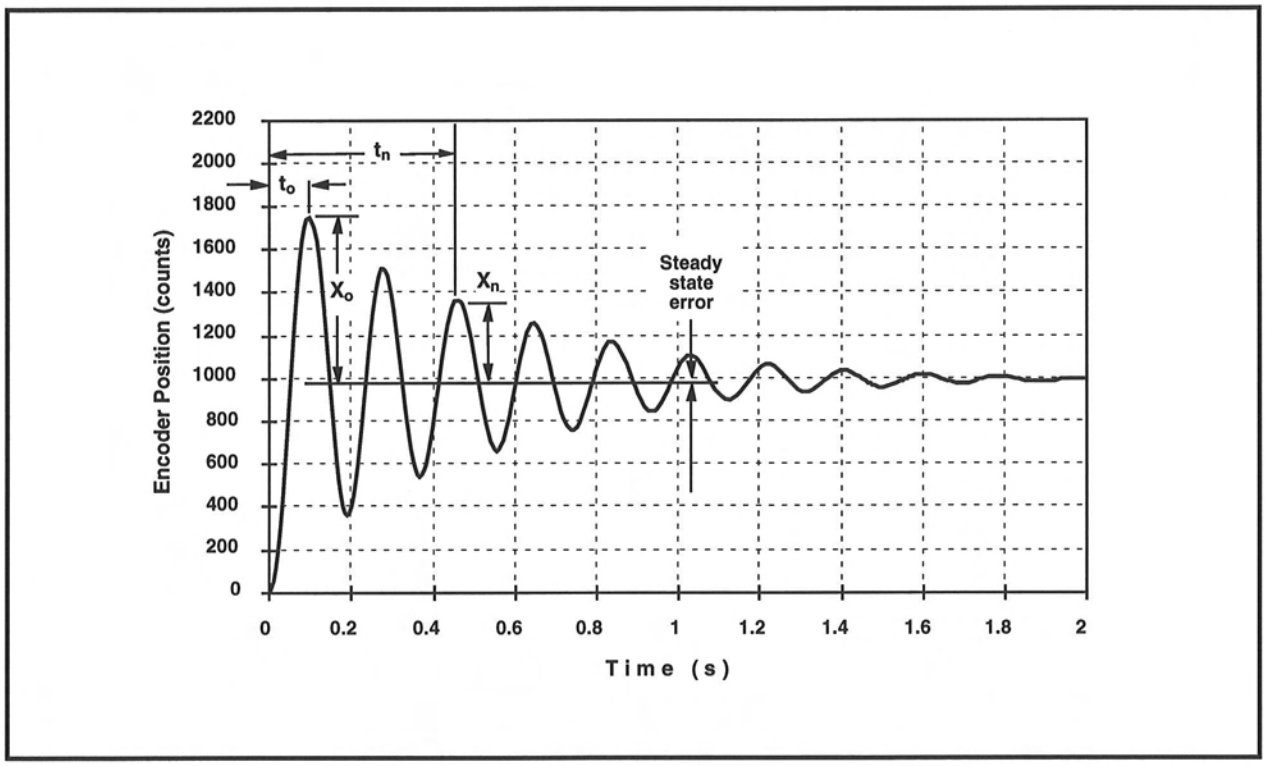

Figure 6.1-2. Typical Step Response for ω_d and ζ Measurement

7. Measure the amplitude and time to peak of the first one or two consecutive cycles as shown in Figure 6.1-2 (The smaller amplitude of the later cycles become dominated by nonlinear friction effects and do not reflect the salient system dynamics. From a stability point of view it is conservative to use the lower indicated damping of the higher amplitude cycles.) Measure the reduction from the initial cycle amplitude X_0 to the last cycle amplitude X_n for the n cycles. For

© ECP 1995, All Rights Reserved

more precise measurements you may "zoom in" to the area of interest in the plot via **Axis Scaling** under **Plotting.**[1]

The following relationship is associated with the *logarithmic decrement* for underdamped second order systems:

$$\frac{\zeta}{\sqrt{1-\zeta^2}} = \frac{1}{2\pi n} \ln\left(\frac{X_o}{X_n}\right) \tag{6.1-9}$$

For small ζ this expression becomes

$$\zeta \approx \frac{1}{2\pi n} \ln\left(\frac{X_o}{X_n}\right) \tag{6.1-10}$$

Solve for ζ_3 (where "3" denotes Test Case 3) by first estimating it via Eq (6.1-10) then solving Eq (6.1-9) by trial and error[2].

8. Divide the number of cycles, n, by the time taken to complete them (t_n - t_o). Convert the resulting frequency in Hz to radians/sec. This *damped frequency*, ω_d, is related to the *natural frequency*, ω_n, according to:

$$\omega_n = \frac{\omega_d}{\sqrt{1-\zeta^2}} \tag{6.1-11}$$

which becomes

$$\omega_n \approx \omega_d \tag{6.1-12}$$

for lightly damped systems. Hence determine ω_{n3}.

Close the graph window by clicking on the left button in the upper right hand corner of the graph. This will collapse the graph to icon form where it may later be brought back up by double-clicking on it.

9. Set up the system as shown in Test Case #4. Make certain that the belt pulleys are properly tightened -See Section 2.2 for instructions. Repeat Steps 1 through 8 for Test Case 4. You will need to increase the trajectory duration in Step 3 to ≥2000 ms to satisfactorily view the lower frequency motion.

Note: It is recommended that test cases be run with the drive disk (and hence the drive actuator) in the same clocked position so that any non-ideal torque characteristics (e.g. cogging torque) are common to each test.

---

[1]For an even more precise measurement, the data may be examined in tabular numerical form – see **Export Raw Data,** Section 2.1.7.3. This is not generally necessary though if the data curves are sufficiently magnified using **Axis Scaling.**

[2]Two significant digit precision is sufficient here and may often be obtained via Eq (6.1-9) for the lightly damped cases such as test case #1 and #2 but is imprecise for other more highly damped system tests.

© ECP 1995, All Rights Reserved

10. Having found k_{hw} in Section 6.1.1, use the result of Step 8 to solve Eq (6.1-3) for J_{dd}. How does the experimentally derived value compare with the calculated value from Steps b and c at the beginning of Section 6.1.1? The pulley inertias may be obtained using the same technique as the above. Their values have been found to be those listed in Table 6.1-2. Based on these values and your measurement of J_{dd} determine $(J_{dl})_{\text{reflected}}$ from the results of Step 9 and hence find J_{dl}.

Table 6.1-2 SR Pulley Inertia Values

Number of Pulley Teeth	Pulley Inertia, J_{pl} or J_{pd} (kg-m^2)
18 tooth	$3 * 10^{-6}$
24 tooth	$8 * 10^{-6}$
36 tooth	$3.9 * 10^{-5}$
72 tooth	$5.5 * 10^{-4}$
Backlash device (incl. attachment screws) – add to J_p	$3.1 * 10^{-5}$

From the above we have the system hardware gain k_{hw} and the unknown inertia components J_{dd}, J_{dl}, and J_p. Since J_{wd} and J_{wl} are easily calculated for a given setup of the brass weights, the system inertia is readily found via Eqs.(5.1-7, -8) for an arbitrary system configuration.[1]

6.1.3 Damping Measurement

Use the ζ of Step 7 in 6.1.1 for Case #4 and Eq (6.1-4) to determine the plant damping coefficient c_4.[2] Note that since the damping is largely the result of belt/pulley friction, its value will vary from set-up to set-up and should be measured for each specific configuration when an accurate plant model is necessary. Note also that a substantial portion of the friction is Coulomb rather than viscous as the model implies. By using measurements taken at relatively high speeds however (e.g. the use of the first rather than last several cycles in Step 7) the resulting "equivalent" viscous friction is conservatively low. In subsequent control cases where control torques are large relative to friction torques (e.g. when $k_d k_{hw}/J >> c$ for PD control) then the damping constant c may be neglected.

---

[1] A more straightforward (and generally more accurate) method of determining net system inertia (reflected to the motor) is to perform Steps 1 through 8 on the mechanism in its identical inertia and speed reduction configuration for later controls testing. This method however is not useful when either drive flexibility or backlash are introduced.

[2] This method will not yield reliable measurement of c for the light friction in Cases 1 & 2.

© ECP 1995, All Rights Reserved

6.1.4 Flexible Drive Measurements

In this procedure, frequency and damping ratio measurements are used to determine the equivalent torsional spring constant, k, of the flexible drive (elastomer belt) and the resulting damping constant, c_2, at the load disk.

This procedure is necessary only if flexible drive control (e.g. Section 6.4) studies are to be undertaken.

Procedure:

1. Disconnect the drive power cord from the mechanism. Keep drive power disconnected for the remainder of this procedure.

2. Set the mechanism in the Test Case #11 configuration with the flexible belt installed between the SR assembly and the load. (see Section 2.2.2.4 for installing the flexible drive belt). Install the drive clamp[1] to immobilize the drive disk.

3. Enter the **Control Algorithm** box under the **Set-up** menu and set T_s = **0.002652 s** and select **Implement**. Enter the **Command** menu, go to **Trajectory** and select **Step, Set-up**. Select **Closed Loop Step** and input a step size of **0 counts**, a duration of **2500 ms** and **1 repetition**. Exit to the Background Screen. This provides for collecting 2.5 s of data without commanded motion.

   Go to **Set up Data Acquisition** in the **Data** menu and select **Encoder #2** as data to acquire and specify data sampling every **1** (one) servo cycles Select **OK** to exit. Select **Zero Position** from the **Utility** menu to zero the encoder positions.

   Prepare to manually displace the load disk approximately 10 deg. With the load disk displaced approximately 10 deg in either direction, select **Run** from the **Execute** box and release the disk approximately 1 second later. Plot the Encoder #2 response.

4. Use the method described in Section 6.1.2 Steps 7& 8 to determine the ω_n and ζ.

5. Using the relationships

$$\omega_n = \sqrt{\frac{k}{J}} \tag{6.1-13}$$

$$\zeta = \frac{c}{2J\,\omega_n} \tag{6.1-14}$$

   and the previously calculated load inertia, J_l, calculate k and c and hence c_{12}. (See Eq.(5.2-21) for definition of c_{12}).

[1]The aluminum spacer and 0.25" bolt that clamps between the brass weight attachment slots on the drive disk and the 0.25" hole in the mechanism base plate.

© ECP 1995, All Rights Reserved

6.2 Rigid Body PD & PID Control

This experiment demonstrates some key concepts associated with proportional plus derivative (PD) control and subsequently the effects of adding integral action (PID). Such a control, acting on plants modeled as rigid bodies, finds broad application in such diverse fields as machine tools, automobiles (cruise control), and spacecraft (attitude and gimbal control). The block diagram for forward path PID control of a rigid body is shown in Figure 6.2-1[1] where friction is neglected.[2] The closed loop transfer function is:

$$c(s) = \frac{\theta(s)}{r(s)} = \frac{(k_{hw}/J)(k_p s + k_i)}{s^3 + (k_{hw}/J)(k_d s^2 + k_p s + k_i)} \tag{6.2-1}$$

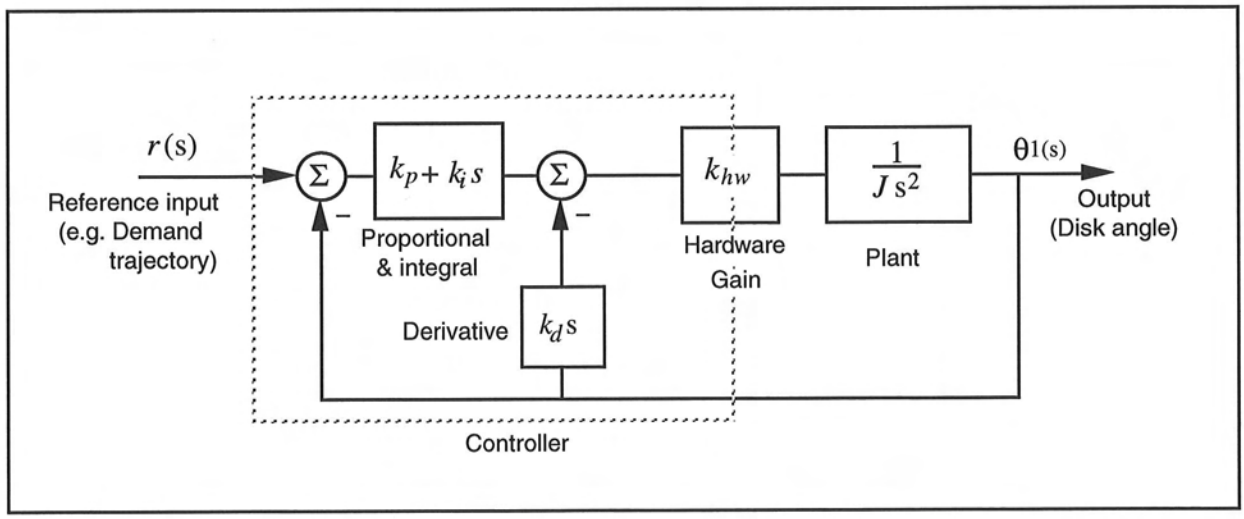

Figure 6.2-1. Rigid Body PID Control – Control Block Diagram

---

[1]Another common form of PID control in which the derivative term is in the forward path is shown below with its transfer function:

$$c(s) = \frac{\theta(s)}{r(s)} = \frac{(k_{hw}/J)(k_d s^2 + k_p s + k_i)}{s^3 + (k_{hw}/J)(k_d s^2 + k_p s + k_i)}$$

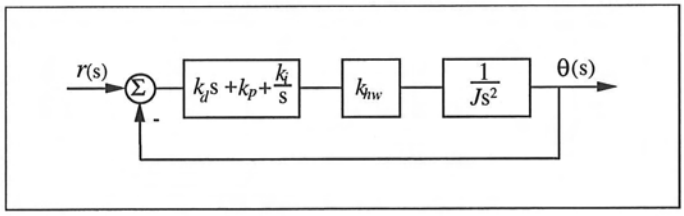

This form has generally better tracking performance but can lead to high instantaneous control effort. We chose the form shown in Figure 6.2-1 to more clearly demonstrate the classical properties of the PID denominator roots as the control parameters are varied.

[2]The student may want to later verify that for the relatively high amount of control damping in the scheme that follows – induced via the parameter k_d – the plant damping is very small.

© ECP 1995, All Rights Reserved

For the first portion of this exercise we shall consider PD control only ($k_i = 0$) which reduces the closed loop system to:

$$\mathbf{c}(s) = \frac{\theta(s)}{r(s)} = \frac{(k_{hw}/J)(k_d s + k_p)}{s^2 + (k_{hw}/J)(k_d s + k_p)} \tag{6.2-2}$$

As before, we define:

$$\omega_n \triangleq \sqrt{\frac{k_p k_{hw}}{J}} \tag{6.2-3}$$

$$\zeta \triangleq \frac{k_d k_{hw}}{2J\omega_n} = \frac{k_d k_{hw}}{2\sqrt{J k_p k_{hw}}} \tag{6.2-4}$$

so that we may express:

$$\mathbf{c}(s) = \frac{\omega_n^2}{s^2 + 2\zeta\omega_n s + \omega_n^2} \tag{6.2-5}$$

The effect of k_p and k_d on the roots of the denominator (damped second order oscillator) of Eq (6.2-2) shall considered in the work that follows.

6.2.1 Effects of k_p and k_d Independently

Procedure :

1. Using the results of Section 6.1 construct a dynamic model of the plant with hardware gain (i.e. k_{hw}/Js^2)) when configured as described in Test Case 2 of Table 6.1-1.

2. Set-up the apparatus in the Test Case 2 configuration. Verify that the plexiglass safety cover is in place and the brass weights are securely fastened - see Section 2.3.

3. From Eq (6.2-3) determine the value of k_p ($k_d = 0$) so that the system behaves like a 2 Hz spring-inertia oscillator.

4. Set-up to collect **Encoder #1** data via the **Set-up Data Acquisition** box in the **Data** menu. Set up a closed-loop step of **0 (zero)** counts, dwell time = **5000 ms**, and **1 (one)** rep (**Trajectory** in the **Command** menu). This puts the controller board in a mode for acquiring 10 sec of data on command while the control system will maintain regulation ($r(s) = 0$). This procedure may be repeated and the duration adjusted to vary the data acquisition period.

5. Enter the **Control Algorithm** box under **Set-up** and set **T_s=0.000884 s** and select **Continuous Time Control**. Select **PI with Velocity Feedback** and **Set-up**

© ECP 1995, All Rights Reserved

Algorithm. Enter the k_p value determined above for 2 Hz oscillation (k_d & k_i = 0, do not input values greater than $kp = 0.2$[1]) and select **OK**.

Stay clear of the mechanism and select **Implement Algorithm**.

6. Enter **Execute** under **Command**. Prepare to manually rotate the drive disk roughly 60 deg. Select **Run**, rotate about 60 deg. and release disk. Do not hold the rotated disk position for longer than 1-2 seconds as this may cause the motor drive thermal protection to open the control loop.

7. Plot encoder #1 output (see Step 6 Section 6.1). Determine the frequency of oscillation. What will happen when proportional gain, k_p, is doubled? Repeat Steps 5 & 6 and verify your prediction. (Again, for system stability, do not input values greater than $kp = 0.2$). Noting that the units of k_p are [DAC counts / controller input counts], what are the units of $k_p k_{hw}$?

8. Determine the value of the derivative gain, k_d, to achieve $kdkhw = 0.05$ N-m/(rad/s).[2]. Repeat Step 5, except set[3] **T_S=0.006188 s** and input the above value for k_d and set k_p & $k_i = 0$. Do not input values greater than $k_d = 0.05$.

9. After checking the system for stability by displacing it with a ruler, manually move the disk back and forth to feel the effect of viscous damping provided by k_d. Do not excessively coerce the disk as this will again cause the motor drive thermal protection to open the control loop.

10. Repeat Steps 8 & 9 for a value of k_d five times as large (Again, $k_d \leq 0.05$). Can you feel the increased damping? What are the units of $k_d k_{hw}$?

6.2.2 PD Control Design

1. From Eq's (6.2-3,-4) design controllers (i.e. find k_p & k_d) for a system natural frequency $\omega_n = 4$ Hz, and three damping cases: 1) $\zeta = 0.2$ (under-damped), 2) $\zeta = 1.0$ (critically damped), 3) $\zeta = 2.0$ (over-damped).[4]

---

[1]Here due to friction, the system remains stable for small k_p. For larger values, the time delay associated with sampling causes instability.

[2]For the discrete implementation you must divide the resulting value by T_S for the controller input value Here, since the PD controller is improper, the backwards difference transformation: $s = (1-z^{-1})/T_S$ is used.

[3]Here we increase the sample period (still a relatively low value) to avoid noise from numerical differentiation. In Step 5 we used a very small period to essentially eliminate any time delay effects on the closed loop frequency. These issues are studied in Section 6.3.

[4]Recall that for discrete implementation, you must divide the k_d values by T_S for controller input.

© ECP 1995, All Rights Reserved

2. Implement the underdamped controller (T_s = 0.00442 s)and set up a trajectory for a 2000 count closed-loop Step with 1500 ms dwell time and 1 rep.

3. Execute this trajectory and plot the commanded position and encoder position (Plot them both on the same vertical axis so that there is no graphical bias.)

4. Repeat Steps 2 & 3 for the critically damped and over-damped cases. Save your plots for later comparison. Does the response agree with that expected for a damped second order system. How does the response compare with that of a classical spring/mass/damper system with the natural frequency and damping ratios specified in Step 11?

6.2.3 Adding Integral Action

1. Compute k_i such that $k_i k_{hw}$ = 5 N-m/(rad-sec).[1] Implement a controller with this value of k_i and the critically damped k_p & k_d parameters from Step 11. (Do not input $k_i > 0.4$). Be certain that the following error seen in the background window is within 20 counts prior to implementing (if not, chose **Zero Position** from the **Utility** menu). Execute a 2500 count closed-loop step of 2000 ms duration (1 rep). Plot the encoder #1 response and commanded position.

2. Increase k_i by a factor of two, implement your controller (do not input k_i >0.4) and plot its step response. Manually displace the disk by roughly 5 deg. Can you feel the integral action increasing the restoring control torque with time? (Do not hold for more than 5 seconds to avoid excessive torque build-up.) What happens when you let go?

3. Review the above two plots and the critically damped plot ($k_i = 0$) of Step 14. What is the integral action's effect on steady state error? Explain this in terms of the Final Value Theorem. How does integral action affect overshoot?

6.2.4 Tracking Response

In this section we consider the characteristic tracking response of PD and PID control with the differentiator in the forward (as per the footnote at the beginning of Section 6.2) and return (as per Fig. 6.2-1) paths. Important differences in tracking characteristics and control effort are seen.

1. Set up the mechanism as in the previous sections (Test Case #2). Using T_s = 0.00442 s implement a PI with velocity feedback controller ($k_i = 0$) using k_p and k_d for ω_n = 4 Hz and critical damping (step 1 of Section 6.2.2). Set up to collect data (**Setup Data Acquisition, Data menu**) every 4 servo cycles.

---

[1]For discrete implementation you must multiply the resulting value of k_i by T_s before inputting into the controller.

© ECP 1995, All Rights Reserved

2. Set up a closed loop ramp trajectory with **Distance = 8000 counts, Velocity = 20,000 counts/sec, and Dwell Time = 400 ms.** Execute this maneuver, collect data and plot **Commanded Position, Encoder #1 Position**, and **Control Effort**. Save your plot.

3. Repeat steps 1 and 2 with $k_i k_{hw}$ = 3 N-m/(rad-s). Repeat steps 1 and 2 using forward path PID control (**PID**, under **Setup Control Algorithm**), first with k_i = 0, then with $k_i k_{hw}$ =3 N-m/(rad-s).[1]

4. (Optional) Setup a closed loop parabolic trajectory with **Distance = 8000 counts, Velocity = 40,000 counts/sec, Acceleration = 300 ms and Dwell Time = 200 ms.** Implement forward path PD control using k_p and k_d from step 1 ($k_i = 0$). Execute this maneuver, collect and plot the same data as in step 2.

5. Describe the error to the ramp trajectory in each case (except for step 4). Explain the difference between k_d in the forward and return paths in terms of the theoretical steady state error to a unit ramp input for each case. Does either case overshoot? Why? What was the effect of adding integral action on overshoot with k_d in the forward path and in the return path? Why? Compare and explain the differences in control effort in all cases. How does the parabolic trajectory of step 4 compare to the others in terms of tracking and control effort? Why?

6.2.5 Frequency Response (Sine Sweep)

In this section we consider the characteristic frequency response[2] of the under- over- and critically damped systems with k_d in the return path[3]. We then consider the case when k_d is placed in the forward path.

1. Set up the mechanism as in the previous sections. Using T_s = 0.00442 s implement a PI with velocity feedback controller ($k_i = 0$) using k_p and k_d step 1 of Section 6.2.2 (use ζ=0.2 for the first trial). Set up to collect (**Setup Data Acquisition, Data menu**) every 4 servo cycles.

2. Set up a closed loop sine sweep trajectory with **Amplitude = 500 counts, Start Frequency = 0.1 Hz, End Frequency = 10 Hz and Sweep Time = 30 s.** Execute this maneuver, collect data (to keep the collected data file size from becoming large you may wish to acquire only Encoder #1 position data) and plot, **Encoder #1 Position**. Save your plot.[4]

3. Repeat steps 1 and 2 with ζ = 1.0 and 2.0. Repeat steps 1 and 2 using forward path PID control (**PID**, under **Setup Control Algorithm**) and ζ = 1.0. Here you will need to reduce the sine sweep input trajectory amplitude to 250 counts to avoid drive saturation at higher frequencies.

---

[1]Can you hear the difference in the drive (due to peak control effort) between the responses with forward path and return path differentiators?

[2]What is seen here is actually a pseudo-frequency response since the change in frequency with time imparts a component of transient response. Frequency response is the response at constant frequency and hence is approached for sufficiently slow changes in frequency.

[3]We first consider the case with k_d in the return rather than forward path because it more clearly shows the effect of damping on the characteristic roots.

[4]For the underdamped case, you may want to repeat and sweep slowly through the frequencies in the resonant band to get a more precise resonant frequency estimate.

© ECP 1995, All Rights Reserved

4. (Optional) Repeat steps 1 and 2 (k_d in the reverse path) with $k_i k_{hw}$ = 10 N-m/(rad-s).
5. What is the resonant frequency of the underdamped case and how does it compare with theoretical predictions for an underdamped oscillator? Compare the various frequency responses and explain their differences in terms of their asymptotic Bode response characteristics and S-plane roots.

6.3 Fundamentals of Servo Control

In this section we consider the effects of changes in parameters and of certain properties that are present in most control systems and in all digitally controlled mechanical systems. These effects have implications to design and analysis of the mechanism, control hardware and control scheme. While the work in this section shall include only PD, PID and simple filter control, the effects studied have implications to all practical control methodologies.

In some cases we shall control the system about the drive disk and in some about the load disk. The former is referred to as *collocated* control since the sensor and actuator are rigidly coupled and hence kinematically lie at the same location. The latter potentially involves flexibility, backlash, and drive nonlinearity between the actuator and sensor and is referred to as *noncollocated* control.

In the instructions that follow it is assumed that the user has become familiar with the apparatus and the ECP Executive interface software so that detailed instructions are unnecessary in most cases. The safety related procedures described in the previous two experiments (6.1 & 6.2) and in Section 2.3 must be strictly followed at all times.

6.3.1 Effect of Gear Ratio and Inertia

Gear ratio and inertia have fundamental effects on the system dynamics since they effectively scale the system gain. In the procedure that follows these relationships are demonstrated experimentally. Gear ratio and inertia effects also are coupled with many of the other effects studied in Section 6.3 and will be redressed in later experiments.

Procedure:

1. Set-up the system in the configuration of Test Case 6 of Table 6.1-1 (1.5:1 gear ratio). Setup to collect data every 1 servo cycle. Utilizing the underdamped PD controller of Experiment 6.2.2 with T_s = 0.00884 s, execute a 2000 count Step of 2500 ms duration. Compare the response with that from the Experiment 6.2.2 underdamped case. Save your plot. Measure the damped natural frequency ω_d and, using Eqs (6.1-9, -11), calculate ω_n and ζ for both cases.

© ECP 1995, All Rights Reserved

Now change the gear ratio to 24:1 and repeat the above procedure and calculations for Test Cases 8 and 9 of Table 6.1-1.[1]

2. How do the responses from Step 1 compare with the Experiment 6.2.2 underdamped response? Explain this result in terms of the effect of gear ratio on reflected inertia and hence on system gain. Based on the measured values of inertia from 6.3.1 what are the predicted values of ω_n and ζ? Compare these with the measured values.

3. In many practical systems the feedback sensor (in some cases there are additional ones elsewhere) is placed at the load output. This generally allows more precise control of the load position or rate. What is the effect of gear ratio on effective system open loop gain, if the control loop is closed about the load position? (e.g. for the Model 220 apparatus, if encoder #2 is used).

6.3.2 Effect of Friction

Friction exists to some extent in all practical mechanical systems. It may be modeled as being a combination of static and Coulomb (kinetic) and viscous types. Coulomb and static friction are often of greater magnitude than viscous and exacerbate the control design problem in that they are nonlinear. In small amounts they may actually help to stabilize a system, but are generally deleterious to tracking and regulation performance[2]. In this section we consider the effect of Coulomb and static friction at the load output and the dependence of performance on gear ratio and sensor location.

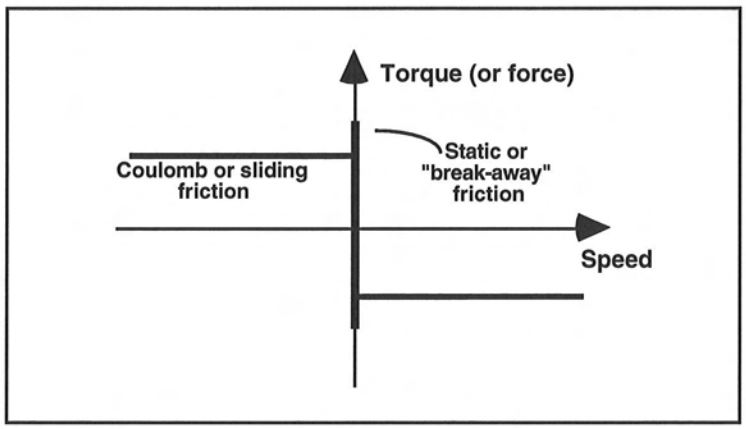

Figure 6.3-1. Simplified Model of Static and Coulomb Friction

1. Assure that power to the Controller Box is turned off. Turn the apparatus on its side so that the inertia disks are vertical and the underside is accessible. Tighten the friction brake clamp so that approximately 0.5 N-m of friction torque is applied to the load shaft when it rotates. This may be achieved by placing a single 500 g brass weight at r=10 cm on the load disk. With the weight roughly horizontal relative to the load shaft, adjust the clamp such that the load disk

[1]For test case 9 you should reduce the servo sample period to T_S = 0.000884 s to more closely approximate the continuous time response and to improve acquired data resolution.

[2]In precision mechanisms for servo control, there is often a premium (higher cost) placed on low friction linkages.

© ECP 1995, All Rights Reserved

rotates very slowly (or rotation is initiated by very slight downward force on the weight). I.e. the friction torque is approximately equal to the torque generated by gravity acting on the weight. Do not over tighten the friction adjustment screw. Only light torque is needed to achieve the desired friction. Over-tightening can damage the clamp and lead to stalling of the motor and potential amplifier burnout.

2. Configure the mechanism according to Test Case #5. Power up the Controller Box. Input the following PD gains in the **PI with Velocity Feedback** dialog box: $k_p = 0.16$, $k_d = 0.025$. Choose Encoder #1 for feedback and implement the control. Make certain that the encoder positions are nearly zero (within say 10 counts – use **Zero Position** in the **Utility** menu if necessary). Perform a ramp maneuver with 3000 count distance, 7500 count/s velocity, and 2500 ms dwell. Plot and save the Encoder #2 (load) position response

3. Determine the gain correction necessary to keep the same nominal closed loop control performance when using the load output sensor (Encoder #2) as the feedback sensor. Correct k_p and k_d accordingly and input these gains under **PI with Velocity Feedback** choosing Encoder #2 for feedback. Implement the controller and perform a ramp with 2000 count distance, 5000 count/s velocity, and 2500 ms dwell. (nominally the same motion as in Step 2) and again plot the Encoder #2 output. Compare the output with that of Step 2.

4. Repeat Step 2 for the plant in the Test Case #7 configuration using the gains: $k_p = 0.068$, $k_d = 0.011$.[1] Repeat step 3.

5. For many control applications it is desirable to control the position of the load. Compare the results of the above with respect to the response at the load including the steady state error in each case. Which scheme is most effective in reducing steady state error? Explain. The *static servo stiffness* (k_{ss}) is the steady state torque (or force for rectilinear systems) generated at the output (load disk) for a unit static displacement. It has units identical to those of a torsional spring. Compute k_{ss} in N-m/rad for each of the above controllers. For the purposes of this computation, consider the output to be the load (Encoder #2) in each case.[2]

6. Adding Integral Action (Optional). Repeat Step 3 Test Case #5 except now add $k_i = 0.8$. You may want to increase the step duration to say 20 s. for the system to reach steady state. Compare this response with the those of Step 4 and explain the differences. What are the static servo stiffness and steady state error here?

Very Important: Verify that the friction brake has been released before proceeding

[1]The gains in steps 2, 3, and 4 provide the same ω_n & ζ (~2 Hz, critically damped) for each gear ratio and output and hence provide the same *nominal* performance. The student may wish to verify this by inspecting the step response shape and rise time in each case with the brake action removed.

[2]Hint: For cases where the output is Encoder #1, you will need to reflect the stiffness to Encoder #2.

© ECP 1995, All Rights Reserved

6.3.3 Effect of Disturbances

In most servo applications, an important requirement of the control design is that it reject forces or torques that tend to disturb the system from its intended set point or tracking trajectory. Examples of disturbances include motor cogging torque, gravity induced loads on the kinematic linkage, interactions with the payload inertia (e.g. material added or removed from a conveyor) and interaction with other operating equipment or control axes (e.g. tool drag on a lathe spindle).

In this section we shall consider the effect of slow spatially dependent disturbances as well as low and high frequency time dependent ones. While these effects are studied in the context of tracking and regulation separately, the tracking results are extendible to regulation and vice versa.

Slow disturbances during tracking (Effect of gear ratio)

1. Set up a spatially dependent sinusoidal disturbance (**Sinusoidal (theta)**, under **Disturbance, Command** menu) of 1.0 volt, 8 cycles/rev., 10,000 ms duration. Input the k_p and k_d values from Step 3 of Section 6.3.2 for the Test Case #5 configuration using **PID** (not **PI with Velocity Feedback**) control and Encoder #2 for feedback. With the mechanism set as per Test Case #5, perform a 8000 count ramp maneuver at 2000 counts/s velocity with dwell time of 1000 ms. Make sure that you check the box labeled "Include sinusoidal disturbance" when commanding the system to execute the trajectory. Plot and save the Commanded Position and Encoder #2 data.
2. Repeat Step 1 for Test Case #7 using the k_p and k_d values from Step 4 of Section 6.3.2 under load sensor feedback (Encoder #2).
3. Are the differences in disturbance rejection between the low and high gear reduction configurations what you might expect based on the results of Section 6.3.2? Although we have not shown it here explicitly, which sensor configuration (collocated or noncollocated) would you expect to be more effective in rejecting low frequency disturbances?

Disturbances during regulation (Effect of disturbance frequency)

In this subsection, we consider the performance of three distinct controller designs in rejecting low and higher frequency disturbances. The plant should be setup as per Test Case #10.

4. The three controllers are as follows:
   a) PD control with ω_n = 2 Hz and ζ = 0.707, and feedback at Encoder #1[1]. I.e. kp = 0.08, kd = 0.009

[1]Here we use collocated feedback since the drive flexibility becomes significant and couples with the system dynamics in testing the higher frequency disturbances. Methods for dealing with flexibility using noncollocated control schemes are studied later in this chapter.

© ECP 1995, All Rights Reserved

b) Same as "a" plus added integral action: $k_i = 1.0$.

c) Same as "a" plus a cascaded lead/lag filter with the following specifications: Zero at 0.2 Hz, Pole at 1.0 Hz, DC gain = 1.

Design the lead/lag filter for controller "c". (Hence find n_o, n_1, d_o, and d_1 in $F(s) = (n_o+n_1 s)/(d_o+d_1 s)$

5. Set up a time dependent sinusoidal disturbance (**Sinusoidal (time)**) of 0.5 volt, 0.1 Hz, 40,000 ms duration. (You should reduce the data acquisition sampling frequency to say once every 20-50 servo cycles to avoid an unnecessarily large data file). Input the k_p and k_d values for controller "a" under **PID** control using Encoder #1 for feedback with $T_s = 0.00442$ s. With the mechanism set as per Test Case #10, perform a 0 (zero) count closed loop step of 30,000 ms duration and 1 repetition. This sets the system up to acquire data during closed loop regulation. Execute this regulation for controllers "a" and "b" above making sure to check the box labeled "Include sinusoidal disturbance" when commanding the system. Plot and save encoder #2 data.

6. Input controller "c" via **PID + Notch** in the **Setup Control Algorithm** box. Execute the same regulation with disturbance as in Step 5, again plotting and saving your data.

7. Repeat Steps 5 and 6 with the disturbance frequency changed to 2.0 Hz. You may reduce the step duration to 10 s and increase the data acquisition frequency to every 5-10 servo cycles.

8. Consider the block diagram of Figure 6.3-2. Derive the open loop transfer function

$$\frac{N_{ol}(s)}{D_{ol}(s)} = K(s)\, k_{hw} P(s) \qquad (6.3\text{-}1)$$

and closed loop transfer function $\theta_1(s) / T_d(s)$ for each controller. Plot the Bode response for the open and closed loop transfer functions in each case. Explain the disturbance attenuation characteristics of each controller in terms of their Bode response.

© ECP 1995, All Rights Reserved

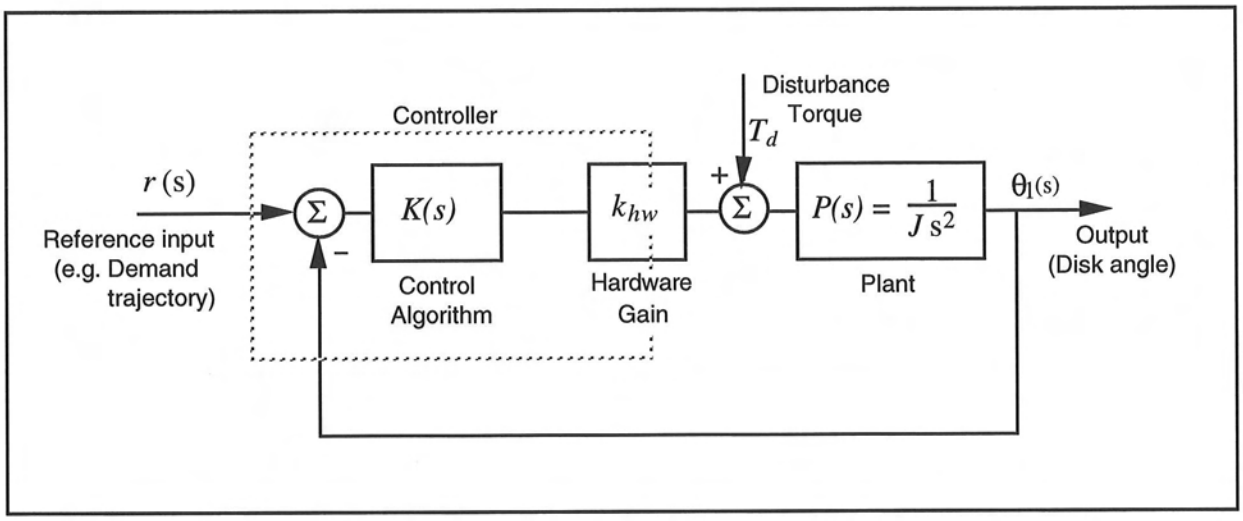

Figure 6.3-2 Disturbance Torque Input To Rigid Body Control Scheme

6.3.4 Effect of Drive Saturation

Saturation is when the output of a device is held at some positive (negative) value for all input values above (below) some limit. This is illustrated in Figure 6.3-3 which depicts the input/output relationship for an otherwise linear device. Saturation may occur due to the control effort signal exceeding the range or capability of the DAC, servo amplifier, or even the sustainable magnetic field of the actuator. In practice however the amplifier and actuator are selected to accept full scale DAC voltage or the control electronics are programmed such that the DAC output saturates below control magnitudes that would saturate or damage other drive components.[1]

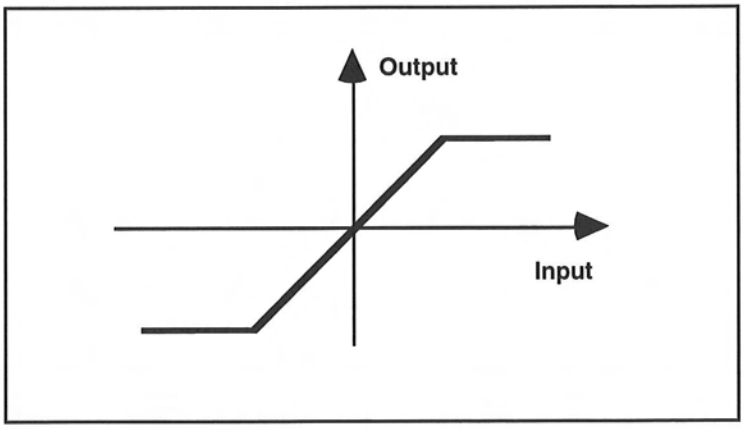

Figure 6.3-3. Linear Device Saturation

[1]In either case, the DAC is generally programmed to saturate below or at its full scale output. Without programmed saturation the DAC, which typically accepts two's-complement input numbers, would output full scale voltage of reverse polarity upon exceeding its input range. This would clearly be disastrous!

© ECP 1995, All Rights Reserved

Gear Ratio Effect & Characteristic Response Shape

1. Set up the mechanism inertias as follows:

   Load inertia: Four 500 g weights at 10 cm radius.
   Drive inertia: Two 200 g weights at 4 cm radius.

   The three controllers and gear ratios listed in Table 6.3-1 will be considered.

Table 6.3-1. Parameters for First DAC Saturation Tests

Gear Ratio, gr	Proportional Gain, k_p	Derivative Gain, k_d
1.5:1	0.54	0.075
4.5:1	0.30	0.040
24:1	0.75	0.10

   The parameters shown have been designed to provide 2 Hz natural frequency and a damping ratio of 1[1] for the three gear ratio cases. The student should may wish to verify by analysis or by observing a small (say 1000 count) step response that the nominal performance is equivalent in each case

2. Set up the mechanism in one of the three gear ratios shown in Table 6.3-1 and implement the corresponding PD controller via in the **PI with Velocity Feedback** dialog box. Choose Encoder #2 for feedback and T_s = 0.00442.[2] Perform a 5000 count step of 1500 ms duration and plot and save the Control Effort and Encoder #2 position responses. (Plot these on separate vertical axes for better data resolution.) You may also want to plot Commanded Position on the same axis as Encoder #2. Repeat this process for the remaining two gear ratios in Table 6.3-1

3. Measure rise time to 90% of peak (use actual position output peak, not commanded peak) What is the shape of the position trace during saturation? Plot Encoder #2 velocity and control effort. Is the shape of the velocity curve during saturation what you would expect? Explain.

4. Consider the following expression regarding available torque and acceleration:

$$\ddot{\theta}_{max} = \frac{T_{max}}{J} \qquad (6.3\text{-}2)$$

[1]Here the k_d values have been reduced form their nominal values to reflect the apparatus damping coefficient, c, for each configuration.
[2]Data sampling ever 4 servo cycles is recommended.

© ECP 1995, All Rights Reserved

where T_{max} is the torque available at saturation. For accelerating the payload (or "load") we have[1]:

$$\left(\ddot{\theta}_{max}\right)_{load} = \frac{T_{max}\,(gr)}{J_l + J_d(gr)^2} \tag{6.3-3}$$

Use calculus maxima/minima techniques to solve Eq. (6.3-3) for the gear ratio, expressed in terms of J_l and J_d, that provides the greatest load acceleration. Given that the load and drive inertias for the tests in this section are approximately J_l = 0.0271 kg-m^2 and J_d = 0.00108 kg-m^2, qualitatively explain the degree of saturation for the three test cases.

Qualitative Changes in Step Response For High Bandwidth Controller

5. Remove the belt from the drive disk to the SR assembly so that the load disk is decoupled. Remove the brass weights from the drive disk. Thus setup the apparatus as per Test Case #3. Implement the following parameters under **PID** control (not **PI with Velocity Feedback**): k_p = 0.011, k_d = 0.0015. These correspond to ω_n = 2 Hz and ζ = 1.0. Perform a 1000 count step maneuver, then a 16,000 count maneuver. Sample data every 1 servo cycle. Plot and save the Control Effort and Encoder #1 position responses. Repeat the 16,000 count step using the same control gains but using **PI with Velocity Feedback**.

6. Describe the differences in the response of the forward path differentiating (**PID**) controller and explain in terms of DAC saturation. How does its shape in the large amplitude response compare with that of the backwards path differentiating controller? (Note that since the backwards path differentiator did not saturate its smaller amplitude response is essentially identical to its large amplitude one)

6.3.5 Effect of Discrete-time Sampling

With modern high speed data processing capability, sampling rates are often high enough that control may be analyzed and implemented using continuous time analytical methods. In cases where either the objective control bandwidth is high, the control processor is otherwise heavily burdened, or economic considerations require lower speed processing capability, sample rate may be sufficiently low that its effect is significant.

Of particular interest is the phase lag due to the time delay associated with sampled data systems. Such time delays propagate from signal sampling and holding in ADC conversion of analog feedback sensors (not the case for the Model 220 system) and in the control algorithm itself. Further time delay and phase lag results from DAC conversion of control effort and in the analog servo amplifier. While a detailed analysis of the associated time delay is beyond the scope of this exercise, the phase lag associated with discrete time sampling is on the order of that of a pure time delay of length equal to the sample period, T_s. Such a delay, denoted here as $\phi(s)$, is expressed in the Laplace domain as:

[1]Here we do not consider the relatively mall inertia of the drive pulleys and other components.

© ECP 1995, All Rights Reserved

Here we shall consider the effect of the position measurement quantization of the feedback encoders. The discrete encoder position measurement may be operated on by high bandwidth control law terms such as the backwards differentiator in discrete-time PD control which can result in quantization noise. The backwards differentiator approximates angular rate as

$$\omega_n \cong \frac{\theta_n - \theta_{n-1}}{T_s} \tag{6.3-7}$$

where θ_n is the current encoder measurement and θ_{n-1} is the immediately prior one. Calling the encoder measurement resolution Δ_θ, the backwards difference rate quantum, Δ_ω, becomes

$$\Delta_\omega = \frac{\Delta_\theta}{T_s} \tag{6.3-8}$$

The associated incremental control torque T_{Δ_ω} is

$$T_{\Delta_\omega} = k_d \Delta_\omega k_{hw} = \frac{k_d \Delta_\theta k_{hw}}{T_s} \tag{6.3-9}$$

As T_{Δ_ω} becomes large, a single encoder pulse (which can occur at infinitesimal rates) can cause relatively high instantaneous control effort. This propagates through the system causing high frequency motion in the sensed position further causing high instantaneous torque – i.e. noise is propagated.

From Eq.(6.3-9) torque (or control effort) quantization increases with reduced encoder resolution.[1] For a given encoder, the torque quantization and hence torque noise increases with increased derivative[2] gain and with reduced sampling period.

Procedure

1. Set up the mechanism as per Test Case #2. Input the following parameters under **PI with Velocity Feedback**: $k_d = 0.02$, $k_p = 0$, $k_i = 0$ (i.e. the controller will implement a pure backwards differentiator) Set $T_s = 0.00442$ s. Before proceeding, note the following:

   If at any time in this experiment excessive noise occurs, shut down open the control loop immediately via **Abort Control**. Any sustained operation with high frequency noise (and/or high torque) can cause loosening or other damage of drive components.

[1] Eq.(6.3-9) should not be viewed as a predictor of noise onset. Many other effects such as system bandwidth, mechanical flexibility, and nonlinear behavior all influence noise propagation and generally have a different effect at different sampling frequency. For a given system and controller, however, high frequency torque (or control effort) quantization is often a dominant factor in quantization noise propagation.

[2] Or more generally with increased high bandwidth gain.

© ECP 1995, All Rights Reserved

$$\phi(s) = e^{-sT_s} \tag{6.3-6}$$

In the frequency domain, its phase angle is:

$$\arg\left(\phi(j\omega)\right) = -T_s\omega \tag{6.3-7}$$

where T_s is in seconds, and $\arg\left(\phi(j\omega)\right)$ and ω are in consistent angular units.

Procedure

1. Set up the mechanism as per Test Case #3 (drive disk decoupled and weights removed). Implement the following parameters under **PI with Velocity Feedback**: $k_p = 0.011$, $k_d = 0.0015$. Use Encoder #1 for feedback and set T_s = 0.00442 s. As before, these gains correspond to ω_n = 2 Hz and ζ = 1.0. Perform a 4000 count step. Gradually increase the sample period and repeat the procedure until significant oscillations occur and the system exhibits near instability. Do not implement sampling periods greater than 75 ms. Record the highest value of T_s prior to instability.

2. Repeat step 1 for ω_n = 10 Hz and ζ = 1.0 ($k_p = 0.27$, $k_d = 0.009$). Do not implement sampling periods greater than 15 ms in this case.

3. Compute the continuous-time Bode phase margin of the two (2 & 10 Hz) systems and note the associated critical frequency (the frequency where the gain curve crosses 0 db). Using this information and the (rough) approximation for sampling related phase lag from Eq. (6.3-7) to explain the instability. Explain the difference in instability inducing sample rate for the two systems.

6.3.6 Effect of Sensor Quantization

Numerical quantization occurs by necessity in all control systems that contain digital control elements. Such effects (also known as finite word-length effects) include coefficient and data quantization, DAC and ADC resolution, signal dynamic range, and round-off noise. These effects can have profound consequences for system stability and performance. High dynamic order controllers require particular care in providing robust algorithmic treatment and high data fidelity.[1]

[1]The DSP controller and imbedded control firmware provide very high data and parameter resolution including a 16 bit DAC, and 48 bit multiplication with 96 bit products. These combined with internal data scaling for numerical conditioning make this system immune to most quantization related problems.

© ECP 1995, All Rights Reserved

2. Implement the control and displace the drive disk with a ruler and note if any noise occurs. Reduce T_s by one increment (0.000884 s) and re-implement, displace the drive disk and check for noise. Repeat this procedure (one T_s increment at a time) until quantization noise is clearly detected. Abort control immediately upon hearing noise and do not repeat at a lower sample period. Note the last sample period.

3. Repeat Steps 1 and 2 for $k_d = 0.05$.

4. Is the relationship between derivative gain, sampling period, and torque noise implied by Eq.(6.3-9) generally consistent with the results of Steps 2 and 3?

© ECP 1995, All Rights Reserved

6.4 Control of Plant With Drive Flexibility

In this section, we consider the implications of drive flexibility to plant control and implement several control schemes to mitigate its effect. The model of our plant belongs to a class having two *degrees of freedom* (DOF) corresponding to *normal modes of oscillation* (actually one oscillatory and one rigid body mode in our case) and hence is of fourth order. The block diagrams of the system for time and Laplace domain analyses are shown in Figure 6.4-1 which gives details of the location of k_{hw} gain elements in the signal flow. The signals θ_{1e} and θ_{2e} are the respective angle measurements in encoder counts.

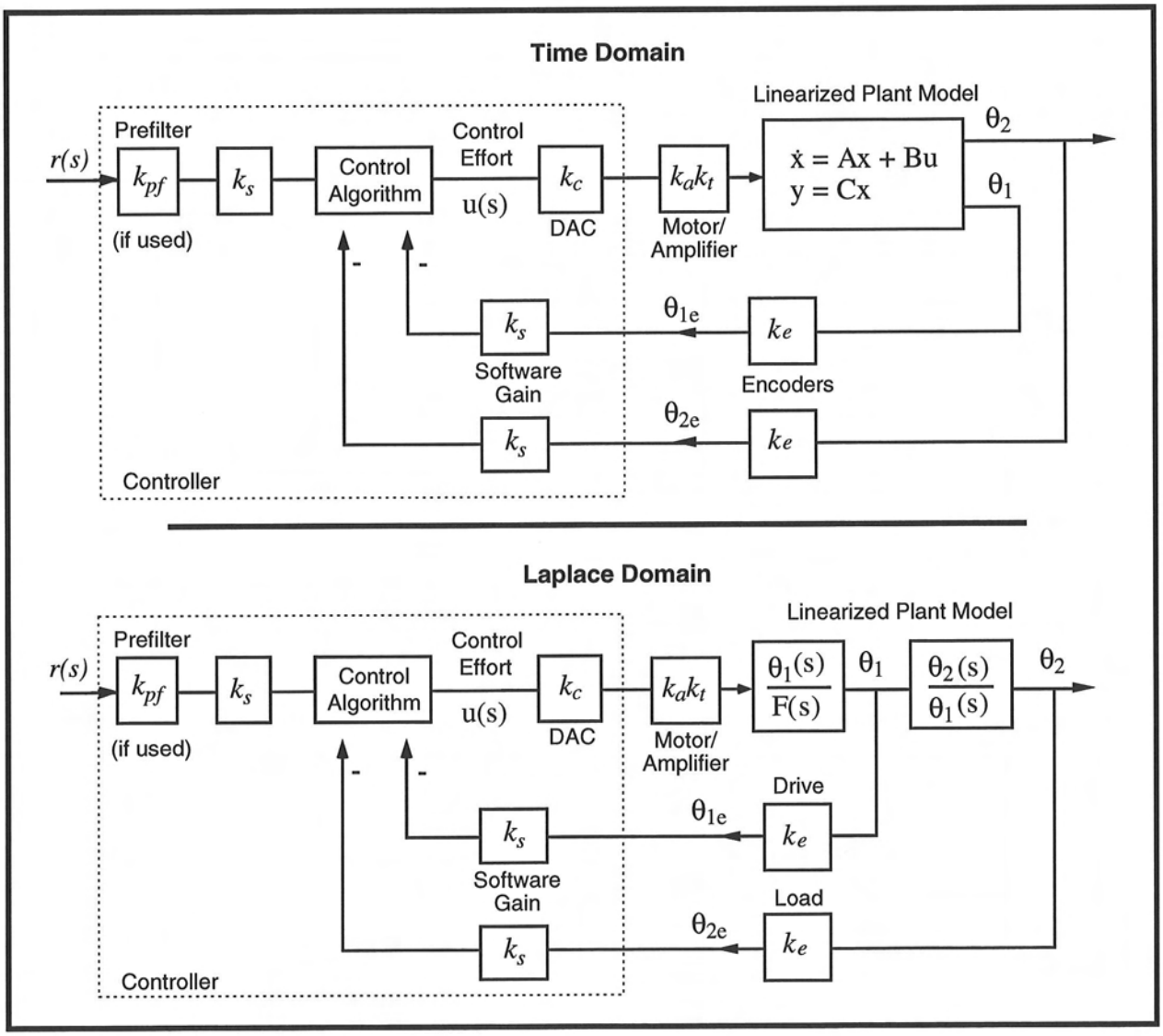

Figure 6.4-1. Block Diagram For 2 DOF Control (SIMO)

© ECP 1995, All Rights Reserved

6.4.1 Collocated Control

In this experiment we consider PD control of the 2-disk system where the controlled output, θ_1, is of the drive disk. Such a scheme is referred to as *collocated* since the sensor output is rigidly coupled to the actuator input.

The addition of flexibility (and load inertia) increase the rigid body plant order by two and adds an oscillatory mode to the plant dynamics. This may be thought of, in a sense, as a dynamic disturbance to the rigid body plant studied in Section 6.2. The collocated control implemented here may be practically employed when there is flexibility between the actuator and some inertia, with the location of objective control being near the actuator.

Procedure:

1. Set-up the system as per test case #11.
2. Implement the following gains under **PI with Velocity Feedback**: $k_p = 0.1$, $k_d = 0.005$, $k_i = 0$ with $T_s = 0.002652$ s. Set-up data acquisition for encoders 1 & 2 and for commanded position and gather data every 5 servo cycles. Execute a 1000 count step response and plot the result for commanded position and encoder #1.
3. Now iteratively adjust the gains k_p & k_d and plot results to obtain an improved response. Make your gain adjustments gradually (not more than 50% at a time) and note the effects of increasing or reducing each of them. Do not input k_p >1.5 or $0.005 < k_d > 0.015$. Attempt to achieve performance goals of ≤ 100 ms rise time (0-90% amplitude) and ≤ 10% overshoot without excessive oscillation. Save your best step response plot. Manually displace the drive disk and note the relative stiffness of the servo system.
4. For your last iteration in Step 3, plot the step response of the load disk. (There is no need to rerun the step, simply re-setup the plot for "encoder #2" & "commanded position" and plot data.) What is the predominant characteristic of the load disk motion?
5. Now using the existing values of k_p & k_d as starting points, iteratively change (lower) gains and plot θ_2 results to provide a well-behaved step response with ≤ 10% overshoot, without excessive oscillation, and as fast a rise time as possible. Save your final plot and record the corresponding gains. Manually displace the drive disk and note the relative stiffness. How does the steady state error compare with the high gain controller from Step 3?
6. Calculate the poles of the closed-loop transfer functions: $\theta_1(s)/r(s)$ and $\theta_2(s)/r(s)$ for your final controllers in Steps 3 & 5 respectively. How close to the imaginary axis (& right half plane) are the most lightly damped poles in each case? How close are the complex poles of $\theta_1(s)/r(s)$ to its zeros in each case?
7. Consider the block diagram of Figure 6.3-1. The torque from manually displacing the disk in Steps 3 & 5 entered the system as the disturbance T_d.

© ECP 1995, All Rights Reserved

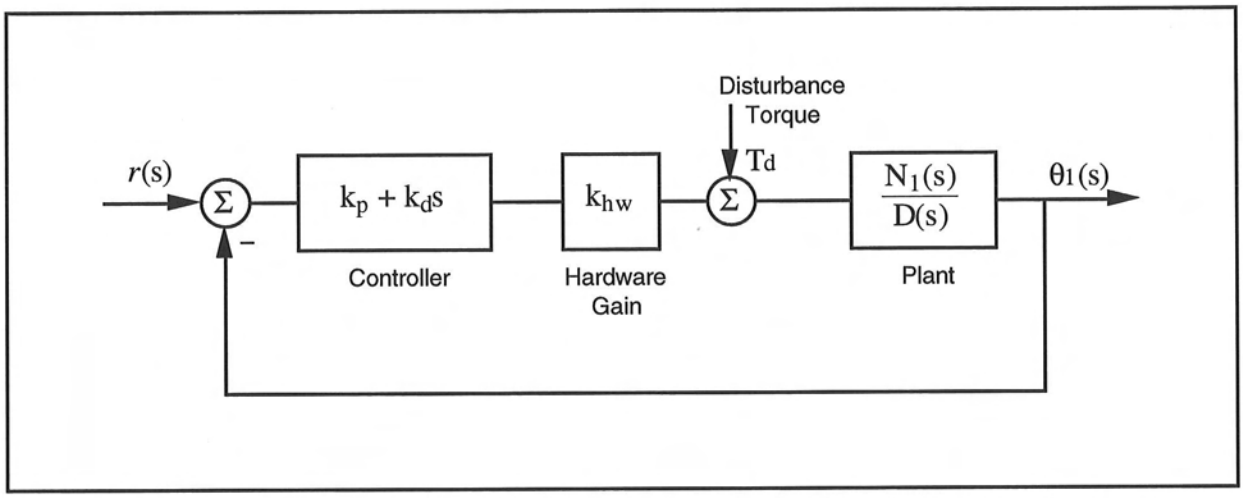

Figure 6.4-2. Disturbance Torques On PD Controlled 2-DOF Plant

The transfer function between the torque disturbance and the drive disk angle is:

$$\frac{\theta_1(s)}{T_d(s)} = \frac{N_1(s)}{D(s)+k_{hw}(k_p+k_d s)\,N_1(s)} \qquad (6.3\text{-}1)$$

where $N_1(s)$ is the numerator in the right hand side of Eq(5.1-4).

What is the static servo stiffness of your final controllers from Steps 3 &5 for the drive disk? What is the equivalent expression for the load disk (i.e. defining static servo stiffness at the load disk as the torque required to displace the disk one radian) and what is its value for the two controllers? Recalling Section 6.3.2, what is the static servo stiffness, k_{ss}, with integral action in the controller (i.e. $k_i \neq 0$)?

Important Note: The flexible belt should be in place only for the duration of active testing. Prolonged periods (more than several hours) may permanently stretch the belts.

6.4.2 PD Plus Notch Filter Control

In this experiment a control scheme is implemented which first closes the collocated loop with simple rate feedback to dampen the oscillatory mode. Then a notch filter is designed to further attenuate the transmission of signals at the damped mode frequency (i.e. nearly canceling the poles with zeros). Finally, PD control is used to achieve certain performance goals.

© ECP 1995, All Rights Reserved

Procedure :

1. The plant studied here is that of the previous exercise, i.e. Test Case #11. Consider the block diagram of Figure 6.4-2. Use root locus techniques to find the rate feedback gain, k_v, that best damps the complex roots of the inner loop $\theta_1(s)/r^*(s)$.

2. Implement this gain as the **f_1** coefficient in the **General Form** controller specification box. Be sure that you select encoder #1 for feedback loop #3 before exiting the box and implementing. Attempt to manually excite the oscillatory mode via the load disk and notice the damping effect of velocity feedback.

3. We may now design for the new "plant" $G^*(s)$ where $N_2(s)$ is as before, and:

$$D^*(s) = D(s) + k_v s N_1(s) \tag{6.4-1}$$

Design a notch filter, $N_n(s)/D_n(s)$ with a pair of stable complex poles (roots of $D_n(s)$) at 6.0 Hz and 80% damping and a stable real pole at 60 Hz. Make the zeros (roots of $N_n(s)$) at the poles of $D^*(s)$. Normalize the notch filter transfer function to have unity DC gain.[1]

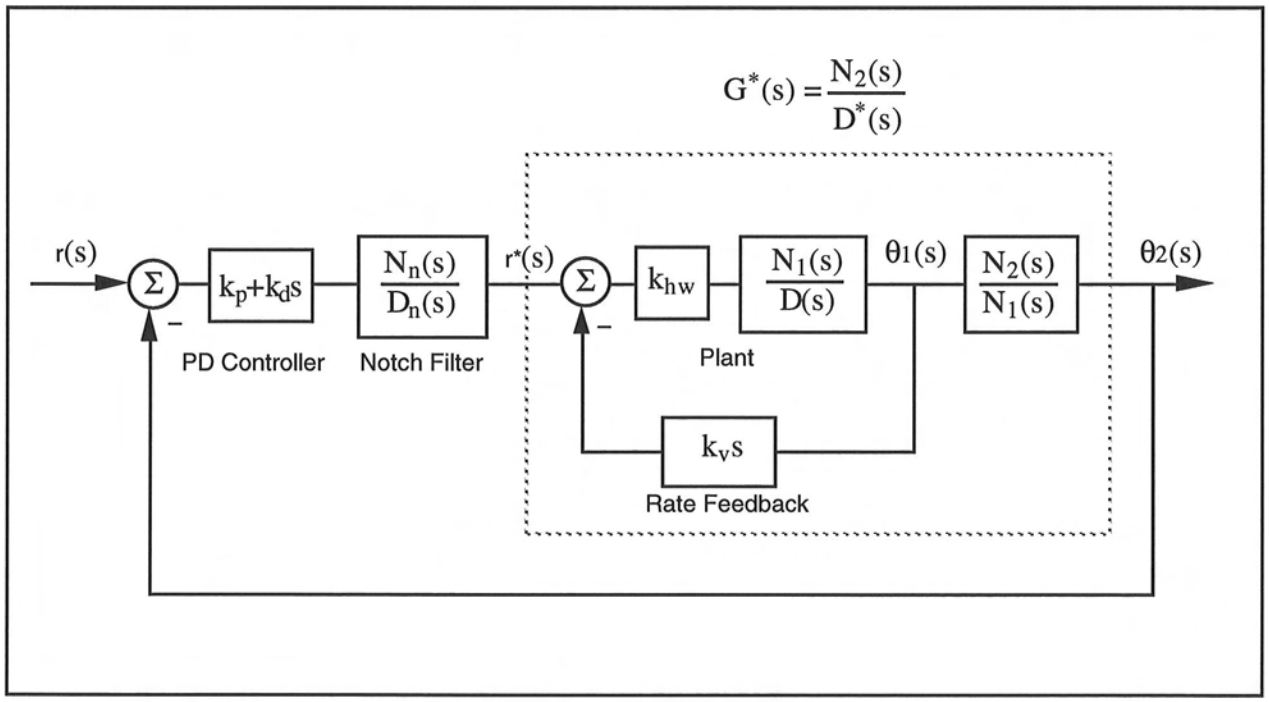

Figure 6.4-2. Control Structure For Section 6.4.2 Experiment

[1]For discrete time design, convert your notch filter design to the z domain using the Tustin (bilinear) transformation:

$$s = \frac{2}{T_s}\frac{1-z^{-1}}{1+z^{-1}}$$

© ECP 1995, All Rights Reserved

4. Select some initial PD gains for control of θ_2. Values in the range of $k_p = 0.02$, $k_d = 0.002$ should be safe to start with. Do not exceed $kp = 0.05$ and $k_d = 0.005$ in the initial run. Since this control scheme uses multiple loop feedback, the Executive program requires that it be implemented via the general control algorithm form. A short-cut to controller coefficient entry is as follows: Input your notch & PD controller coefficients via the dialog box **PID + Notch** , exit and select **Preview In General Form.** You will see the PD + notch controller in the form that it is implemented in the generalized controller form.[1] In the **General Form** window, enter the $\mathbf{f_1}$ coefficient calculated in Step 1 (i.e. k_V). Make sure that Encoder #1 is selected for Loop #3 and Encoder #2 is selected for Loop #1. Exit the box and **make sure that General Form is selected** (i.e. the little red dot is next to it), then **Implement**. Now check performance of the control using step trajectories of 500 counts.
5. Iteratively change PD gains by repeating Step 4 to obtain performance goals of 0.25 sec rise time and overshoot less than 10%. Do not exceed $k_p = 0.50$ or $k_d = 0.07$. Recalling the results of Section 6.3, you may notice a trend here that for relatively high values of k_d the system transmits excessive noise and appears "twitchy". As k_p becomes large, the system becomes oscillatory and further increases lead to instability.
6. Record your best performance step response. Use a ruler or similar object to feel the static stiffness of the load disk under this control. How does it compare with the drive disk stiffness? How does the static servo stiffness at θ_2 for this controller compare with the one from Step 5 of Section 6.4.1? Can you see the drive disk move in opposition to your disturbance? How does the steady state error from the step plots compare?

Important: Disconnect the flexible belt after completing tests.

6.4.3 Full State Feedback LQR Control

In this experiment a linear quadratic regulator is implemented using full state feedback. The plant used is again that of Test Case #11. The states chosen are the disk angles and rates according to the model of Eq (5.2-15) with the output taken as θ_2, i.e.

$$C = [\,0 \;\; 0 \;\; 1 \;\; 0\,] \tag{6.5-1}$$

[1] $\mathbf{r(s)}$ will be the same as $\mathbf{D_n(s)}$ and $\mathbf{s(s)}$ & $\mathbf{t(s)}$ will be identical and equal to the polynomial convolution of $\mathbf{N_n(s)}$ with (k_p+k_ds). Upon selecting **Preview In General Form** the algorithm is also converted to discrete time form (by the Tustin transform for N_n *and* N_n, Backwards difference for (k_p+k_ds) then by convolving the two.). Hence the discrete time equivalent controller may be viewed in the discrete time **General Form** controller box.

© ECP 1995, All Rights Reserved

The angular outputs are measured by the feedback encoders. The encoders are backwards differentiated in the controller to provide a rate measurement[1] and hence the four defined states are available for control.

Procedure :

1. Construct a state space model of the plant using the realization of Eq (5.1-3) and measured parameter values from Section 6.1.
2. The following notation shall be used for LQ optimization:

   Feedback law:

   $$u = -Kx \tag{6.5-2}$$

   with notation: $$K = [\ K_1 \quad K_2 \quad K_3 \quad K_4\ ] \tag{6.5-3}$$

   Perform LQR synthesis via the Riccati equation solution[2] or numerical synthesis algorithms to find the controller K which minimizes the cost function (scalar control effort):

   $$J = \int (x'Qx + u^2 r)dt \tag{6.5-4}$$

   In this synthesis choose Q=C'C so that the error at the intended output, θ_2, is minimized subject to the control effort cost. Perform synthesis for control effort weight values: r = 100, 10, 1.0, 0.01, and 0.001. Calculate the closed loop poles for each case as the eigenvalues of [A–BK]

3) From this data, select a control effort weight to put the lowest pole frequency between 3.5 and 4 Hz. Use one of the above obtained K values if it meets this criteria, or interpolate between the appropriate r values and perform one last synthesis iteration. Do not use K_1 or K_3 values greater than 1, or K_2 or K_4 values greater than 0.12.[3]
4) Implement your controller via the **State Feedback** box under **Control Algorithm**.[4] Using the block diagrams of Figure 6.4-1, show that for tracking, the prefilter gain K_{pf} must be set equal to $grK_1 + K_3$.
5) Execute a 1000 count step and plot the result. How do the rise time, overshoot, servo stiffness, and steady state errors compare with previous controllers? What is k_{ss} for disturbances at the load and drive disks?

Important: Disconnect the flexible belt after completing these tests.

---

[1]Strictly speaking, the rate feedback is an estimate rather than a measurement. In practice however, with high sensor resolution, low signal noise, and relatively high sample rate, system performance and stability are not adversely affected. Hardware cost is generally lowered by eliminating a dedicated rate sensor(s).

[2]See for example Kwakernaak and Sivan, "Linear Optimal Control Systems", Wiley & Sons, 1972.

[3]K_1 and K_3 scale control effort proportional to position errors; K_2 and K_4 scale control effort proportional to the respective velocities. Excessive values of K_1 or K_3 can lead to low stability margin and in the presence of time delays, instability. Large K_2 or K_4 cause excessive noise propagation and lead to "twitching" of the system.

[4]If using discrete time implementation, be sure to divide your K_2 and K_4 values by T_s before entering them.

© ECP 1995, All Rights Reserved

6.5 Control of Plant With Backlash

In this section, we consider the effects of backlash on plant dynamics and control. We first consider the effects of backlash in a conventionally controlled PD system, then implement a control scheme to mitigate the adverse effects.

6.5.1 Effects on Conventionally Controlled Systems

1. Setup the mechanism in the Test Case #12 configuration using a timing belt to connect the SR assembly to the load disk. Make certain that the backlash adjustment screw is fully engaged so that no backlash is present. Input the following parameters under **PI with Velocity Feedback**: $k_p = 1.0$, $k_d = 0.080$, $k_i = 0$. Choose Encoder #2 for feedback (noncollocated) and set $T_s = 0.00884$ s.[1] Execute and plot a 500 count, 2000 ms, step observing the encoder #1 and #2 response. Save your plot.
2. Repeat step 1 but with[2] $k_p = 0.25$, $k_d = 0.020$, and Encoder #1 for feedback (collocated). You will need to increase the step size to 2000 counts to account for the change in sensor location. The response in each case should be similar.
3. Disconnect power from the mechanism and adjust the backlash device to give 60 – 70 counts of backlash as read at the load disk. Make sure that the SR assembly clamp screw is securely tightened. The backlash adjustment process is simplified by temporarily installing the drive clamp[3] to immobilize the drive disk. With the feedback (not the drive power) connector still connected to the mechanism you may rotate the load disk back and forth and read the resulting backlash on the background screen (ECP Executive program) while adjusting the backlash. You may **Zero Position** (**Utility** menu) while fully displacing (lightly) the load disk in one direction. The amount that the encoder reads when the load disk is (lightly) rotated in the opposite direction is the backlash.
4. Repeat step 2 for this setup reducing the amplitude to 250 counts. Can you see the effects of backlash in the response?
5. Prepare to implement the noncollocated control of Step 1. Be prepared to **Abort Control** immediately after implementing. Implement the control algorithm. If the system oscillates wildly, abort control immediately. If not, use an object such as a ruler to perturb the drive disk. The system should exhibit unstable behavior. Abort control immediately.
6. Return to the collocated control of Step 2 and implement the indicated control gains. Set up a step disturbance (**Command** menu) of 0.25 volt, 2000 ms duration and 2 repetitions. Setup a 10,000 ms closed loop step trajectory of zero amplitude. This configures the system for regulation in the presence of the step disturbance. Run this maneuver making sure that **Include Step Disturbance** is checked in the **Execute Trajectory** dialog box. Plot and save the response at both θ_1 and θ_2.

---

[1] If the system rattles or buzzes, make certain that the drive belts are taught.

[2] Recall the relationship between sensor location, gear ratio, and gain from Section 6.3.1.

[3] The aluminum spacer and 0.25" bolt that clamps between the brass weight attachment slots on the drive disk and the opposing 0.25" hole in the mechanism base plate.

© ECP 1995, All Rights Reserved

7. Compare the response from Steps 2 and 4. Is the backlash effect clearly seen? What is the effect of backlash on the noncollocated controlled system? Describe the effect of backlash on regulation for collocated control.

6.5.2 Control for Mitigation of Backlash Effects

1. With the mechanism set for 60–70 counts of backlash (measured at θ_2 - see step 3 of the previous section) enter the general form control algorithm dialog box. enter the following coefficients: $\mathbf{t_0} = 0.5$, $\mathbf{s_0} = 0.5$, $\mathbf{s_1} = 0.04$, $\mathbf{r_1} = 0.001$, $\mathbf{f_1} = 0.02$. (All other coefficients should be zero except for $e_o = h_o = r_o = j_o = g_o = 1$) Chose Encoder #2 for Loop #1 feedback and Encoder #1 for Loop #3 feedback. Verify that this sets the system up for proportional plus velocity feedback control ($k_p = 0.5$, $k_d = 0.040$) about θ_2, with a rate feedback loop ($k_v = 0.020$) closed about θ_1. The coefficient $\mathbf{r_1}$ corresponds to a pole at 1000 rad/s and does not appreciably affect system behavior.[1]

   Set $T_s = 0.00884$ s then implement[2].
2. Perform a 250 count step and compare the plotted result with that of step 6 of the previous section. Interactively change the noncollocated proportional gain ($\mathbf{t_0}$ and $\mathbf{s_0}$), and the collocated rate feedback gain ($\mathbf{f_1}$) to attain a more rapid response and higher servo stiffness, but without excessive oscillation. Do not input $\mathbf{t_0}$, $\mathbf{s_0} > 1.5$, or $\mathbf{f_1} > 0.05$. Perform a 250 count step each time to characterize the response. Save your final plot.
3. Using your final design from step 2, perform a step disturbance test according to the instructions of Step 6 of the previous section. Plot and save the result at both θ_1 and θ_2.
4. How does the step response from the final controller in step 2 compare with that from the first trial? How does it compare with the collocated controller of step 4 of the previous section? Why? What is the effect of changes in k_p of the noncollocated loop and k_v of the collocated loop? How does the disturbance response of this section compare with that of the previous section?

---

[1] It is needed for properness of T(s)/R(s) and S(s)/R(s) in the bilinear transformation to T(z)/R(z) and S(z)/R(z). This transformation is performed by the Executive program prior to downloading to the control board for real-time execution.

[2] If the system rattles or buzzes, make certain that the drive belts are taught.

© ECP 1995, All Rights Reserved

6i. Instructor's Supplement To Experiments

This is the instructor's supplement to the experiments described in Chapter 6 of the main manual. It contains some of the expected experimental results as well as suggestions for further experiments and further detail on certain analytical developments. There are many dynamics and controls topics that relate to these experiments which are not explored in the manual, but which the instructor may wish to bring out. The methodologies presented here demonstrate some fundamental principles and behaviors, but are not represented to be necessarily superlative practical control solutions. They do in the least however, give the undergraduate student a hands-on introduction to control implementation, and the more advanced user a working orientation to the system from which much more general topics may be explored.

This supplement is organized with section numbers consistent with those of the five experiments in the main manual body. In addition to describing experimental results, Section 6.1i contains numerical models of three plant configurations. Suggestions for further experiments are given in Section 6.6i. Appendix Ai contains some MATLAB® scripts useful in building numerical plant models and performing certain steps in the experiments.

The analysis and design techniques described in Chapter 6 are in the context of continuous time implementation. Analogous discrete-time methodologies are easily substituted in the appropriate areas as indicated by footnotes.

Note to instructors and advanced users:

If you or your students synthesize and implement a control structure that is of particular academic or instructional interest, please share it with us! Pending ECP review it may be included in a future revision of this manual with credits of course to the inventor. You will receive a complementary software and manual upgrade!

6.1i System Identification

The procedure given is for identifying the plant parameters in Eq's (5.1-13 through -14, 5.2-15 through -18, and 5.2-24 through -27). Experimental values given here are for a particular system and may not precisely match the results of another. In particular, k_{hw} could vary by as much as 20% from system to system and friction is dependent on a particular apparatus setup. Inertia values given here are relatively accurate however. All values – experimentally and analytically derived – stated here are mutually consistent.

Two methods are used in determining gain and inertia, namely: acceleration under a known fixed control (DAC voltage), and natural frequency measurement of a lightly damped closed loop system. In practice, the acceleration method first used in measuring system gain may be employed

© ECP 1995, All Rights Reserved

on the motor alone where reasonably accurate inertia specifications are generally available from the supplier. Either method may be used exclusively for both gain and inertia measurement[1].

Finally, it is worth noting that for applications where the plant may be modeled as a rigid body with fixed inertia, a single test by either method may be used to find (k_{hw}/J^*) and hence the total effective system gain.

6.1.1 Gain Measurement

1. In Part a: $J_w = 2.0 \text{ kg}*(.05^2 + .0495^2/8) = 0.00561 \text{ kg-m}^2$

   In Part b: Calculated mass of drive disk = 0.174 kg $\Rightarrow J_{drive\ disk} = 0.000381 \text{ kg-m}^2$

   In Part c: $J_{motor} = 3.8*10^{-5} \text{ kg-m}^2$ (given)

   The above $\Rightarrow J_{dtest} = 0.00603 \text{ kg-m}^2$

2. In Step 4: $\ddot{\theta}_1 = 197{,}000 \text{ counts/s}^2$.

   $\Rightarrow k_a k_t k_e = 595$ (N-m encoder count/ volt rad)

   $\Rightarrow k_{hw} = 5.81$ [(N-m / rad) * (controller count) / (DAC count)] (this value could vary by as much as 20% from system to system).

6.1.2 Inertia Measurement

Reasonable values for experimental results are on the order of (Use the values in Table 6.1.-1i in later work for more precise modeling):

In Steps 8, 9, & 10:

$\zeta_3 = 0.05$

$\omega_{n3} = 86.8$ rad/s

$\zeta_4 = 0.1$

$\omega_{n4} = 28.3$ rad/s

$J_{dd} = k_p k_{hw}/(\omega_{n3})^2 = 0.00039 \text{ kg-m}^2$

$(J_{dl})_{\text{gross, reflected to drive}} = k_p k_{hw}/(\omega_{n4})^2 = 0.00363 \text{ kg-m}^2$

$\Rightarrow (J_{dl})_{\text{net, reflected to drive}} = 0.00363 - J_{dd} - (J_{backlash\ device} + J_{18\ tooth} + J_{72\ tooth})/(\text{gear ratio to SR} = 1.5)^2$

$\Rightarrow (J_{dl})_{\text{net, reflected to drive}} = 0.00297 \text{ kg-m}^2$

$\Rightarrow J_{dl} = (J_{dl})_{\text{net, reflected to drive}} * (1.5)^2 = 0.0067 \text{ kg-m}^2$

[1]E.g. if the closed loop method is used exclusively, then two tests may be run. One with the basic system inertia (J_o) , one with an added known inertia (preferably on the order of the basic system inertia). Two equations of the form (6.1-3) are then solved for the two unknowns J_o and k_{hw}. Similarly the acceleration method may be used without a priori knowledge of inertia or gain.

© ECP 1995, All Rights Reserved

6.1.3 Damping Measurement

$c = 2\zeta\omega_n J - k_d k_{hw}$

Substituting the above values for Case 4, we have

$c_4 = 0.015$ N/(rad/s) (reflected to drive)

The friction coefficients listed in Table 6.1-1i were obtained by direct physical measurement and only approximate what might exist for a given physical setup. A measurement as per Step 7 is more accurate for a given setup.[1] If the values in Table 6.1-1i are used, c_2 must be divided by the gear ratio squared to be reflected to the motor (or "drive").

The Pulley inertia values of Table 6.1-2 are repeated in Table 6.1-2i for convenience.

Table 6.1-1i System Dynamic Parameters

Parameter	Value
J_{dd}	0.00040 kg-m^2
J_{dl}	0.0065 kg-m^2
J_{wd} (with 4 *0.20 kg masses at r = 5.0 cm)†	0.0021 kg-m^2
J_{wl} (with 4 *0.50 kg masses at r = 10.0 cm)†	0.0206 kg-m^2
c_1 (drive friction (modeled as viscous)). No belt to SR assembly	0.002 N-m/rad/s (approximately)
c_1 (drive friction (modeled as viscous)). Belt connected to SR assembly	0.004 N-m/rad/s (approximately)
c_2 (load friction at load (modeled as viscous)) Includes load disk-to-SR belt	0.05 N-m/rad/s (approximately)

† Includes inertia of weights about their c.g.

Table 6.1-2i SR Pulley Inertia Values

Number of Pulley Teeth	Pulley Inertia, J_p (kg-m^2)
18 tooth	$3 * 10^{-6}$
24 tooth	$8 * 10^{-6}$
36 tooth	$3.9 * 10^{-5}$
72 tooth	$5.5 * 10^{-4}$
Backlash device (incl. attachment screws) – add to J_p	$3.1 * 10^{-5}$

[1]The method of Step 7 is inaccurate for relatively small friction measurement such as for the drive alone.

© ECP 1995, All Rights Reserved

6.1.4 Flexible Drive Measurement

Typical results are $\omega_n = 17.7$ rad/s , $\zeta = 0.07$

For this setup, $J_l = 0.0271$ kg-m^2 which results in the parameters given in Table 6.1-3i. The load disk damping c_2 must be subtracted from the ζ derived damping, c, of this experiment in to obtain c_{12}.

In practice it is often not necessary to include the such a detailed dynamic term as c_{12}. We include it here because it renders closer agreement between later simulation and test results.

Table 6.1-3i Flexible Drive Parameters

Parameter	Value
k	8.45 N-m/rad
c	0.067 N-m/rad/s
c_{12}	0.017 N-m/rad/s

This section covered:

1. Creation of the plant model including inertia for arbitrary gear ratio.
2. Measurement of combined amplifier / motor torque gain and unknown inertia by two methods: open loop acceleration and closed loop natural frequency.
3. Measurement of friction (modeled as viscous).
4. Measurement of flexible drive spring and damping constants

Example Numerical Plant Models.

The following are some example plant models using the parameters stated above and a specific hardware gain, $k_{hw} = 5.81$. These models may be generated using the scripts in Appendix A.1i . Since they include hardware gain, any control parameters consistent with these models may be input directly via the Executive program. Below the variable u(s) refers to the control effort signal at the output of the control algorithm, and θ_i(s) is the output at location "i" scaled by k_e and k_s (see e.g. Figure 6.4-1).

1) As-delivered (rigid body, same as Test Case #12 except no weights on either disk):

TF:

$$\frac{\theta_1(s)}{u(s)} = \frac{7036}{s(s+8.63)} \qquad (6.1\text{-}1i)$$

$$\frac{\theta_1(s)}{u(s)} = \frac{1759}{s(s+8.63)}$$

© ECP 1995, All Rights Reserved

SS: $$A = \begin{bmatrix} 0 & 1 \\ 0 & -8.63 \end{bmatrix},\ B = \begin{bmatrix} 0 \\ 7036 \end{bmatrix},\ C = [\,1\ \ 0\,]\ (\theta_1 \text{ output})$$ (6.1-2i)

$$A = \begin{bmatrix} 0 & 1 \\ 0 & -8.63 \end{bmatrix},\ B = \begin{bmatrix} 0 \\ 1759 \end{bmatrix},\ C = [\,1\ \ 0\,]\ (\theta_2 \text{ output})$$

2) Test Case #3:

TF: $$\frac{\theta(s)}{u(s)} = \frac{1310}{s(s+.71)}$$ (6.1-1i)

SS: $$A = \begin{bmatrix} 0 & 1 \\ 0 & -10 \end{bmatrix},\ B = \begin{bmatrix} 0 \\ 14{,}500 \end{bmatrix},\ C = [\,1\ \ 0\,]\ (\theta_1 \text{ output only})$$ (6.1-2i)

3) Test Case #6:

TF: $$\frac{\theta_1(s)}{u(s)} = \frac{399}{s(s+1.80)}$$ (6.1-1i)

$$\frac{\theta_2(s)}{u(s)} = \frac{266}{s(s+1.80)}$$

SS: $$A = \begin{bmatrix} 0 & 1 \\ 0 & -1.80 \end{bmatrix},\ B = \begin{bmatrix} 0 \\ 598 \end{bmatrix},\ C = [\,1\ \ 0\,]\ (\theta_1 \text{ output})$$ (6.1-2i)

$$A = \begin{bmatrix} 0 & 1 \\ 0 & -1.80 \end{bmatrix},\ B = \begin{bmatrix} 0 \\ 266 \end{bmatrix},\ C = [\,1\ \ 0\,]\ (\theta_2 \text{ output})$$

4) Test Case #11 (rigid body):

$$\frac{\theta_1(s)}{u(s)} = \frac{2750}{s(s+3.37)}$$

$$\frac{\theta_2(s)}{u(s)} = \frac{687}{s(s+3.37)}$$

$$A = \begin{bmatrix} 0 & 1 \\ 0 & -3.37 \end{bmatrix},\ B = \begin{bmatrix} 0 \\ 2750 \end{bmatrix},\ C = [\,1\ \ 0\,]\ (\theta_1 \text{ output})$$

$$A = \begin{bmatrix} 0 & 1 \\ 0 & -3.37 \end{bmatrix},\ B = \begin{bmatrix} 0 \\ 687 \end{bmatrix},\ C = [\,1\ \ 0\,]\ (\theta_2 \text{ output})$$

5) Test Case #11 (Flexible - 0.25" flex. belt):

TF: $$\frac{\theta_1(s)}{u(s)} = \frac{N_1(s)}{D(s)}$$ (6.1-3i)

$$\frac{\theta_2(s)}{u(s)} = \frac{N_2(s)}{D(s)}$$

© ECP 1995, All Rights Reserved

where:

$$N_1(s) = 2306((s+1.236)^2+17.61^2)$$
$$N_2(s) = 361.6(s+497.1)$$
$$D(s) = s(s+1.691)((s+1.395)^2+22.79^2)$$

SS: (6.1-4i)

$$A = \begin{bmatrix} 0 & 1 & 0 & 0 \\ -209.6 & -2.009 & 838.5 & 1.687 \\ 0 & 0 & 0 & 1 \\ 77.95 & 0.1568 & -311.8 & -0.2472 \end{bmatrix}, \quad B = \begin{bmatrix} 0 \\ 2306 \\ 0 \\ 0 \\ 0 \end{bmatrix}, \quad C = [\,0\ 0\ 1\ 0\,]$$

6.2i Rigid Body PD & PID Control

This section first demonstrates the equivalence of $k_p k_{hw}$ to a mechanical spring and $k_d k_{hw}$ to a damper. It then shows the relationship of these to the natural frequency and damping ratio of the closed loop system. Parameters are selected to implement under-, over-, and critically damped systems and characteristic step responses are plotted. Integral action is then added and its effect on response, steady-state error, and stability are studied. These experiments may also be performed in the context of discrete time implementation where k_d must be divided by T_s and k_i multiplied by T_s when inputting parameters in the discrete time PID control window.

6.2.1 Effects of k_p and k_d Independently

1) In step 3, $k_p \approx 0.068$.
2) In step 7, $\omega_n \approx 2$ Hz, after doubling k_p, $\omega_n \approx \sqrt{2}$ *2 (Hz). Units of $k_p k_{hw}$ are N-m/rad same as for a torsional spring.
3) In step 8, $k_d \approx 0.009$ for $k_d k_{hw} = 0.05$ N-m/(rad/s)
4) In step 10, units of $k_d k_{hw}$ are N-m/(rad/s) same as for a rotary damper.

This section showed:

1. The equivalence of proportional-to error feedback to a mechanical spring and of derivative feedback to a damper.
2. The square root proportionality of natural frequency to proportional gain.

© ECP 1995, All Rights Reserved

6.2.2 PD Control Design

Gains for the respective under-, critically-, and over-damped cases are approximately k_p = 0.27, k_d = 0.0043, 0.022, and 0.043. Their step responses are shown in Figure 6.2-1ia, b, & c. Figure 6.2-1id shows critically damped case with $k_i k_{hw}$ = 5 N-m/(rad-sec) added (Sect 6.2.3). Note the characteristic overshoot and damped oscillation of the underdamped system, the rapid rise time with no overshoot of the critically damped system, and the sluggish response of the overdamped system.

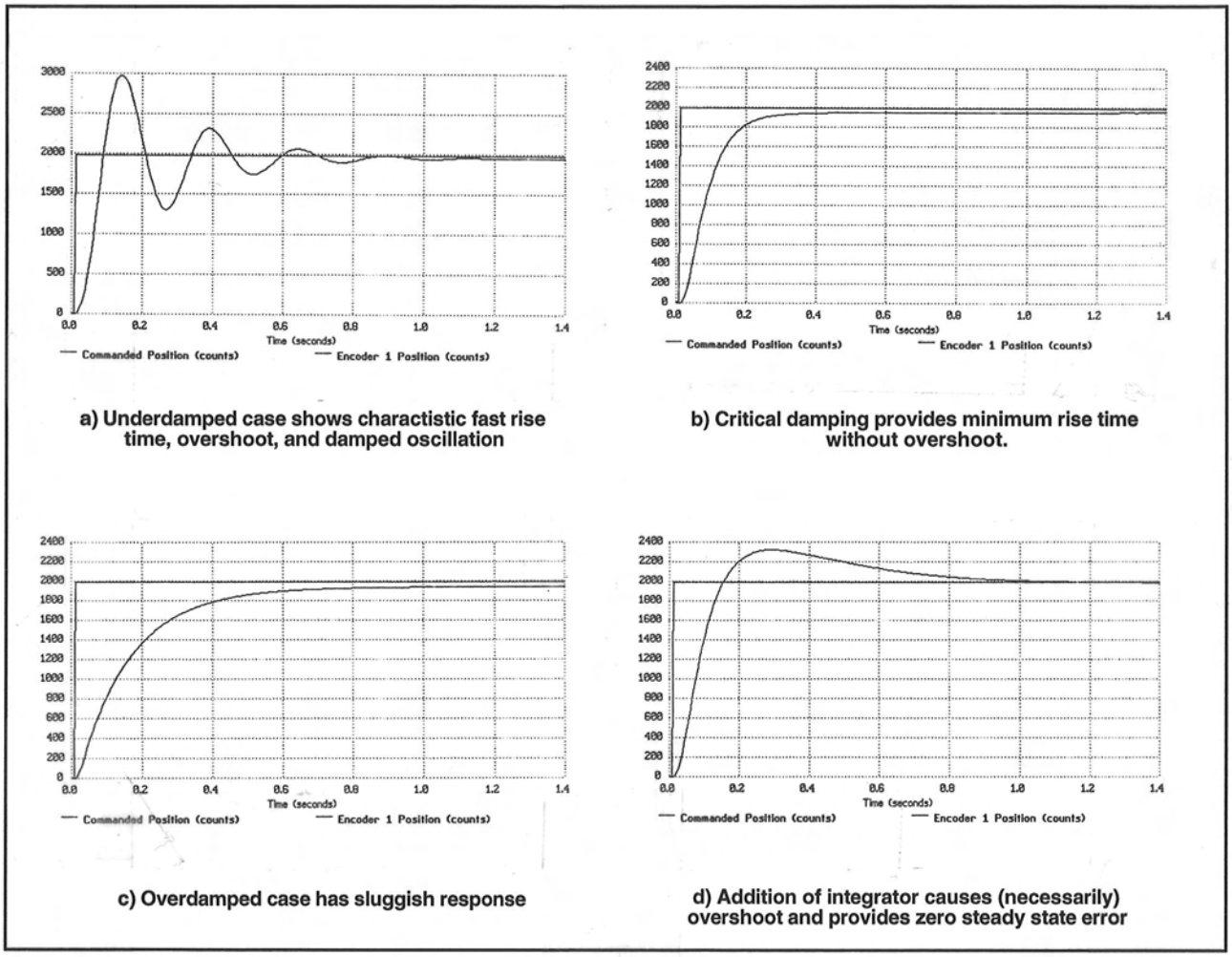

a) Underdamped case shows charactistic fast rise time, overshoot, and damped oscillation

b) Critical damping provides minimum rise time without overshoot.

c) Overdamped case has sluggish response

d) Addition of integrator causes (necessarily) overshoot and provides zero steady state error

Figure 6.2-1i Test Results Show Classical PD and PID Step Responses

6.2.3 Adding Integral Action

1) k_i = 0.86. See Figure 6.2-1i(d) for step response.

2) In step 3: *ans: Integral action eliminates steady state error. System will always overshoot (in the absence of Coulomb friction) due to the integration of error over the period before the output reaches the step demand amplitude.*

© ECP 1995, All Rights Reserved

The last two sections showed:

1. Pole placement PD control design.
2. The characteristic under- over- and critically damped second order system step responses.
3. The elimination of steady state error (fixed input) and necessary overshoot by introduction of integrating control.

6.2.4 Tracking Response

Tracking response plots are shown in Figure 6.2-2i

1) In step 1: $k_p \approx 0.27$, $k_d \approx 0.022$

2) In step 5: *ans: For k_d in the return path:*

$$e_{ss} = \lim_{s\to 0} s \frac{\alpha}{s^2} \frac{Js^2 + k_{hw}k_d s}{Js^2 + (k_p + k_d s)k_{hw}} = \frac{k_d \alpha}{k_p} \qquad (6.2\text{-}1i)$$

where α is the velocity constant of the ramp input.

For k_d in the forward path:

$$e_{ss} = \lim_{s\to 0} s \frac{\alpha}{s^2} \frac{Js^2}{Js^2 + (k_p + k_d s)k_{hw}} = 0 \qquad (6.2\text{-}2i)$$

Hence in the absence of friction or other disturbances, the return path differentiator has a ramp steady state error proportional to k_d/k_p while the forward path differentiator has zero ramp steady state error.

The forward path differentiated system overshoots (as it does to a step input) due to "momentum carryover" at the velocity discontinuities (Since there is nominally zero tracking error at these points, infinite control bandwidth would be required to abruptly stop the inertia and avoid overshoot)

Adding integral action causes overshoot when k_d is in the return path because following error (Eq. 6.2-1i @ steady state) is integrated during the course of the ramp following so that residual control effort exists when the input becomes stationary. When k_d is in the forward path, the ramp following errors are small and added overshoot due to integral action is also small.

The peak control effort is much higher (approximately 4x) for the forward path than for the return path differentiator in this case. The greater control effort is due to differentiation of the discontinuous error at the beginning and end of the dwell points. The return path differentiator on the other hand operates on the output velocity and which is effectively low pass filtered by the system bandwidth and has no abrupt changes.

Figure 6.2-2i(d) shows that the effects of high peak control effort and overshoot can be mitigated by use of a more smooth input trajectory. It is worth noting that since the acceleration and deceleration periods are nominally parabolic, the control effort is piece-wise approximately constant.

© ECP 1995, All Rights Reserved

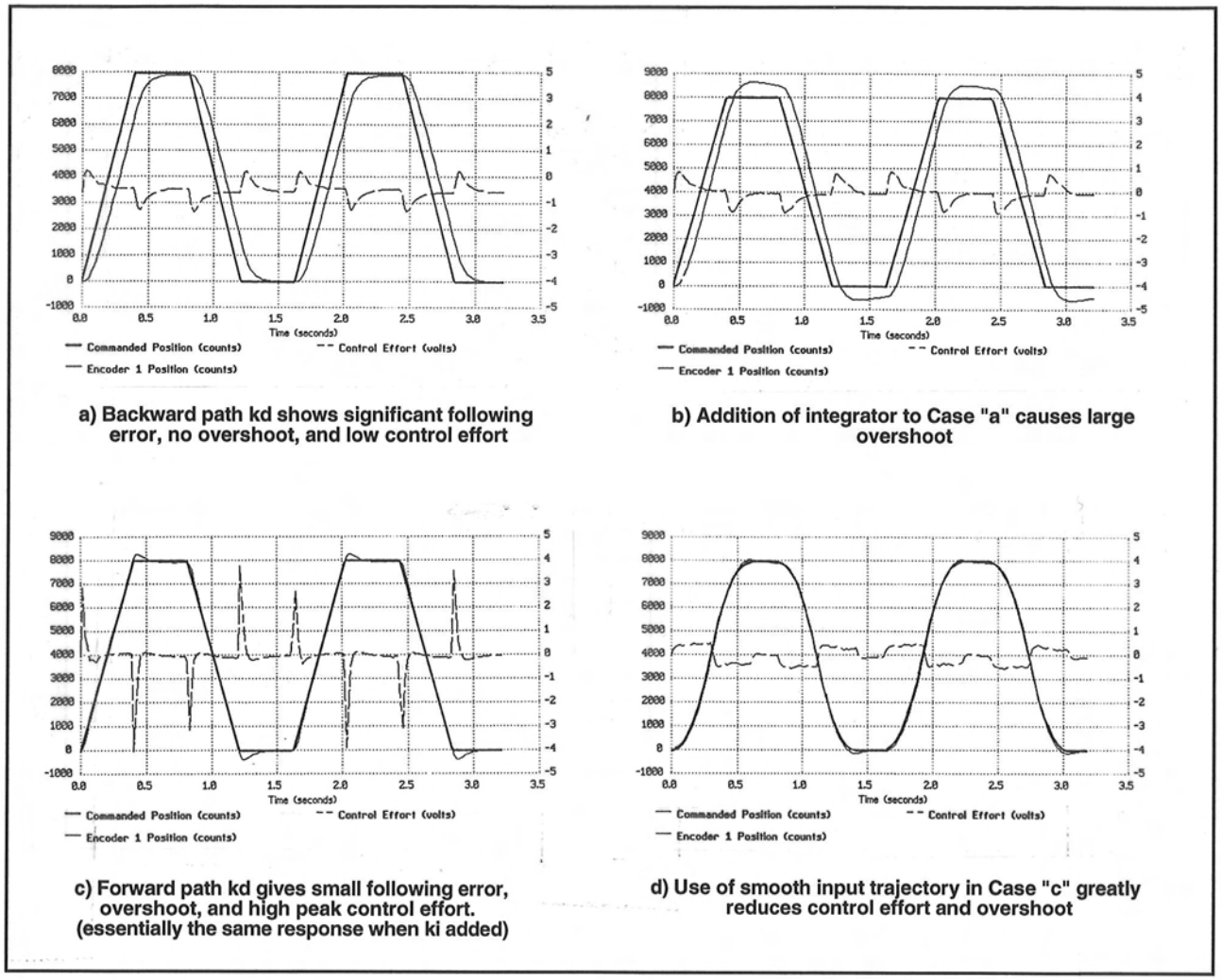

a) Backward path kd shows significant following error, no overshoot, and low control effort

b) Addition of integrator to Case "a" causes large overshoot

c) Forward path kd gives small following error, overshoot, and high peak control effort. (essentially the same response when ki added)

d) Use of smooth input trajectory in Case "c" greatly reduces control effort and overshoot

Figure 6.2-2i Tracking Responses Showing Effect of Various PID Configurations & Trajectory Smoothness

The above results are representative of arbitrary inputs in most cases and hence in industry, PID tracking controllers generally have k_d in the forward path. Integral action may be added if set point regulation is desired. Trajectories are usually planned that have no velocity discontinuities to avoid excessive peak power torque (current) demands. For pure regulation or if following errors are not a concern then return path differentiation may be employed

This section showed:

1. Steady state error to a ramp input is proportional to k_d/k_p for a return path k_d and equal to zero when k_d is in the forward path.
2. Integral action with return path k_d is generally unacceptable for tracking due to high overshoot.
3. The characteristic overshoot and high peak control effort for forward path k_d are significantly mitigated by modest smoothing of the input.

© ECP 1995, All Rights Reserved

6.2.5 Frequency Response (Sine Sweep)

1) In step 1: $k_p \approx 0.27$, $k_d \approx 0.0043$, 0.022, and 0.043

2) In step 6: $\omega_r = \omega_n\sqrt{1 - 2\zeta^2} = 3.8$ Hz (for $\zeta = 0.2$). Typical sine sweep responses are shown in Figure 6.2-3i. The underdamped case shows the 3.8 Hz resonance and the theoretically predicted resonant amplitude gain of approximately 8 db. The poles lie near the imaginary axis at $s = -\zeta\omega_n \pm j\omega_n\sqrt{1 - \zeta^2}$. The critical and overdamped cases show gain roll-off at successively lower frequencies as predicted by their lower frequency real poles. The asymptotic attenuation is 40 db/decade due to the two pole excess.

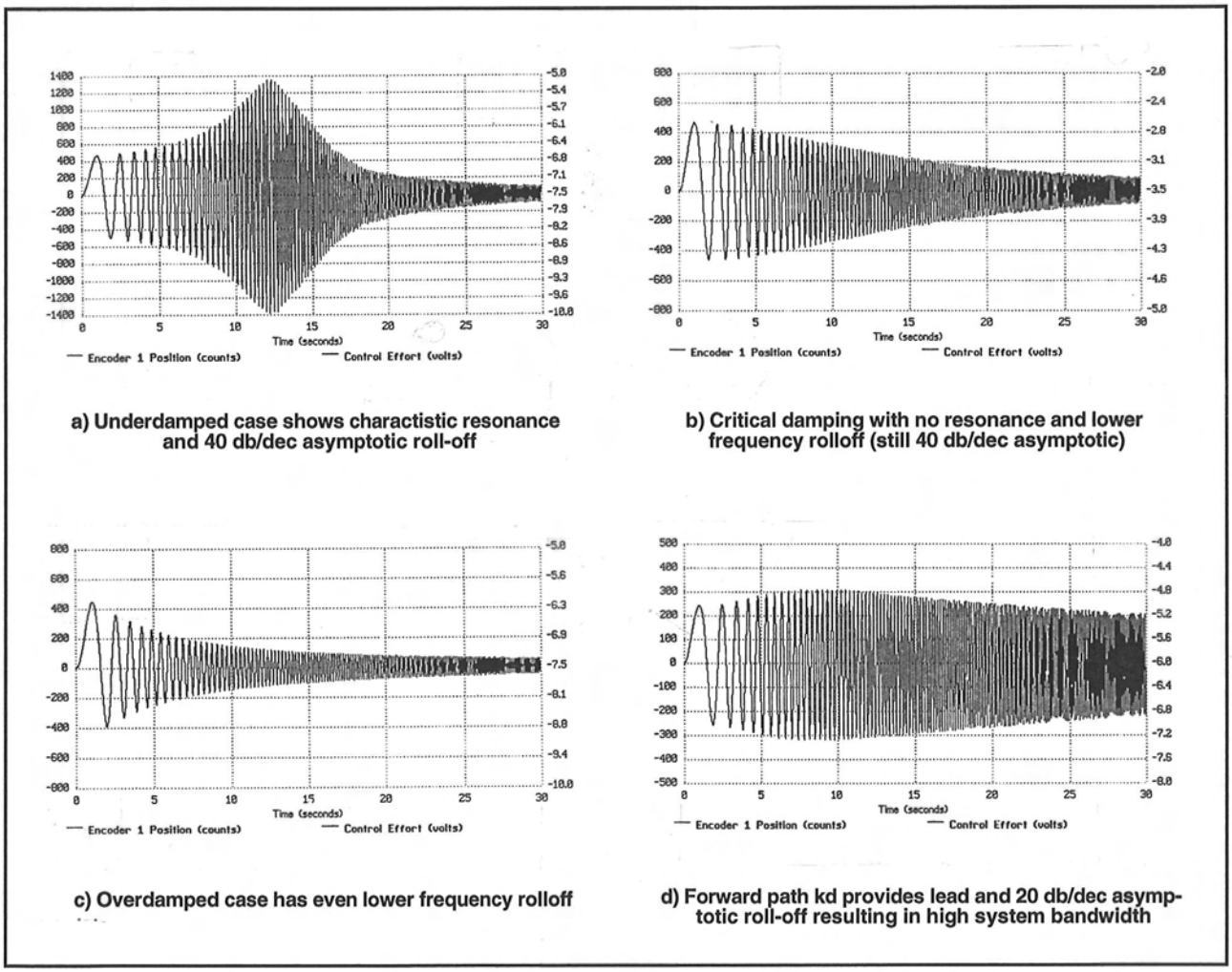

a) Underdamped case shows charactistic resonance and 40 db/dec asymptotic roll-off

b) Critical damping with no resonance and lower frequency rolloff (still 40 db/dec asymptotic)

c) Overdamped case has even lower frequency rolloff

d) Forward path kd provides lead and 20 db/dec asymptotic roll-off resulting in high system bandwidth

Figure 6.2-3i Test Results Reflect Classic Bode Response

© ECP 1995, All Rights Reserved

With the differentiator in the forward path, there is a zero at $s = -k_p/k_d \approx -12$ rad/s ≈ 2 Hz leading to the slight mid-band gain increase seen in the response. This zero along with a 20 db/decade roll-off (single pole excess) leads to much higher system bandwidth reflected in the closer tracking and higher peak control effort seen in the tracking exercises of Section 6.2.4.

The sine sweep with the integrator added (step 5, not shown in Figure 6.2-3i) exhibits a low frequency resonance due to two lightly damped poles which arise due to the integrator. This correlates to the step response overshoot with this controller. The asymptotic attenuation is 40 db per decade.

This section showed:

1. Characteristic frequency response of under- over- and critically damped second order systems including bandwidth, resonance, and asymptotic gain roll-off.
2. Much increased bandwidth and lower asymptotic gain slope with k_d in the forward path.
3. Resonance induced by complex pole pair being drawn near the imaginary axis by introduction of integral action (optional exercise).

Further Example Questions & Topics:

1. What are the phase and gain margins under PD control? *ans: Gain margin is ideally infinite, however as the ratio* k_p/k_d *increases to large values phase margin becomes vanishingly small. In practical systems, there are time delays and nonlinearities which lead to instability when the ratio* k_p/k_d *is large. There are also discretization issues which affect the stability of all sampled data systems. For sufficiently large* T_s *the associated time delay leads to instability. Conversely if* T_s *is too small, excessive noise is propagated due to numerical differentiation with finite sensor measurement (and numerical processor-internal) resolution.*
2. Discuss the root locus implications to stability for PID control of a rigid body when $k_i \neq 0$. *ans: The locus of roots where* k_p, k_i & k_d all *increase proportionally, begins at the triple integrator with one root tending toward* $-\infty$ *and the other two toward the roots of* $(s^2 + (k_p/k_d)s + k_i/k_d)$. *The angles of departure of the three loci from the triple pole are at 60, 180, and 300 deg and therefore the system is unstable at sufficiently <u>low</u> gains for all relative ratios of* k_p, k_i & k_d. *Via the Routh-Hutwitz criterion, the requirement for closed loop stability is* $K_s(k_p k_d) > k_i$ *where* K_s *is the system gain* k_{hw}/J_d^*. *Thus sufficient increase in relative magnitude of* k_i *leads to instability.*
3. The results regarding instability with increased k_i may be shown by slowly and successively increasing its value and implementing the resulting PID controller on the

© ECP 1995, All Rights Reserved

system. The system will become increasingly oscillatory and then unstable. Be certain that k_i is increased slowly and that the safety instructions of Section 2.3 are followed strictly during this procedure.

4. The Bode phase characteristics may be examined as were the magnitude characteristics by comparing the phasing of the Commanded Position sinusoids with the output sinusoids in Section 6.2.5.

6.3i Fundamentals of Servo Control

6.3.1 Effect of Gear Ratio and Inertia

The term k_{hw}/J_d^* (J_d^* is the total reflected inertia at the drive) may be viewed as net system gain. According to Eq's (6.1-3,-5) both ω_n and ζ scale with the inverse square root of inertia. Hence for a given set of PD gains, the response will become slower and more lightly damped with increased inertia. Equivalent load inertia reflected to the motor (J_l^*) scales with the inverse of the gear ratio squared (see Eqs.(5.1-3 through 5.1-6)).

In most applications the load inertia is much greater than the drive inertia . Under very low gear ratios the load inertia tends to dominate the system gain. Most practical systems therefore utilize some form of speed reduction.

In Step 2: The analytical values for the test cases are as follows (comparisons with underdamped controller from Section 6.2.2 using Test Case #2 Configuration):

For Test Case 6:

$J_d = J_{wd}+J_{dd} = 0.0021 + 0.00040 = 0.0025\ kg\text{-}m^2$

$J_{l_{reflected}} = (J_{wl}+J_{dl})(1/gear\ ratio)^2 + (J_{18\ tooth} + J_{72\ tooth} + J_{backlash\ device})(12\ teeth/18\ teeth)^2$

$= (.0206+.0065)(1/1.5)^2 + (3*10^{-6} + 5.5*10^{-4} + 3.1*10^{-5})(1/1.5)^2$

$= (0.0271)(1/1.5)^2 + (0.00058)(1/1.5)^2$

$= 0.0123\ kg\text{-}m^2$

The effect on ω_n and ζ scales with the inverse square root of inertia

i.e. $\omega_n = \omega_{n_o}\sqrt{\frac{J_o}{J}} = 4*\sqrt{\frac{.0025}{.0025+.0123}} = 4*0.41 = 1.64$ Hz, $\zeta = 0.2*0.41 = 0.08$

© ECP 1995, All Rights Reserved

For Test Case 8:

$J_{l_{reflected}} = (0.0271)(1/24)^2 + (0.00058)(12/72)^2$

$= 0.000063\ kg\text{-}m^2$

$\omega_n = 4*\sqrt{\frac{.0025}{.0025+.000063}} = 4*0.988 = 3.95\ Hz, \quad \zeta = 0.2*0.99 = 0.2$

i.e. no appreciable change from ω_{n_o}

For Test Case 9:

$J_d = J_{dd} = 0.00040\ kg\text{-}m^2$

$J_{l_{reflected}} = 0.000063\ kg\text{-}m^2$

$\omega_n = 4*\sqrt{\frac{.00250}{.00040+.000063}} = 4*2.32 = 9.30\ Hz, \quad \zeta = 0.2*2.32 = 0.46$

Representative experimental results are shown in Table 6.3-1i. Measured ζ values will vary somewhat due to their dependence on belt tensioning. The natural frequency measurements however should agree quite well with the analytical predictions.

Table 6.3-1i Typical Results of Section 6.3.1 Experiments.

Test Case Configuration	Description	ω_n (Hz)	ζ
2	Max drive inertia, load disconnected	4.0	0.25
6	Max drive inertia, max load inertia, min gear ratio (1.5:1)	1.7	0.13
8	Max drive inertia, max load inertia, max gear ratio (24:1)	4.0	0.25
9	Min drive inertia, max load inertia, max gear ratio (24:1)	9.6	0.5

In Step 3, When the load (vs. the drive) is taken as the output, the open loop gain is increased by the gear ratio but the reflected inertia, J^*, is increased by gr^2. The net system gain, k_{hw}/J^*, is therefore reduced by gr^{-1}.

© ECP 1995, All Rights Reserved

This section showed:

1. Under low gear ratio, the load inertia (generally much greater than the drive inertia) dominates and lowers the system gain, bandwidth, and damping. (Test Case 6).
2. Under high gear ratio, the load inertia becomes negligible.(Test Case 8).
3. Under high gear ratio the drive inertia dominates and by reducing it, higher gain, bandwidth, and damping result (Test Case 9).

See also Section 6.3.4 for optimum gear ratio and effect on saturation.

6.3.2i Effect of Friction

1. In Step 2: The gains selected provide a critically damped (ideally without friction or drive flexibility) response with ω_n approximately 2 Hz.
2. In Step 3: k_p= 0.24, k_d= 0.037 (i.e. the net system gain for output at Encoder #2 is reduced by the gear ratio – see answer to step 3 Section 6.3.1. The control gains must therefore be increased by this ratio)
3. In Step 5: By closing the loop about the load output, load tracking is generally improved and steady state error reduced since feedback occurs beyond the drive[1] flexibility. I.e. the static servo stiffness at the load includes the drive flexibility when the loop is closed about the drive sensor but not when closed about the load sensor.

   Static servo stiffness (k_{ss}) may be found by injecting a unit disturbance at the plant output and computing the resulting control effort at the plant input (with $r(s)$ =0). By the Final Value Theorem for a stable system, s is set equal to zero throughout the loop (Fig. 6.1-3) Hence when $k_i = 0$ for this system, $k_{ss} = k_p k_{hw}$. For output at the load, when the control is closed about the drive sensor, stiffness is increased by a factor of the gear ratio squared – same as for reflected stiffness in any drive train.

   For Test Case #5, Step 2:

   $k_{ss} = 0.16*5.8\ (1.5)^2 = 2.1$ (N-m/rad).

   In Step 3

   $k_{ss} = 0.24*(5.8*1.5) = 2.1$ (N-m/rad).[2]

   That the above are equivalent corresponds to their gains being adjusted in Step 3 to give the same closed loop dynamic properties.

[1] I.e. the overall drive train – from the drive disk to the load disk in this case

[2] Here the net system gain is reduced by the gear ratio for output at Encoder #2. In this treatment we do not consider the drive compliance in the k_{ss} calculation. See Sect. 6.4 for a discussion of the effect of feedback sensor location on steady state error when drive flexibility exists.

© ECP 1995, All Rights Reserved

For Test Case #7, Step 4:

k_{ss} = 0.068*5.8 $(24)^2$ = 227 (N-m/rad). (Same for case of Encoder #2 as feedback)

4. In Step 6:

   For Test Case #5

   With integral action, k_{ss} is infinite and steady state error is zero

Typical results are given in Table 6.3-2i and Figure 6.3-1i. The advantage of increased static servo stiffness at the output resulting from increased gear ratio is clearly seen. The improvement by using the noncollocated load sensor results from effective elimination of compliance in the drive train. Such compliance between the drive and the load and reduces k_{ss} as per a spring in series.

It should be mentioned to students that while adding integral action may be a satisfactory means for eliminating steady state position error (e.g. in regulation applications) it may not be suitable for tracking because of its effective underdamped (overshoot) characteristic. Also as may be observed, the stick-slip phenomenon of dry friction makes the settling time to steady state very long under integral action and low gear ratio. A low amplitude limit cycle may be seen in some cases. This is alleviated by higher gear ratio.

It may also be mentioned that the higher servo stiffness in step 4 vs. step 3 could be achieved via increased control gains. These gains in the latter case would have to be 256 times higher however to provide the same k_{ss} and would require excessive control effort and result in severe DAC saturation. These issues are studied later in this section (especially 6.3.4).

Finally, it may be mentioned that increased friction (and inertia under dynamic conditions) increases the effect of the flexibility of drive components (mostly in the drive train belts in this case): I.e. lowered flexible mode frequencies and greater disparity between the scaled drive and load sensor indications.

Table 6.3-2i Typical Results of Section 6.3.2 Experiments.

Test Case Configuration	Description	Typical Steady State Error, e_{ss} (Counts)
5	Low gear ratio (1.5:1), drive (collocated) feedback	600
5	Low gear ratio (1.5:1), load (noncollocated) feedback	400
7	High gear ratio (24:1), drive (collocated) feedback	10
7	High gear ratio (24:1), drive (noncollocated) feedback	5
5	High gear ratio (1.5:1), noncollocated, integral action	0

© ECP 1995, All Rights Reserved

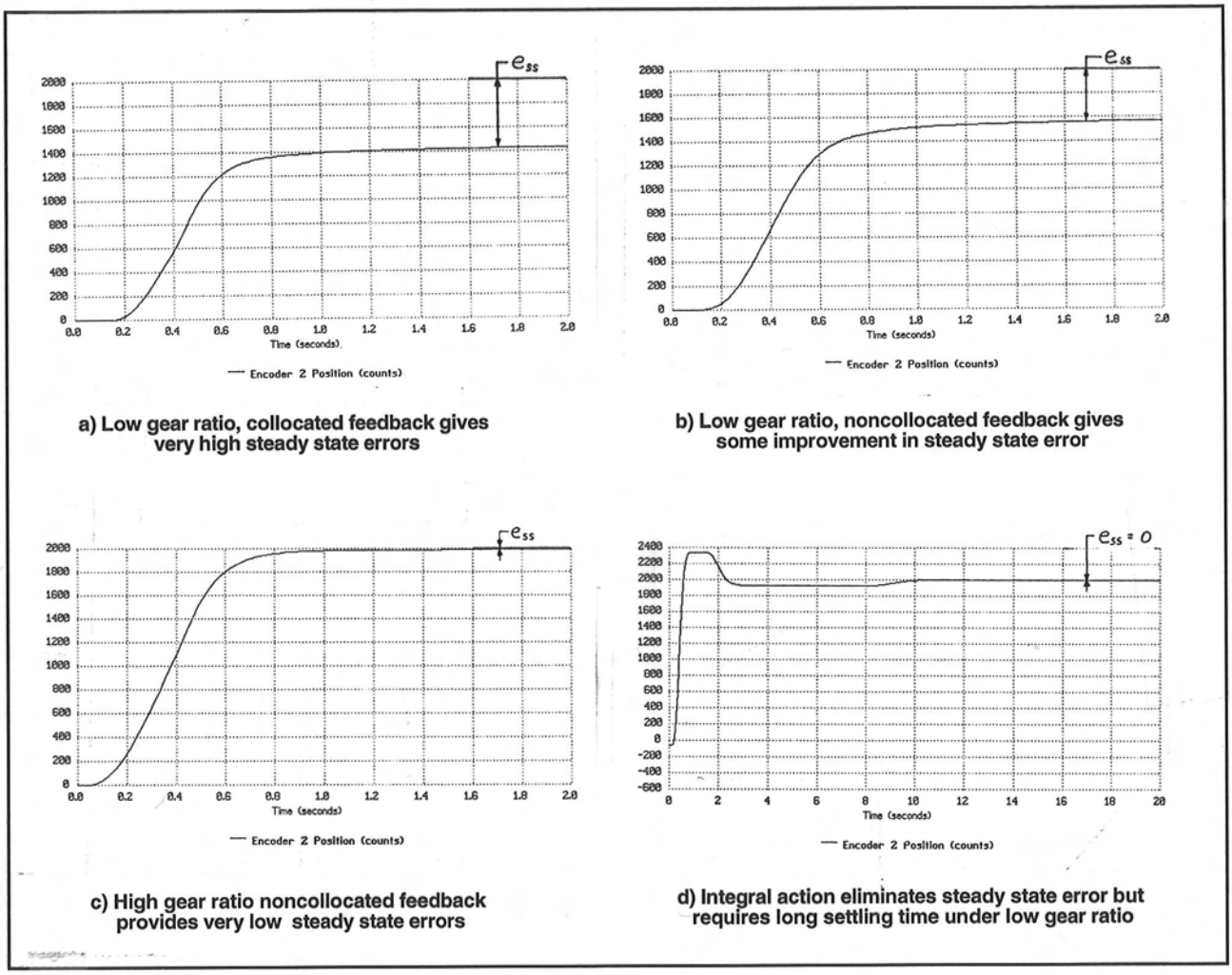

Figure 6.3-1i Experimental Results Show Effects of Gear Ratio and Integral Action on Friction Induced Steady State Error

This section showed:

1. Static servo stiffness, k_{ss}, is proportional to, and steady state error is inversely proportional to, the gear ratio squared.
2. Noncollocated control (with sensor at the location of objective control) generally yields lower steady state error than collocated.
3. Integral action is an effective way of eliminating steady state error but may involve high control effort and long settling time in low gear reduction plants.

© ECP 1995, All Rights Reserved

6.3.3i Effect of Disturbances

1. Typical results for steps 1 and 2 are shown in Figure 6.3-2i.
2. In Step 3: The advantage of high gear ratio in attenuating low frequency disturbances at the load is clearly seen. This is again because the static servo stiffness increases by the gear ratio squared. The noncollocated scheme is more effective than collocated for low frequency disturbance rejection.

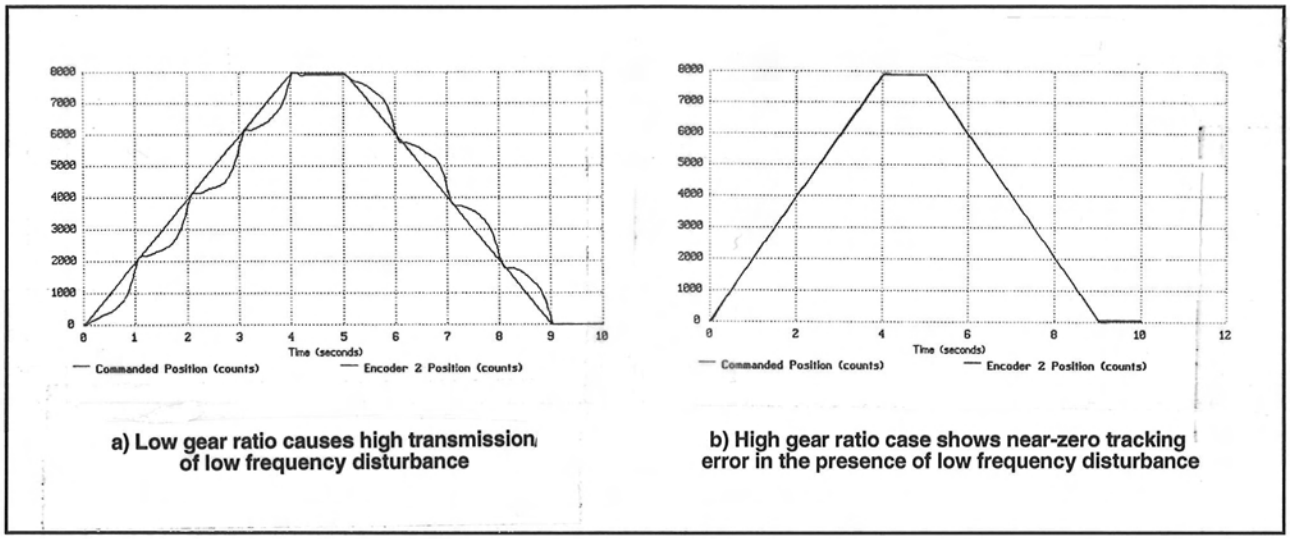

a) Low gear ratio causes high transmission of low frequency disturbance

b) High gear ratio case shows near-zero tracking error in the presence of low frequency disturbance

Figure 6.3-2i Test Results Show Strong Reduction In Disturbance Induced Tracking Error With Increased Gear Ratio

3. In Step 4c: The filter is: $F(s) = \dfrac{6.28 + 5s}{6.28 + s}$
4. In Step 8: Open Loop Transfer Functions:[1]

Controllers "a" & "b":

$$\frac{N_{ol}(s)}{D_{ol}(s)} = \frac{k_d s^2 + k_p s + k_i}{s} \frac{k_{hw}}{Js^2} \qquad (6.3\text{-}1i)$$

$$= \frac{5.81(0.009s + 0.08)}{0.0029s^2} \quad \text{(Controller "a")}$$

$$= \frac{5.81(0.009s^2 + 0.08s + 1)}{0.0029s^3} \quad \text{(Controller "b")}$$

[1]The transfer function parameter values shown are for output at the Drive disk, for output at the Load disk, the open loop expressions should be multiplied by the gear ratio and the closed loop divided by the gear ratio.

© ECP 1995, All Rights Reserved

Controller "c":

$$\frac{N_{ol}(s)}{D_{ol}(s)} = (k_d s + k_p)\frac{N_f(s)}{D_f(s)}\frac{k_{hw}}{Js^2} \qquad (6.3\text{-}2i)$$

$$= \frac{5.81(0.009s+0.08)(5s+6.28)}{0.0029s^2(s+6.28)}$$

$$= \frac{(0.261s^2+2.65s+2.92)}{s^2(0.0029s+0.0182)}$$

Closed Loop $\theta_1(s)/T_d(s)$:

Controllers "a" & "b":

$$\frac{\theta_1(s)}{T_d(s)} = \frac{s}{Js^3 + k_{hw}(k_d s^2 + k_p s + k_i)} \qquad (6.3\text{-}3i)$$

$$= \frac{1}{0.0029s^2 + 5.81(0.009s+0.08)} \quad \text{(Controller "a")}$$

$$= \frac{s}{0.0029s^3 + 5.81(0.009s^2+0.08s+1)} \quad \text{(Controller "b")}$$

Controller "c":

$$\frac{\theta_1(s)}{T_d(s)} = \frac{D_f(s)}{Js^2 D_f(s) + k_{hw}(k_d s + k_p)N_f(s)} \qquad (6.3\text{-}4i)$$

$$= \frac{s+6.28}{0.0029s^3 + 0.280s^2 + 2.65s + 2.92}$$

Example test results are given in Figure 6.3-3i. The Bode magnitude of the above transfer functions is given in Figures 6.3-3i and -4i. The correlation between the closed loop gain and the experimentally obtained disturbance attenuation at the two test frequencies is clear. The integrator in controller "b" provides high low frequency attenuation but has a high gain peak between one and two Hz making it ineffective at these frequencies. The lead-lag filter made no improvement over the PD controller at very low frequencies but was effective in the higher frequencies as predicted in the closed loop Bode response.

The correlation between the open and closed loop gains is also clear. The integrator is manifested as the -60 db/dec. low frequency slope and provides complete disturbance attenuation (zero DC gain) in the closed loop. The low open loop gain slope near crossover correlates (significant phase lag also exists at this frequency) to the closed loop resonance near two Hz. The added gain from the lead-lag filter for frequencies beyond 0.1 Hz yields higher frequency attenuation in the closed loop.

© ECP 1995, All Rights Reserved

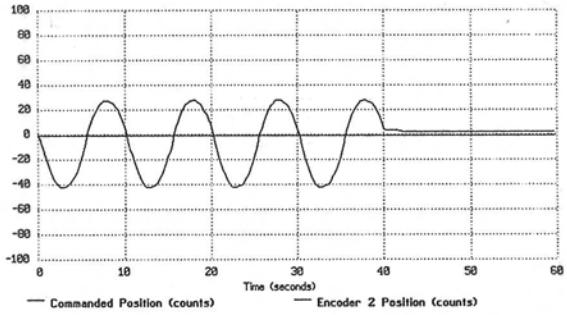

a) PD control with 0.1 Hz disturbance frequenciy shows high disturbance transmission

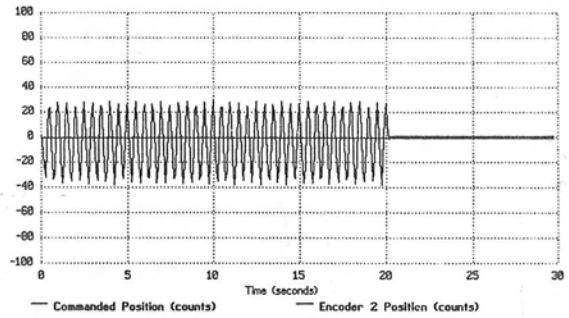

d) PD control shows only slightly less disturbance transmission at higher frequency (2.0 Hz)

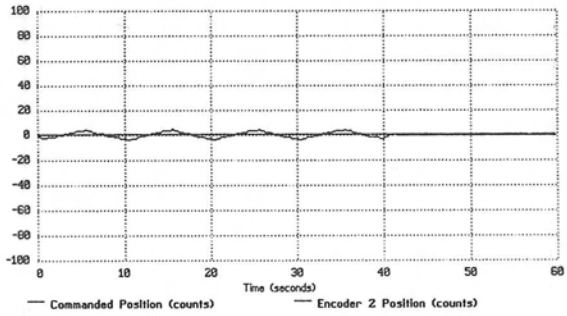

b) Integrator added to PD control is effective in attenuating low frequency disturbances

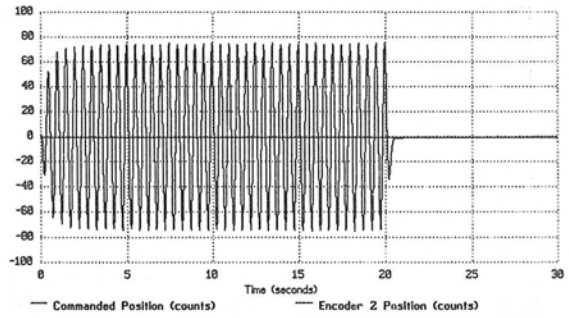

e) Integrator shows high transmission at 2 Hz

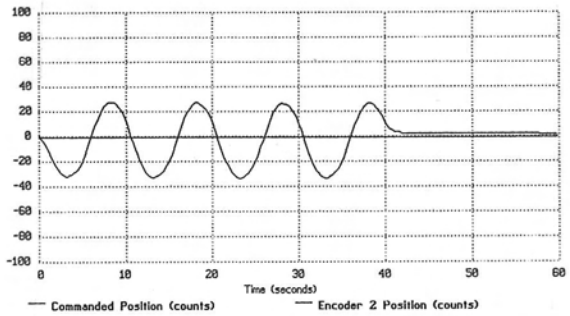

c) Lead/lag filter added to PD controller does not improve low frequency attenuation

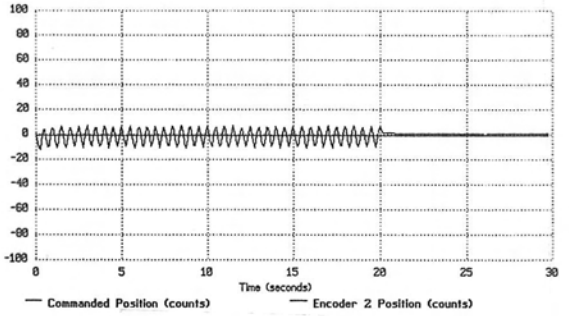

f) Lead lag filter has considerably improved attenuation at higher frequency

Figure 6.3-3i Effects Of Integral Action And Lead On Low and High Frequency Disturbance Transmission

© ECP 1995, All Rights Reserved

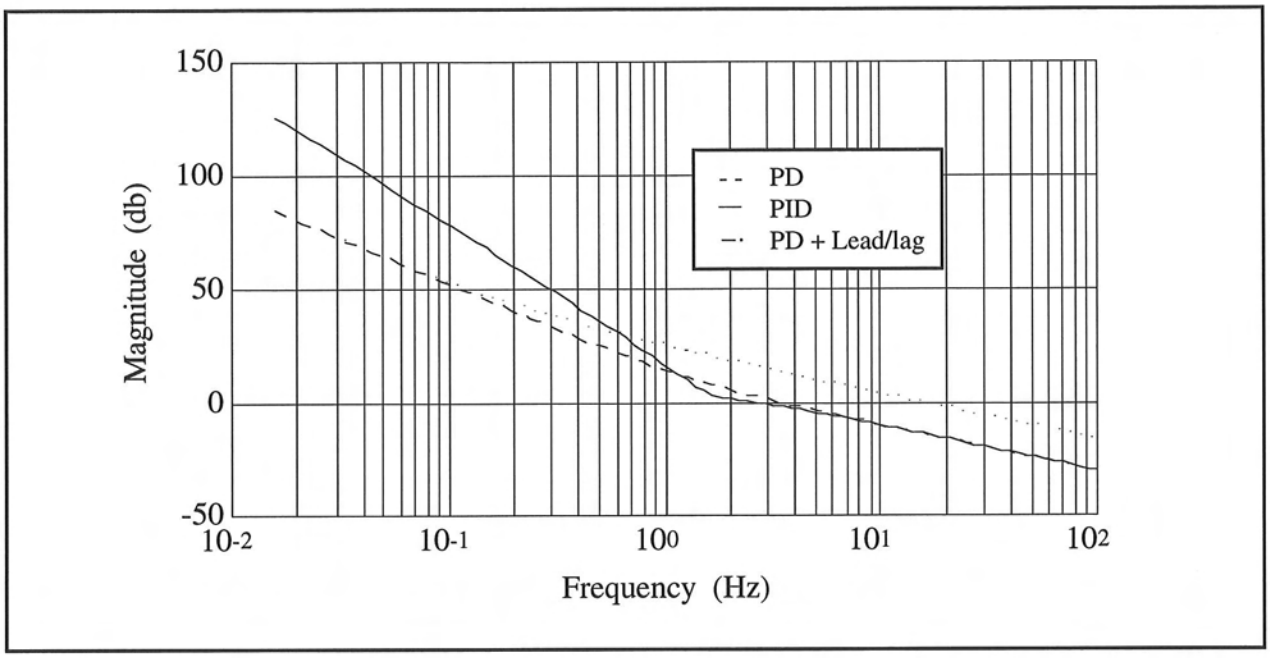

Figure 6.3-4i Open Loop Frequency Response of Disturbance Test System

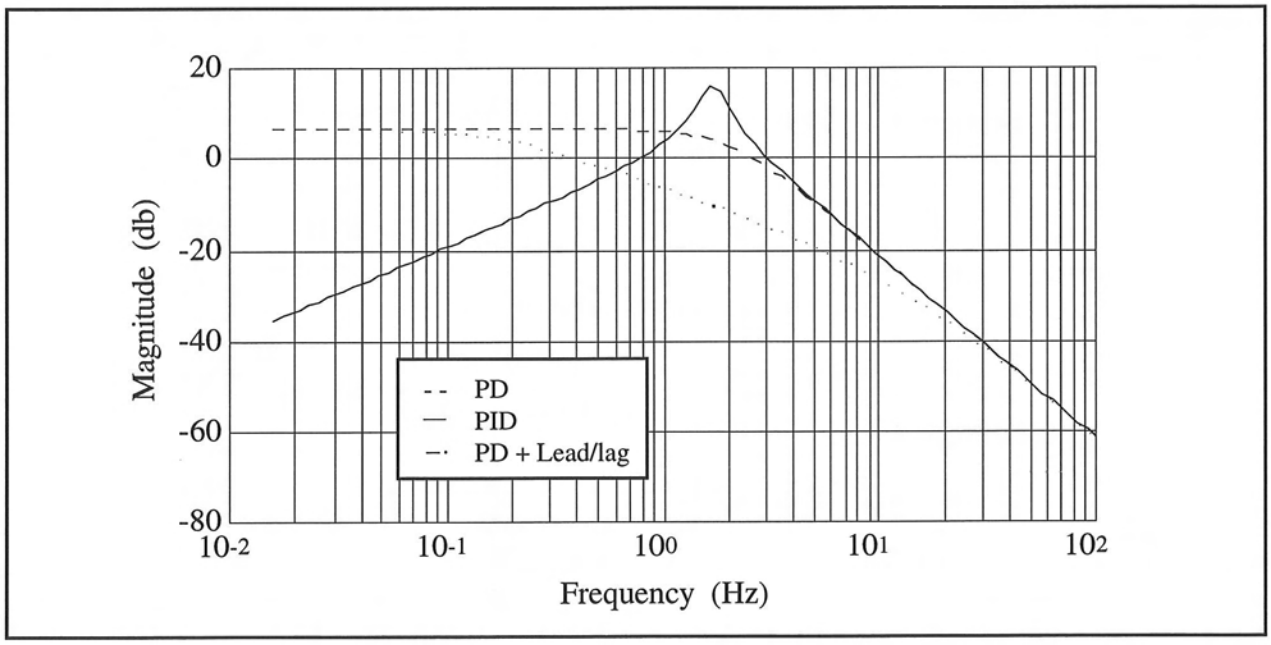

Figure 6.3-5i Closed Loop Frequency Response, $\theta_1(s)/T_d(s)$

© ECP 1995, All Rights Reserved

This section showed:

1. The results of Section 6.3.2 regarding strong reduction in e_{ss} with increased gear ratio is extendible to disturbance attenuation - at least for lower frequency disturbances
2. An integrator in the control can be an effective way to attenuate disturbances at low frequencies but can be deleterious for higher frequency disturbances.
3. Providing high open loop gain in the expected disturbance frequency band of is an effective attenuation approach (subject of course to the requirement for closed loop stability).

6.3.4i Effect of Drive Saturation

1. In Step 2: Typical test results are shown in Figure 6.3-6i.
2. In Step 3: 90% rise time ≅ 390 ms, 320 ms, and 460 ms for the respective 1.5, 4.5, and 24:1 gear ratios. The response shape during saturation is nominally parabolic since a constant torque is being applied to a rigid body. The velocity is nominally linear.
3. In Step 4: By taking $d\left(\ddot{\theta}_{max_{load}}\right)/d\,(gr) = 0$ and verifying that the result is a maximum, the optimum gear ratio is:

$$gr_o = \sqrt{\frac{J_l}{J_d}} \qquad (6.3\text{-}4i)$$

This expression leads to the rule of thumb in servo design that the optimum gear ratio is such that the reflected payload inertia (reflected to the drive or motor) is equal to the drive inertia.

The experiment was designed for an optimal gear ratio of 5:1 hence the 4.5:1 gear ratio was near optimal and resulted in the least saturation.

The function $\ddot{\theta}_{max}(gr)$ in Eq. (6.3-3) is geometrically symmetric about its optimum. That is, the accelerations under a fixed torque with the gear ratios gr_o*x and gr_{or}/x (for some positive real x) are identical. Since $gr = 1.5$ is 3.3 times smaller, and $gr = 24$ is 4.8 times greater than the optimum (here $gr_o = 5.0$), the greater saturation in the latter case is to be expected.

4. In Step 5: The inertia was minimized to obtain a satisfactory low amplitude response with the forward path differentiating controller. This scheme otherwise saturates for very low step amplitudes. (E.g. with full load inertia at gr=1.5, and ω_n=2 Hz, saturation occurs for a 25 count step.) Typical test results are shown in Figure 6.3-7i which includes a discussion of the response differences. The reduction in rise time due to saturation in the forward path k_d controller is dramatic and accompanies a qualitative change in shape.

© ECP 1995, All Rights Reserved

It should be mentioned to students however that a step input, while useful for characterization, is extremely harsh and normally would not be employed in practice. The forward path k_d controller performs quite well in many systems using a smoothed trajectory (e.g. Figure 6.2-2i).

The above results lead to more broad generalizations. In some control systems – particularly those involving plant inversion or near plant inversion – saturation can lead to completely unacceptable performance because the drive components are unable to follow the large transient control effort. Such schemes are not practical in some cases since they may require relatively large (costly) drive components.

Equation (6.3-4i) shows the value in obtaining very low drive inertia so that a large gear ratio may be used. This in turn reduces the torque and current requirements (lower equipment cost) of the servo motor and amplifier. It also reduces the required electrical power (lower operating cost). Thus modern high performance servo motors typically have very low inertia relative to their rated torque.

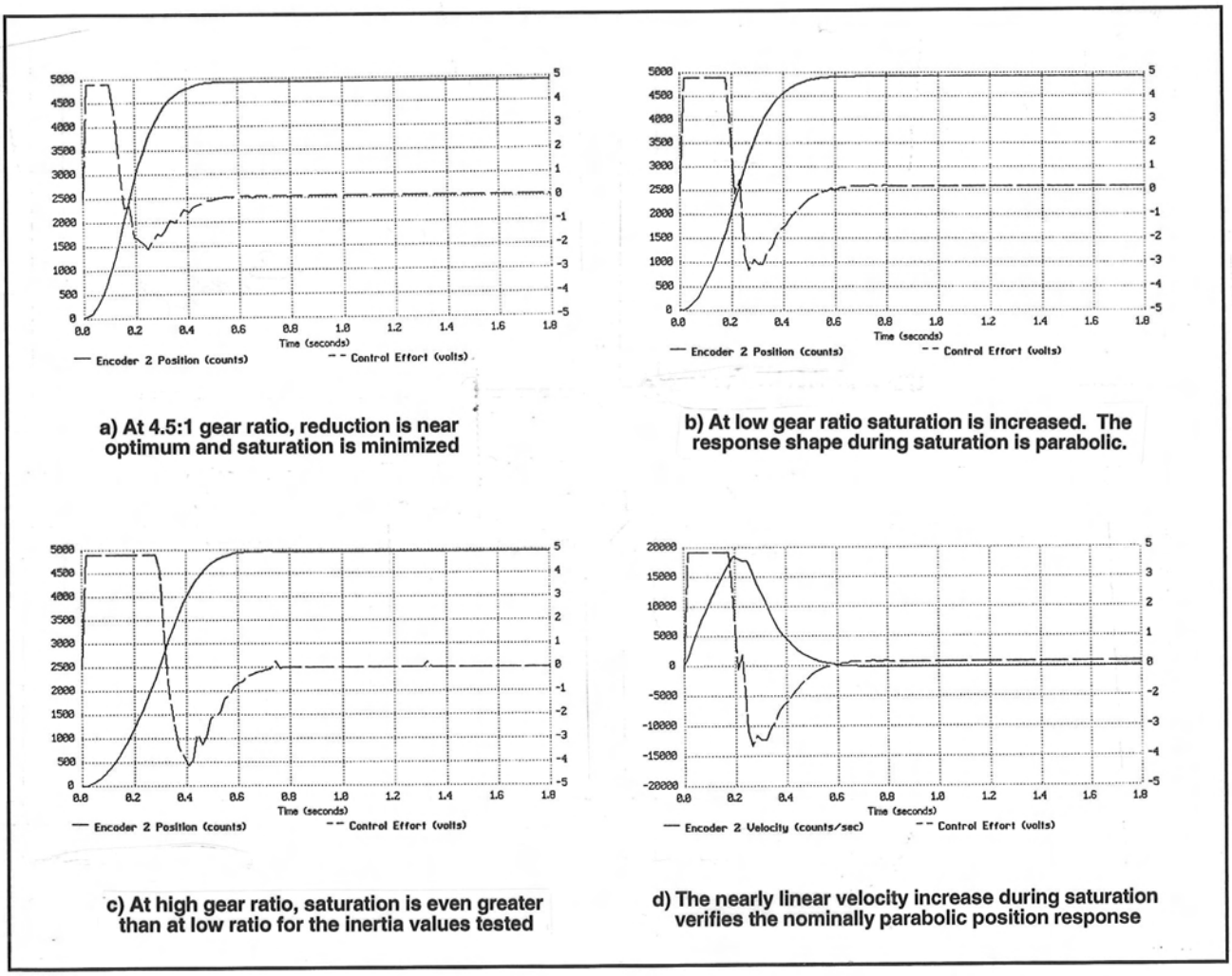

a) At 4.5:1 gear ratio, reduction is near optimum and saturation is minimized

b) At low gear ratio saturation is increased. The response shape during saturation is parabolic.

c) At high gear ratio, saturation is even greater than at low ratio for the inertia values tested

d) The nearly linear velocity increase during saturation verifies the nominally parabolic position response

Figure 6.3-6i Experimental Results Show Effects of Gear Ratio on Saturation and Characteristic Parabolic Response

© ECP 1995, All Rights Reserved

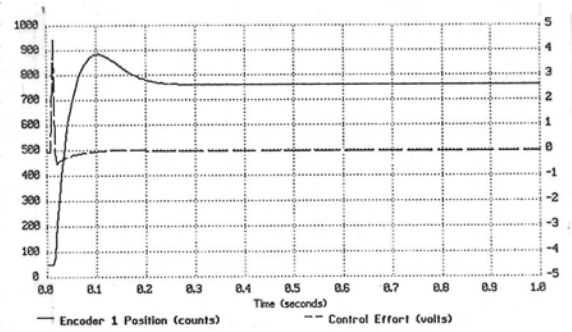

a) Low amplitude step response with forward path differentiator has near ideal shape (including overshoot for zeta = 1). Peak DAC output is just below saturation

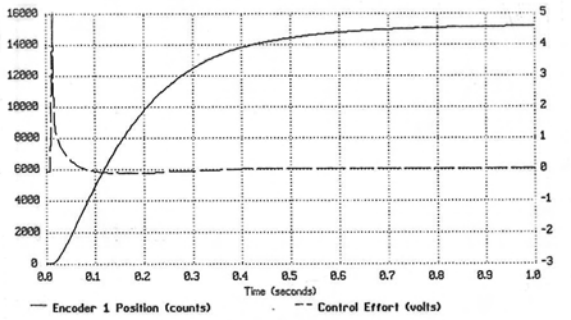

b) High ampl. step causes truncation of impulsive initial control effort. (Peak DAC level would be ~ 80 V (at this Ts) if not saturated!) Response is essentially identical to suplot "c".

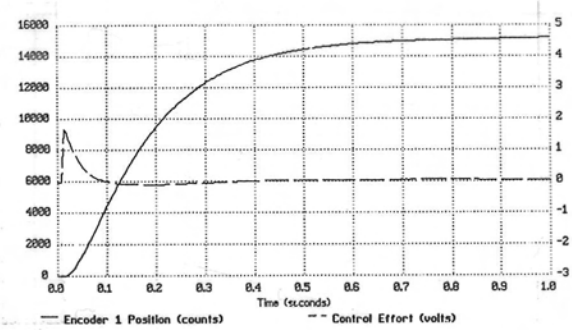

c) Backward path kd does not attempt to differentiate step input. Low control effort req'd. Response shape indep. of ampl. except for very high and low values

For all but low amplitude steps, the forward path kd gives nearly identica response to the reverse path one because the initiai impulsive control effort is highly truncated and because the two control schemes are identical under constant reference input

Figure 6.3-7i Effect Of Saturation in Forward Path Differentiator Control on Response Shape

This section showed:

1. Saturation can significantly reduce the system response time.
2. The optimal gear ratio to minimize saturation is $gr_o = \sqrt{J_l/J_d}$ corresponding to the rule of thumb that the optimum gear ratio results in the reflected load inertia and the drive inertia being equal.
3. High bandwidth forward path control terms can lead to substantial saturation and significantly alter the tracking response - particularly for abruptly changing input trajectories.

© ECP 1995, All Rights Reserved

6.3.5i Effect of Discrete Time Sampling

1. In Step 1: Experimental instability occurs for sample periods greater than about 60 ms.
2. In Step 2: Experimental instability occurs for sample periods greater than about 9 ms.
3. In Step 3: Bode phase margins are both 76° (1.33 radians) and occur at 26 and 129 rad/s for the respective 2 and 10 Hz systems. Using the approximation by way of Eqs.(6.3-6, -7)[1], we would expect instability when $T_s\omega$ is roughly equal to the phase margin (PM) at the critical frequency. I.e. at:

$$T_s = PM/\omega \qquad (6.3\text{-}5i)$$

$$= 51 \text{ ms for the 2 Hz system}$$

$$= 12 \text{ ms for the 10 Hz system}$$

Approximations similar to the pure time delay of Eq.(6.3-6) give rise to a often used rule of thumb that the sample frequency should be at least 1 decade higher than the open loop crossover frequency ω_c. In many cases however, one should consider the continuous time phase margin to be certain that the thumb's rule is sufficiently conservative. For the pure time delay approximation, 36° of lag is levied when sampling at $10\omega_c$ – i.e. a substantial and in some cases destabilizing amount. For sampling two decades higher than ω_c, the phase loss is only 3.6°, which is negligible in most systems.

It may be mentioned to students that well before increases in T_s cause instability, they cause significant changes in plant dynamics – e.g. measurable changes in natural frequency and damping for the simply controlled system studied here. These topics are more rigorously studied in the context of z-domain and discrete time linear systems analyses and are readily supported by the Model 220 system and Executive software.

6.3.6i Effect of Sensor Quantization

Important Note:

Before allowing students to proceed with this experiment, make certain that power to the mechanism is disconnected and that the belt connecting the drive motor and the drive disk

[1]In most industrial implementations, sampling related phase lag is not less than that of a zero order hold which has one half the phase lag of a pure time delay for a given T_s. Generally the sample and hold process is the dominant phase lag source and hence at modest sample rates Eq 6.3-5 tends to be conservative. For high sample rates, other non T_s related phase lags including those in analog signal and power processing may become significant hence the non conservative prediction for the 10 Hz system.

© ECP 1995, All Rights Reserved

(underneath the horizontal base plate) is taught. Any appreciable looseness will adversely affect test results and could lead to damage of the mechanism. If necessary, have an experienced technician loosen the motor mounting screws and apply 10-20 lb. force on the belt via the motor while re tightening.

It is important that students shut down (via **Abort Control**) the system promptly after inducing quantization noise and that the sampling rate is lowered not more than one increment at a time when identifying T_s for noise onset.

1. In Step 2: Noise onset should be at 0.001768 s ± 1 T_s increment (0.000884 s).
2. In Step 3: Noise onset should be at 0.002652 s ± 1 T_s increment.
3. In Step 4: The higher minimum T_s for quantization noise onset with greater k_d is consistent with the associated control torque quantization as defined in Eq.(6.3-9).

This last two sections showed:

1. The phase lag associated with discrete-time sampling can lead to performance changes and instability when continuous-time techniques are exclusively employed.
2. The maximum sample period to induce instability, T_{smax}, for this and many servo systems is approximately: $T_{smax} = PM/\omega$. This value should be reduced by a factor of 2 or more to furnish adequate phase margin and a more close approximation of continuous time performance.
3. Sensor quantization noise increases with high frequency gain and with increased sampling frequency.

6.4 Control of Plant With Drive Flexibility

6.4.1 Collocated Control

This experiment illustrates the affect of dynamic coupling on the plant, the characteristic differences between collocated and noncollocated dynamics, and the inherent controllability difficulties in the use of a collocated scheme when point of objective control is not at the actuator location.

Expected Results:

1) In Step 3: Step responses at θ_1 and θ_2 are shown in subplots a and b of Figure 6.4-1i where $k_p = 1.5$, $k_d = .015$ were selected.

© ECP 1995, All Rights Reserved

2) In Step 4: The predominant feature is the lightly damped oscillation @ roughly 2.8 Hz[1] . The fairly high PD gains have brought the closed loop poles very near the collocated zeros (roots of N_1 (s)); thus the oscillations are largely attenuated in θ_1.

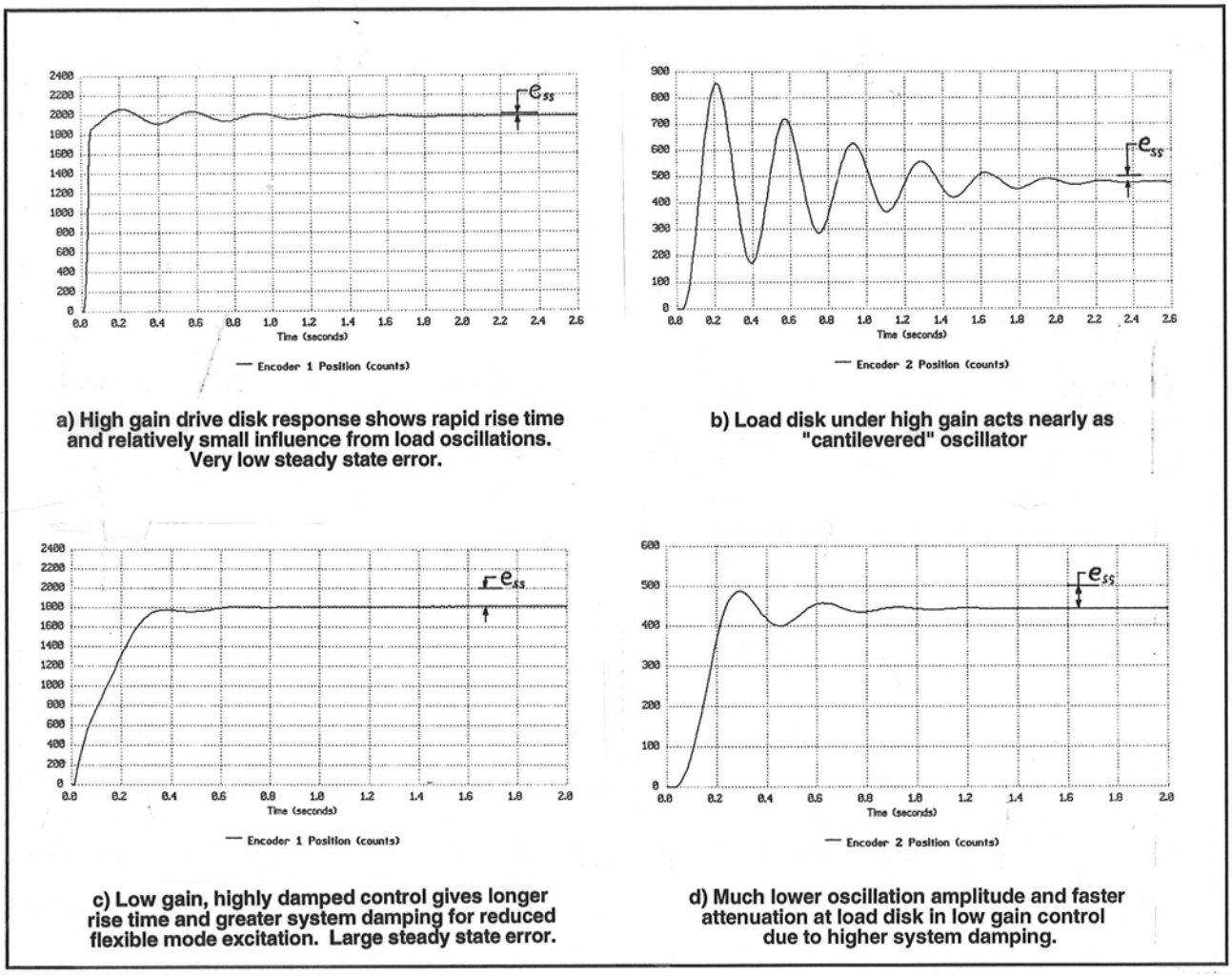

a) High gain drive disk response shows rapid rise time and relatively small influence from load oscillations. Very low steady state error.

b) Load disk under high gain acts nearly as "cantilevered" oscillator

c) Low gain, highly damped control gives longer rise time and greater system damping for reduced flexible mode excitation. Large steady state error.

d) Much lower oscillation amplitude and faster attenuation at load disk in low gain control due to higher system damping.

Figure 6.4-1i. Step Responses At Drive and Load Under High and Low Gain Collocated Control

3) In Step 5: Step responses at θ_2 are shown in subplots c and d of Figure 6.4-1i where k_p = .12, k_d = 0.015 were selected. This provided a fairly highly damped response at the drive disk to dampen and minimize excitation of the vibration mode.

4) In Step 6: Closed loop poles for the gains above are roughly {-18± 16i, -0.2± 2.7i} (Hz, from step 3), and { -33,-1.4, -0.6± 2.6i} (Hz, step 5). The closed loop zeros are identical to the open loop ones. Again, the high PD gains in step 3 have brought the closed loop poles very near the collocated zeros (at -0.2± 2.8i). This pole pair is not canceled in the θ_2 output. The lower gain control has dampened the oscillatory poles.

[1]Because of the stiff collocated control, the oscillation is essentially the same as that of the clamped-free ("cantilevered") configuration used in measurement of k in Section 6.1.4.

© ECP 1995, All Rights Reserved

5) In Step 7: Static servo stiffness, k_{ss}, at the drive is equal to $k_p k_{hw}$ (N-m/rad). It is more than ten times greater in the stated higher gain controller than in the lower gain one. The static servo stiffness at θ_1 couples in series with the torsional spring and reduces the effective stiffness at θ_2 according to: $(T_d/\theta_2)_{ss} = (k_p k_{hw} gr^2)k/(k_p k_{hw} gr^2+k)$. With $k_i \neq 0$, k_{ss} is infinite at the collocation and is equal to k at the load.

Further Topics:

1) It is illustrative to demonstrate frequency response behavior via sine sweeps of the closed (& open) loop systems. Shown in Figure 6.4-2i is the sweep output at θ_1 and θ_2 with sweep frequency starting at 0.01 and ending at 6.0 Hz for the high gain PD controller from step 3. Note the near pole-zero cancellation in the collocated response with the pole occurring just below the zero frequency and hence the lower amplitude at higher frequency. The collocated amplitude does not begin to roll off at 6 Hz. The noncollocated response clearly shows the structural resonance. This is the frequency response correlation to the much larger oscillation in the θ_1 step response than in the θ_2 one. The noncollocated response attenuates at a lower frequency with faster roll-off due to its lower gain and four pole excess (collocation has two pole excess).

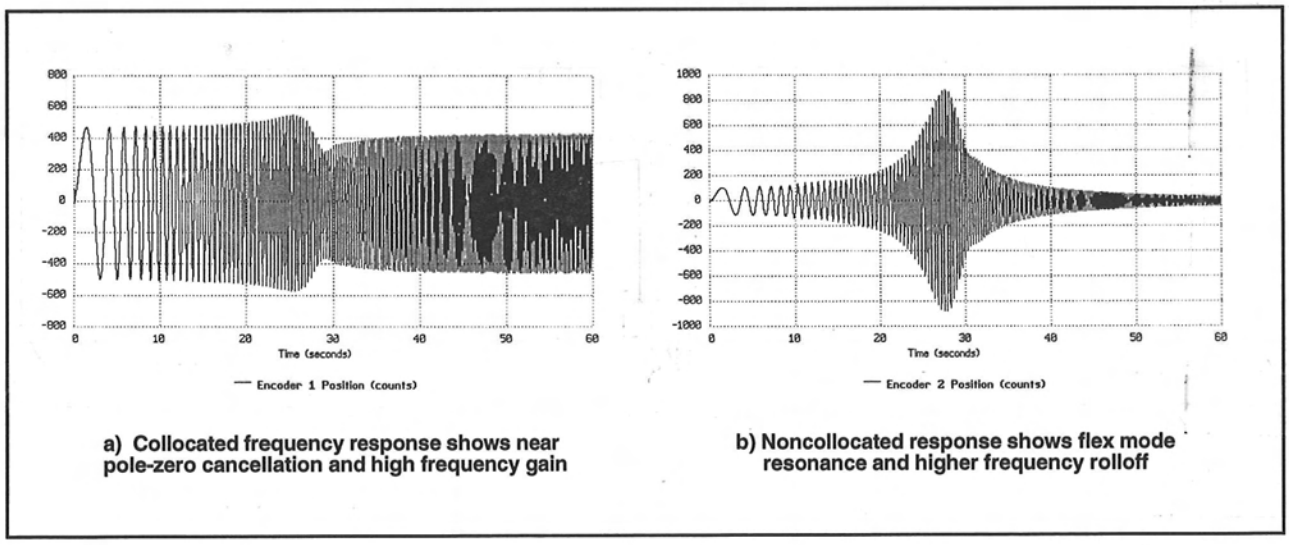

a) Collocated frequency response shows near pole-zero cancellation and high frequency gain

b) Noncollocated response shows flex mode resonance and higher frequency rolloff

Figure 6.4-2i. Frequency Response Magnitude (Sine Sweep) At θ_1 and θ_2

2) It is also instructive to perform tracking control and regulation under disturbance torques. These are shown later in Figures 6.4-9i, -10i and discussed in Section 6.4-4.

3) Comparison of the stability margins in this and the next section is also a very useful exercise. Generally speaking, the phase and margins of collocated control can be made greater than those for noncollocated control, but collocated schemes of course generally have poorer performance at the noncollocation (load disk).

© ECP 1995, All Rights Reserved

4) In all experiments, it is insightful to consider control effort and to examine the price paid in power consumption and component size (read "cost") in providing high gain tracking. In some cases the effects of DAC saturation are also evident.

This section showed:

1. That high bandwidth collocated control is effective in attenuating flexible mode oscillations at the collocation but results in large oscillations at other locations (the load in our case).
2. Lower bandwidth, well damped, collocated control can result in more damping of the mode(s) and provide more acceptable performance at noncollocations
3. Collocated control has limited capability to provide high performance at noncollocations if significant flexibility exists in the drive train.

6.4.2i PD Plus Notch Filter Control

This experiment illustrates an approach often used in noncollocated structural control where a collocated rate feedback loop is first closed to improve plant stability. An outer loop is then closed about the location where control is desired. This approach generally yields superior performance to purely collocated schemes in cases with significant structural flexibility.

Expected Results:

1) In Step 1: The root locus of the plant given in Eq (6.1-3i) is shown in Figure 6.4-3i where $k_v = 0.0030$ is selected as providing the greatest damping.

2) In Step 3: For the above value of k_v the specified notch filter is:

$$N_n = 526.7\left((s+19.07)^2+(25.56)^2\right) = 526.68s^2+20092s+535788 \quad (6.4\text{-}1i)$$

$$D_n = \left((s+9.6\pi)^2+(7.2\pi)^2\right)(s+120\pi) = s^3+437.310s^2+24160.8s+535788 \quad (6.4\text{-}2i)$$

Note that this filter also adds phase lead in the crossover frequency region and hence helps stabilize the system.

3) In step 5: A step response for $k_p = 0.5$, $k_d = 0.040$ is shown in Figure 6.4-4i.[1] The steady state error here is reduced by a factor of about three from that seen in Figure 6.4-1i. The static servo stiffness here is $(T_{d\theta_2}/\theta_2)_{ss} = grk_pk_{hw} = 11.6$ (N-m / rad). The drive disk is now less stiff according to: $(T_{d\theta_1}/\theta_1)_{ss} = k_pk_{hw}/gr$ I.e. with collocated control (previous section) the structural compliance and gear ratio inverse increase the effective control compliance at the noncollocated output and hence the steady state error. With noncollocated control, the servo stiffness is independent of structural compliance

[1]The response shown has slower rise time and less oscillation than the ideal. This is because of momentary DAC saturation from differentiation of the input at the step leading edge. The more ideal response can be viewed by reducing the step size to say 50 counts.

© ECP 1995, All Rights Reserved

and can generally be made greater. The noncollocated control stiffness at the drive disk is lower than at the load disk by the inverse gear ratio squared. The student should notice the drive disk moving in opposition to the disturbance direction when the load disk is manually perturbed, i.e. the servo stiffness is greater than the flexible belt stiffness.

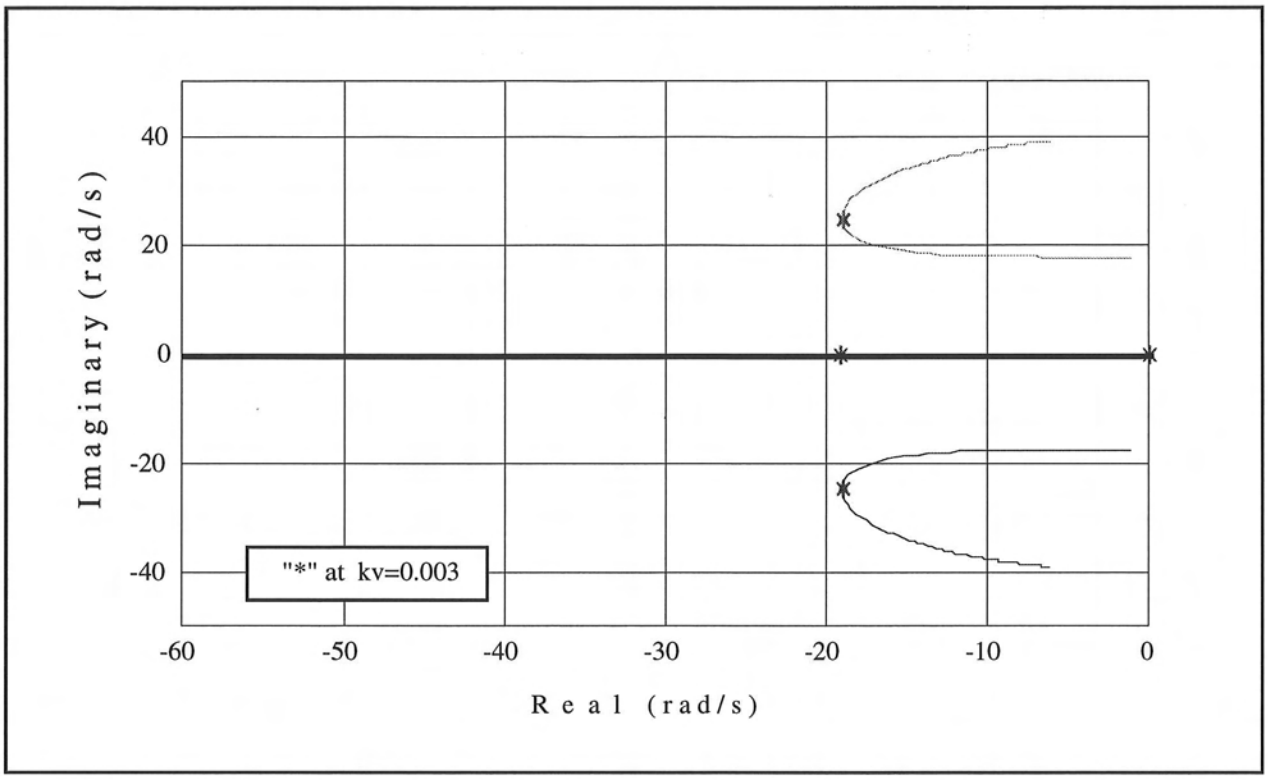

Figure 6.4-3i. Collocated Rate Feedback Root Locus

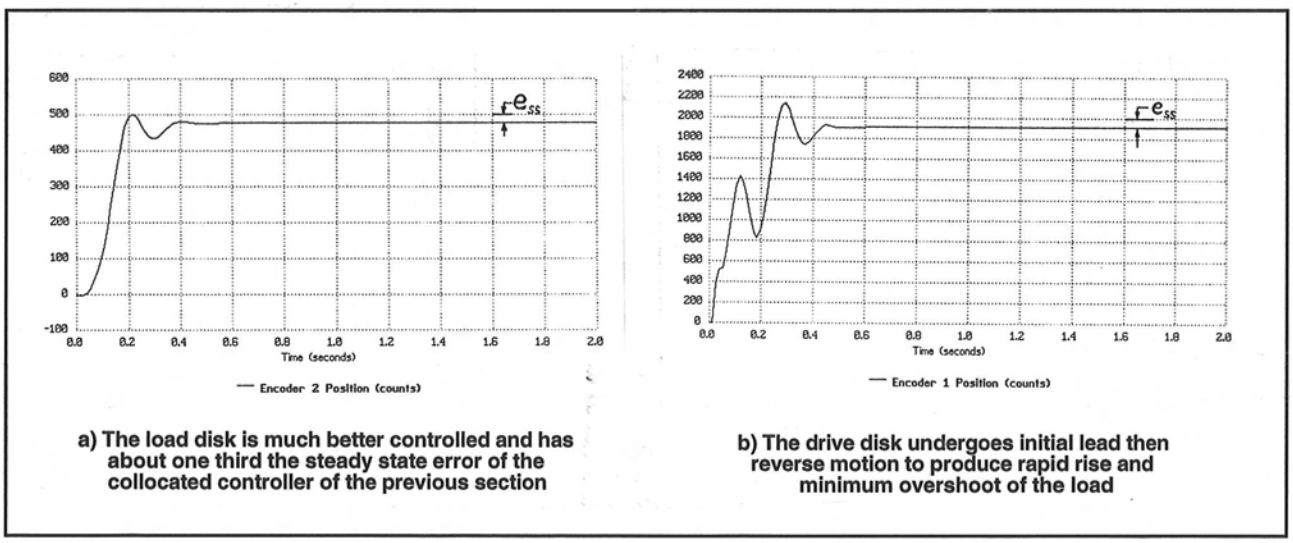

a) The load disk is much better controlled and has about one third the steady state error of the collocated controller of the previous section

b) The drive disk undergoes initial lead then reverse motion to produce rapid rise and minimum overshoot of the load

Figure 6.4-4i. Step Responses at the Drive and Load For Successive Loop / Notch Filter Design

© ECP 1995, All Rights Reserved

Further Topics:

1) A saw-tooth tracking response is shown later in Figure 6.4-9i. The reduction in lag and error over the collocated controllers in the previous experiment is apparent. Figure 6.4-10i gives the disturbance response and again shows improvement over the collocated designs.

2) Many other schemes are readily implemented including collocated (drive disk only) controller plus cascaded notch; or outer loop pole placement, loop shaping (e.g. H2 or H∞, m-synthesis), or QFT based on the multiple loop approach. In all cases, collocated rate feedback and notch filtering may be included or left out.

This section showed:

1. In many practical cases such as this, the SIMO control problem may be satisfactorily solved via successive loop closure.
2. Satisfactory results for flexible plants may be obtained by first closing a collocated rate feedback loop then designing/implementing SISO control about the desired output location.
3. When successfully implemented, noncollocated control can provide improved performance (regulation, tracking, disturbance rejection) over collocated control at the noncollocated output .

6.4.3i Full State Feedback LQR Control

Expected Results:

1) In Step 2: Using the numerical plant of Eq. (6.1-6i) the poles of the closed loop transfer function for the specified values of "r" are plotted in Figure 6.4-5i.[1]

2) A suitable controller from these which meets the closed loop pole specification is the case of $r = 1.0$ which has a corresponding controller:

$$K = [\ 0.0897 \quad 0.0030 \quad 0.6414 \quad 0.0545\ ] \tag{6.5-1i}$$

[1]Scripts for Lqr synthesis using MATLAB® are included in Appendix Ai.

© ECP 1995, All Rights Reserved

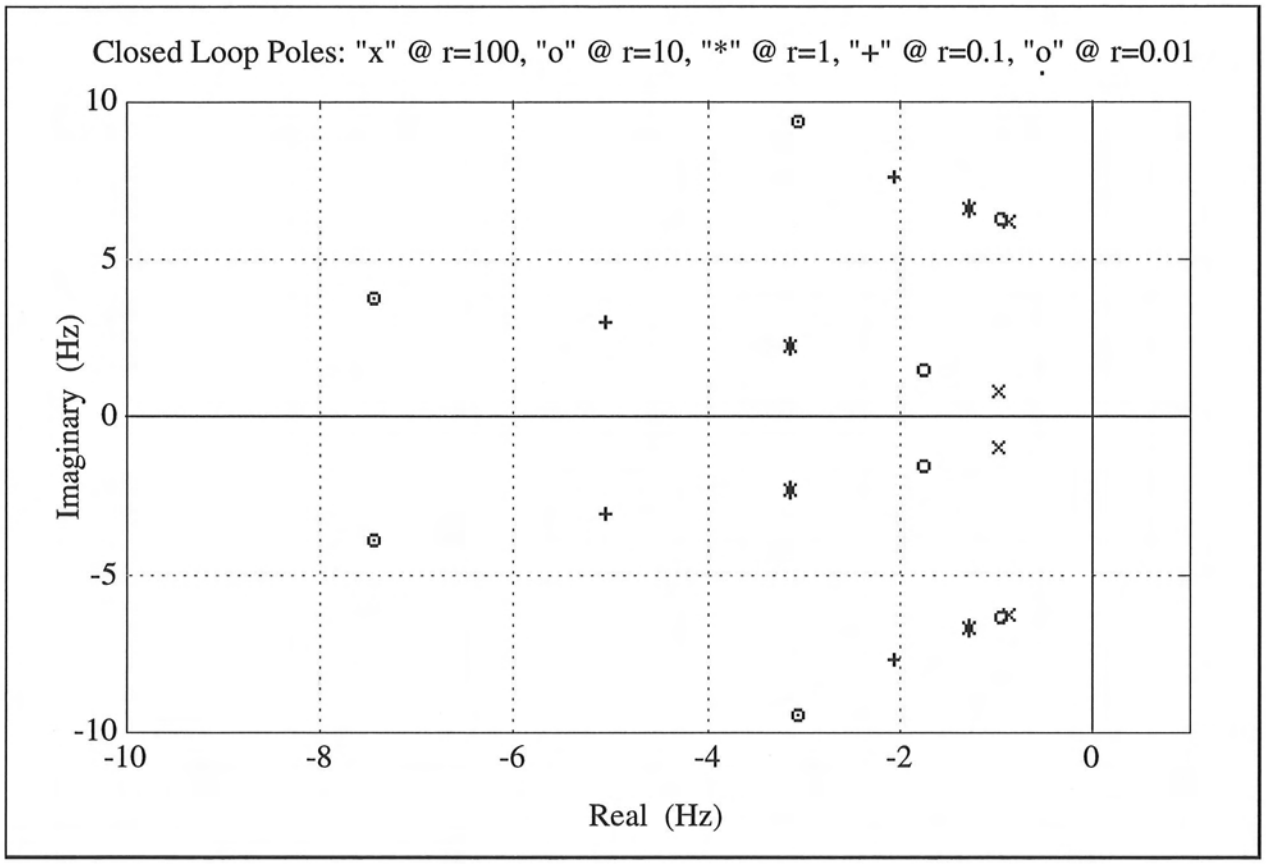

Figure 6.4-5i. Closed Loop Pole Locations For Various Control Effort Weights

Since the tracking error weight was levied against θ_2 only, the LQR solution in this case has higher K_1 than K_3 gains[1] for values of $r \geq 0.1$ and hence rejects low frequency disturbances at the base disk better than at the top within this range. The resulting performance, however is better than for the previous controllers.

3) A step response using this controller is shown in Figure 6.4-6i. Notice the reduced rise time and steady state error. Notice also the irregular motion in θ_1 in which as the control "attempts" to minimize the error in θ_2. Figure 6.4-7i shows the simulated step response at θ_1 and θ_2 using the Matlab® script "LQR.M" given in Appendix Ai. Note the close agreement between the simulation and actual response.

[1]This does not hold for higher control effort weights

© ECP 1995, All Rights Reserved

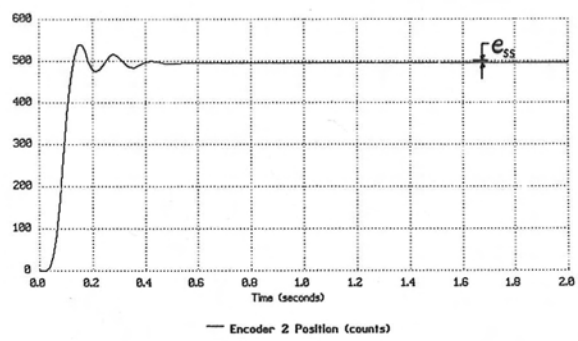

a) The load disk response is roughly 30% faster than for the notch filter design and has very low steady state error

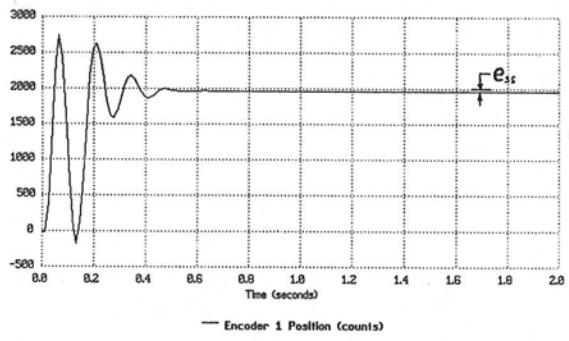

b) As in the previous noncollocated control case, the drive disk undergoes initial lead then reverse motion minimize error af the load

Figure 6.4-6i. Step Responses at the Drive and Load For LQR Design

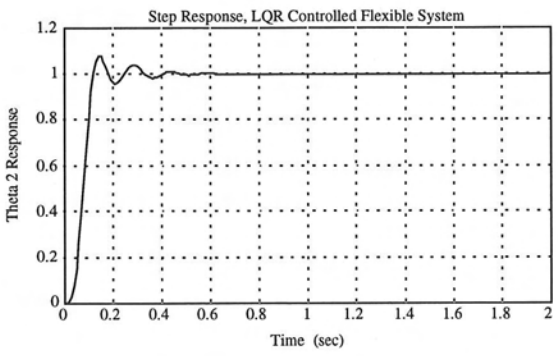

a) Nonollocated (θ_2) response

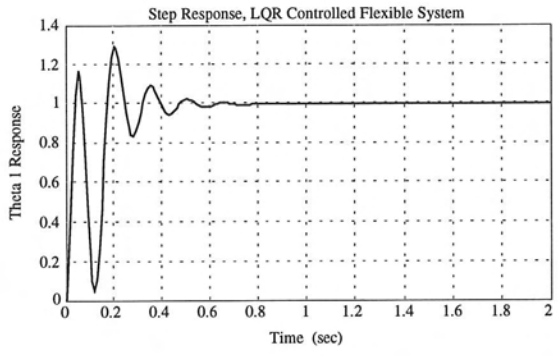

b) Collocated (θ_1) response

Figure 6.4-7i. Simulated Response Agrees Closely With Experimental Results

4) For static disturbances T_d, the control torque, T_u, reacts to changes in position according to: $T_u = -K_1\theta_1 - K_3\theta_2$. For disturbances at the collocation (disk #1), neglecting friction $\theta_2 = gr^{-1}\theta_1$ and $T_{d\theta_1} = -T_u$, so that the static stiffness is: $T_{d\theta_1}/\theta_1 = K_1 + gr^{-1}K_3$ and $T_{d\theta_1}/\theta_2 = grK_1 + K_3$. For disturbances at the load disk we have $T_{d\theta_2} = -grT_u$ and $T_{d\theta_2} = k(\theta_2 - gr^{-1}\theta_1)$ where k is the spring constant. This results in $T_{d\theta_2}/\theta_2 = k(K_1gr^2 + K_3gr)/(k + K_1gr^2)$. Hence for large values of K_1 the effective servo stiffness approaches the spring stiffness, k, and for large k the servo stiffness approaches $K_1gr^2 + K_3gr$ (i.e. it is gr^2 times greater than $T_{d\theta_1}/\theta_1$). It is also easily shown that $T_{d\theta_2}/\theta_1 = k(K_1gr + K_3)/(k - K_3gr)$ so that θ_1 may react to disturbances at θ_2 in either the same or reverse direction depending on the relative values of k and K_3gr.

© ECP 1995, All Rights Reserved

Full state feedback for a fourth order system (one rigid body and one flex mode) nominally requires rate and position sensors at both the input and output, i.e. the nominal cost of full state feedback is additional sensors. When high resolution end relatively low noise sensors already exist (e.g. the high resolution encoders in the Model 220 apparatus) their signals may be differentiated for rate measurement[1] and hence four states become available. If noncollocated control is to be used, then both a collocated and a noncollocated sensor are generally required to implement it. In many cases therefore, full state feedback control can be effected using only $n/2$ sensors where n is the system order.

Further Topics:

1) A sine sweep showing both outputs is shown in Figure 6.4-8i. (Trajectory parameters are: 0.1 to 12.0 Hz range, 60 s duration ($\Rightarrow$ 5 s. $\approx$ 1 Hz), 100 count amplitude.) The plant zero is clearly seen in the θ_1 output while the resonance associated with the common pole frequencies are seen in both (only slightly in θ_2). The second disk response is nearly flat out to the system bandwidth, then rolls off at -80 db/decade (four pole excess), while the first disk rolls off at -40 db/decade (two pole excess).

2) Tracking control and regulation under disturbance torques are shown in Figures 6.4-9i, -10i and discussed in Section 6.4-4.

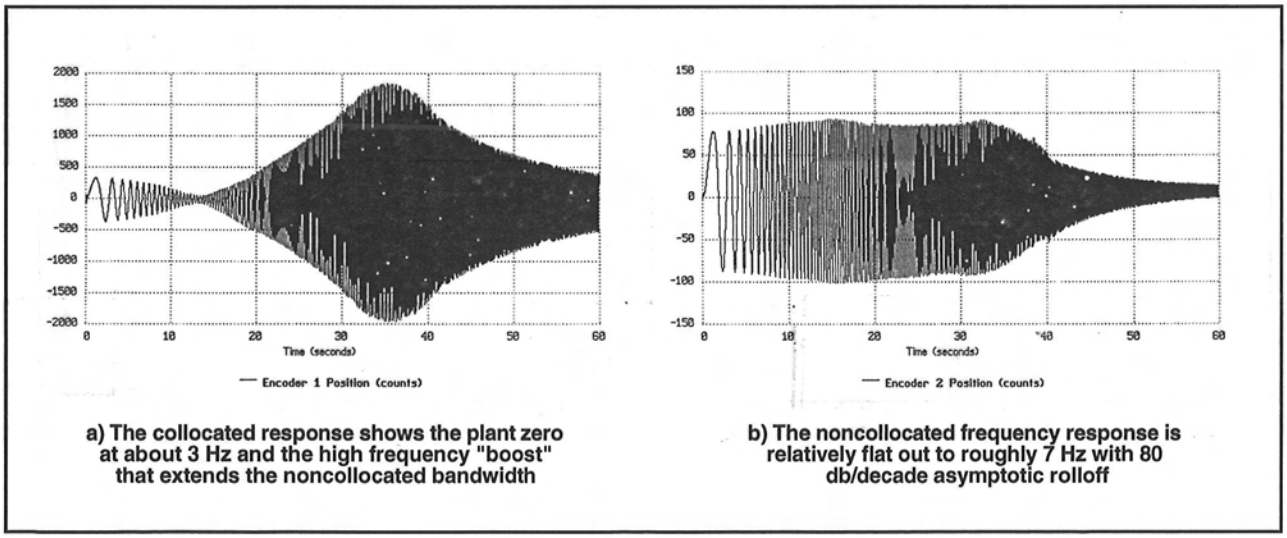

a) The collocated response shows the plant zero at about 3 Hz and the high frequency "boost" that extends the noncollocated bandwidth

b) The noncollocated frequency response is relatively flat out to roughly 7 Hz with 80 db/decade asymptotic rolloff

Figure 6.4-8i. Frequency Response Magnitude (Sine Sweep)of Collocated LQR System

[1]Strictly speaking, the rate feedback is an estimate rather than a measurement.

© ECP 1995, All Rights Reserved

This section showed:

1. LQR design often provides well-behaved, relatively high performance controllers for servo equipment with drive flexibility. It may be readily implemented whenever full state feedback is available.
2. With sufficient sensor resolution and low signal noise, position measurement may be differentiated to provide a rate estimate thereby reducing the sensor requirement to $n/2$ where n is the number of states.
3. Low steady state errors are often achievable through relatively high proportional gain at both the drive and load outputs.

6.4.4i Further Tests of Flexible Control Designs

Further tests that give insight into the relative performance and stability merits of the two collocated (6.4.1) and two noncollocated (6.4.2 & 6.4.3) designs in Section 6.4 are easily performed.

1) Tracking of a rapid saw-tooth trajectory[1] is shown in Figure 6.4-9. The collocated controllers clearly show poor input trajectory following with the structural oscillation clearly present. The collocated (drive disk) response (not shown) during these maneuvers closely follows the scaled demand. Control effort for the high gain controller is large with intermittent saturation as the "disturbance" caused by the uncontrolled flexible mode is resisted at the drive disk.

   The noncollocated controllers both show considerable tracking improvement over their collocated counterparts. The successive loop closure / notch filter control has low constant-velocity following error and moderate overshoot at the rate discontinuities. The LQR design has moderate following error[2] and virtually no overshoot. In both cases, the collocated (drive disk) response (not shown) digresses wildly from the input as the systems "automatically" compensate for the flexible motion to minimize error at the load disk. The notch filter design requires high peak control effort including brief saturation at the rate discontinuities. The LQR design requires about one third the peak torque.

[1] I.e. a ramp with: 8000 count amplitude, 16000 count/s velocity and 2.0 s dwell. For the collocated controllers, PD control was implemented via the **General Form Algorithm** in loop 3 ($e_o = f_o = k_p$, $f_1 = k_d$) and t_1 multiplied by the gear ratio so that the Commanded Position data scaled with the θ_2 output.

[2] This can of course be eliminated with velocity feedforward

© ECP 1995, All Rights Reserved

2) Disturbance rejection with a step torque[1] at the output is shown in Figure 6.4-10. The collocated controllers show poor regulation at the load. As is expected, the high gain version has lower steady state disturbance response than the low gain design but has greater oscillation because of the low flexible mode damping. The two noncollocated designs have about one fourth the disturbance response of the collocated schemes. The notch filter design is more oscillatory in the initial transient but the steady state values are quite similar. This coincides with similar k_{ss} at the outputs.[2]

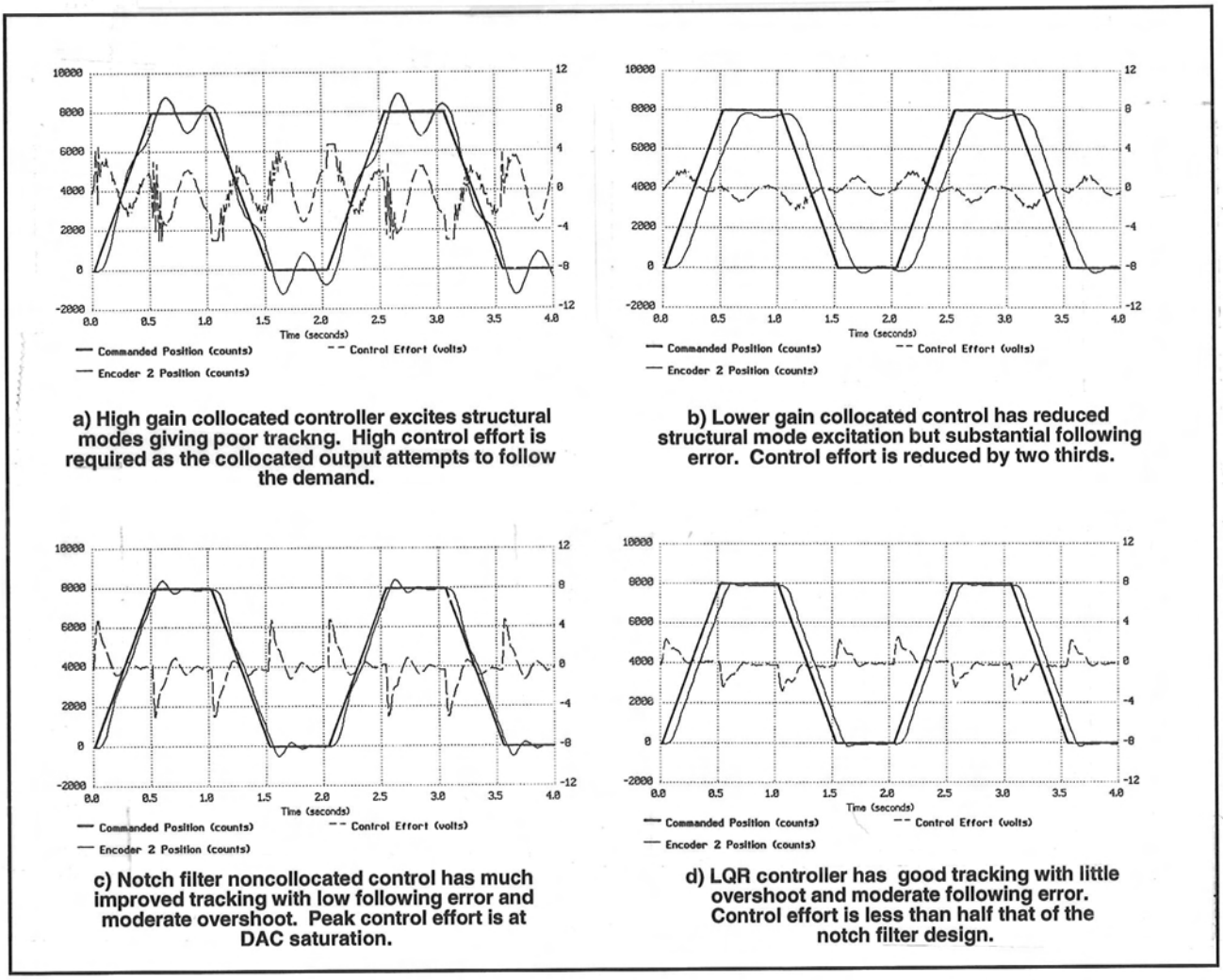

a) High gain collocated controller excites structural modes giving poor trackng. High control effort is required as the collocated output attempts to follow the demand.

b) Lower gain collocated control has reduced structural mode excitation but substantial following error. Control effort is reduced by two thirds.

c) Notch filter noncollocated control has much improved tracking with low following error and moderate overshoot. Peak control effort is at DAC saturation.

d) LQR controller has good tracking with little overshoot and moderate following error. Control effort is less than half that of the notch filter design.

Figure 6.4-9i. Trajectory Tracking Of Section 6.4 Controllers

[1]Disturbance amplitude = 0.5 V, duration = 2.0 s, 2 repetitions.

[2]This result may at first look seem to be inconsistent with the LQR step response steady state error being considerably less than for the notch filter design. The LQR system however has a proportional gain term at θ_1 as well as θ_2 and hence more strongly resists disturbances such as friction that occur near the low (motor) end of the drive train.

© ECP 1995, All Rights Reserved

3) System stability and performance robustness to parameter changes is easily tested and compared by adding and removing from the load disk. All four systems can tolerate arbitrarily large inertia increases without instability (this in essence reduces system gain). The collocated designs can also tolerate complete removal of all load inertia. The LQR and notch filter designs can each withstand roughly 50% inertia loss before instability.

   Performance at the load improves dramatically with reduced load inertia for the collocated controllers but heavily degrades as it is increased. The notch filter design response becomes more oscillatory with both increased and reduced inertia since the notch filter no longer corresponds to the modal frequency. The LQR performance is satisfactory over an inertia variation range of about -20% to +50% .

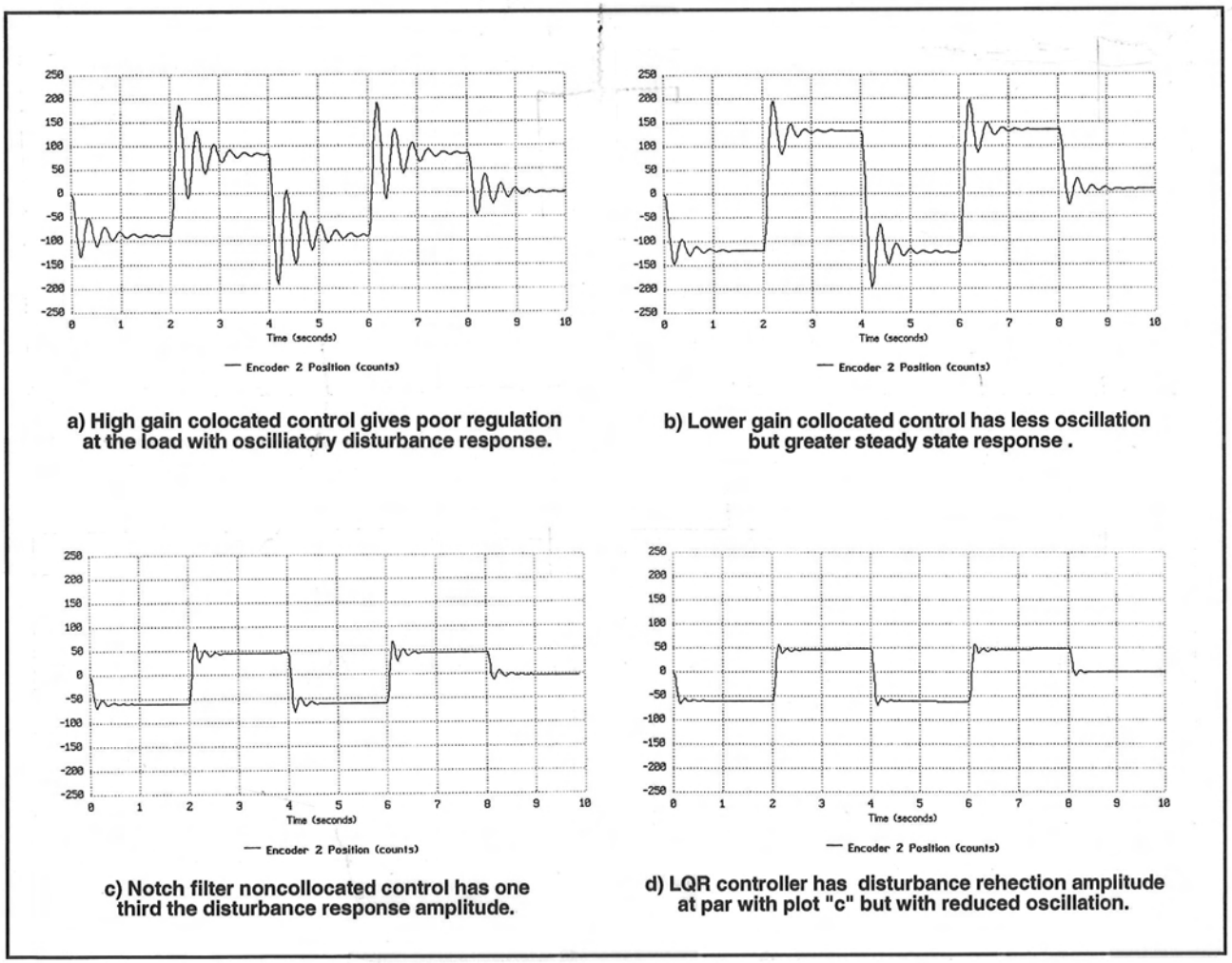

a) High gain colocated control gives poor regulation at the load with oscilliatory disturbance response.

b) Lower gain collocated control has less oscillation but greater steady state response .

c) Notch filter noncollocated control has one third the disturbance response amplitude.

d) LQR controller has disturbance rehection amplitude at par with plot "c" but with reduced oscillation.

Figure 6.4-10i. Output Disturbance Rejection Of Section 6.4 Controllers

© ECP 1995, All Rights Reserved

6.5 Control of Plant With Backlash

In this section, the effect of backlash is first shown in the context of its effect under a typical PD control implementation. An empirical approach to mitigating its effect is then developed.

General Discussion on Backlash:

Backlash is common in mechanical drives and exists to some extent in nearly all gear boxes and in many mechanical couplings. Backlash as seen at the load is *reduced* by the gear ratio between the backlash location and the load and backlash as seen at the motor is *increased* by the gear ratio between the backlash location and the motor. Thus it is the usually backlash at the high end of the gear train (closest to the load) that is most problematic.

It is worth noting that in practice, backlash is sometimes eliminated via torque biasing at the load or through internal counter-torqueing devices such as anti-backlash gears. If the first of these is employed, a feed-forward torque may be simultaneously applied through the control to offset the output error bias. This usually requires continuous control torque and hence can lead to drive power and thermal problems. In either of these mechanical backlash remedies, pure noncollocated control is only viable if the control torque does not overcome the torque bias.

6.5.1 Effects on Conventionally Controlled Systems

1. In Steps 1 and 2: The response should be similar to the ones shown in Figure 6.5-1a - i.e. an approximately critically damped system with about 200 ms rise time. The θ_1 and θ_2 responses track closely with amplitude scaled by the gear ratio. The response is similar for the collocated and noncollocated feedback cases.
2. In Steps 3 and 4: The step with the collocated controller is shown in Figure 6.5-1b.[1] The effects of backlash are clearly seen. The collocated output tracks the reference input is well behaved and settles fairly closely (within 15 counts) to the reference input. The noncollocated output however tracks in an ill-behaved and inconsistent way and may settle anywhere within the backlash amount (plus friction and other disturbance related steady state error sources).
3. In Step 6: The disturbance effect at θ_1 and θ_2 are shown in Figure 6.5-2 where the right and left hand axes are appropriately scaled by gear ratio. As would be expected, the collocated output is only mildly affected by the disturbance (servo compliance only) while the noncollocated output is displaced by the backlash distance plus the servo compliance.

[1] In all plots involving backlash, the relative position of θ_1 and θ_2 will vary depending on their initial positions when control was first implemented (or "zero position" commanded) and when a maneuver is executed. The plots will then vary from trial to trial by the amount of the backlash and may not appear as shown here.

© ECP 1995, All Rights Reserved

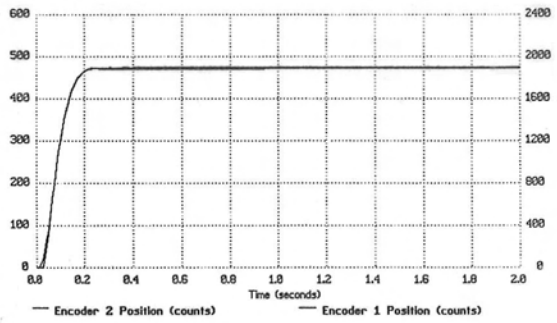

a) Rigidly coupled drive and load track closely and give well behaved response

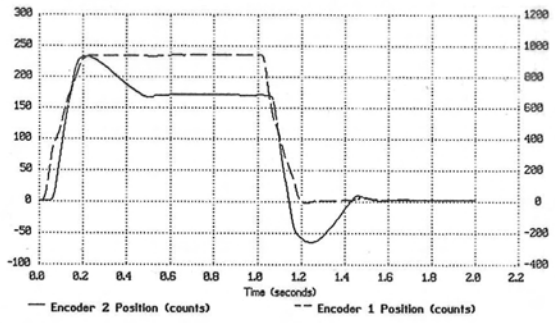

b) Collocated control with backlash results in large load position errors and unpredictable response. (Noncollocated controlled system is unstable.)

Figure 6.5-1i. Step Responses With and Without Backlash

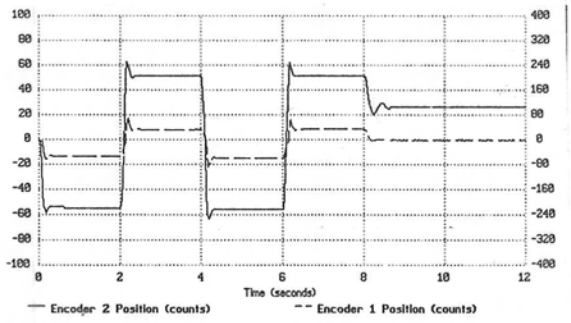

Errors at the load include both backlash and servo compliance. Those at the drive include only servo compliance.

Figure 6.5-2i. Response To Output Disturbance With Backlash

This section showed:

1. When backlash is present, purely collocated control can lead to significant output errors at the load. Purely noncollocated control is often unstable (nearly always unless very low gains are used).
2. Output disturbance errors include the output equivalent backlash (which can be large) and the servo compliance error.

© ECP 1995, All Rights Reserved

6.5.2 Control for Mitigation of Backlash Effects

1. In Step 1: The initial step response is given in Figure 6.5-3i, subplot "a" shows a well damped but slow response with large steady state error.

2. In Step 2: An example step response following interactive gain selection is shown in Figure 6.5-3i, subplot "b" where the gains $\mathbf{t_0} = \mathbf{s_0} = 1.2$ (k_p), $\mathbf{f_1} = 0.04$ (k_v) were used. The response shows typical "backlash "rattling" but is generally well damped and has dramatically improved rise time and steady state error over the initial controller.

3. In Step 3: The disturbance response is shown in Figure 6.5-3i, subplot "d". The resulting steady state error is reduced by a factor of three over the collocated control of Section 6.5.1. The collocated disk moves in opposition to the disturbance and drives through the backlash so that only the servo compliance (plus friction and cogging torque) contributes to steady state error.

4. In Step 4: Increase in the noncollocated proportional gain increases responsiveness of the output and reduces steady state error, but also can increase oscillation and/or "backlash rattle". Increase in collocated rate feedback improves system stability margin and reduces oscillation, but slows the response. Increase (or reduction) reduction in noncollocated derivative gain (not changed in this exercise) may either increase or reduce stability margin depending on other gain values and plant dynamic conditions. Acceptable results are usually obtained by setting this gain value near midrange between its lower and upper bound for instability onset.

© ECP 1995, All Rights Reserved

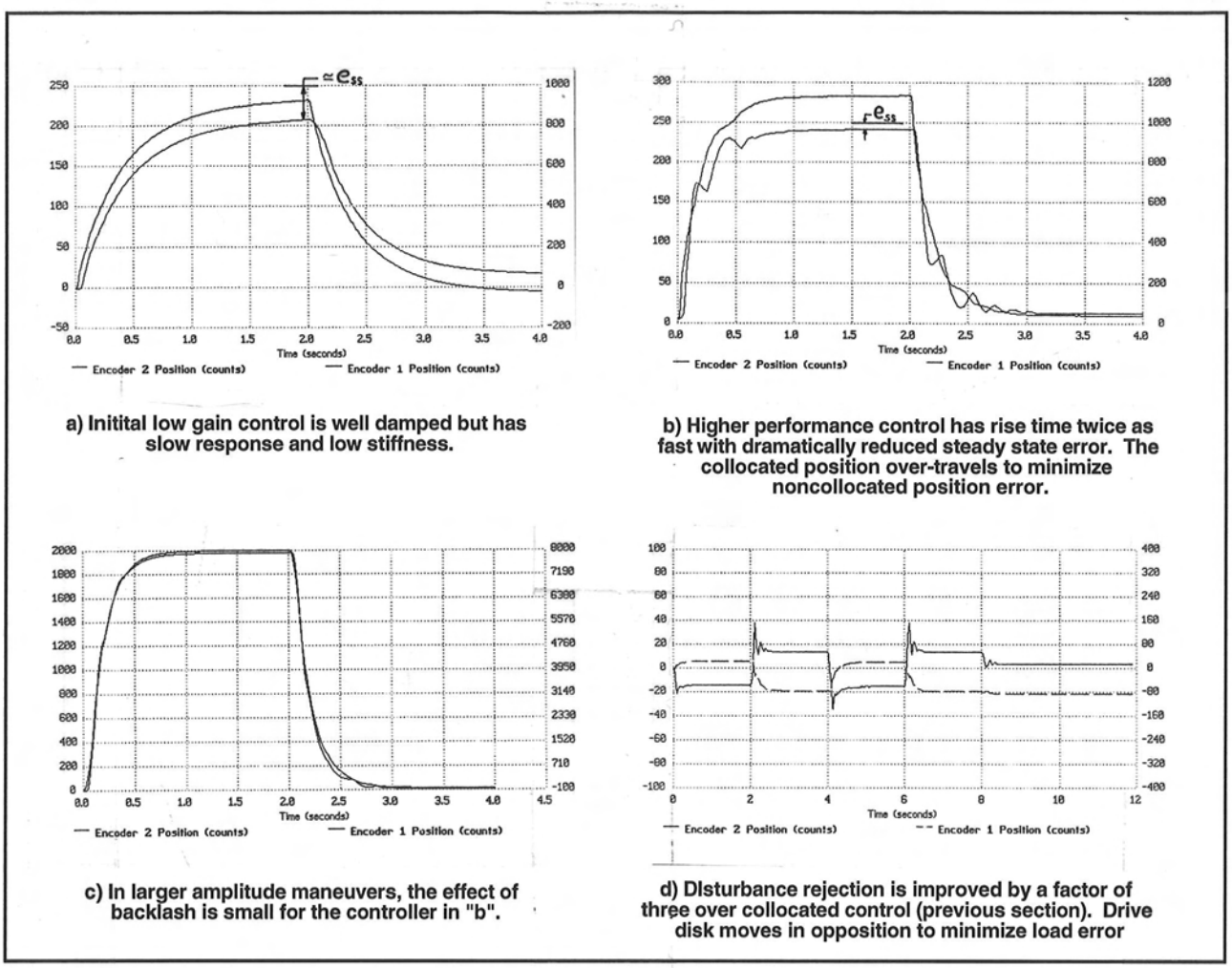

a) Initital low gain control is well damped but has slow response and low stiffness.

b) Higher performance control has rise time twice as fast with dramatically reduced steady state error. The collocated position over-travels to minimize noncollocated position error.

c) In larger amplitude maneuvers, the effect of backlash is small for the controller in "b".

d) Disturbance rejection is improved by a factor of three over collocated control (previous section). Drive disk moves in opposition to minimize load error

Figure 6.5-3i. Characteristic Responses With Collocated Rate Feedback Plus Outer Loop Noncollocated Control For System With Backlash

This section showed:

1. The effects of backlash may be effectively mitigated in some systems by use of collocated rate feedback and higher authority (gain) outer loop noncollocated control.
2. For outer loop PD control, k_p increases responsiveness and servo stiffness, but tends to make the output more oscillatory. Increases *or* reductions in k_d from some stabilizing value may lead to instability. Increase in collocated rate feedback gain improve system stability but slow response.

© ECP 1995, All Rights Reserved

6.6i Suggestions For Further Experiments

The following experiments are readily supported by the ECP control system and emulator apparatus. Still others are possible.

1) Dynamics: Many aspects of coupled discrete inertia systems may be demonstrated on this system. Specifically:
   a) The interrelationship between stiffness and inertia and the modal shapes and frequencies may be analyzed, then demonstrated.
   b) Viscous friction may be added via rate feedback and/or the disturbance motor.
   c) The plant may be identified by modal techniques with data gathered via the encoders. (See e.g. Eqs.(5.2-19, -20).
   d) The equations of motion may be efficiently derived using generalized coordinates and variational techniques such as those employing Lagrange's equations or the Hamiltonian methods.

2) Digital Control:
   a) Demonstrate that a significantly larger T_s can be accommodated by designing in discrete rather than time.
   b) Demonstrate digital controller implementation by simulating a controller response (i.e. the controller only O/I response) to an input then implement the controller and see the same. This may be accomplished via the general controller form by setting feedback or "downstream" gains to zero. Then perform a closed loop move (e.g. step response) while collecting data at the appropriate node (See Figure 4.1-1).[1]

3) System Robustness:
   a) Characterize a controller designed for the nominal plant, then vary the disk inertia(s) (changes both plant gain & frequencies) and test system performance.
   b) Continue changing inertia until instability is approached (often instability only occurs via inertia reduction).
   c) Design robust controllers and test comparatively with nonrobust designs.

[1]It is a good idea to do this check on any complicated controller before implementing it.

© ECP 1995, All Rights Reserved

4) Tracking Performance:

   a) Feed-forward design for improved tracking performance is readily implemented through the **Setup Feedforward** box under **Setup Control Algorithm**.

   b) Trajectories may be optimized for characteristics such as rapid response, minimum tracking error, or minimum peak control effort. The user may select from the library of geometric trajectories, or develop and implement custom shapes via **User Defined** in the **Trajectory Configuration** dialog box.

5) Advanced Control:

   The general control form supports virtually any linear controller up to and including seventh order (e.g. observer based, LQG/LTR, H∞, QFT).[1] The data acquisition, trajectory generation, and file management features of the system provide for rapid implementation and system characterization.

Closing Note:

The control designs given here are in no sense optimized, but rather are designed to demonstrate several fundamental principles of control. The user is invited to implement other designs or invent other approaches and share them with us at ECP.

[1]The authors for example, have had good luck designing high performance and robust controllers for the flexible drive system using the loop shaping techniques and algorithms found in the MATLAB® Robust Control Toolbox. The approach for noncollocated control is generally to use collocated rate feedback and then close the high performance or robust loop through the noncollocated encoder.

© ECP 1995, All Rights Reserved

Appendix Ai. Useful Scripts

Listed in this appendix are Matlab® scripts for building the numerical plant models, and some LQR related design work from Section 6.4. These are not represented as being numerically or methodologically optimal, but may be useful to some users.

A.1i Plant Model Builders

A.1.1i General Form

The following script builds models of both the rigid body and flexible plants. Parameter values (e.g. k_{hw} and the flex. constant, *k*)used here are for a specific measured plant. For more precise results, use the identified values for your plant. Use only the script portion for one configuration at a time. Shorter forms for the rigid body or flexible models alone are given in A.1.2i and A.1.3i.

```
%plant.m
%This script Calculates inertias and builds the rigid body
%or flexible plant models
%*************************  Input Parameters  *****************************

%Select output location, Out:
                    %  "1" = Encoder #1
                    %  "2" = Encoder #2
Out=2

%Plant configuration, Confg:
                    %  "1" = Drive disk only, (use only Out=1)
                    %  "2" = Drive & load disk - rigid drive train
                    %  "3" = Drive & load disk - flexible drive belt
Config=3

%Select mass parameters
mwd=0.8, %(mass of brass weights on drive disk)
rwd=0.05, %(radius from center of plate on drive disk)
mwl=2.0, %(mass of brass weights on load disk)
rwl=0.1, %(radius from center of plate on load disk)

%Lower (Drive) Pulley: Select (decomment) one of the following as appropriate:
%npd=18,Jpd=0.000003; %(18 tooth)
npd=24,Jpd=0.000008; %(24 tooth)
%npd=36,Jpd=0.000039; %(36 tooth)
%npd=72,Jpd=0.00055; %(72 tooth)

%Upper (Load) Pulley: Select (decomment) one of the following as appropriate:
%npl=18,Jpl=0.000003; %(18 tooth)
%npl=24,Jpl=0.000008; %(24 tooth)
```

© ECP 1995, All Rights Reserved

```
npl=36,Jpl=0.000039; %(36 tooth)
%npl=72,Jpl=0.00055; %(72 tooth)

%Default frict coeff's - change if setup-specific measurements available
c1=0.004 %if belt from drive to SR ass'y attached
%c1=0.002 %if belt from drive to SR ass'y not attached
c2=0.05 %if belt from drive to SR ass'y attached
c12=0.017 %viscous coupling between drive & load

k=8.45 %Torsional spring constant

khw=5.81 %(Hardware gain, assume kg=1, it will be corrected below if Out=2)

%************************  The Rest Is Automatic   ************************
gr=6*npd/npl %gear ratio
grprime=npd/12 % drive to SR pulley gear ratio

%First calculate known inertias
Jdd=0.00040;
Jdl=0.0065;
Jpbl=0.000031;%Backlash mechanism
Jp=Jpd+Jpl+Jpbl

%Calculate Drive inertia,
rwdo=0;%initializing
rwlo=0;
%First find which size weight used, can use only 0, 2, or 4 weights
if mwd < 0.81
 if mwd > 0.39
  rwdo=0.016 %(smaller brass weight used)
 end
end
if mwd < 2.1
 if mwd > 0.9
  rwdo=0.025 %(larger brass weight used)
 end
end
%Calculate inertia about weights own cg.
Jwdo=(1/2)*mwd*rwdo^2;
%Combined drive inertia:
Jd=Jdd+mwd*rwd^2+Jwdo

%Calculate Load inertia,
if mwl < 0.81
 if mwl > 39
  rwlo=0.016  %(smaller brass weight used)
 end
end
if mwl < 2.1
 if mwl > 0.9
  rwlo=0.025  %(larger brass weight used)
 end
end
%Calculate inertia about weights own cg.
```

© ECP 1995, All Rights Reserved

```
Jwlo=(1/2)*mwl*rwlo^2;
%Combined load inertia:
Jl=Jdl+mwl*rwl^2+Jwlo

%Build transfer functions and state space models
if Config==1, %Drive disk only:
 %Transfer Function:
 N=khw
 D=[Jd c1 0]
 %State Space model:
 A1=[0 1]
 A2=[0 -c1/Jd]
 Aol=[A1;A2]
 B=[0 khw/Jd]'
 C=[1 0],%Theta1 output
end

if Config==2, %Drive & load disks - rigid drive train
 if Out==1, %Encoder %1 output
  Jr=Jd+Jp*grprime^(-2)+Jl*gr^(-2), %Reflected inertia at drive
  cr=c1+c2*gr^(-2), %Reflected damping to drive
  %Transfer Function:
  N=khw
  D=[Jr cr 0]
  %State Space model:
  A1=[0 1]
  A2=[0 -cr/Jr]
  Aol=[A1;A2]
  B=[0 khw/Jr]'
  C=[1 0]
end
 if Out==2,%Encoder #2 output
  Jr=Jd*gr^2+Jp*(gr/grprime)^2+Jl,%Reflected inertia at load
  cr=c1*gr^2+c2,%Reflected damping at load
  %Transfer Function:
  N=khw*gr
  D=[Jr cr 0]
  %State Space model:
  A1=[0 1]
  A2=[0 -cr/Jr]
  Aol=[A1;A2]
  B=[0 khw*gr/Jr]'
  C=[1 0]
 end
end

if Config==3,%Drive & load disks - flexible drive train

 Jdstr=Jd+Jp*grprime^(-2),%Pulley inertias combined with drive
 %Transfer Function:
 %The following do not include the coupled damping c12
 %N1=khw*[Jl c2 k];
 %N2=khw*k/gr;
 %D=[Jdstr*Jl (c2*Jdstr+c1*Jl) (k*(Jdstr+Jl/gr^2)+c1*c2) (k*(c1+c2/gr^2)) 0];
```

© ECP 1995, All Rights Reserved

```
 %The following include c12
 N1=khw*[Jl c2+c12 k];
 N2=khw/gr*[c12 k];
     D=[Jdstr*Jl      (c2*Jdstr+c1*Jl+(Jdstr+Jl/gr^2)*c12)
(k*(Jdstr+Jl/gr^2)+c1*c2+(c1+c2/gr^2)*c12) (k*(c1+c2/gr^2)) 0];

 %State Space model:
 A1=[0 1 0 0];
 A3=[0 0 0 1];
 %The following do not include the coupled damping c12
 %A2=[-k/Jdstr/gr^2 -c1/Jdstr k/Jdstr/gr 0];
 %A4=[k/Jl/gr 0 -k/Jl -c2/Jl];
 %The following include c12
 A2=[-k/gr^2/Jdstr -(c1+c12/gr^2)/Jdstr k/gr/Jdstr c12/gr/Jdstr];
 A4=[k/gr/Jl c12/gr/Jl -k/Jl -(c2+c12)/Jl];
 Aol=[A1;A2;A3;A4];
 B=[0 khw/Jdstr 0 0]';
 if Out==1,%Encoder #1 output
   C=[1 0 0 0];
 end
 if Out==2,%Encoder #2 output
   C=[0 0 1 0];
 end
end
```

A.1.2i Abbreviated Form for Rigid Body Plants

```
%rgdplnt.m
%This script builds the Rigid Body plant model
%Its is shorter than plant.m but requires up front inertia calculations for
%each plant configuration.
%*****************************  Input Parameters  ****************************
%Select output location, Out:
                    %  "1" = Encoder #1
                    %  "2" = Encoder #2
Out=2

%Plant configuration, Confg:
                    %  "1" = Drive disk only, (use only Out=1)
                    %  "2" = Drive & load disk - rigid drive train
Config=2

gr=4 %gear ratio
grprime=2 %gear ratio between drive and idler

%Drive Disk Inertia - Calculate value if not given below
Jd=0.0025 %(4*200g wts. at r=5.0 cm)
%Jd=0.00040 %(no wts.)
%Jd=0.00145 %(2*200g wts. at r=5.0 cm)
%Pulley Inertia - Calculate value
```

© ECP 1995, All Rights Reserved

```
Jp=0.000078  %(Add Jpl+Jpd+Jbacklash device from Table 6.1-2)
%Load Inertia - Calculate value if not given below
Jl=0.0271 %(4*500g wts. at r=10.0 cm)
%Jl=0.0065 %(no wts.)

%Default frict coeff's - change if setup-specific measurements available
c1=0.004 %if belt from drive to SR - ass'y attached
%c1=0.002 %if belt from drive to SR - ass'y not attached
c2=0.05 %if belt from SR ass'y to load attached

khw=5.81; %(Hardware gain, assume kg=1, it will be corrected below if Out=2)

%*********************   Build Rigid Body Plant Model   **********************
%Build transfer functions and state space models
if Config==1, %Drive disk only:
 %Transfer Function:
 N=khw
 D=[Jd c1 0]
 %State Space model:
 A1=[0 1]
 A2=[0 -c1/Jd]
 Aol=[A1;A2]
 B=[0 khw/Jd]'
 C=[1 0],%Theta1 output
end
if Config==2, %Drive & load disks - rigid drive train
 if Out==1, %Encoder %1 output
  Jr=Jd+Jp*grprime^(-2)+Jl*gr^(-2), %Reflected inertia at drive
  cr=c1+c2*gr^(-2), %Reflected damping to drive
  %Transfer Function:
  N=khw
  D=[Jr cr 0]
  %State Space model:
  A1=[0 1]
  A2=[0 -cr/Jr]
  Aol=[A1;A2]
  B=[0 khw/Jr]'
  C=[1 0]
end
 if Out==2,%Encoder #2 output
  Jr=Jd*gr^2+Jp*(gr/grprime)^2+Jl,%Reflected inertia at load
  cr=c1*gr^2+c2,%Reflected damping at load
  %Transfer Function:
  N=khw*gr
  D=[Jr cr 0]
  %State Space model:
  A1=[0 1]
  A2=[0 -cr/Jr]
  Aol=[A1;A2]
  B=[0 khw*gr/Jr]'
  C=[1 0]
 end
end
```

© ECP 1995, All Rights Reserved

A.1.2i Abbreviated Form for Flexible Plants

```
%flxplnt.m
%Short Form Plant Builder for Flexible drive plants
%Its is shorter than plant2.m but requires up front inertia calculations for
%each plant configuration.
%*************************  Input Parameters  *****************************
%Select regulation or tracking output location, Out:
%   "1" = Encoder #1
%   "2" = Encoder #2
Out=2

gr=4 %gear ratio
grprime=2 %Drive to SR pulley (i.e. first stage) gear ratio

%Drive Disk Inertia - Calculate value if not given below
Jd=0.0025 %(4*200g wts. at r=5.0 cm)
%Jd=0.00040 %(no wts.)
%Jd=0.00145 %(2*200g wts. at r=5.0 cm)
%Pulley Inertia - Calculate value
Jp=0.000078  %(Add Jpl+Jpd+Jbacklash device from Table 6.1-2)
%Load Inertia - Calculate value if not given below
Jl=0.0271 %(4*500g wts. at r=10.0 cm)
%Jl=0.0065 %(no wts.)

%Default frict coeff's - change if setup-specific measurements available
c1=0.004 %if belt from drive to SR - ass'y attached
%c1=0.002 %if belt from drive to SR - ass'y not attached
c2=0.05 %if belt from SR ass'y to load attached
c12=0.017 %viscous coupling between drive & load

k=8.45 %Torsional spring constant
khw=5.81; %(Hardware gain, assume kg=1, it will be corrected below if Out=2)

%**********************   Build Flexible Plant Models   **********************

Jdstr=Jd+Jp*grprime^(-2);%Pulley inertias combined with drive

%Transfer Function:
%The following do not include the coupled damping c12
%N1=khw*[Jl c2 k];
%N2=khw*k/gr;
%D=[Jdstr*Jl (c2*Jdstr+c1*Jl) (k*(Jdstr+Jl/gr^2)+c1*c2) (k*(c1+c2/gr^2)) 0];
%The following include c12
N1=khw*[Jl c2+c12 k];
N2=khw/gr*[c12 k]
D=[Jdstr*Jl       (c2*Jdstr+c1*Jl+(Jdstr+Jl/gr^2)*c12)
(k*(Jdstr+Jl/gr^2)+c1*c2+(c1+c2/gr^2)*c12) (k*(c1+c2/gr^2)) 0];
```

© ECP 1995, All Rights Reserved

```
%State Space model:
A1=[0 1 0 0];
A3=[0 0 0 1];
%The following do not include the coupled damping c12
%A2=[-k/Jdstr/gr^2 -c1/Jdstr k/Jdstr/gr 0];
%A4=[k/Jl/gr 0 -k/Jl -c2/Jl];
%The following include c12
A2=[-k/gr^2/Jdstr -(c1+c12/gr^2)/Jdstr k/gr/Jdstr c12/gr/Jdstr];
A4=[k/gr/Jl c12/gr/Jl -k/Jl -(c2+c12)/Jl];
Aol=[A1;A2;A3;A4];
B=[0 khw/Jdstr 0 0]';
if Out==1,%Encoder #1 output
  C=[1 0 0 0];
 end
 if Out==2,%Encoder #2 output
  C=[0 0 1 0];
 end
```

A.2i PD Gain Selector

This simple script finds the PD gains once the plant model parameters have been established.

```
kpkd.m
%Finds PD gains kp and kd given wn, z, Jl, & Jd.
%This version neglects friction
%Select output at load disk or at drive disk below

%**************************  Input Parameters    ************************
wnHz=4 % Desired natural frequency in Hz.
wn=wnHz*(2*pi) %natural freq. in rad/s
z=1 % Desired damping ratio
gr=4 % Gear ratio
Jl=0.00651; %Load disk inertia
Jdstr=.00040; %Drive disk inertia including reflected pulley inertia
khw=5.81; %Hardware gain

%**************************  Compute kp & kd    ************************

%For output at load disk:
kp=wn^2*(Jl+Jdstr*gr^2)/khw/gr
kd=2*z*wn*(Jl+Jdstr*(gr)^2)/khw/gr

%For output at drive disk:
%kp=wn^2*(Jl/gr^2+Jdstr)/khw
%kd=2*z*wn*(Jl/gr^2+Jdstr)/khw
```

© ECP 1995, All Rights Reserved

A.3i LQR Designer

This script generates the gain vector K for full state feedback LQR control. The error weighting is on the output(s) specified in the C vector. Various K are generated for a range of control effort weightings. The script also plots the closed loop poles. For plotting step response, specify the desired closed loop system(s) near the bottom of the script.

```
%lqr.m
%  The following Generates a family of LQR controllers and plots the
%  resulting closed loop poles and selected step responses.
%  You must first have generated the Aol, B, & C matrices.

Q=C'*C;

Klqr1=lqr(Aol,B,Q,100);
Klqr2=lqr(Aol,B,Q,10);
Klqr3=lqr(Aol,B,Q,1);
Klqr4=lqr(Aol,B,Q,.1);
Klqr5=lqr(Aol,B,Q,.01);
Klqr6=lqr(Aol,B,Q,.001);

Pcl1=eig(Aol-B*Klqr1)/2/pi;
Pcl2=eig(Aol-B*Klqr2)/2/pi;
Pcl3=eig(Aol-B*Klqr3)/2/pi;
Pcl4=eig(Aol-B*Klqr4)/2/pi;
Pcl5=eig(Aol-B*Klqr5)/2/pi;
Pcl6=eig(Aol-B*Klqr6)/2/pi;

% Plot Roots
axis([-10,1,-10,10])
plot(Pcl1,'x')
hold;
plot(Pcl2,'o');
plot(Pcl3,'*');
plot(Pcl4,'+');
plot(Pcl5,'.');
plot(Pcl5,'o');
plot(Pcl6,'*');
plot(Pcl6,'o');
title('LQR Controller, Closed Loop Poles For Various Control Effort Weights')
%title('Closed Loop Poles: "x" @ r=100, "o" @ r=10, "*" @ r=1, "+" @ r=0.1,
"o" @ r=0.01')
xlabel('Real  (Hz)')
ylabel('Imaginary  (Hz)')
grid;
hold;
pause
% User may define labels, frequencies in Hz.
% Stike any key to continue

% Compute Step Response:
t=0:.01:2;
steplq1=(gr*Klqr1(1)+Klqr1(3))*step([Aol-B*Klqr1],B,C,0,1,t);
```

© ECP 1995, All Rights Reserved

```
steplq2=(gr*Klqr2(1)+Klqr2(3))*step([Aol-B*Klqr2],B,C,0,1,t);
steplq3=(gr*Klqr3(1)+Klqr3(3))*step([Aol-B*Klqr3],B,C,0,1,t);
steplq4=(gr*Klqr4(1)+Klqr4(3))*step([Aol-B*Klqr4],B,C,0,1,t);
steplq5=(gr*Klqr5(1)+Klqr5(3))*step([Aol-B*Klqr5],B,C,0,1,t);
steplq6=(gr*Klqr6(1)+Klqr6(3))*step([Aol-B*Klqr6],B,C,0,1,t);

%Example Step Response Plot
axis([0,2,0,1.2]);
plot(t,[steplq3 steplq4 steplq5]);
%plot(t,[steplq1]);
title('Step Response, LQR Controlled Flexible System')
xlabel('Time  (sec)')
ylabel('Theta 2 Response')
grid
```

© ECP 1995, All Rights Reserved